Frontispiece
Bragg reflection of an argon laser beam from the structure induced in a medium by a ruby laser beam

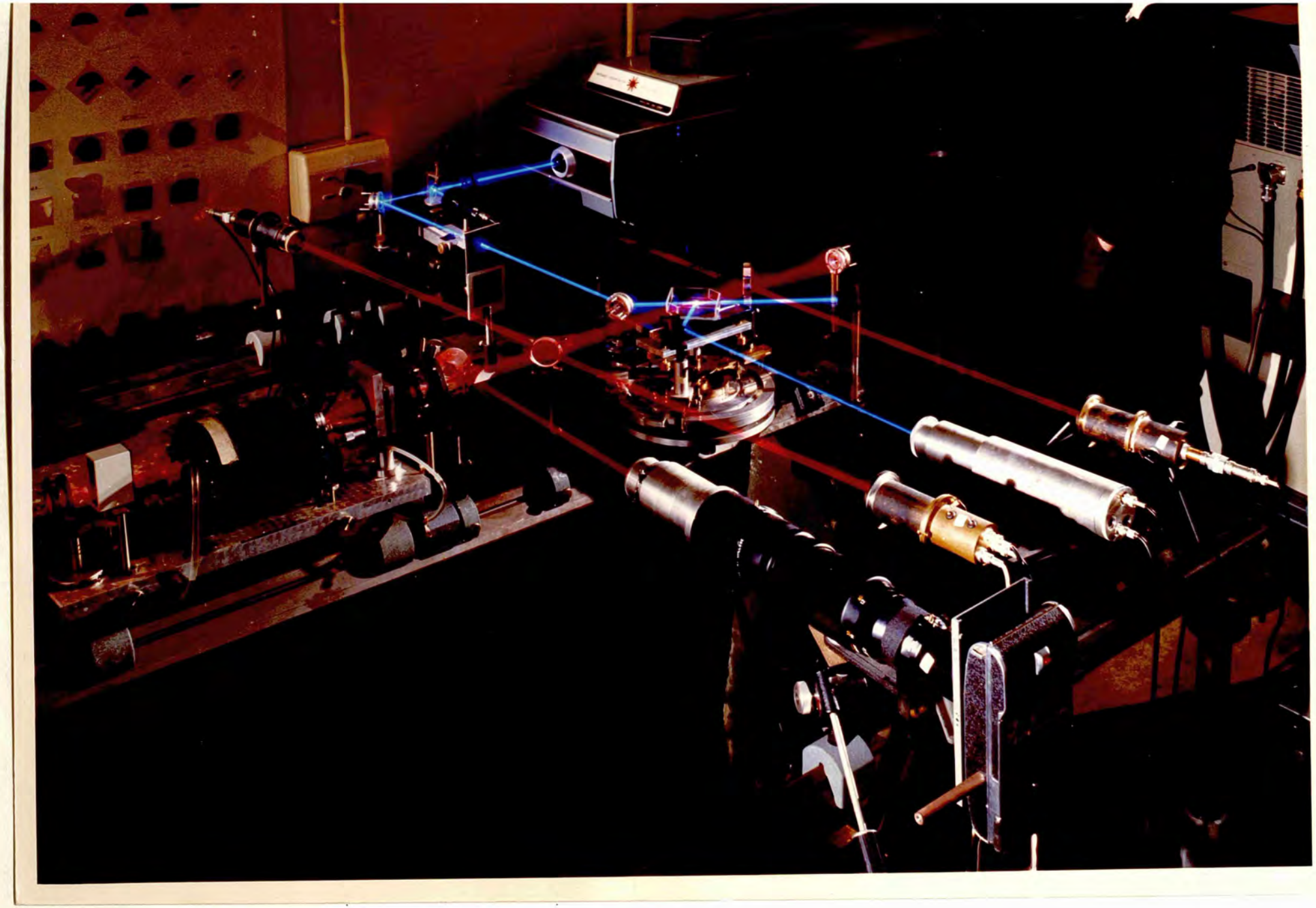

THE SCATTERING OF LIGHT FROM LIGHT INDUCED STRUCTURES IN LIQUIDS

by

PAUL YENAN KEY

Thesis presented for the
Degree of Doctor of Philosophy
in the University of London

July, 1970

Department of Physics,
Royal Holloway College

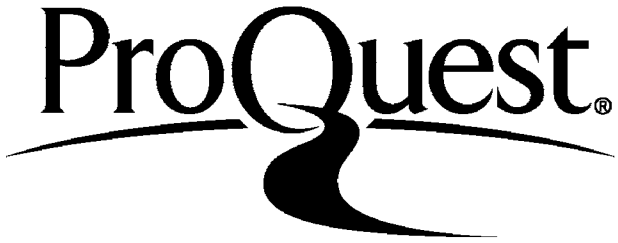

A B S T R A C T

The development of the study of light scattering, from the early work of Stokes and Rayleigh to the modern investigations of non-linear stimulated scattering processes has been reviewed.

The conventional theory of stimulated scattering has been extended to describe the scattering of an independent probe laser beam. This scattering is the result of the effect on the refractive index of a medium of the electric field due to two oppositely directed, high intensity light beams. The standing wave of electric field, generated by these beams, spatially modulates the refractive index of the medium by electrostriction, the Kerr effect and absorptive heating, all of which are proportional to the mean square of the local field. When the beams are of slightly different frequency the standing wave, and the resulting modulation, travel through the medium with a velocity proportional to that difference. Under these circumstances the modulation and the standing wave travel through the medium with the same velocity but with different phase as a result of the inertia associated with each of the above mechanisms. The usual stimulated scattering is determined entirely by the out of phase component of the refractive index modulation while the probe scattering described in this thesis is determined by the whole amplitude of that modulation.

A Q-switched ruby laser has been used to generate such modulations in a liquid and these have been detected by the scattering of a frequency

doubled portion of the ruby laser beam and of an independent argon laser beam. The refractive index modulation associated with the temperature modulation induced by absorption of the ruby laser light has been investigated in some detail and the lifetimes of such modulations in a number of media have been measured.

Other related non-linear scattering processes have been investigated using a variety of experimental techniques, particularly interesting results being obtained in the study of non-linear fluorescence from saturable absorbers.

C O N T E N T S

C O N T E N T S
(Continued)

C O N T E N T S
(Continued)

CHAPTER I

DEVELOPMENT OF THE STUDY OF LIGHT SCATTERING

1.1 EARLY WORK

The first scientific studies of the scattering of light by material media were made in the second half of the 19th century, particularly by Stokes[1] and Rayleigh[2]. Stokes studied the frequency shifted fluorescence which occurs when certain absorbing media are strongly illuminated. He discovered empirically that this light is always depolarized and that its spectrum is a band of comparable width to the absorption band, but with its maximum always at a lower frequency than the maximum of the absorption band. These observations received a satisfactory and simple explanation only on the development of the quantum theory. Lord Rayleigh considered from a classical theoretical point of view the scattering of light from very small particles. He was able to show that the scattering is essentially unshifted in frequency and proportional to the inverse fourth power of the wavelength of the illuminating light and thus explained the blue colour of the sky.

The next major development was achieved by Brillouin[3] in 1922 who used Debye's[4] method of analysing the random fluctuations of a medium into its acoustic modes to show that the light scattered from such a medium will be shifted up or down in frequency by a Doppler shift due to the velocity of the acoustic waves. This splitting was detected by Gross[5] in 1930. The theory was developed in more detail by Mandelshtam[6] (1926) and Landau and Placzek[7,8] (1934) who showed that in addition to the 'Brillouin doublet' there exists scattering, due to non propagating entropy fluctuations, which is unshifted in frequency. This is usually known as the 'Rayleigh line'. Scattering from induced

ultrasonic waves was also demonstrated[9] and theoretically analysed[10].

In the meantime Raman[11,12] in 1928 had discovered an entirely new type of molecular scattering (Raman scattering). Like the fluorescence investigated earlier by Stokes it was predominantly down-shifted in frequency but unlike fluorescence it was strongly polarized. Furthermore the spectrum of the scattered light consisted of sharp lines reduced in frequency from the illuminating lines by integral multiples of certain fixed frequencies characteristic of the medium. There were also much fainter lines of increased frequency. This scattering he correctly explained in terms of the quantum theory, the frequency shifts being determined by the difference between energy levels of the molecule.

At the same time Raman and Krishnan[13] considered the problem of scattering from anistropic molecules and showed that, as distinct from the case of the Rayleigh line and Brillouin doublet, a depolarization of the scattered light occurs. Further work[7,14,15,23] showed that the depolarized light contributes a broad wing to the light scattering spectrum (the Rayleigh wing) with a frequency spread which is the inverse of the molecular re-orientation time.

This wing was very difficult to observe, the results obtained often being contradictory. The first definite observation was probably that of Gross[16].

1.2 IMPLICATIONS OF LIGHT SCATTERING OBSERVATIONS

The Raman scattering was soon well investigated[17-19] and shown to be a powerful tool in spectroscopy allowing very precise measurement of molecular energy levels. Along with infra-red ultra-violet absorption, and nuclear magnetic resonance spectra it has been used primarily as a diagnostic tool in physical chemistry.

The existence of the fine structure of the Rayleigh scattering (Rayleigh line, Rayleigh wing and Brillouin doublet) was shown by a number of workers[5,16,20-22] in the thirties and forties, though quantitative work was made very difficult by the lack of spectroscopic resolution and the feeble light sources available. The practical work was however accurate enough to demonstrate the inadequacy of the then current hydrodynamic theory of liquids[23] which predicted a square law dependence of sound absorption on frequency. Using this relationship extrapolation of the ultrasonic data to the frequencies involved in Brillouin scattering shows such a high sound absorption that the Brillouin lines, whose widths are determined by absorption, would be much wider than their separation and therefore indistinguishable. Clear Brillouin lines were however easily observable.

The problem was resolved in 1937 by Mandelshtam and Leontovich[24,25] who proposed the relaxation theory of liquids. This shows the same features at low frequencies as the earlier theory but shows that at high frequencies the static 'constants' are modified due to their finite relaxation times.

The relaxation theory however, also implies a dispersion in the velocity of sound which had not been found at that time. It thus remained a matter of controversy until such dispersion had been experimentally demonstrated particularly by the Brillouin scattering measurements of Fabelinskii and co-workers[26-28] in the fifties.

One further source of controversy was the non-observance of Brillouin lines in viscous liquids. This result also was in contradiction with the relaxation theory but was shown by Fabelinskii[29] to be

due only to experimental difficulties when he observed the Brillouin doublet of glycerine. The relaxation theory then adequately explained the light scattering phenomena observed at that time[30]. (Though later more detailed investigations of Brillouin spectra have required it to be modified for high viscosity liquids[31].

1.3 THE DEVELOPMENT OF THE LASER

This situation, with the phenomena of light scattering broadly understood but impossible to investigate in great detail, was to be dramatically changed by the development of the laser.

The first stimulated emission device was the maser developed by Townes[32] in 1954. This, employed the fact that the transition coefficients for a stimulated transition between two energy levels are equal in each direction. Thus if the majority of the atoms in a medium can be put in an upper state the medium will amplify microwaves (or light) at a frequency where it normally absorbs them. In a suitable resonator this amplification can result in oscillations in one or a number of modes of the oscillator near the peak of the gain (ground state absorption) curve.

A laser, an identical device except that the emission is in the optical region, was first constructed by Maiman in 1960[33]. He used a small ruby rod surrounded by a helical flash tube which produced a train of 3 kW, 2 μsec pulses lasting about 1 msec. The power available was soon extended into the megawatt region particularly by the work of Hellwarth[34] who developed the technique of Q-switching. In this technique a large population inversion built up in the laser material in a lossy cavity which was then switched to higher gain by electro-optic means. All the stored energy then appeared as a single 'giant pulse'

of megawatt intensity and some tens of nanoseconds duration.

At the same time the continuous Helium-Neon laser was developed by Javan[36]. While the power of this laser was less than a milliwatt the divergence, spectral width and beam diameter were much smaller than those of the ruby laser. In 1962 Kleinman[32] suggested improvement of the spectral output of all types of laser by using a resonant reflector in place of the output mirror, to ensure single longitudinal mode operation, and this was achieved by various workers[38,40]. The technique of Q switching was greatly simplified in 1964 by the development by Sorokin of the passive Q-switch[41,42]. This employs a highly absorbent dye inside the resonator which bleaches when the laser pulse starts to develop. The gain of the resonator thus increases suddenly and a giant pulse occurs.

Another important development in that year was the achievement of mode locking by Hargrove et al[43,44] who synchronized the phase of the longitudinal modes of a gas laser by modulating the cavity losses at the difference frequency. This converted the output to a train of high power pulses of picosecond duration separated by the cavity loop time. Similar results[45,46] were obtained in ruby and neodymium lasers simply by using a suitable (fast relaxation) bleachable dye (and Brewster angled surfaces to avoid mode selection). A new technique for measurement of these picosecond pulses was developed by Giordmaine[47,48] using the fact that two such pulses overlapping produce more two photon fluorescence (see Section 1.5) than two acting separately.

Transverse mode selection has since been developed by Soncini and Svelto[49,50] and transverse mode locking was recently reported by Arakelyan[51].

A further advance was achieved in 1966 with the development of the Pulse Transmission Mode Laser[54,55]. Here a Pockels cell is used in conjunction with a Glan Thompson prism to give first a low Q cavity to build up population inversion, then a very high Q cavity to transfer the energy from the inverted population to the photon flux, then back to the first situation with the light energy switched out of the cavity. This results in a pulse length of the order of the cavity loop time and can be used in conjunction with mode locking to give a single picosecond pulse[54] of very high power.

The 'state of the art' at present is that the powers available are up to 10^4 watts continuous (CO_2 laser), 10^9 watts pulsed (PT M Neodymium laser) and 10^{12} watts in picosecond pulses. Diffraction limited divergence has been obtained for both continuous and pulsed lasers. Longitudinal and transverse mode selection allow line widths of 10^{-3} Å for pulsed lasers and a few cycles per second for carefully stabilized continuous lasers. Pulses of a few nanoseconds can be obtained from mode selected lasers while mode locked, non-linear optically shortened, pulses can be less than one picosecond[55,115]. A wide variety of materials allow lasing at frequencies throughout the optical spectrum while the dye laser developed by Sorokin[56] has the further advantage of being continuously tunable over a range of frequencies.

The development of these light sources has affected light scattering studies in two main ways: First, an enormous improvement in the accuracy and ease of spontaneous light scattering experiments, and secondly the development of the entirely new field of non-linear optics.

1.4 SPONTANEOUS LIGHT SCATTERING STUDIES USING LASERS

The crude features of the light scattering spectrum had already been worked out by 1959[57,220]. The development of the laser has however increased the accuracy of measurement by many orders of magnitude and led to the discovery of some entirely new features. The spectral purity of the continuous gas laser has made it the main experimental tool for spontaneous scattering studies in spite of the higher powers available from solid state lasers.

The high power argon-ion laser has allowed Raman scattering to be developed as a very convenient spectroscopic tool. Furthermore it is now possible to make absolute measurements of Raman cross-sections[58,59] while studies of line-widths and correlation counting has given new information on intermolecular forces and optical phonon properties[60-62].

The first studies of the spontaneous Brillouin scattering using helium/neon lasers were done in 1964 by Benedek et al[63] for the case of solids and by Chiao and Stoicheff for liquids[64]. These together with further work[65-70,74] provided accurate knowledge of hypersonic velocity in a large range of media. Such measurements were extended to gases by the work of Eastman et al in 1966[71]. With the improved spectral resolution available it was also possible to measure the width of the Brillouin lines and hence deduce the hypersonic absorption coefficient. This was first done by Mash et al[72] in 1965 and a quantity of accurate information was soon available[68,70,73,74].

In the meanwhile investigations had been carried out on the scattering in the Rayleigh line and wing. The angular dependence of such scattering was investigated first by George et al[75] in 1963 and then by Leite et al[76] who found good agreement with theory. The

depolarization of the different parts of the scattering spectrum were investigated by various workers[77-79]. The exact frequency dependence was studied particularly by Staranov[80-85] from 1963 onward, who was first to discover a fine structure in the depolarized Rayleigh wing scattering spectrum of liquids[86-88](1967) which he identified as the result of transverse or shear waves.

The spectral width of the central Rayleigh line was first measured in 1964 by Cummins et al[89] for the case of a solution of macromolecules. The homodyne and Heterodyne light beating techniques developed for this experiment are capable of a few cycles per second resolution and were soon applied to determine the width of the central Rayleigh line in pure gases[90] and liquids[91] and at the critical point[92].

In addition to these greatly refined measurements an entirely new feature of the scattering spectrum originating in the relaxation of the shear and volume viscosities was predicted by Mountain in 1966[93-96], and discovered by Gornal et al[97] later that year. This consisted of a broad peak centred on the incident frequency but distinguished from the Rayleigh wing by being completely polarized.

Further investigations of the central line scattering promise to reveal the existence of second sound in solids. The conditions for such an experiment to succeed have been discussed[98,99] but no successful observations have yet been reported.

The overall spectrum of the spontaneous scattering as known at present is shown in the upper curve of Fig.2.3.[168]. The spectrum shown is that of the polarized scattering. In the depolarized spectrum the sharp peaks due to the Rayleigh line, Brillouin doublet and Raman scattering are absent leaving a broad band centred on ω_L. The

spectrum can be analysed as the sum of the scattering due to the Rayleigh line. Rayleigh wing, Brillouin doublet and Raman line. These are due to fluctuations in refractive index associated with variations of entropy, anisotropy, density and molecular polarizability respectively. Each resulting component of the curve represents the solution (in terms of the frequency dependence of amplitude) of the equation of a damped resonant system. These components are of the form:

$$I \propto \frac{1}{\left(1 - \frac{\Delta\omega^2}{\Omega^2}\right)^2 + \left(\frac{2\,\Gamma\Delta\omega}{\Omega^2}\right)^2}$$

[Throughout this thesis the variables introduced are defined in the Appendix at the back.]

The central peaks occur for processes where $\frac{\Omega}{\Gamma} > \sqrt{2}$, and the double peaks where $\frac{\Omega}{\Gamma} > \sqrt{2}$. This simple picture is in fact complicated by the fact that relaxation theory shows τ and Ω are themselves frequency dependent.

The various spontaneous scattering processes have been well reviewed by a number of authors[30,62,69,74,93,94,95,96,100].

1.5 NON-LINEAR OPTICS

Before the laser was invented the possibility of light changing the refractive index of a medium by the Kerr effect had been suggested by Buckingham[101], but this possibility seemed so remote that there was no further practical or theoretical investigation of the phenomenon. However the high power and spectral brightness of the laser soon made this a very active subject. The phenomena observed may be divided into two categories. Those involving the polarization of the medium under the influence of a number of waves and those involving only the transitions induced in individual molecules by the light flux. Both types of

phenomena were first observed in 1961. We shall consider the latter category first as less work has been done in this field.

The first experiment of this sort was the detection by Kaiser and Garrett[102] of the effect of non-linear two photon absorption. In this phenomenon a molecule absorbs two photons of ruby laser light though there is no real energy level at the photon energy. Quantum mechanically the process depends on a transition to a virtual level followed rapidly by a second induced transition which allows energy conservation. The absorption was revealed by the blue fluorescence due to the transition back to the ground state from the two photon level. Such absorption was directly measured by Giordmaine and Howe[103] in 1963. In 1964 Sorokin et al[41] used the reversible bleaching of cyanine dyes to Q-switch a ruby laser. In this process the rate of absorption is such that the populations of the ground and first singlet state become equalized thus reducing the absorption. This phenomenon has since been extensively investigated experimentally and theoretically[104,106,109] and Mack has demonstrated[107] that under some circumstances it can even result in amplification of a beam which would usually be absorbed. Gibbs in 1967[108] used the fluorescence technique of Kaiser and Garrett to demonstrate excited state absorption. In the Q-switching dyes there is an energy level at the single photon energy and a second at the two photon level. Molecules can be successively excited from ground to first and first to second levels. The real energy level distinguishes this process from two photon absorption and the power dependence of the fluorescence is also different. The extension of such fluorescence studies to a number of other dyes and solvents is reported in this thesis[248].

The first non-linear polarization effect detected was the frequency doubling of light in a piezoelectric crystal. This was observed by Franken et al[109] in 1961. This, and non-linear effects in general, may be understood as a result of the fact that the mathematical expression

for the polarization of a medium contains terms in the square, cube, etc. of the applied field, in addition to the linear term[110]. The coefficients of these terms are so small that they were negligible for the optical field strengths attainable before the use of lasers. With the high fields produced by lasers it is necessary to take into account the effect of these terms. When the applied field is sinusoidal the expression for the polarization is a sum which may contain terms at all integral multiples of the fundamental frequency. If two or more fields are applied all the sum and difference frequencies can also occur.

In centrosymmetric media there can be no asymmetric terms in the polarizability and therefore the expression for the polarization can contain no terms in even powers of the magnitude of electric field. Thus only odd multiples of the applied frequency can occur. Third harmonic generation was detected in such media by Terhume et al[111] 1962.

The production of harmonics in this way is limited by any dispersion in the medium. This causes the fundamental and second harmonic beams to get out of phase so that further production of the second harmonic is subtracted from that already produced. This problem was ingeniously overcome by Maker et al[112] in 1962, who used the fact that for a particular angle of propagation in some birefringent media the ordinary refractive index at the fundamental frequency is equal to the extraordinary refractive index at the second harmonic. Using this technique conversion efficiencies with giant pulse lasers of up to 20% were soon obtained[113] and even second harmonic generation induced by a 1 mW continuous He-Ne laser[114] was detected. Much later it was demonstrated that under certain conditions third harmonic generation may also be phase matched[115].

The multiple of the frequency by zero of course represents a D.C. potential. Such a potential (or more precisely a pseudo-D.C. potential as the total light pulse duration was $\sim 10^{-8}$ secs) was observed by Bass et al[116] in 1962.

Difference frequency generation was observed in 1963 by Niebuhr[117] who used a laser oscillating in two modes to generate the two incident frequencies. When such difference frequency generation occurs, energy conservation demands that one photon at the higher frequency is destroyed while one is created at a lower frequency and another at the difference frequency. Thus if the lower frequency signal is much weaker than the main 'pump' light it can be greatly amplified at the same time as producing the 'idler' difference frequency. This process, known as parametric amplification, which has long been known at lower frequencies[118] was achieved in the optical region by Peterson and Yariv in 1964[119]. With the non-linear material in a feedback cavity this amplification can result in oscillation without any signal input and the phase matching conditions allow this to be used as a tunable source of coherent radiation[129,121].

It is interesting that the parametric oscillator mentioned was constructed three years before study of the underlying parametric fluorescence by Akhanov et al[122,123] in 1967. They examined the light emitted for various directions of the incident and resultant beams when no feedback was present.

All these non-linear polarization processes have undergone exhaustive theoretical examination[110,124-132,217-219] particularly in the work of Bloembergen from 1962 onward, and in conference proceedings[127-129].

A non-linear polarization phenomenon of a rather different kind, involving a change in the bulk refractive index of the medium was predicted by Askaryan in 1962[133]. When an intense light beam propagates in a medium it increases the refractive index by electrostriction and the Kerr effect. This increase is greater in the regions of higher field resulting in a concentration of the light into these regions. When the intensity is so high that this effect overcomes diffraction, the light self-focuses and is finally self-trapped into long narrow filaments. The caused by such filaments in a transparent solid was observed by Hercher in 1964[134] and the filaments themselves by Pilipetskii et al in 1965[135].

This thesis contains some study of such filaments undertaken in order to investigate the interesting scattering process which takes place when two such filaments intersect[245].

The precise explanation of such self-trapping has been the subject of some controversy[136-142] recently renewed after investigation of the self-trapping of picosecond pulses[143,144]. The opposite phenomenon of defocusing has also been observed[145-148] as a result of the decrease in refractive index with increased temperature when the light beam passes through an absorbing medium. Similarly self-bending has been observed with a non-uniform incident beam[149,150]

The bulk change of refractive index causing these phenomena has been quantitatively determined by Gires et al in 1964[151-153] who measured the rotation it induces in the axis of elliptically polarized light. Longaker and Litvak[154] have recently used one laser to take Mach-Zender interferometer pictures of the disturbance of refractive index induced by another. This technique has the advantage of allowing spatial resolution of the disturbance.

1.6 STIMULATED SCATTERING

Another remarkable consequence of non-linear optics was discovered accidentally in 1962 by Woodbury and Ng[155] but was soon understood and investigated by Eckhardt et al[196] and other workers[62,139,157-164]. This phenomenon was stimulated Raman scattering. The very weak wave produced by Raman scattering beats with the main laser wave at the difference frequency. This frequency is of course the characteristic frequency of the atom which gave rise to the Raman scattering in the first place. A very strong interaction can therefore occur with the Raman scattered wave and the atomic excitation being amplified at the

expense of the 'pump' wave in a variation of the parametric amplification process. Any small antistokes shifted signal itself acts as a pump wave and there is therefore induced absorbtion at these frequencies[165] though stimulated antistokes generation can occur as a result of more complicated four photon interactions[110,104,166,167].

It is accepted that each of the contributions to the spontaneous scattering curve[74,164,168] can under appropriate conditions, give rise to stimulated scattering (though this may be obscured by competition between the possible processes). The gain contributed by each process is a function of the difference in frequency between the amplified light and pump light of the form:

$$G \propto \frac{\frac{2\Gamma\Delta\omega}{\Omega^2}}{\left(1 - \frac{\Delta\omega^2}{\Omega^2}\right)^2 + \left(\frac{2\Gamma\Delta\omega}{\Omega^2}\right)^2},$$

where the constants are the same as those in the appropriate spontaneous scattering curve. The overall gain curve[108] shown in Fig.2.3 is a sum of such terms. The gain curve for a signal polarized perpendicularly to the pump of course, contains only those terms which exist in the depolarized scattering spectrum.

When the stimulated scattering builds up from spontaneous noise usually only the frequency with the highest gain will occur. Under various conditions this can be due to the different scattering processes. A complete picture of the gain curve is however more easily obtained by generating the shifted frequency separately and subjecting it to a relatively small amplification. (This technique was first developed in 1964 by Bret and Meyer[169] to measure stimulated Raman gain.)

The next stimulated scattering effect observed, discovered in solids by Chiao et al in 1964[170,221,222] was stimulated Brillouin scattering

In this process a hypersonic wave takes the place of the atomic excitation and coupling is provided by electrostriction. Extensive work[170-177] was soon carried out on this process including observations in liquids[170] and gases[171]. A major difficulty of this work was that focused light was necessary to achieve the intensities required, however Brewer in 1965[178] was able to observe the stimulated Brillouin scattering in an unfocused beam, allowing much more precise experimental and theoretical investigation[162,163,178-189].

In 1965 another stimulated scattering process, that of the Rayleigh wing was observed by Mash et al[184]. The polarization of this scattering was perpendicular to that of the laser light allowing separation from other scattering processes. The depolarized scattering has been further studied[185-189] and the special case of stimulated scattering from shear waves has been observed in solids[177].

With the discovery of self-focusing it became necessary to re-interpret the quantitative significance of most of these experiments. In particular the use of the stimulated amplifier technique was necessary as lower powers can be used with this method. Comprehensive results were obtained on both stimulated Brillouin and stimulated Rayleigh wing scattering by Bret and Denariez using this technique[168]. Pohl et al[190] were able to use it to estimate the lifetime of the phonons involved in the stimulated Brillouin process.

The last stimulated scattering to be discovered was that associated with the Rayleigh central line. The reason for this was that coupling of the light wave to the entropy wave is normally provided by the very weak electrocaloric effect[191-193] resulting in very small gains. This problem was avoided by Bespalov and Kubarev in 1967[194] who used

a mixture of liquids and observed stimulated Rayleigh scattering from the concentration fluctuations. In the same year Zaitsev et al[193] observed stimulated thermal scattering due to the electrocaloric effect in a pure liquid. Both these methods involved experimental difficulties and the very small Stokes frequency shift of about half the laser line-width was not measured. The frequency shift in gases is much larger and this was later measured in hydrogen by Mash et al[195].

At the same time Herman and Gray[196] considered the modification of the scattering process in an absorbing medium. There is in this case a very strong coupling between the light and temperature waves which has the unusual feature that the energy transferred to the medium by absorption results in a gain for the antistokes rather than the Stokes scattering. This type of scattering and its very small frequency shift was immediately detected by Rank et al in liquids[197-199] and later in gases[200]. The time and frequency dependence of the thermal Rayleigh gain was investigated by Pohl et al[201] who also detected a change in the stimulated Brillouin gain[202] as predicted by Herman and Gray.

The use of picosecond pulses to stimulate Rayleigh scattering offerred interesting possibilities. Earlier experiments by Shapiro et al[203] had shown strong inhibition of stimulated Raman and Brillouin scattering under these conditions. The stimulated Rayleigh scattering usually observed depends on the change in refractive index with entropy at constant pressure. For such short pulses, because of the inertia of the medium, the change would be at constant density. An experiment of this type was performed by Mack in 1968[204] but it has since been pointed out by Pohl[205] that owing to his use of a pulse train, not a

single picosecond pulse, the conditions would have to be much more strictly controlled to nullify the density change effect.

While these fundamental scattering processes were under study, more complicated interactions involving three and four photons had been discovered[206-211]. In 1965 Maker and Terhune[132] generated a frequency at $\omega + \Delta\omega$ from input frequencies of ω and $\omega - \Delta\omega$ by three wave mixing in a medium where $\Delta\omega$ was not a characteristic frequency and Bloembergen et al[206] showed that the process could iteratively produce a very large number of side bands. Carman et al[208] observed a degenerate four photon interaction which scattered light without change of frequency and Chaban[211] predicted a breakdown of the Fresnel reflection laws for a similar reason.

Another form of four photon interaction can be used to overcome a major inadequacy of all previous stimulated scattering investigations. This inadequacy lay in the fact that only the two optical waves in the scattering process were measured while the disturbance of the medium had to be inferred from them. If the medium is appropriately probed with an independent light source this disturbance can be directly measured at the same time as the incident and scattered beams. The first experiment of this type was performed by Giordmaine and Kaiser in 1966[212] who probed the effect of stimulated Raman scattering in calcite using a frequency doubled portion of the laser beam as the probe light. A related experiment was performed by Boersch and Eichler[213] who used an argon laser to probe variations of population inversion in a ruby. Experiments of this type can be viewed simply as Bragg reflection of the probe light from the periodic refractive index generated in the medium by the main scattering process. Bragg reflection of the light of an He-Ne laser by the phase grating generated in the stimulated Brillouin

process was observed in 1967 by Walder and Tang[214] and in 1968 by Winterling and Heinick[215] used a delayed probe at the fundamental frequency to directly measure phonon lifetimes in quartz at very low temperatures.

The extension of this technique to study in detail the properties of the disturbance involved in the various scattering processes is the main aim of the work reported in this thesis[249].

Comprehensive reviews concerned with stimulated scattering have been writen by Bloembergen[104], Fabelinskii[74] and others[131,132,168,216,223] and have also been given in conference proceedings[127-129].

C H A P T E R II

THEORETICAL ASPECTS OF THE INTERACTION OF LIGHT AND MATTER

2.1 QUANTUM PROCESSES

Fig.2.1 shows an energy level diagram indicating schematically the most important linear and non-linear interactions between electromagnetic radiation and matter[164]. Such a diagram is helpful in visualizing certain aspects of these processes, especially the involvement of the energy states of the medium, but of course contains no information concerning the phases of the waves involved.

In Rayleigh scattering it can be seen that there is no resultant effect on the medium and the photon frequency is unchanged. When the direction of the wave vector is also unchanged, the diagram corresponds to ordinary propagation.

The case of resonant scattering can be viewed as absorption of the photon followed by emission at unchanged frequency. The emission has random direction and phase so there is a loss from the forward beam. This process is closely related to fluorescence in which absorption, which excites a molecule to an energy band, is followed by a non-radiative transition before re-emission. Thus in fluorescence the emitted photon is lower in frequency than the absorbed one. When there is a long-lived state of lower energy than the absorption band, population inversion can build up between this state and the ground state resulting in laser action[32,33].

The Raman scattering (which may be taken to include Brillouin and Rayleigh wing scattering where the excited states correspond to phonons and molecular rotations respectively) involves, in the Stokes case, excitation from the ground state to a virtual level followed by emission

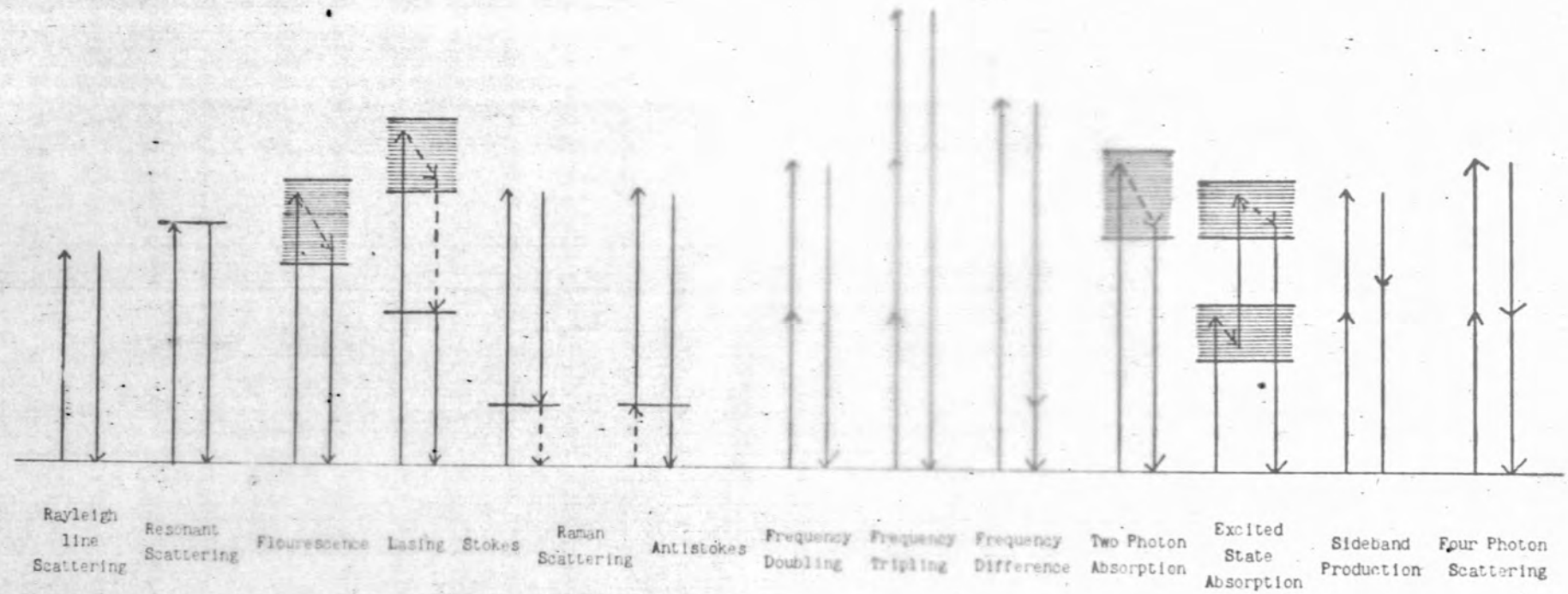

FIG. 2.1 Basic Quantum Processes in the Interaction of Light with Matter

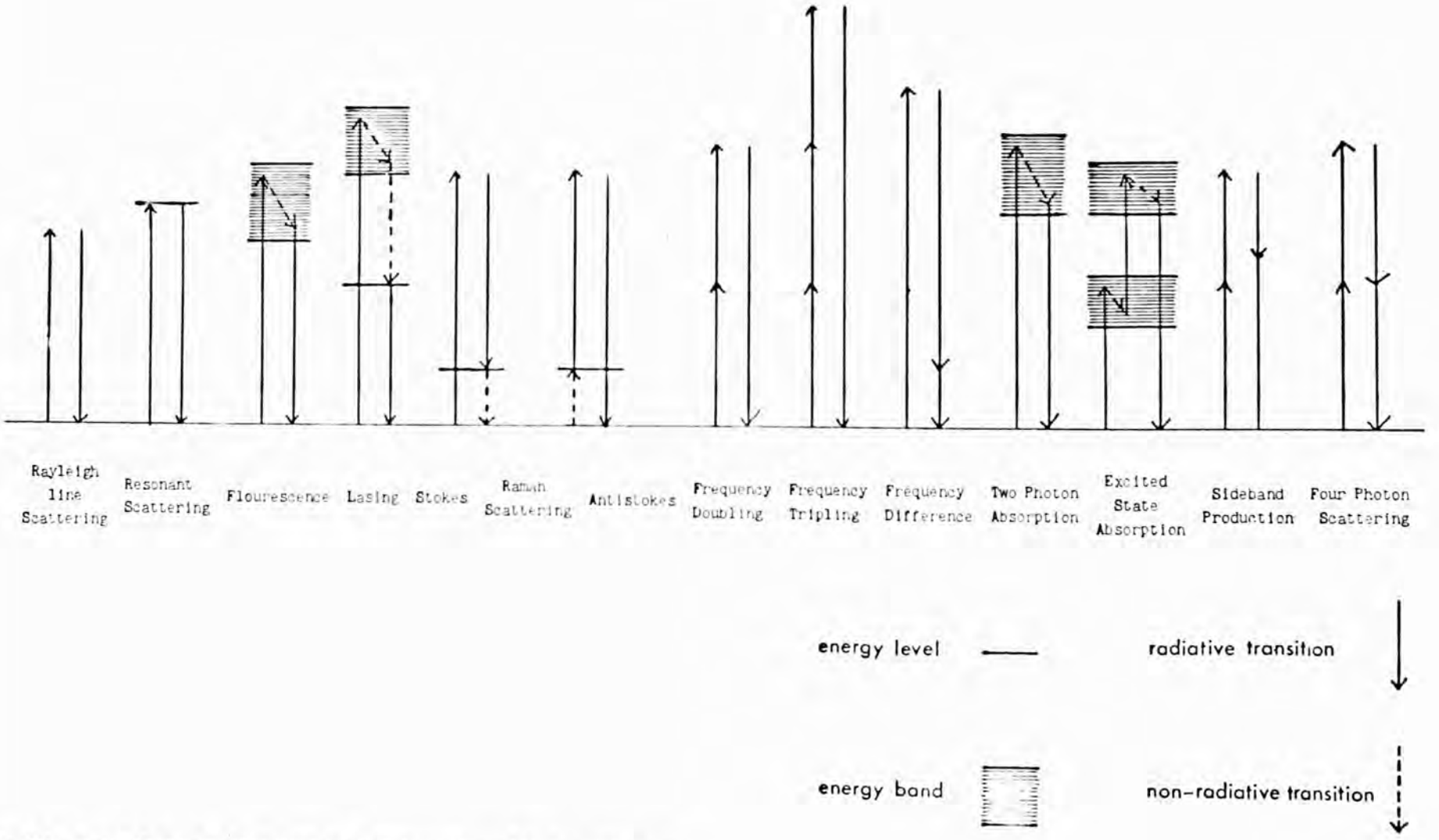

FIG. 2.1 Basic Quantum Processes in the Interaction of Light with Matter

on returning to a real excited state[11,12,110,126,164]. The related antistokes process can occur only for those molecules initially in the excited state and is therefore much weaker. Stimulated Raman scattering is represented by the same diagram but in this case the transition from the virtual to the real excited level is stimulated by the presence of radiation at that frequency in a manner analogous to laser action.

Harmonic and difference frequency generation is seen to be the result purely of the non-linear polarizability of the medium without involving its real energy states[124,164]. The same is true of the degenerate four photon interaction and sideband production represented in the diagram though in general these processes can involve real levels as intermediate or final stages[132,104,208].

Two photon absorption is similar to the single photon case except that the high intensities allow coupling of two photons via a virtual transition to achieve a real excited state[102,107,164]. The subsequent transitions and fluorescence are entirely analogous to linear flourescence. Excited state absorption on the other hand, proceeds by two successive excitations between real energy levels or bands[104-106]. The subsequent fluorescence is very similar to that from two photon absorption. Excited state absorption has been observed in bleachable dyes and can be distinguished from two photon absorption by the change of the dependence of fluorescent on incident intensity when the first excited state of the dye becomes saturated[108].

The intensity of two photon fluorescence is directly proportional to the square of the incident intensity for all accessible power levels[102]. The intensity of fluorescence due to excited state absorption can be derived by consideration of Fig.2.2[248].

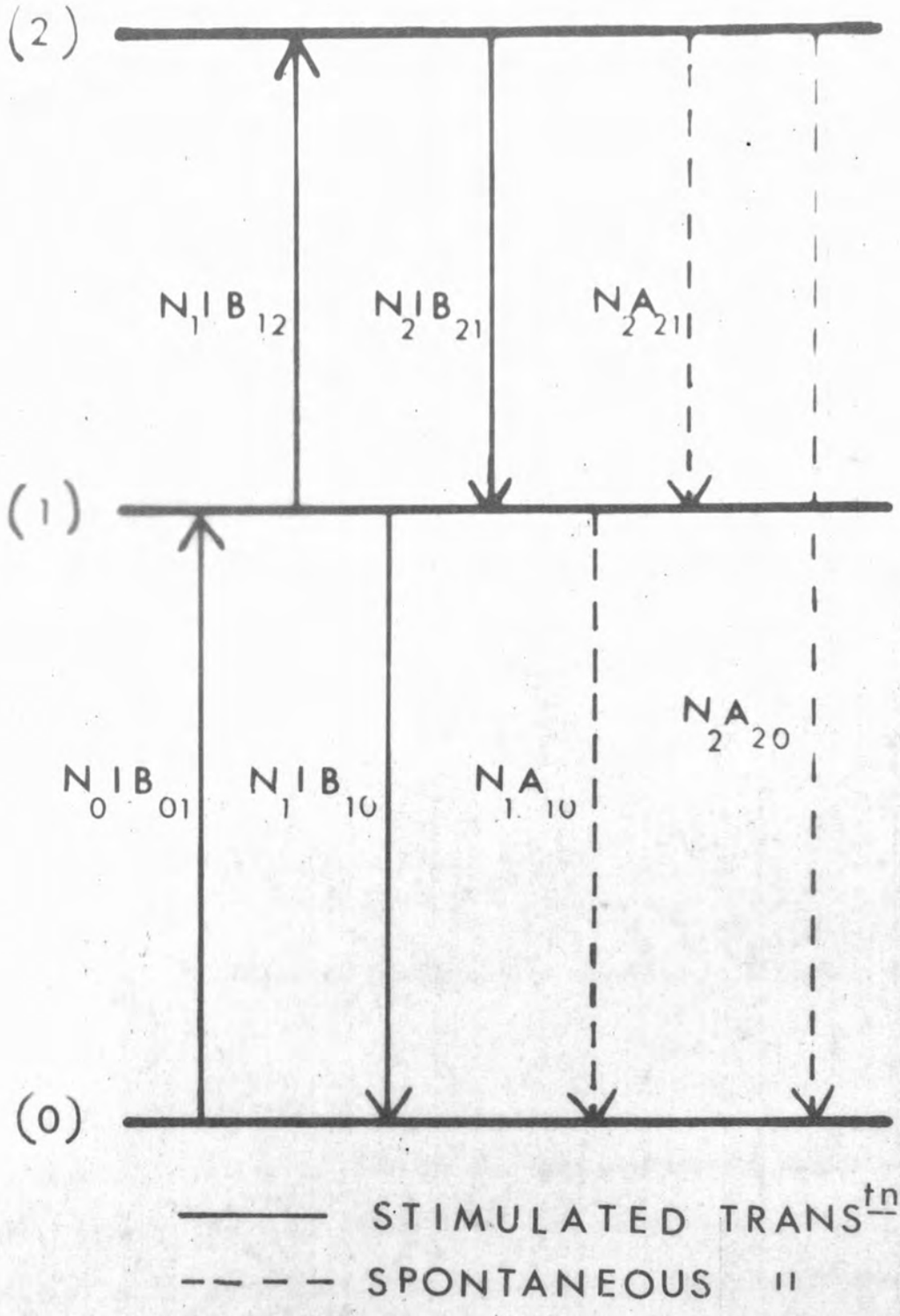

Fig.2.2
Transitions Occurring in the Molecules of a Saturable Absorber

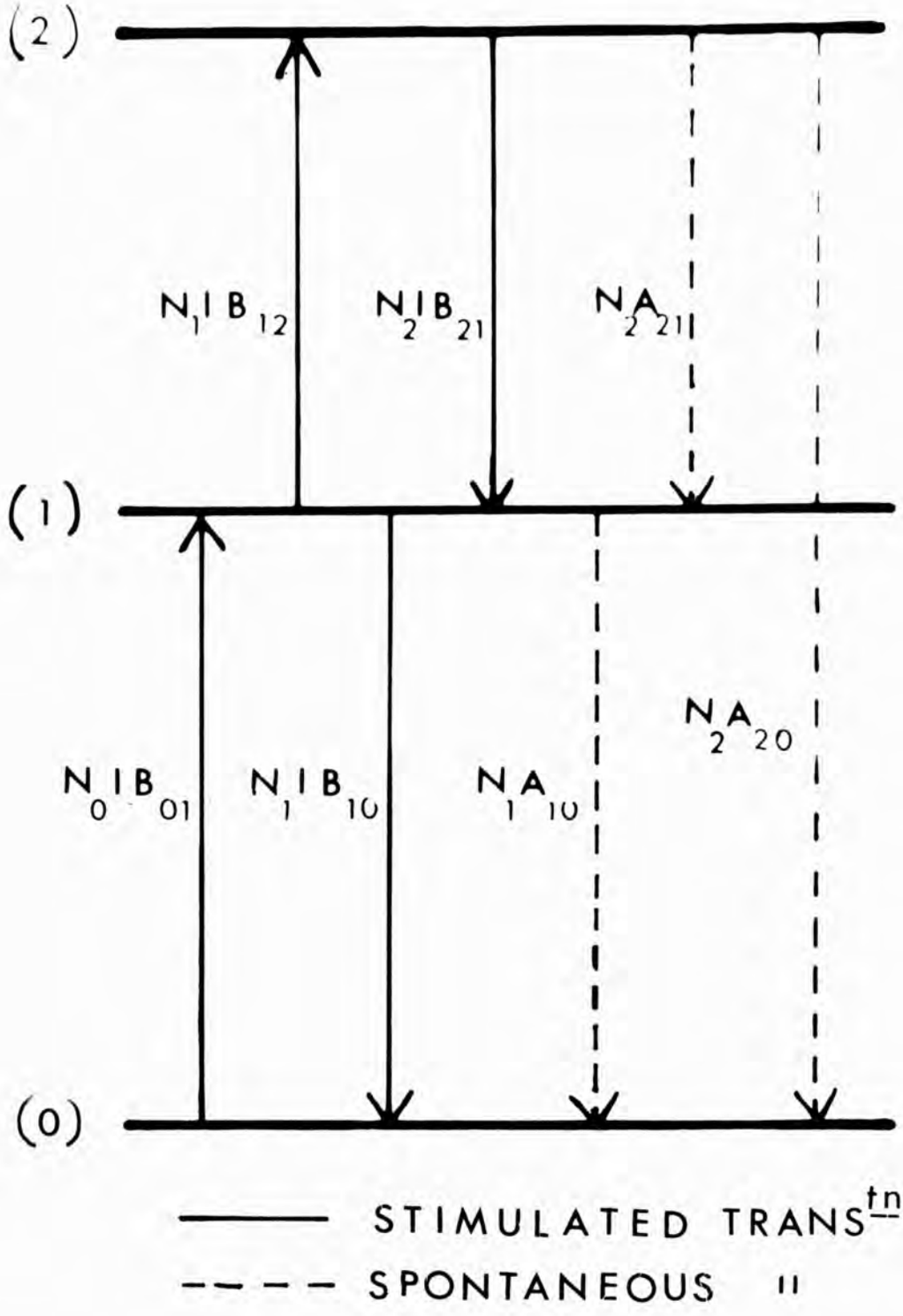
(2)
(1)
(0)
$N_1 I B_{12}$
$N_2 I B_{21}$
$N A_{21}$
$N_0 I B_{01}$
$N_1 I B_{10}$
$N A_{10}$
$N A_{20}$
STIMULATED TRANSTN
SPONTANEOUS "

At equilibrium the number of transitions per unit time ending in a particular state must equal the number starting from that state. Hence, considering the ground and second state:

$$N_0 B_{01} I = N_1 B_{10} I + N_1 B_{10} + N_2 A_{20}$$

$$N_1 B_{12} I = N_2 B_{21} I + N_2 A_{21} + N_2 A_{20}$$

but $B_{01} = B_{10}$ and $B_{12} = B_{21}$,

and $N = N_0 + N_1 + N_2$ therefore:

$$\frac{N_2}{N} = \frac{B_{01} B_{12} I^2}{B_{12} I (3B_{01} I + A_{10} + A_{20}) + (A_{21} + A_{20})(2B_{01} I + A_{10})} .$$

In real cases the first excited state has a much longer lifetime than the second so $A_{21} + A_{20} \gg A_{10}$, the dyes considered are bleachable so $B_{01} \gg B_{12}$ and the power levels attainable are much lower than those required to saturate the second excited state so $B_{21} + B_{20} \gg A_{12} I$.[104-106,224]

The expression thus becomes:

$$\frac{N_2}{N_1} = \frac{\frac{B_{01}}{A_{01}} \cdot \frac{B_{12}}{A_{21} + A_{20}} \cdot I^2}{1 + \frac{2B_{01} I}{A_{10}}}$$

or:

$$\frac{N_2}{N_1} \propto \frac{\frac{I^2}{I_c^2}}{1 + 2\frac{I}{I_c}}$$

Where $I_c = \frac{A_{10}}{B_{01}} \propto \frac{1}{\sigma_1 T_1}$ is the intensity required to saturate the first excited state.

2.2 SPONTANEOUS SCATTERING

It is instructive to consider the same processes from the classical point of view. The description of the spontaneous scattering is greatly simplified by the fact that in any fluid the fluctuations of pressure, entropy, anisotropy and molecular polarizability are statistically independent[7,9,74]. The spontaneous scattering can thus be considered as the sum of the scatterings caused separately by the fluctuations in

refractive index associated with each of the above fluctuations. These will be seen to result in the Brillouin doublet, the Rayleigh central line, the Rayleigh wing and the Raman scattering respectively.

The process of Brillouin scattering is the most easily understood. The pressure fluctuations in the medium may be Fourier analyzed as the sum of plane adiabatic sound waves propagating in the medium with all possible directions and frequencies[3,4,36,100]. We may now consider the effect of any one of these sound waves on a light wave traversing the medium. The plane wavefronts of the sound wave are associated with a modulation of refractive index, and thus reflect a small fraction of the light incident upon them. Only when the light reflected from consecutive wavefronts is in phase is there a significant resultant reflection[9,10]. The condition for this is identical to the Bragg condition for electron diffraction, i.e.:

$$\lambda_s = \frac{\lambda_L}{2n \sin \frac{1}{2}\theta} ,$$

As the sound wave 'mirror' is moving with a velocity v there will be a Doppler shift in frequency of:

$$\frac{\omega_B}{\omega_L} = \pm 2n\left(\frac{v}{c}\right)\sin\tfrac{1}{2}\theta$$

while the frequency of the sound wave involved is:

$$\omega_s = 4\pi\left(\frac{v}{\lambda_L}\right)\sin\tfrac{1}{2}\theta .$$

Thus it is seen that although the liquid contains sound of all frequencies and directions the light scattered in any direction is affected only by sound of one particular frequency and direction.

This analysis is for an ideal undamped sound wave. In general we must consider the variation of refractive index with density, the density fluctuations being determined by the acoustic wave equation:[93,139,225]

$$-\nabla^2\Delta\rho + \frac{1}{v^2}\frac{\partial^2\Delta\rho}{\partial t^2} - \frac{2\Gamma_B}{v^2}\frac{\partial\Delta\rho}{\partial t} = R$$

where the force term R is a random fluctuation containing all frequencies and wavelengths. For that Fourier component of R with frequency ω and wave vector k, $\Delta\rho$ is a wave with the same frequency and wave vector and an amplitude:

$$\left| \Delta\rho \right|^2_{(\omega,k)} \propto \frac{1}{\left(1 - \frac{\omega^2}{k^2 v^2}\right)^2 + \left(\frac{2\Gamma_B \omega}{k^2 v^2}\right)^2} .$$

The amplitude reflected from each wave is proportional to $\Delta\rho$ and when $k = 2k_L \sin\frac{\theta}{2} = \frac{\omega_B}{v}$ the amplitudes from each wave add in phase the resulting intensity being proportional to $|\Delta\rho|^2$. The light reflected from such a fluctuation is changed in frequency by an amount ω so the spectrum of the scattered light is given by[93,95,220].

$$I \propto \frac{1}{\left(1 + \frac{\Delta\omega^2}{\omega_B^2}\right)^2 + \left(\frac{2\Gamma_B \Delta\omega}{\omega_B^2}\right)^2}$$

Transverse waves can occur in solids (and also in liquids as can be seen when the relaxation of shear viscosity is taken into account)[86,87]. There is no change of density associated with these shear waves but in anisotropic media, and liquids with isotropic molecules, there is a change in polarizability as the principle polarization directions undergo rotation. There is thus a depolarized scattering with a spectrum similar to that of the Brillouin scattering but usually with smaller velocity and greater damping. Thus ω_B is smaller and Γ_B larger. In contrast to the sharp Brillouin lines a rather diffuse doublet occurs which is hard to distinguish from the depolarised Rayleigh wing[86,87].

This wing may be sub-divided into two portions. There is a contribution due to rotational Brownian motion and another as a result of their angular oscillation in the local fields of neighbouring molecules[80]. The fluctuations of anisotropy can be analysed as a randomly driven

rotation or oscillation with viscous damping. The solution of the damped resonance equation gives the frequency dependence of the molecular motion and hence of the resultant depolarized scattering. The resulting equations:[80]

$$I \propto \frac{1}{\left(1 - \frac{I\,\Delta\omega^2}{4\,kT}\right)^2 + \Delta\,\omega^2 \left(\frac{\xi}{6kT}\right)^2} \quad \text{for Brownian rotation}$$

and

$$I \propto \frac{1}{\left(1 - \frac{I\Delta\,\omega^2}{\mu}\right)^2 + \Delta\omega^2 \left(\frac{\xi}{\mu}\right)^2} \quad \text{for oscillation ,}$$

are of the same form as those for the Brillouin scattering. However, molecular rotations and oscillations are heavily damped because $\xi \gg I$ a and the maximum scattering occurs at $\Delta\omega = 0$.

While the main scattering processes arise from the fluctuation of independent parameters the shear wave, molecular rotation and molecular oscillation scattering all involve variation of the orientation of anisotropic molecules. They are thus not truly independent effects which can be simply added but they are nevertheless distinguishable by the different frequency dependence of their contributions to the depolarized wing. The shear waves give a diffuse doublet of very small frequency shift while the Brownian rotation gives a broad central peak. The faster molecular oscillations give even greater frequency shifts and are responsible for the remotest part of the wing[74].

The thermal or entropy fluctuations responsible for the central Rayleigh line decay but do not propagate[7,69,74,191]. (They do in fact tend to propagate if the second sound correction is introduced into the heat conductivity equation[98,99,226].) The half width of the frequency spread induced in the light scattering is the inverse of the lifetime of the waves of suitable length to give Bragg reflection and is given by:

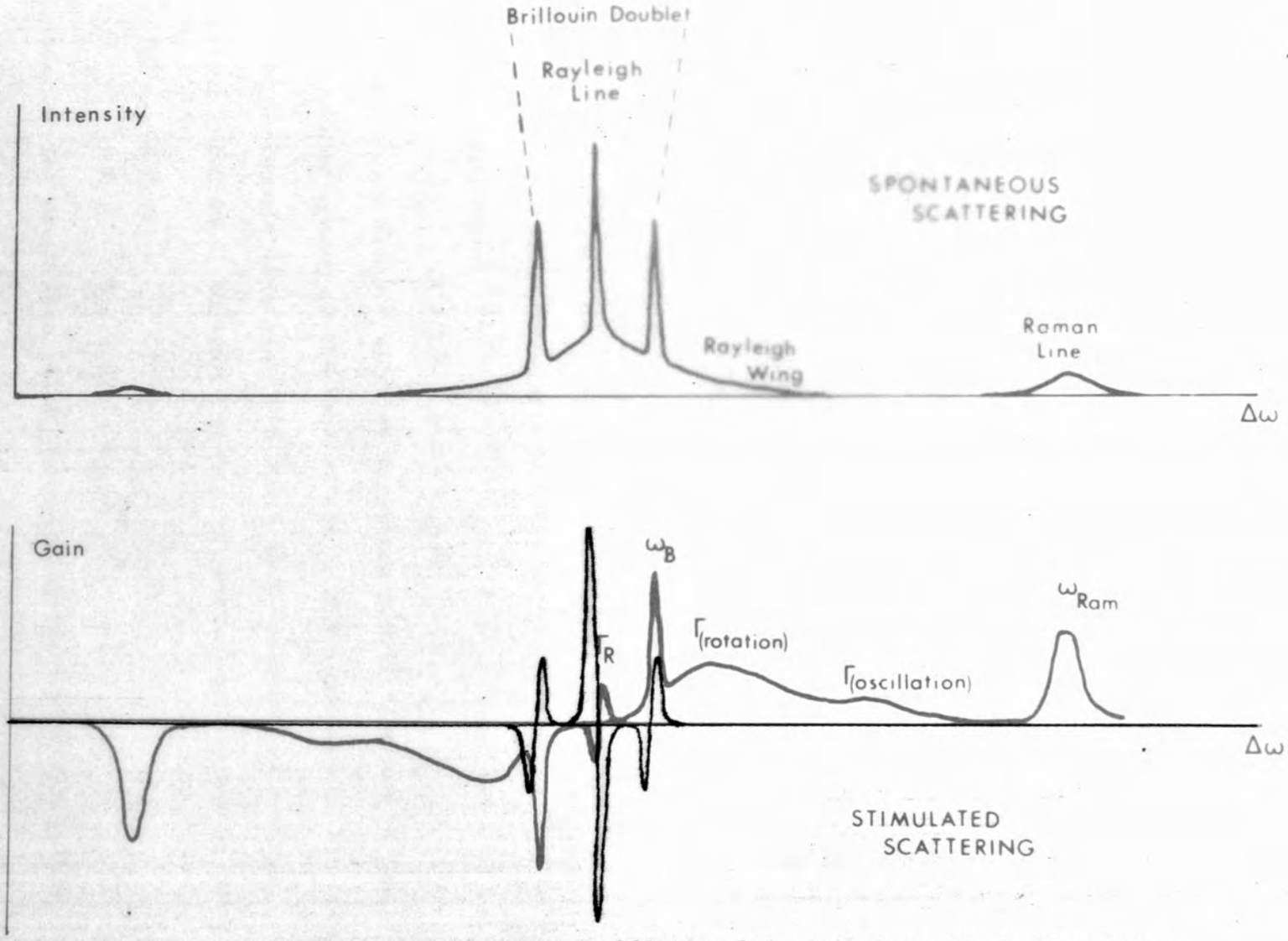

Fig. 2.3
Scattering Spectra

Additional Contribution due to Absorption

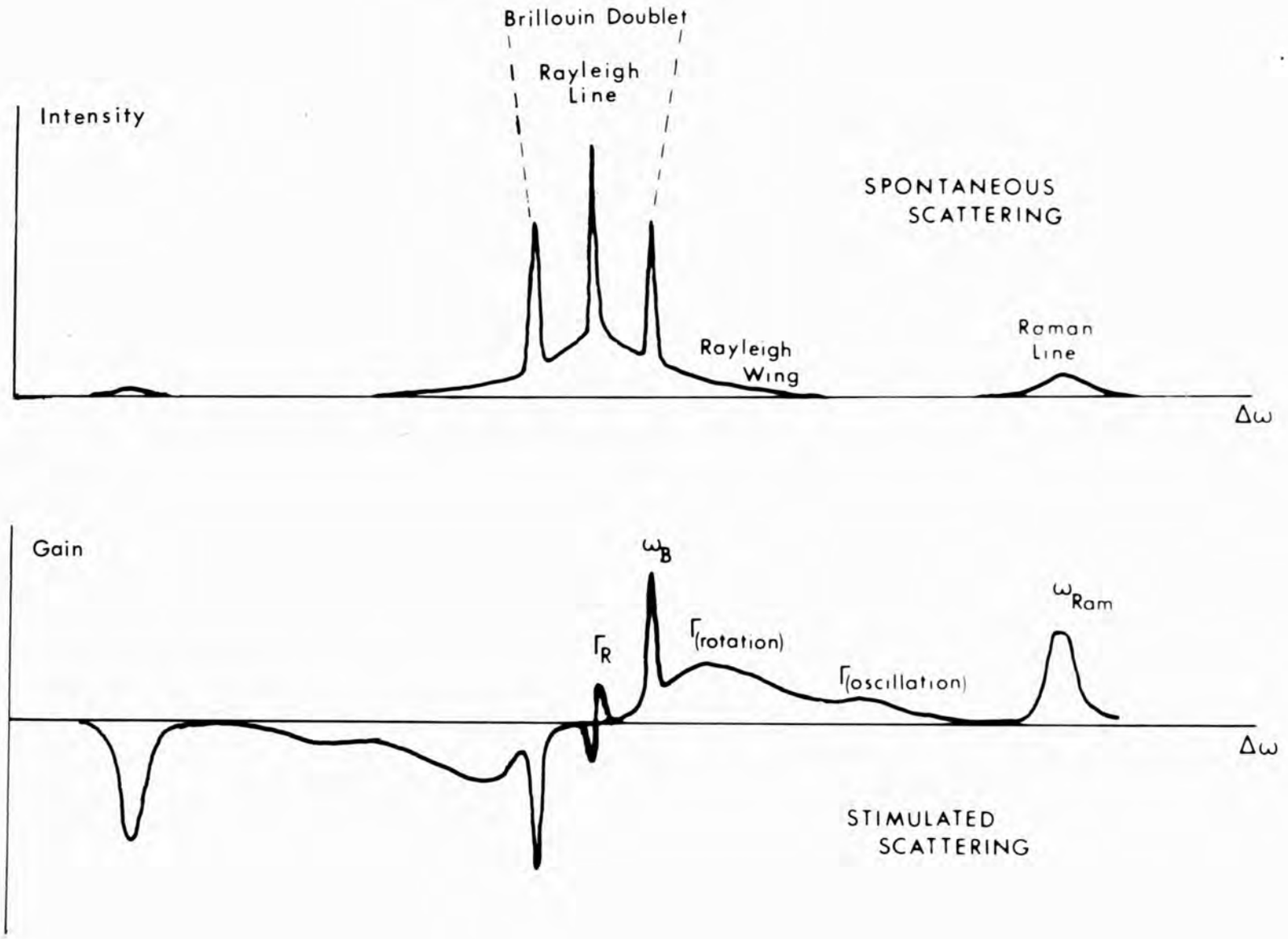
Brillouin Doublet
Rayleigh Line
Intensity
SPONTANEOUS SCATTERING
Rayleigh Wing
Raman Line
Δω
Gain
ωB
ωRam
ΓR
Γ(rotation)
Γ(oscillation)
Δω
STIMULATED SCATTERING

$$\Gamma_R = k^2 D = 4 n^2 D k_L^2 \sin^2 \frac{\theta}{2} .$$

The spectrum of the scattered light is:[74,93,95]

$$I \propto \frac{1}{1 - \frac{\Delta\omega^2}{\Gamma_R^2}} .$$

The frequency dependence of the Raman scattering is dependent on the line shape of the states to be excited. This cannot be derived on a classic basis but is usually well represented by a Lorentzian so the scattered spectrum is represented by:

$$I \propto \frac{1}{\left(1 - \frac{\Delta\omega^2}{\omega_{Ram}^2}\right)^2 + \left(\frac{2\Gamma_{Ram}\Delta\omega}{\omega_{Ram}}\right)^2}$$

The sum of the light scattered by all these mechanisms gives the spontaneous scattering spectrum (upper curve of Fig.2.3).

2.3 NON-LINEAR OPTICS

When very high electric fields are applied to matter the usual linear polarization law breaks down and has to be replaced by the more complicated expression:[110,124,217-219]

$$P = \chi E + \chi_1 E^2 + \chi_2 E^3 \ldots .$$

This is well known for D.C. and low frequency A.C. fields and is the cause of such phenomena as the Kerr effect. The inclusion of the non-linear terms in Maxwell's equations makes them incapable of general analytical solution. However a number of conclusions are easily derived.

We may define:

$$P = P_L(E) + P_{NL}(E^2, E^3, \ldots)$$

and consider the properties of P_{NL} . Taking the lowest order term:

$$P_{NL} = \chi_1 E^2 .$$

Let us consider the case:

$$E = A_1 \cos(k_1 x - \omega_1 t) + A_2 \cos(k_2 x - \omega_2 t)$$

Then

$$P_{NL} = \chi_1 \left[\tfrac{1}{2}(A_1^2 + A_2^2) \right] + \chi_1 \left[\tfrac{1}{2}(A_1^2 \cos(2k_1 x - 2\omega_1 t) + \tfrac{1}{2} A_2^2 \cos(2k_2 x - 2\omega_2 t) \right]$$
$$+ \chi_1 \left[A_1 A_2 \cos\left((k_1 + k_2)x - (\omega_1 + \omega_2)t\right) \right] + \chi_1 \left[A_1 A_2 \cos\left((k_1 - k_2)x - (\omega_1 - \omega_2)t\right) \right] .$$

The non-linear polarization has a D.C. component, components at double each incident frequency and components at the sum and difference frequencies. In general χ_1 may be frequency dependent and which term is most significant depends on the conditions of the experiment.

Each component of polarization of the medium emits light at its own frequency. The velocity of the light emitted in this way is determined by the linear refractive index of the medium which is a function of frequency. In general, for this reason, after a certain distance the light of new frequency being produced gets out of phase with that produced earlier in the medium and interferes destructively with it, limiting the resulting flux obtainable[110,112,124,218]. When the velocity at the new frequency is the same as that at the original frequency a very much greater conversion occurs. This situation is known as phase matching and can sometimes be achieved in anisotropic crystals when the dispersion of velocity with frequency can be compensated, in a particular direction, by the velocity variation due to birefrigence.

In centrosymmetric media in general and fluids in particular there can be no term proportional to E^2 in the polarization as this would lead to a different value of polarization according to the direction of the field[110,124,132,218]. For such media let us consider the effect of the next term :

$$P_{NL} = \chi_2 E^3 ,$$

when $E = A_1 \cos(k_1 x - \omega_1 t) + A_2 \cos(k_2 x - \omega_2 t) + A_3 \cos(k_3 x - \omega_3 t)$. Then :

$$P_{NL} = \frac{3}{4}\chi_2\Big[(A_1^2 + 2A_2^2 + 2A_3^2)A_1\cos(k_1x - \omega_1 t) + (A_2^2 + 2A_3^2 + 2A_1^2)A_2\cos(k_2x - \omega_2 t) + (A_3^2 + 2A_1^2 + 2A_2^2)A_3^2\cos(k_3x - \omega_3 t)\Big]$$

$$+ \frac{1}{4}\chi_2\Big[A_1^3\cos(3k_1x - 3\omega_1 t) + A_2^3\cos(3k_2x - 3\omega_2 t) + A_3^3\cos(3k_3x - 3\omega_3 t)\Big]$$

$$+ \frac{3}{4}\chi_2\Big[A_1A_2^2\cos\Big((2k_2 + k_1)x - (2\omega_2 + \omega_1)t\Big) + A_2A_1^2\cos\Big((2k_1 + k_2)x - (2\omega_1 + \omega_2)t\Big)$$

$$+ A_1A_2^2\cos\Big((2k_2 - k_1)x - (2\omega_2 - \omega_1)t\Big) + A_2A_1^2\cos\Big((2k_1 - k_2)x - (2\omega_1 - \omega_2)t\Big)$$

$$+ \text{similar terms in } E_1E_3 \text{ and } E_2E_3\Big]$$

$$+ \frac{3}{2}\chi_2\Big[A_1A_2A_3\cos\Big((k_1 + k_2 + k_3)x - (\omega_1 + \omega_2 + \omega_3)t\Big) + A_1A_2A_3\cos\Big((-k_1 + k_2 + k_3)x - (-\omega_1 + \omega_2 + \omega_3)t\Big)$$

$$+ A_1A_2A_3\cos\Big((k_1 - k_2 + k_3)x - (\omega_1 - \omega_2 + \omega_3)t\Big)$$

$$+ A_1A_2A_3\cos\Big((k_1 + k_2 - k_3)x - (\omega_1 + \omega_2 - \omega_3)t\Big)\Big]$$

The first group of terms in this expression are at the original frequency and correspond to a change in the polarizability and therefore of the refractive index of the medium. The most important result of these terms is that at sufficiently high intensities the increase in refractive index in the more intense parts of the beam acts as a lens concentrating the light into a number of narrow filaments in which it remains trapped[133-142]. It is interesting to note that since the change in refractive index for the wave of frequency ω_1 is proportional to:

$$A_1^2 + 2A_2^2 + 2A_3^2$$

and that for ω_2 to:

$$A_2^2 + 2A_3^2 + 2A_1^2 \ ,$$

if $A_1^2 \gg A_2^2$, A_3^2 the change at ω_2 is twice that at ω_1. Thus the weaker wave experiences a greater refractive index change than the stronger (this is known as weak wave retardation)[208].

The second group of terms simply represents third harmonic generation[111] which occurs for each wave independently of the others.

The third group can be sub-divided into those terms involving sum frequencies of the type $(2\omega_2 + \omega_1)$ and those with difference frequencies like $(2\omega_2 - \omega_1)$. The second type are of particular interest as may be seen by considering the case $\omega_1 = \omega_L$ and $\omega_2 = \omega_L + \Delta$. The difference terms in ω_1 and ω_2 are then $\omega_L + 2\Delta$ and $\omega_L - \Delta$. This shows that when two slightly different frequencies are present in the medium side-band frequencies are produced which can of course themselves interact with ω_L to produce a large number of further bands[132,206].

The last group of terms consists of those involving ω_1 , ω_2 and ω_3. The sum frequency is produced and also each frequency can be changed by the difference between the other two so if two are close together side-

bands can be produced in the third.

For efficient generation at any of these frequencies phase matching must be achieved. The condition for this is that for the new wave with frequency ω_4 and wave vector k_4 :

$$\omega_4 = \pm \omega_i \pm \omega_j \pm \omega_k \ ,$$

and

$$k_4 = \pm k_i \pm k_j \pm k_k \ .$$

As we are dealing with centrosymmetric media this cannot be achieved in the same way as for the second order non-linear processes. In the side band prodution however the frequency shifts can be very small and the dispersion and phase mismatch may therefore be negligible, allowing efficient generation in this case[206,208].

2.4 STIMULATED SCATTERING

The above analysis has throughout considered P_{NL} as exactly determined by the instantaneous value of the field and χ_2 as a fixed quantity independent of time. In real media χ_2 is determined by the variation of other parameters on which the refractive index depends. In particular there are changes in density due to electrostriction, changes in temperature due to absorption, changes in anisotropy due to realignment of molecules and changes of molecular polarizability due to the non-linear response of the molecules themselves[74,131,132,164,168]. It will be shown that the inertia and damping involved in changing these parameters give rise to stimulated scattering processes associated with each of the spontaneous scatterings discussed earlier[74,168,196].

The changes in the parameters of the medium mentioned are all, at equilibrium, proportional to the square of the electric field[191]. Considering the field due to two waves travelling in opposition directions, let:

$$E = A_1 \cos(k_1 x - \omega_1 t) + A_2 \cos(- k_2 x - \omega t) \ .$$

(This expression is quite general without phase terms since the origins of x and t are arbitrary.) Then:

$$E^2 = \tfrac{1}{2}(A_1^2 + A_2^2) + \tfrac{1}{2}A_1^2\cos(2k_1x - 2\omega_1 t) + \tfrac{1}{2}A_2^2\cos(2k_2x - 2\omega_2 t) + A_1A_2\cos\Big((k_1 - k_2)x - (\omega_1 + \omega_2)t\Big) + A_1A_2\cos\Big((k_1 + k_2)x - (\omega_1 - \omega_2)t\Big).$$

As will be demonstrated when specific effects are considered only the term $A_1A_2\cos((k_1 + k_2)x - (\omega_1 - \omega_2)t)$ is of sufficiently low frequency to significantly affect the parameters of the medium. The equations governing these parameters will be shown to imply that the steady state response to this wave is a wave of the same frequency and wave number but with a phase that may be different.

The resulting dielectric constant change may therefore be expressed as:

$$\Delta\varepsilon = \Delta\varepsilon' \cos\Big((k_1 + k_2)x - (\omega_1 - \omega_2)t\Big) + \Delta\varepsilon'' \sin\Big((k_1 + k_2)x - (\omega_1 - \omega_2)t\Big).$$

Maxwell's wave equation, including non-linear terms, may be written in the form[110,124,139,164]:

$$-\frac{\partial^2 E}{\partial x^2} + \frac{n^2}{c^2}\frac{\partial^2 E}{\partial t^2} = -\frac{1}{c^2}\frac{\partial^2 \Delta\varepsilon \cdot E}{\partial t^2}$$

Substituting the above expressions for E and $\Delta\varepsilon$ and equating coefficients of the terms on each side of the equation with the same dependence on x and t gives the expressions:

$$\frac{\partial A_1}{\partial x} = \frac{\Delta\varepsilon'' k_1}{4n^2} \cdot A_2 ,$$

$$\frac{\partial A_2}{\partial x} = \frac{\Delta\varepsilon'' k_2}{4n^2} \cdot A_1 .$$

Thus A_1 experiences a gain and A_2 a loss or vice versa according to the value of $\Delta\varepsilon''$. (Negative $\Delta\varepsilon''$ implies gain for A_2 as it is a backward going beam.)

We may now consider the effect of the electric field on specific parameters of the medium and find under what circumstances there is a significant gain in A_2 (taking A_1 as the amplitude of the laser field). Under these circumstances stimulated scattering due to amplification of any spontaneous scattering at the frequency ω_2 can take place.

Temperature and density variations within the medium under the influence of the electric field are governed by the equations[93,196,225]

$$\frac{\partial^2 \Delta\rho}{\partial t^2} - \frac{v^2}{c_p/c_v}\frac{\partial^2 \Delta\rho}{\partial x^2} - \frac{\eta}{\rho_o}\frac{\partial}{\partial t}\frac{\partial^2 \Delta\rho}{\partial x^2} - \frac{v^2}{c_p/c_v}\beta\rho_o\frac{\partial \Delta T}{\partial x^2} = -\frac{\gamma}{8\pi}\frac{\partial^2 E^2}{\partial x^2}$$

$$\rho_o c_v \frac{\partial \Delta T}{\partial t} - K\frac{\partial^2 \Delta T}{\partial x^2} - \frac{c_p - c_v}{\beta}\frac{\partial \Delta\rho}{\partial t} = \frac{1}{4\pi} n c \alpha E^2 .$$

These are linear differential equations so solutions can be found separately for each component of E^2. For any component

$$E^2 = A\cos(kx - \omega t) ,$$

there are solutions:

$$\Delta\rho = \Delta\rho'\cos(kx - \omega t) + \Delta\rho''\sin(kx - \omega t)$$

and

$$\Delta T = \Delta T'\cos(kx - \omega t) + \Delta T''\sin(kx - \omega t).$$

Now the change in refractive index due to the effect of temperature on molecular polarizability is negligible compared to the change due to the effect of temperature on density[196] so we need only calculate $\Delta\rho''$ to find the value of $\Delta\varepsilon''$ resulting from both the absorptive and electrostrictive mechanisms. Solution of the above equations gives:

$$\Delta\rho'' = Am \cdot \frac{1}{\Gamma^2} \cdot \frac{\Omega_3\left(1 - \frac{\omega^2}{\Omega_1^2}\right) - \Gamma\left(\frac{1}{\Omega_2^2} - \frac{1}{\Omega_1^2}\right)\omega^2}{\left(1 - \frac{\omega^2}{\Omega_2^2}\right)^2 + \frac{\omega^2}{\Gamma^2}\left(1 - \frac{\omega^2}{\Omega_1^2}\right)^2} \cdot \omega$$

and

$$\left|\Delta\rho\right|^2 = A^2 m^2 \cdot \frac{1}{\Gamma^2} \cdot \frac{(\Omega_3 - \Gamma)^2 + \omega^2}{\left(1 - \frac{\omega^2}{\Omega_2^2}\right)^2 + \frac{\omega^2}{\Gamma^2}\left(1 - \frac{\omega^2}{\Omega_1^2}\right)^2} .$$

In order to simplify these expressions we make use of the fact that $\Gamma \ll \Omega_2 \ll \Omega_1 = kv$. The expressions above thus have resonant maxima in the region $|\omega| \lesssim \Omega_1$ and are negligible outside this region. We need therefore consider only those components of E^2 in which $\frac{\omega}{k} \lesssim v$. The only term for which this can be true is the one for which $A = A_1 A_2$, $\omega = \omega_1 - \omega_2 = \Delta\omega$, $k = k_1 + k_2 \sim 2k_1$. We may now evaluate $|\Delta\rho|^2$ and ρ'' in the regions of their maxima.

When $\alpha = 0$ the expressions are negligible except at $\omega \sim \pm \Omega_1$. Then:

$$\Delta\rho'' = -\frac{\gamma}{8\pi v^2} \cdot \frac{\frac{2\Gamma_B \omega}{\omega_B^2}}{\left(1 - \frac{\omega^2}{\omega_B^2}\right)^2 + \left(\frac{2\Gamma_B \omega}{\omega_B^2}\right)^2} A_1 A_2 ,$$

and

$$|\Delta\rho|^2 = \left(\frac{\gamma}{8\pi v^2}\right)^2 \cdot \frac{1}{\left(1 + \frac{\omega^2}{\omega_B^2}\right)^2 + \left(\frac{2\Gamma_B \omega}{\omega_B^2}\right)^2} A_1^2 A_2^2 ,$$

where

$$\omega_B = kv \quad \text{and} \quad \Gamma_B = \frac{\eta k^2}{2\rho} .$$

But

$$\Delta\varepsilon = \frac{\gamma}{\rho_0} \Delta\rho ,$$

therefore:

$$\frac{1}{A_2} \frac{\partial A_2}{\partial x} = -\frac{\gamma^2 k_2}{32\pi n^2 v^2 \rho_0} \cdot \frac{\frac{2\Gamma_B \omega}{\omega_B^2}}{\left(1 - \frac{\omega^2}{\omega_B^2}\right)^2 + \left(\frac{2\Gamma_B \omega}{\omega_B^2}\right)^2} A_1^2 .$$

This Stokes ($\omega_1 > \omega_2$ implies $\omega > 0$) gain in the backward goin wave, proportional to the intensity of the forward going one is the cause of the Stimulated Brillouin Scattering.

When $\alpha \neq 0$ the values of $|\Delta\rho|$ and ρ'' are significant in two regions:

THE REGION $\omega \sim 0$

where:

$$\Delta\rho'' = \frac{n\, c\, \alpha\, \beta\, \rho_0}{4\pi k^2 K} \quad \frac{\frac{\omega}{\Gamma_R}}{1 + \left(\frac{\omega}{\Gamma_R}\right)^2} \quad A_1 A_2 ,$$

and

$$|\Delta\rho|^2 = \left(\frac{n\, c\, \alpha\, \beta \rho_0}{4\pi k^2 K}\right)^2 \quad \frac{1}{1 + \left(\frac{\omega}{\Gamma_R}\right)^2} \quad A_1^2 A_2^2 ,$$

therefore

$$\frac{1}{A_2} \frac{\partial A_2}{\partial x} = \frac{c\, \alpha\, \beta\, \gamma\, k_2}{16\, \pi\, k^2\, K n} \quad \cdot \frac{\frac{\omega}{\Gamma_R}}{1 + \left(\frac{\omega}{\Gamma_R}\right)^2} A_1^2 ,$$

where $\Gamma_R = \frac{K k^2}{\rho_0 c_p}$.

These expressions describe the antistokes shifted stimulated thermal Rayleigh scattering.

THE REGION $\omega \sim \Omega_1$

In this region there is the stimulated Brillouin term which is the same as in the case for $\alpha = 0$ plus another term dependent on α. This gives:

$$\Delta\rho'' = \frac{nc\, \alpha\, \beta}{4\pi c_p k v} \quad \frac{\frac{\omega}{\omega_B}\left(1 - \frac{\omega^2}{\omega_B^2}\right)}{\left(1 - \frac{\omega^2}{\omega_B^2}\right)^2 + \left(\frac{2\, \Gamma_B \omega}{\omega_B^2}\right)^2} \quad A_1 A_2 ,$$

$$|\Delta\rho| = \left(\frac{nc\, \alpha\, \beta}{4\pi c_p\, kv}\right)^2 \quad \frac{1}{\left(1 - \frac{\omega^2}{\omega_B^2}\right)^2 + \left(\frac{2\, \Gamma_B \omega}{\omega_B^2}\right)^2} A_1 A_2 ,$$

and:

$$\frac{1}{A_2} \frac{\partial A_2}{\partial x} = \frac{c\, \alpha \beta \gamma\, k_2}{16\pi c_p\, kv\, n} \cdot \frac{\frac{\omega}{\omega_B}\left(1 - \frac{\omega^2}{\omega_B^2}\right)}{\left(1 - \frac{\omega^2}{\omega_B^2}\right)^2 + \left(\frac{2\, \Gamma_B \omega}{\omega_B^2}\right)^2} A_1^2 .$$

This describes the stimulated thermal Brillouin scattering or, more strictly the thermal modification of the stimulated Brillouin scattering.

The parameters responsible for the Rayleigh wing and Raman scattering are governed by rather different equations from those concerned with

temperature and density. The molecular rotations oscillations and vibrations responsible for these processes occur more or less independently for each molecule and the associated change in refractive index is therefore governed by an equation of the form:[212]

$$\frac{\partial^2 \Delta\varepsilon}{\partial t^2} + \frac{2\,\Gamma \partial \Delta\,\varepsilon}{\partial t} + \Omega^2 \Delta\varepsilon = \Omega^2\, k\, E^2 \quad .$$

Hence

$$\Delta\varepsilon'' = - K \frac{\dfrac{2\,\Gamma\omega}{\Omega^2}}{\left(1 - \dfrac{\omega^2}{\Omega^2}\right)^2 + \left(\dfrac{2\,\Gamma\omega}{\Omega^2}\right)^2} A_1 A_2 \ ,$$

$$\left|\Delta\varepsilon\right|^2 = K^2 \ \frac{1}{\left(1 - \dfrac{\omega^2}{\Omega^2}\right)^2 + \left(\dfrac{2\,\Gamma\omega}{\Omega^2}\right)^2} \ A_1^2 A_2^2 \ ,$$

$$\frac{1}{A_2}\frac{\partial A_2}{\partial x} = - \frac{K\, k_2}{4\, n^2} \cdot \frac{\dfrac{2\,\Gamma\omega}{\Omega^2}}{\left(1 - \dfrac{\omega^2}{\Omega^2}\right)^2 + \left(\dfrac{2\,\Gamma\omega}{\Omega^2}\right)^2} \cdot A_1^2 \quad .$$

Indicating a Stokes gain for these processes..

For stimulated Raman scattering Ω and Γ are the frequency and linewidth of the excited state, while K is proportional to that part of the Kerr coefficient due to the nonlinear polarizability for which the vibration at frequency Ω is responsible. The total high frequency Kerr coefficient at a frequency ω_K is equal to the sum of those parts involved in all the Raman transitions for which $\Omega > \omega_K$. In general $\Omega \gg \Gamma$ and a sharp maximum in the gain curve is observed[11-13,156].

For Rayleigh wing scattering:

$$\left.\begin{aligned} \Omega^2 &= \frac{4kT}{I} \\ \Gamma &= \frac{\xi}{3I} \end{aligned}\right\} \text{ for the rotational mechanism}$$

$$\left.\begin{aligned} \Omega^2 &= \frac{\mu}{I} \\ \Gamma &= \frac{\xi}{2I} \end{aligned}\right\} \text{ for the oscillatory mechanism.}$$

while K is proportional to that part of the Kerr coefficient due to molecular reorientation[80,188]. For media with highly anisotropic molecules this is approximately equal the total low frequency Kerr coefficient. The stimulated Rayleigh wing gain curve, like the spontaneous scattering is controlled by the rotational mechanism in the region $|\omega| \lesssim \frac{6kT}{\xi}$ and by the oscillatory mechanism[80,188] when $|\omega| \gtrsim \frac{\mu}{\xi}$. Since in both cases $\Gamma \gg \Omega$ the two mechanisms lead to two diffuse maxima in the gain curve, these being at $\omega = \frac{6kT}{\xi}$ and $\omega = \frac{\mu}{\xi}$ respectively.

The overall curve of gain against frequency shift (the lower curve of Fig.2.3) represents the sum of the gains discussed in this section[168].

2.5 PROBE SCATTERING

The stimulated scattering described in the previous section is the result of the action of an induced refractive index wave on the electromagnetic waves producing it. This refractive index variation will also affect any independent light beam traversing the medium[241,246,249]. The refractive index variation acts as a phase grating in its effect on the probe light. From each layer of the grating (one wavelength of the refractive index wave) a small portion of the probe light is reflected. When the angle of incidence is such that the reflected portions from adjacent layers add in phase a maximum overall reflectivity is reached.

The condition for this is the Bragg condition:

$$\theta_{max} = \cos^{-1} p \frac{\lambda_a}{\lambda_r} \cdot \frac{n_r}{n_a} ,$$

where p is any integer. We need only consider $p = 1$ because in the experimental case where λ_r is the wavelength of ruby laser light (6943 Å) and λ_a is that of argon laser light (4880 Å) the only values of p giving real values of θ are unity and the trivial solution zero.

The reflectivity of a length L of phase grating for light incident at any angle θ is given by:

$$\frac{I_R}{I_I} = \left(\frac{2\ k_r\ n_r\ \Delta\ n_a\ L}{8\ \cos^2\ \theta\ n_a}\right)^2 \left(\frac{\sin(k_a\ n_a\ \cos\theta - k_r\ n_r)L}{(k_a\ n_a\ \cos\theta - k_r\ n_r)L}\right)^2 ,$$

[see Appendix of reference 249 enclosed with this thesis]

where Δn_a is the difference between the maximum and minimum refractive index for the probe light.

When $\theta = \theta_{max}$:

$$\left(\frac{I_R}{I_I}\right)_{max} = \left(\frac{\pi N \delta}{2\ \cos^2\ \theta_{max}}\right)^2$$

where:

$N = \frac{2n_r L}{\lambda_r}$ = The number of wavelengths of the refractive index modulation within the interaction region.

and:

$$\delta = \frac{\Delta n_a}{2n_a} .$$

The an ular width at half reflectivity is:

$$\delta\theta = \frac{4 \times 1{\cdot}39}{\pi N \tan\theta_{max}} .$$

Now Δn_a has been defined as the difference between maximum and minimum refractive index, i.e. twice the amplitude of the refractive index modulation whereas $|\Delta\varepsilon|$ was defined in the previous section as the amplitude of the dielectric constant variation. Thus :

$$\Delta n_a = \frac{|\Delta\varepsilon|}{n_a} ,$$

and

$$\delta = \frac{|\Delta\varepsilon|}{2n_a^2} = \frac{\gamma}{2\ \rho_o\ n_a^2}\ |\Delta\rho| .$$

The values of $|\Delta\varepsilon|^2$ or $|\Delta\rho|^2$ due to various interaction mechanisms were derived in the last section. These can now be introduced into the reflectivity equation in order to calculate the proportion of argon laser light reflected, in terms of the intensities of the forward and backward

going ruby laser-beams, the frequency shift between them, the known properties of the medium and the length of the interaction region.

Thus for absorbing media, when $\omega \sim 0$:

$$\left(\frac{I_R}{I_I}\right)_{max} = \left(\frac{\pi N \alpha \beta \gamma}{8 k_r^2 n_r^2 \cos^2\theta_{max} K n_a^2}\right)^2 \frac{1}{1 + \left(\frac{\omega}{\Gamma_R}\right)^2} \cdot I_1 I_2 ,$$

and for non-absorbing media, when $\omega \sim \omega_B$:

$$\left(\frac{I_R}{I_I}\right)_{max} = \left(\frac{\pi N \gamma^2}{4 \rho_o v^2 n_a^2 n_r c \cos^2\theta_{max}}\right)^2 \cdot \frac{1}{\left(1 - \frac{\omega^2}{\omega_B^2}\right)^2 + \left(\frac{2\Gamma_B \omega}{\omega_B^2}\right)^2} \cdot I_1 I_2$$

while at $\omega \sim \omega_B$ in absorbing media there is the additional thermal Brillouin term:

$$\left(\frac{I_R}{I_I}\right)_{max} = \left(\frac{\pi N \alpha \beta \gamma}{4 \rho_o c_p n_a^2 \cos^2\theta_{max} k_r n_r v}\right)^2 \frac{1}{\left(1 - \frac{\omega^2}{\omega_B^2}\right)^2 + \left(\frac{2 \Gamma_B \omega}{\omega_B^2}\right)^2} \cdot I_1 I_2 .$$

The anisotropy and nonlinear polarizability of the molecules of the medium give rise to additional terms of the form

$$\left(\frac{I_R}{I_I}\right)_{max} = \left(\frac{2\pi^2 NK}{n_a^2 n_r c \cos^2\theta}\right)^2 \frac{1}{\left(1 - \frac{\omega^2}{\Omega^2}\right)^2 + \left(\frac{2\Gamma\omega}{\Omega^2}\right)^2} \cdot I_1 I_2 ,$$

corresponding to Rayleigh wing and Raman scattering.

These formulae show that the probe scattering has the same dependence on frequency shift (of one ruby laser beam from the other) as the dependence on frequency shift of spontaneously scattered light (see Fig.2.3). It does not have the same frequency dependence as the stimulated scattering gain because that is a function only of the out of phase part of the refractive index[110,124,126,164,196] change whereas probe scattering depends on the amplitude of the whole change.

CHAPTER III

EQUIPMENT USED IN THE SCATTERING EXPERIMENTS

3.1 LIGHT OUTPUT MEASUREMENT SYSTEMS

Three oscilloscopes were used in the experiments to be described. A relatively slow (rise time ~ 15 nsec) Tektronic 551 oscilloscope, triggered from the ruby laser drive unit was used to measure the long term (millisecond) characteristics of the ruby laser output. In most of the experiments the purpose of the oscilloscope was to make sure that a single giant pulse was being generated by the ruby laser.

A very fast (rise time ~ ·3 nsec) Tektronix 519 oscilloscope was used to give a high time resolution display of the ruby laser-pulses. Unfortunately the photomultiplier used to detect the Bragg reflected pulses of argon laser light in the probe scattering experiment (Chapter VII) did not give enough signal to be displayed on this oscilloscope, the sensitivity of which was only 10 V cm^{-1}. This signal was displayed on a fast (rise time $2\frac{1}{2}$ nsec) Tektronix 454 oscilloscope which had a built in amplifier system giving a maximum sensitivity of 5 mV/cm. This instrument had the added advantage of a two channel input so that the ruby, and Bragg reflected argon, light pulses could be displayed on the same trace but with different gain. The pulses were separated in time simply by using a known length of delay cable.

In the argon probe scattering experiments (Chapter VII, Fig.7.1) the output of three diodes had to be displayed via Channel 1 of the oscilloscope while that of the photomultiplier was displayed via Channel 2.

To do this without introducing electronic distortion, delay cables of 50 Ω characteristic impedance were used. The longest cable was that to the photomultiplier, causing its pulse to appear last on the trace.

The three photodiodes were connected at intervals directly to a shorter length of cable. The internal impedance of the diodes was very large so these connections did not cause mis-match in the cable. Both cables were terminated with a 50 Ω impedance where they were joined to the oscilloscope and the cable to which the diodes were connected was simularly terminated at the other end. The oscillograms obtained showed no spurious pulses due to mis-match.

The Tektronix 454 oscilloscope had, in addition to its two channel input, a very convenient double trigger system. The 'A' trigger was operated by a signal from the laser trigger unit and, after an adjustable delay, prepared the 'B' trigger for operation. The B trigger was operated by the input to Channel 1 of the scope and displayed a trace on the screen. At the same time a synchronization pulse appeared at another terminal and was displayed on the 551 oscilloscope. This system greatly reduced spurious triggering of the 454 scope (there is a large, transit electromagnetic signal when the laser discharge tube is triggered). It also allowed display of the 454 triggering on one trace of the 551 oscilloscope (triggered by the laser trigger unit) while the long term characteristics of the laser output were displayed on the other to check single pulse output.

An absolute measurement of the energy of the ruby laser beam was obtained using a calibrated calorimeter (Laser Associates Model 42). In this calorimeter was a polished copper cone into which the light was directed. The shape of the cone was such that after multiple reflections on its surfaces very little of the incident light escaped from it. The heat produced by absorption of the light was detected by an array of thermocouples on the outer surface of the cone. These were connected to a millivoltmeter calibrated in terms of beam energy and allowed

measurements accurate to about one tenth of a joule. The results of the calorimeter measurements were used to calibrate a photoelectric detection system consisting of an EM I Photodiode Type 9648B connected to a Tektronix 519 or 454 oscilloscope. The light input to the photodiode was obtained by reflection from a beam splitter and attenuated by a diffusing screen and filters. Using the 519 oscilloscope this detection system had a rise time of about two nanoseconds.

The continuous Argon laser output was measured using a calibrated photodiode and voltmeter (Spectra Physics Type 401B). The pulse of argon laser light Bragg reflected in the probe scattering experiment (Chapter VII) was recorded using a Mullard 56 AVP photomultiplier and Tektronix 454 oscilloscope having a combined rise time of about 7 nsec. This system was calibrated by chopping a continuous beam of known power and reflecting the chopped pulses into the photomultiplier with a 50% beam splitter placed in the position of the interaction region of the Bragg reflection experiment. This calibration was not entirely satisfactory as it was not possible to ensure that the sensitivity of detection was the same for the Bragg reflected pulse as for the very much longer chopped pulse. Red light was excluded from the photomultiplier by Jena BG 18 green filters and extraneous blue light from the laser flashlamp minimised by a narrow band (20 Å) filter with peak transmission at the argon laser wavelength.

3.2 THE RUBY LASER

The ruby laser used for the experiments described in this thesis, was a model 351 supplied by G and E Bradley in 1966, It is shown in the Frontispiece and in Fig.3.1.

The laser head consisted of a $6\frac{1}{2}" \times \frac{5}{8}"$ ruby rod and a flash tube at the two foci of a highly polished elliptical aluminium cavity. The

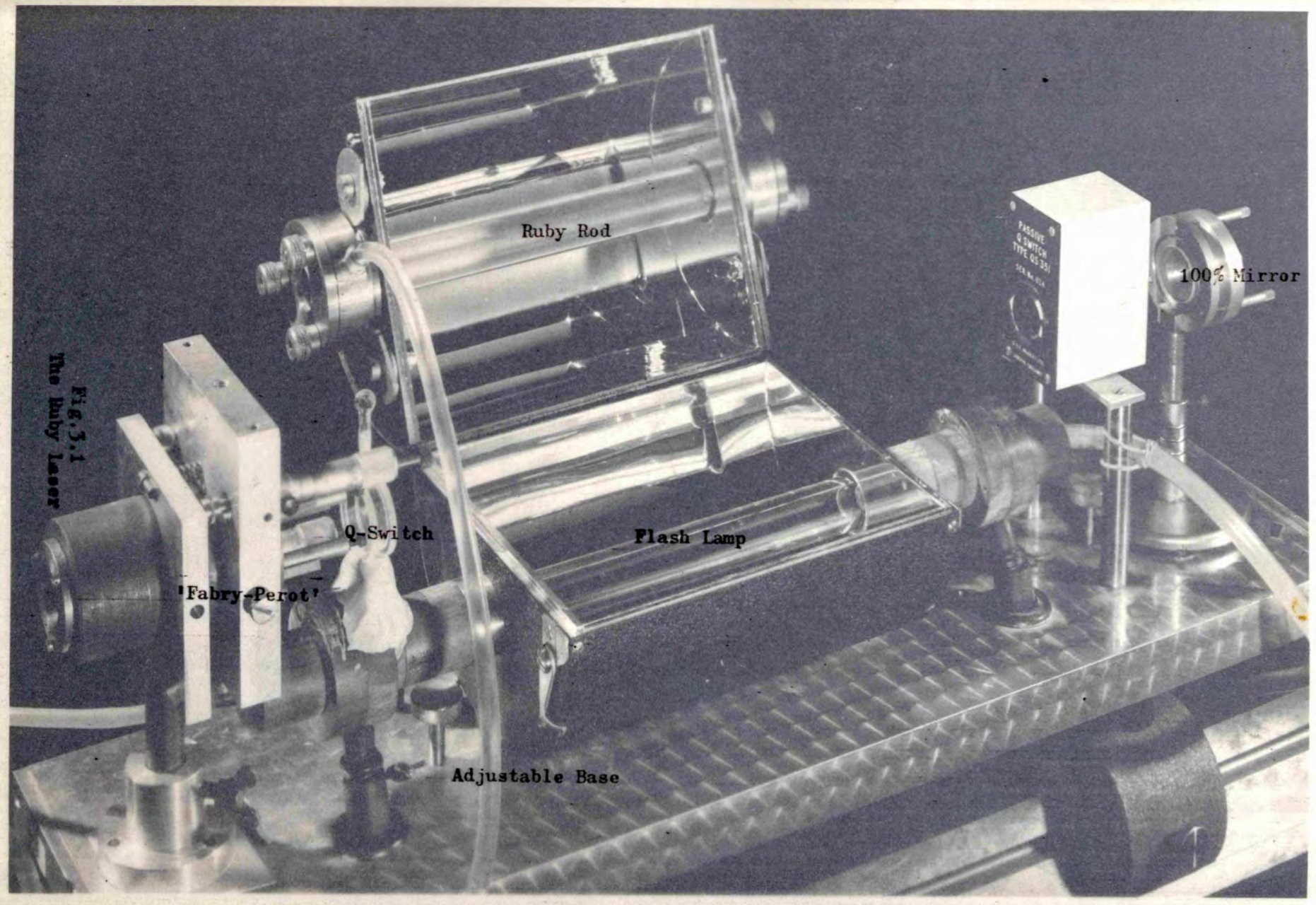

Fig.3.1
The Ruby Laser

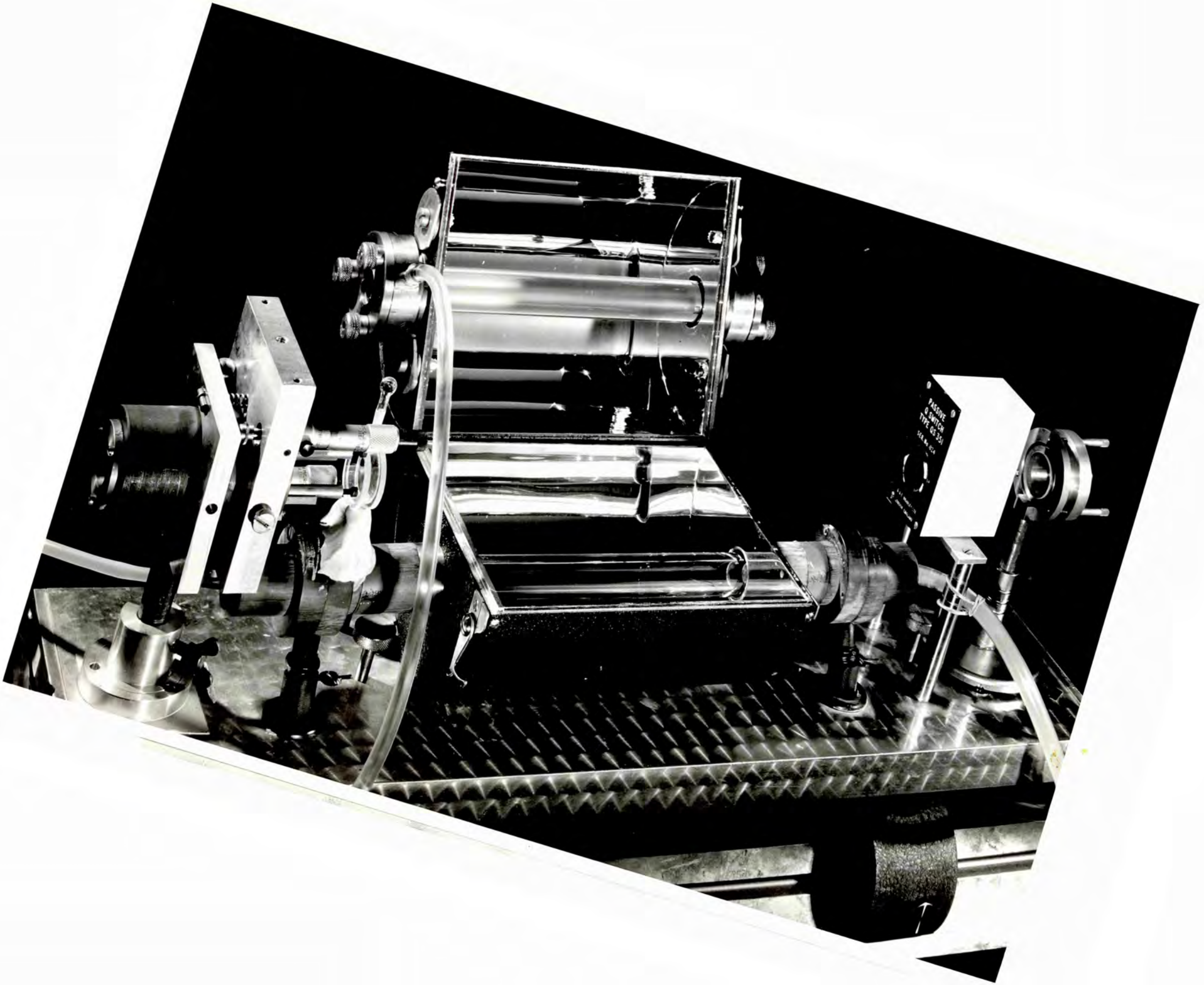
PASSIVE
Q SWITCH
TYPE QS 25i

rod and flash tube were water cooled allowing fairly reproducible firing of the laser about once every two minutes. The discharge through the flash tube had an energy of up to 10,000 J, supplied by a voltage of up to 3000 V on a 2400 mF capacitor bank. The discharge was triggered by a pulse of about 15 kV lasting a few microseconds applied to the same terminals as the main voltage. At the same time as the trigger pulse a small pulse was generated at another terminal to synchronize oscilloscopes and other apparatus (Fig.3.2).

Feedback in the laser cavity was provided at one end by a dielectric mirror coated to reflect 100% of light of 6943 Å incident upon it and at the other end by the quartz window of the water jacket, which had a reflectivity of 10% for the ruby laser-light. Unfortunately the design was such that the ruby faces were immersed in the cooling water which caused some beam deterioration and increased the possibility of non-linear effects within the laser cavity. The laser was passively Q-switched[41,42] by means of a cell containing a solution of cryptocyanine in methanol inserted in front of the 100% mirror.

The output of this system was a pulse of plane polarized light of about 200 M.W. power, 20 nsec duration and 8 m.rad. divergence.

The most serious defect of the system as supplied by the manufacturers was that it operated in a large number of longitudinal and transverse modes. Single longitudinal mode operation was obtained without loss of power by including a second Q-switch within the cavity and providing feedback at the output end of the cavity with a precisely parallel pair of quartz flats instead of the water jacket window (see Fig.3.1)[37,40]. The number of transverse modes could be reduced by inserting a small aperture in the feedback cavity[228]. However this technique reduced the

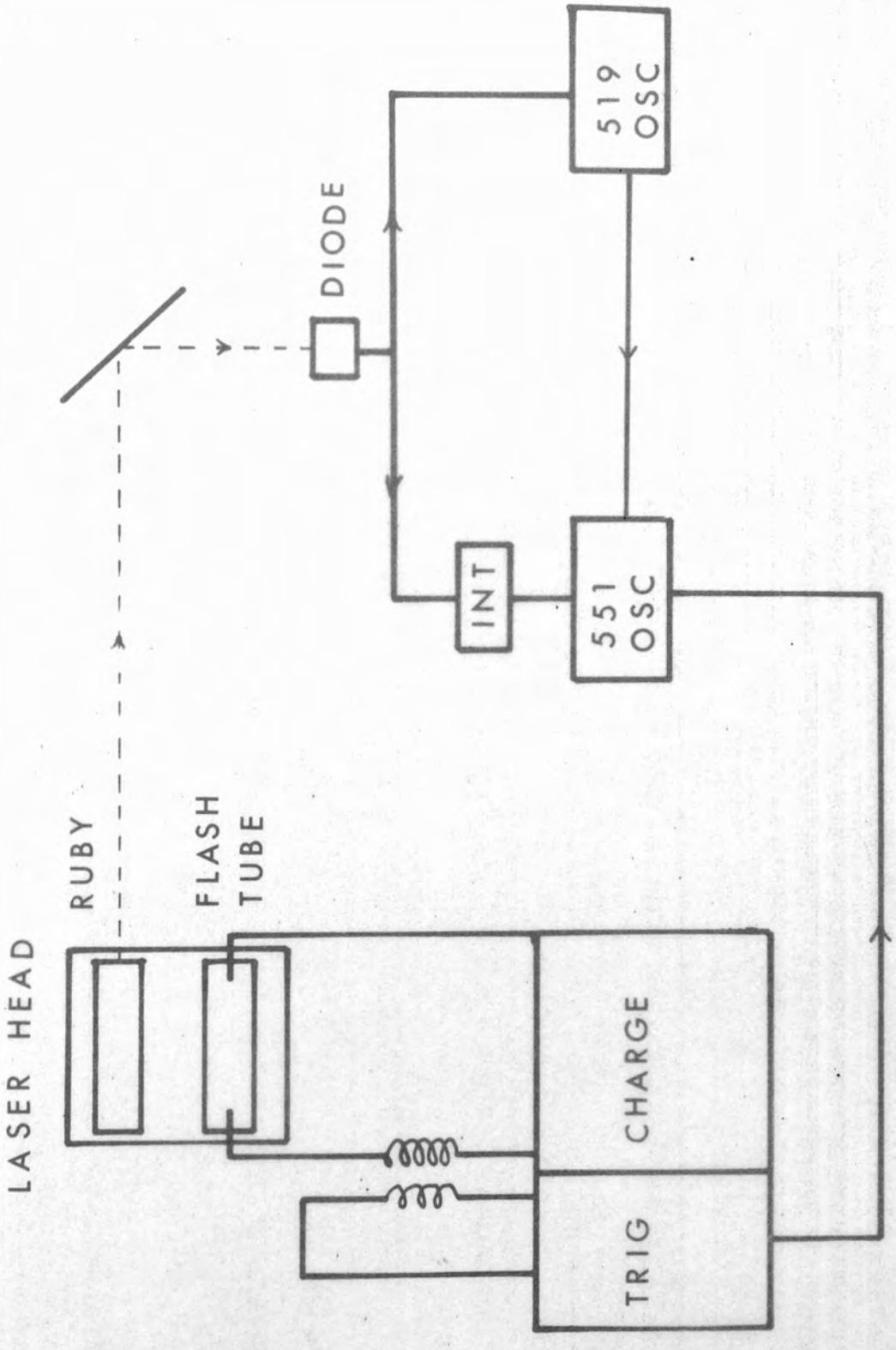

Fig.3.2.
Ruby Laser Electronics

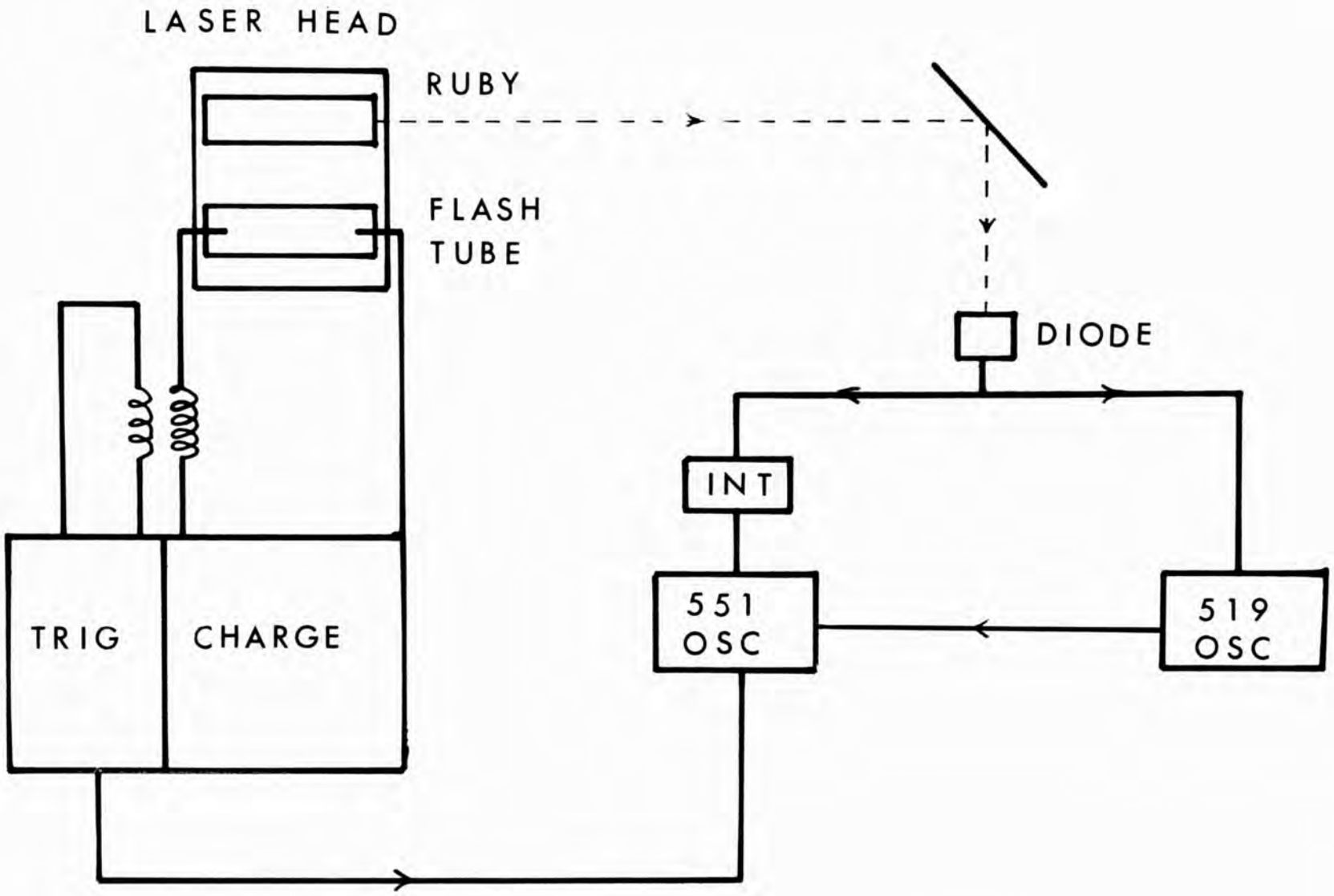
LASER HEAD
RUBY
FLASH
TUBE
DIODE
INT
TRIG
CHARGE
551
OSC
519
OSC

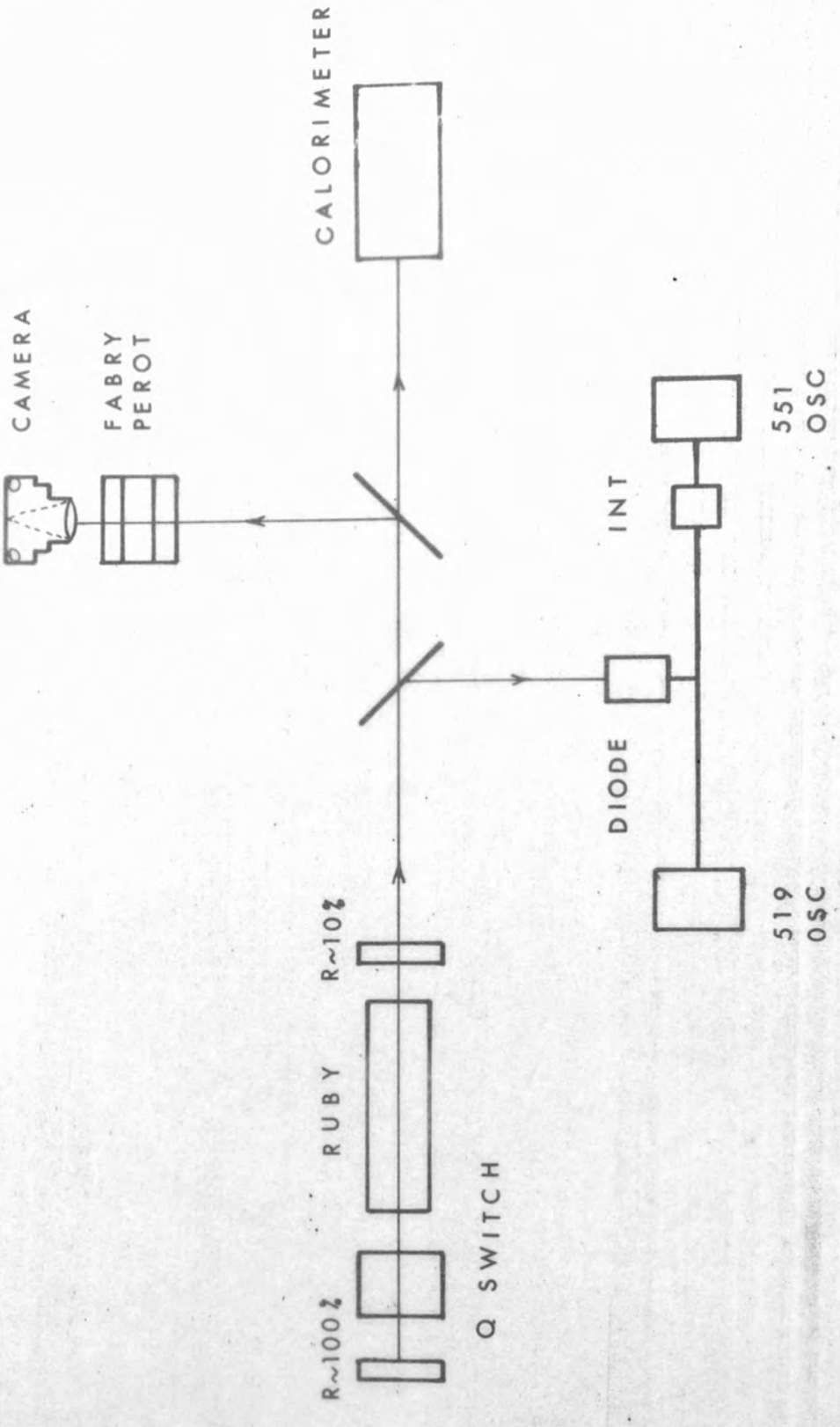

Fig .3.3.
Ruby Laser Calibration

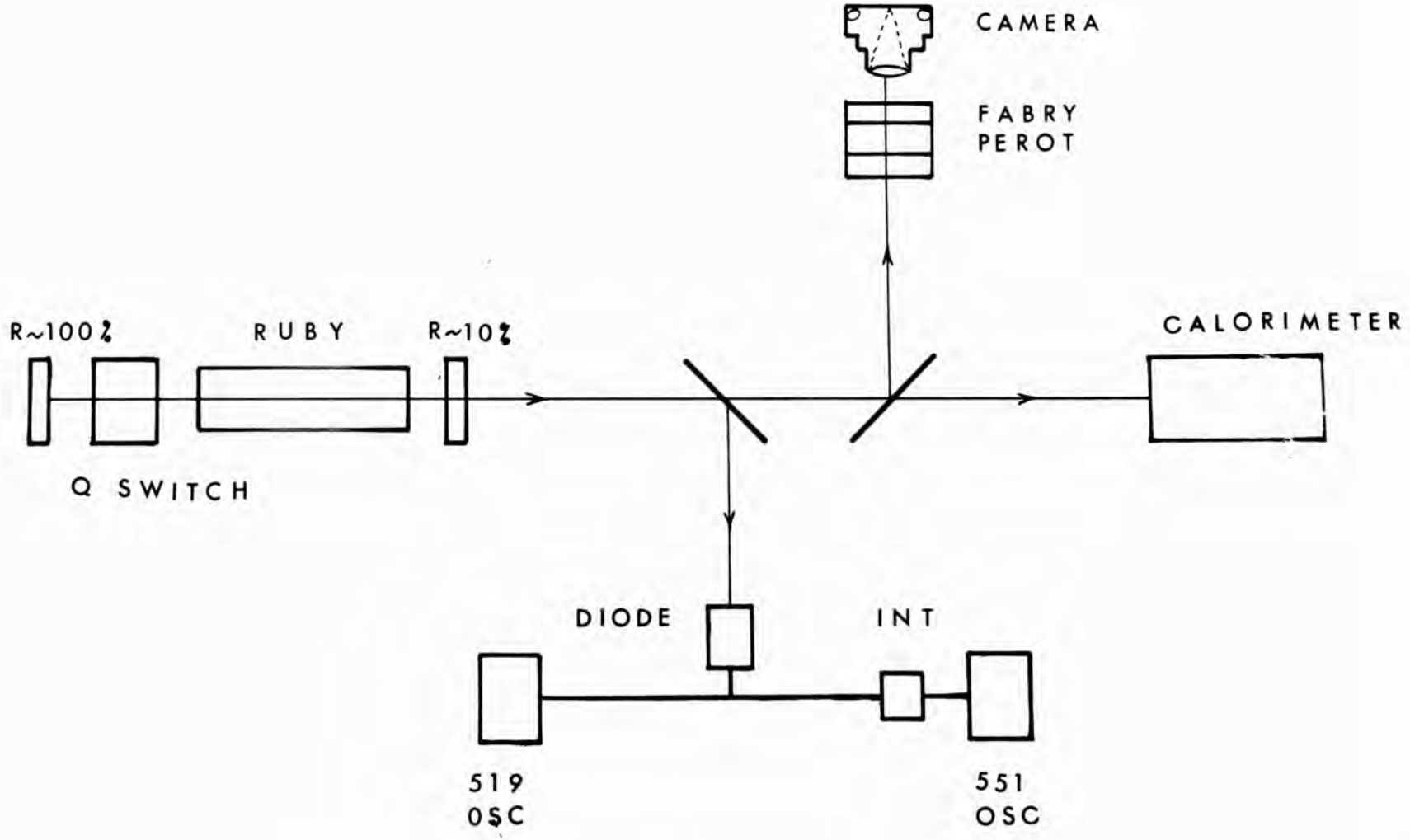
CAMERA
FABRY
PEROT
R~100%
RUBY
R~10%
CALORIMETER
Q SWITCH
DIODE
INT
519
OSC
551
OSC

output power to such an extent that it was impracticable to use it and lack of transverse mode control remained the main source of error in the experiments to be described.

The laser characteristics were investigated using the arrangement shown schematically in Fig.3.3. The signal detected by the photodiode was displayed simultaneously on two oscilloscopes. The signal on the Tektronix 551 oscilloscope was first put through an integrating circuit with a response time of 10^{-5} secs. This converted the very short laser pulses into relatively slow pulses visible on one trace of the 551 oscilloscope. This had a time base of ·2 msec/cm and was triggered by the laser trigger unit. The Tektronix 519 oscilloscope was triggered by the input signal which was displayed directly on the scope trace. The time base of this trace was varied between 20 and 200 nsec. Each time the 519 scope was triggered a syncronization pulse was generated. This was integrated and displayed on the second trace of the 551. In this way the whole pulse train was shown on the 551 while those pulses which triggered the 519 were displayed individually, the second trace of the 551 indicating which pulses these were. At the same time the spectrum of the light output was analysed with a 1 cm Fabry-Perot interferometer (Section 3.5) and the energy of the pulse train measured with a calorimeter.

Typical results obtained are shown in Figs.3.4 and 3.5. (The scales have been changed by the photographic reproduction to those shown with the diagram.)

Fig.3.4 shows the laser output with the flash lamp discharge chosen to be the threshold value for lasing when amounts of dye in the Q-switch were as shown. It is seen that at low dye concentrations there was a large number of feeble pulses of long duration. At greater concentration a single powerful pulse was generated which became still shorter

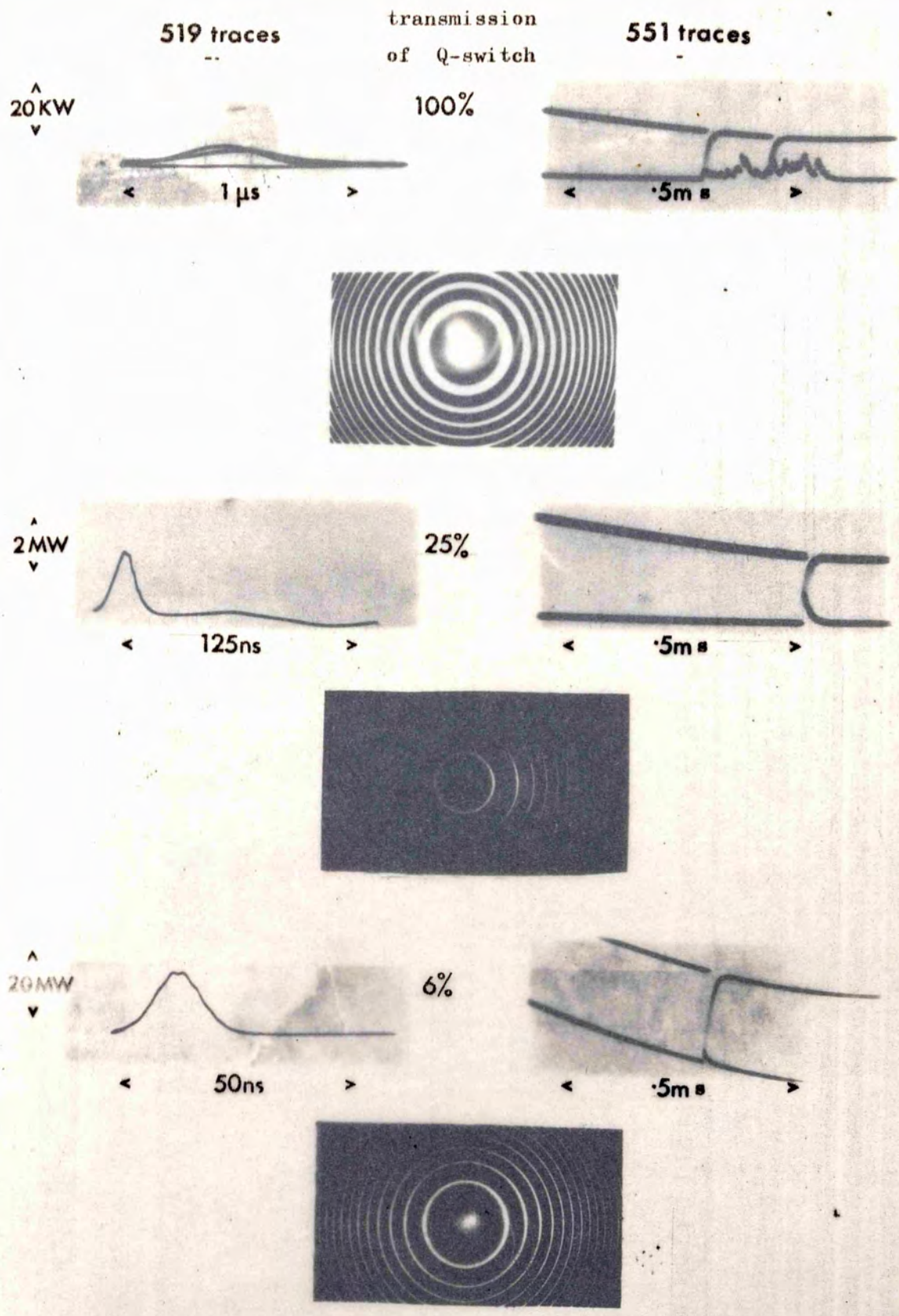

Fig.3.4
Ruby Laser Output at Threshold Pumping

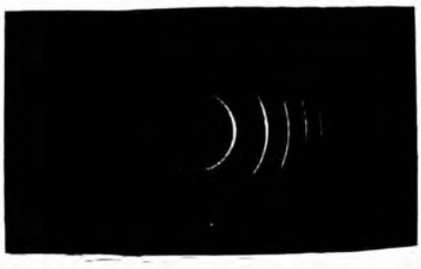

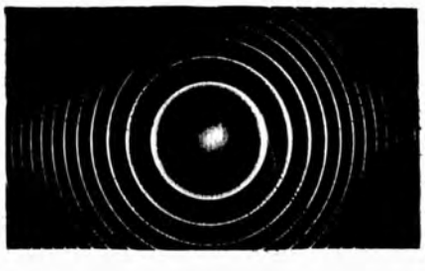

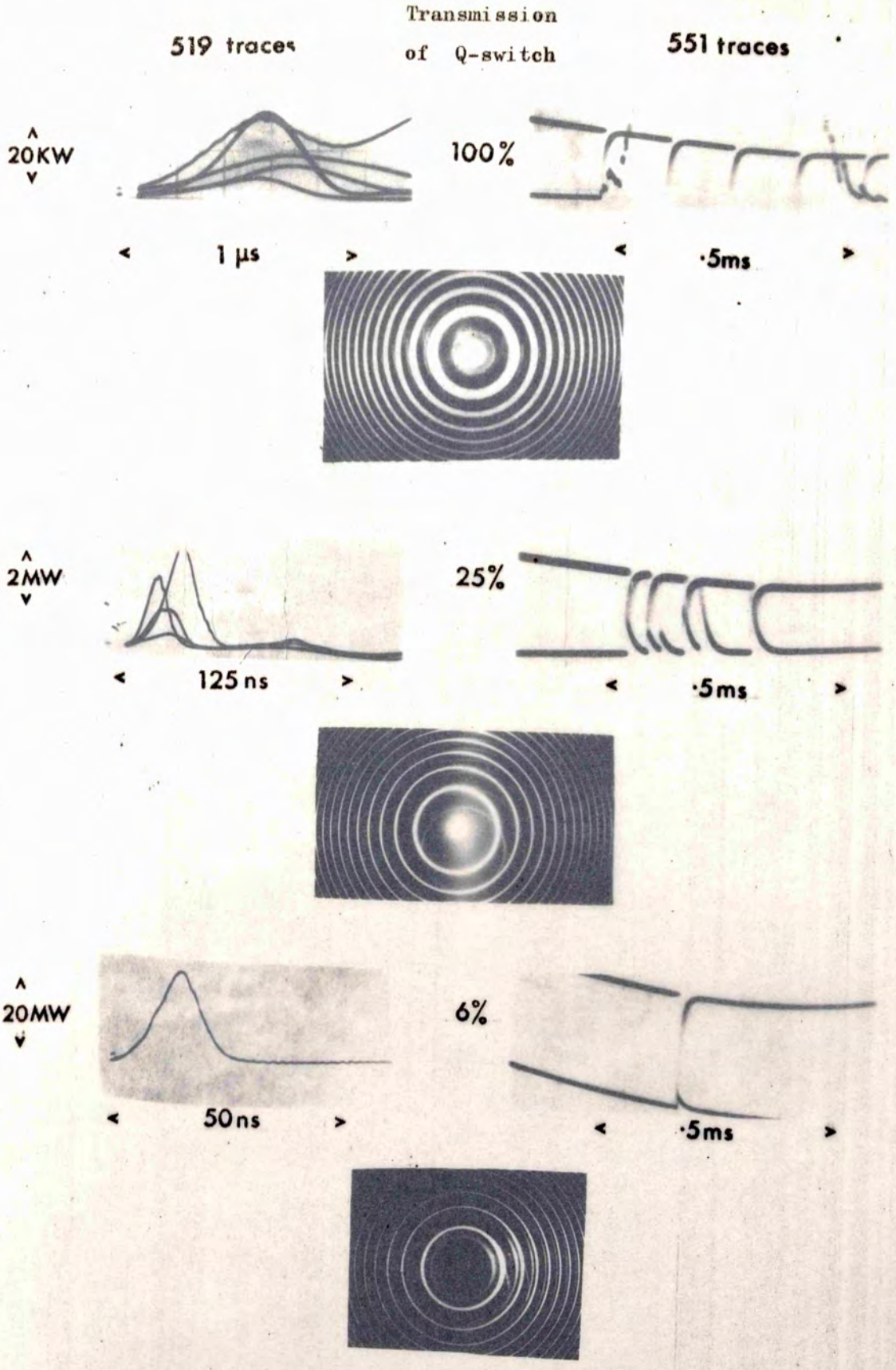

Fig.3.5
Ruby Laser Output at Constant Pumping

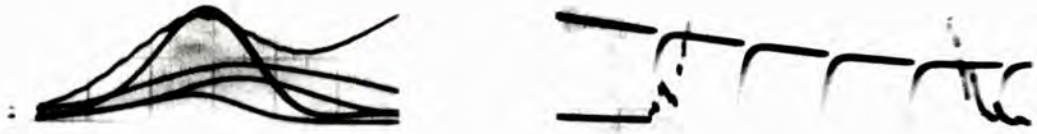

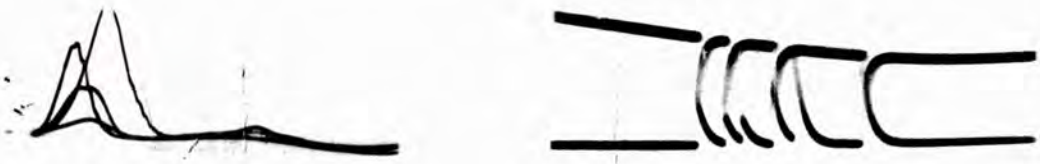

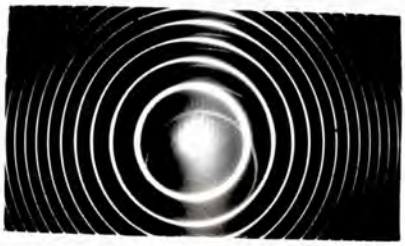

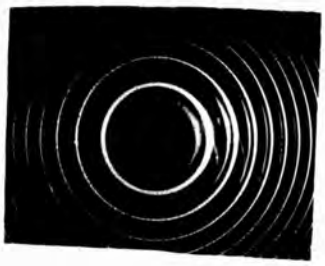

and more powerful with increasing concentration. The spectral output was broad when there was a large number of pulses but narrow enough (about ·002 Å) to indicate single longitudinal mode output when there was only one pulse.

Fig.3.5 shows the output when the flash lamp discharge remained constant and the dye concentration was varied. At low concentrations the discharge was far above threshold and enormous numbers of pulses were generated. With increasing concentration the number of pulses decreased, while they become shorter, more powerful, and of purer spectral composition. Eventually a single pulse was obtained which could be of sufficiently high power to cause stimulated Brillouin scattering in the Q-switch. When this was the case the Fabry-Perot showed the characteristic frequency shift as in the lowest photograph of Fig.3.5.

If the mode selecting elements in the cavity were removed and a Brewster angled ruby rod used, mode locking of the laser system could be achieved. Fig.3.6 shows partly mode locked and non-mode locked output from the ruby and a schematic diagram of the passive mode locking mechanism[227]. When the light intensity is slightly modulated due to the presence of (say) two modes in the cavity the saturable absorber transmits a greater proportion of the peak intensity than of the minimum intensity. In this way the intensity becomes more and more sharply modulated with more side-band frequencies being generated till eventually a series of sharp pulses may be emitted.

In general the presence of more than one mode in the output will result in a modulation of the pulse envelope at the mode separation frequency. This is the frequency of the modulation of the lower pulse in Fig.3.6 so the smoothness of the pulse is an additional check on the single mode output.

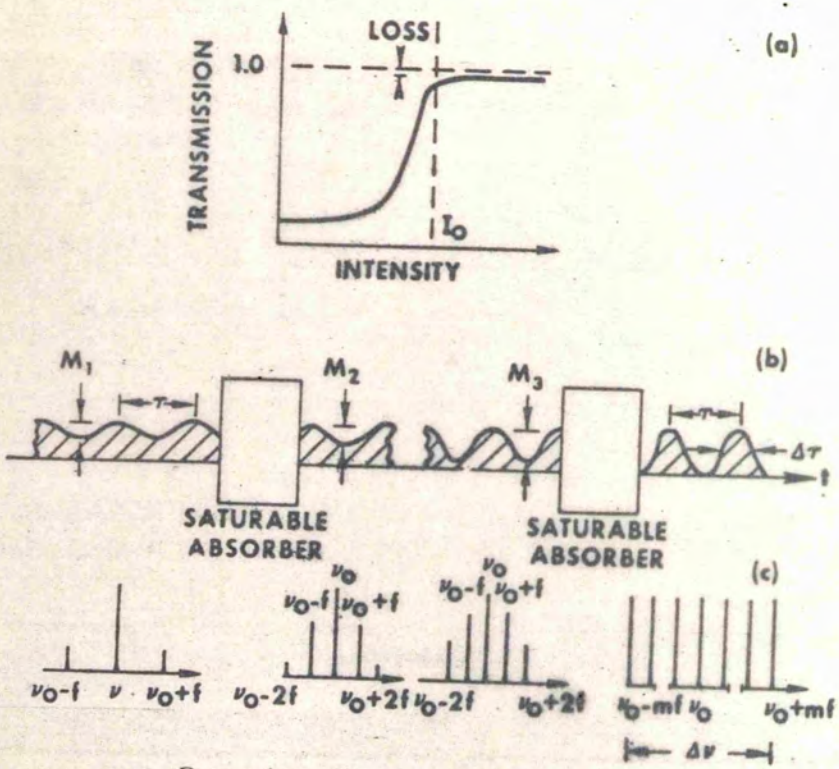

Operation of a saturable absorber in the time and frequency domain.

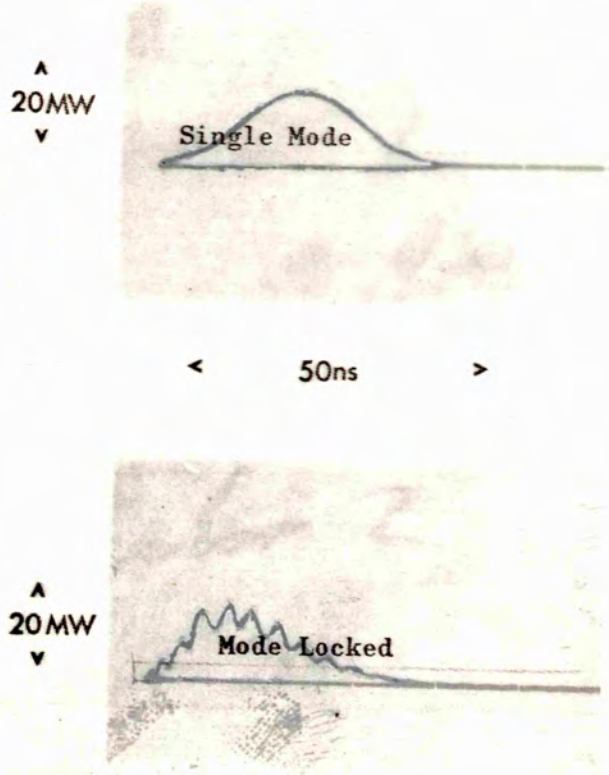

Fig.3.6
Mode Locking in the Ruby Laser

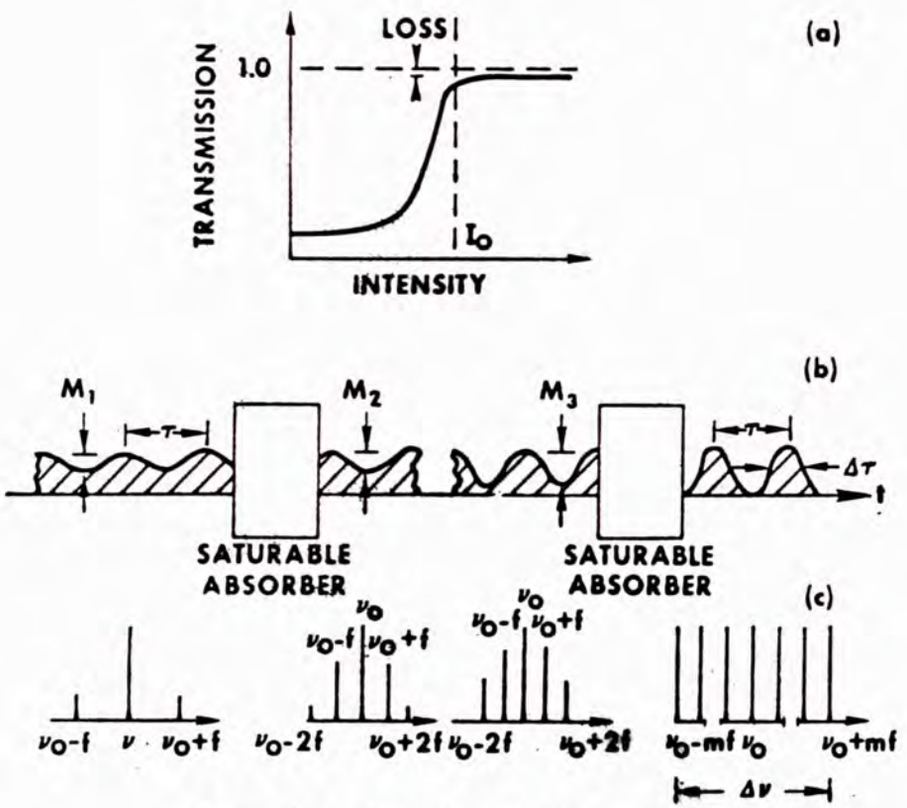

Operation of a saturable absorber in the time and frequency domain.

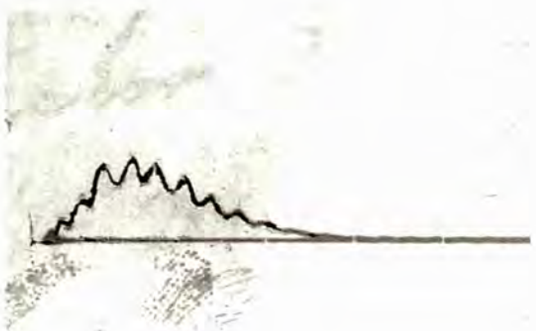

3.3 GAS LASERS

Two gas lasers were used in these experiments. One was a simple helium neon laser (Elliott model 315) giving a one milliwatt continuous beam at 6328 Å. This was used to align the complicated optical arrangements involved in the experiments. The helium-neon laser beam was directed normally through the back mirror (a 100% reflector at 6943 Å but not at 6328Å) of the ruby laser and thus traced out directly the path of the ruby laser beam, greatly facilitating alignment.

The other gas laser was a Spectra-Physics argon-ion laser, model 142 (Frontispiece). In this laser the plasma in a loop of electrodeless quartz discharge tube acted as the secondary coil of a radio frequency transformer. The gas pressure and hence the plasma density were kept at an optimum level by an automatic refilling system which replaced gas lost into the walls during the discharge. This loss was minimized by magnetic focusing of the discharge keeping the dense part of the plasma away from the walls. One side of the loop was a straight tube about one metre long and 2 mm in diameter with Brewster angled windows at its ends. Feedback mirrors were provided outside these windows and laser action occurred along the straight tube.

In an argon ion plasma lasing can occur at a number of frequencies and the total output in all lines was about 3 W of light polarized in the plane perpendicular to that of the Brewster window. For the experiments to be described a single frequency is required and this was achieved by inserting a dispersion prism in front of the rear feedback mirror. By rotating the prism lasing could be achieved at a number of frequencies the principal outputs being about 1 W at 4880 Å and 5145 Å. The long narrow lasing tube ensured single transverse mode operation giving a 1 mm diameter beam with Gaussian intensity distribution and diffraction limited

divergence of about 1 m.rad. Longitudinal mode selection could not be achieved without loss of power and was not used since the lack of ruby transverse mode control was a source of greater error (Chapter VIII).

The laser output was measured with a calibrated photocell and meter supplied by Spectra Physics and was found to be stable to within a few percent over several hours after an initial stabilizing period of about one hour.

3.4 KINEMATICALLY DESIGNED OPTICAL STANDS

In the experiments to be described, especially in the probe scattering experiments, a number of laser beams had to be aligned with an accuracy of 1 m.rad. or better. The complexity of the system and the frequency of damage to optical components[178,229,231] by the very high laser powers made it very desirable that individual mountings should be as mobile and versatile as possible.

For these reasons a number of kinematically designed optical tables were constructed. The 'Fabry-Perot' front mirror of the laser (Fig.3.1) and the A.D.P. crystal (Chapter VI) were supported on kinematic mountings of standard design[230]. The rear mirror of the laser could be removed and replaced without re-adjustment, its stand having three grooves in the base which rested on three steel balls fixed on the main laser table. This table, and thus the whole ruby laser set up was fully mobile, having six thumb screws allowing adjustment in all possible degrees of freedom.

The most important development was however the 'spectrometer table' supporting the scattering cell (Chapters VI,VII) and the components round it (Figs.3.7 and 3.8, and Frontispiece)[247]. The crucial feature of this system was the novel arrangement of the ball bearings fixed to the removable arms. The two balls on the underside of the arm rested in the

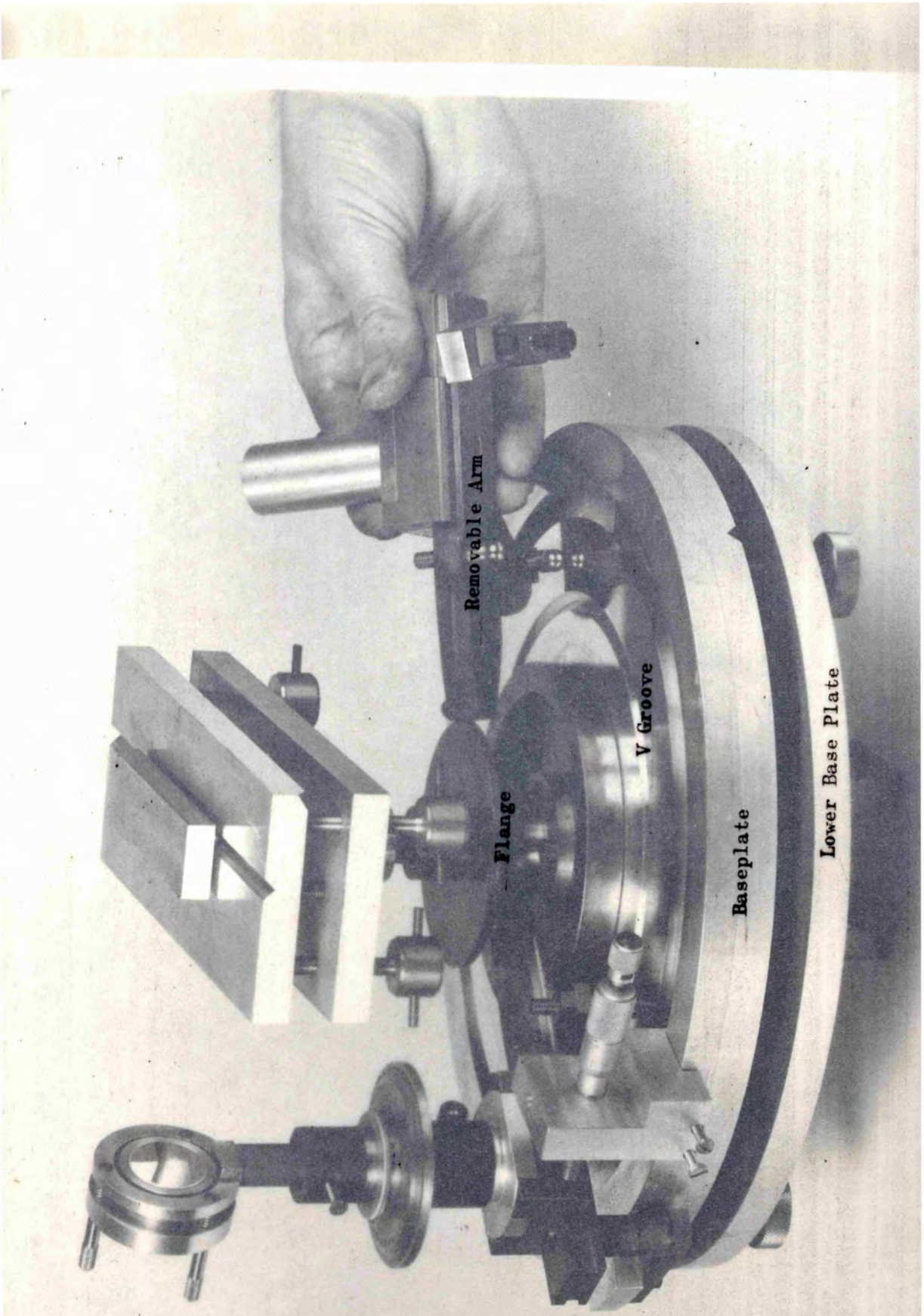

Fig.3.7
Kinematically Designed 'Spectrometer Table'

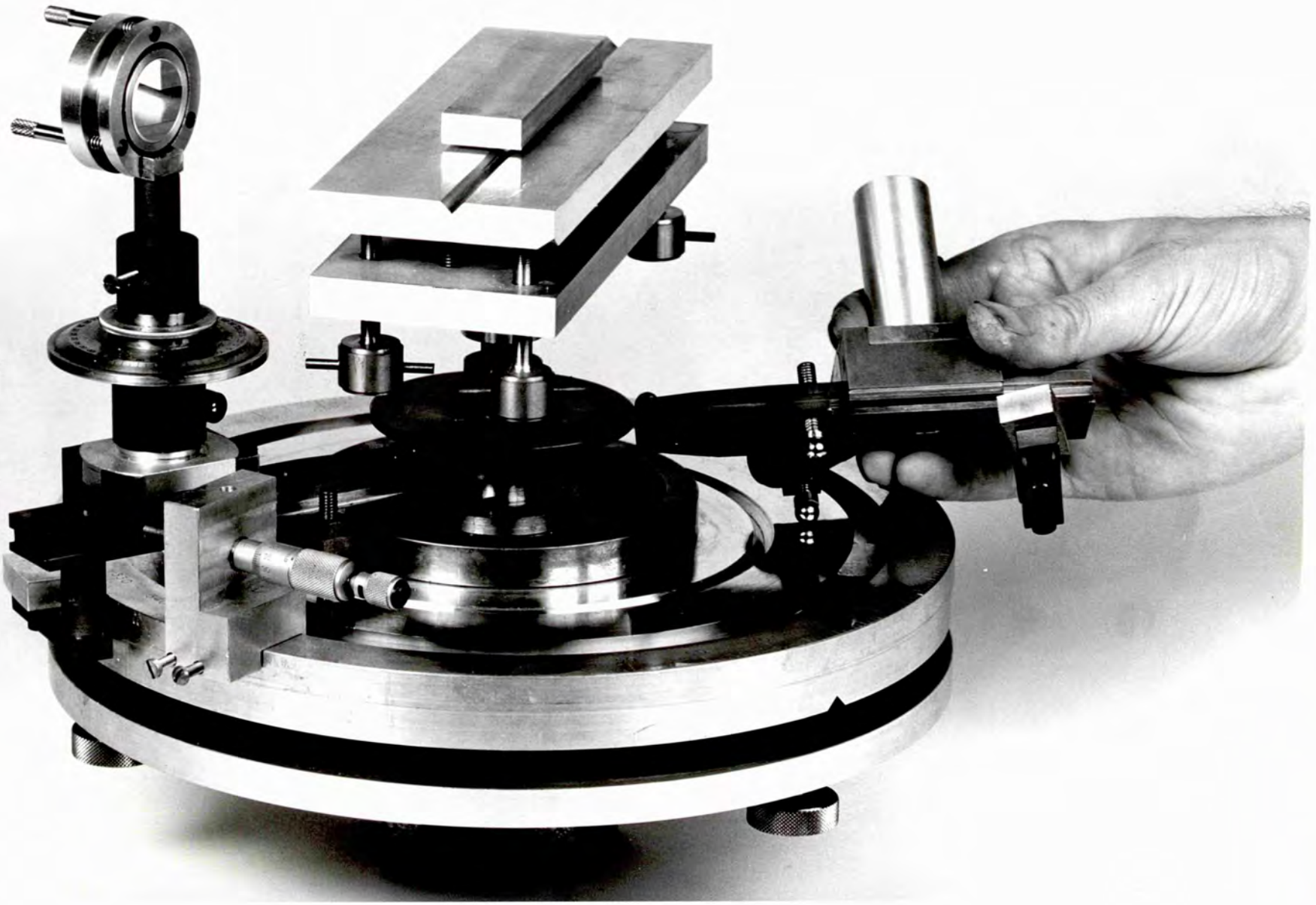

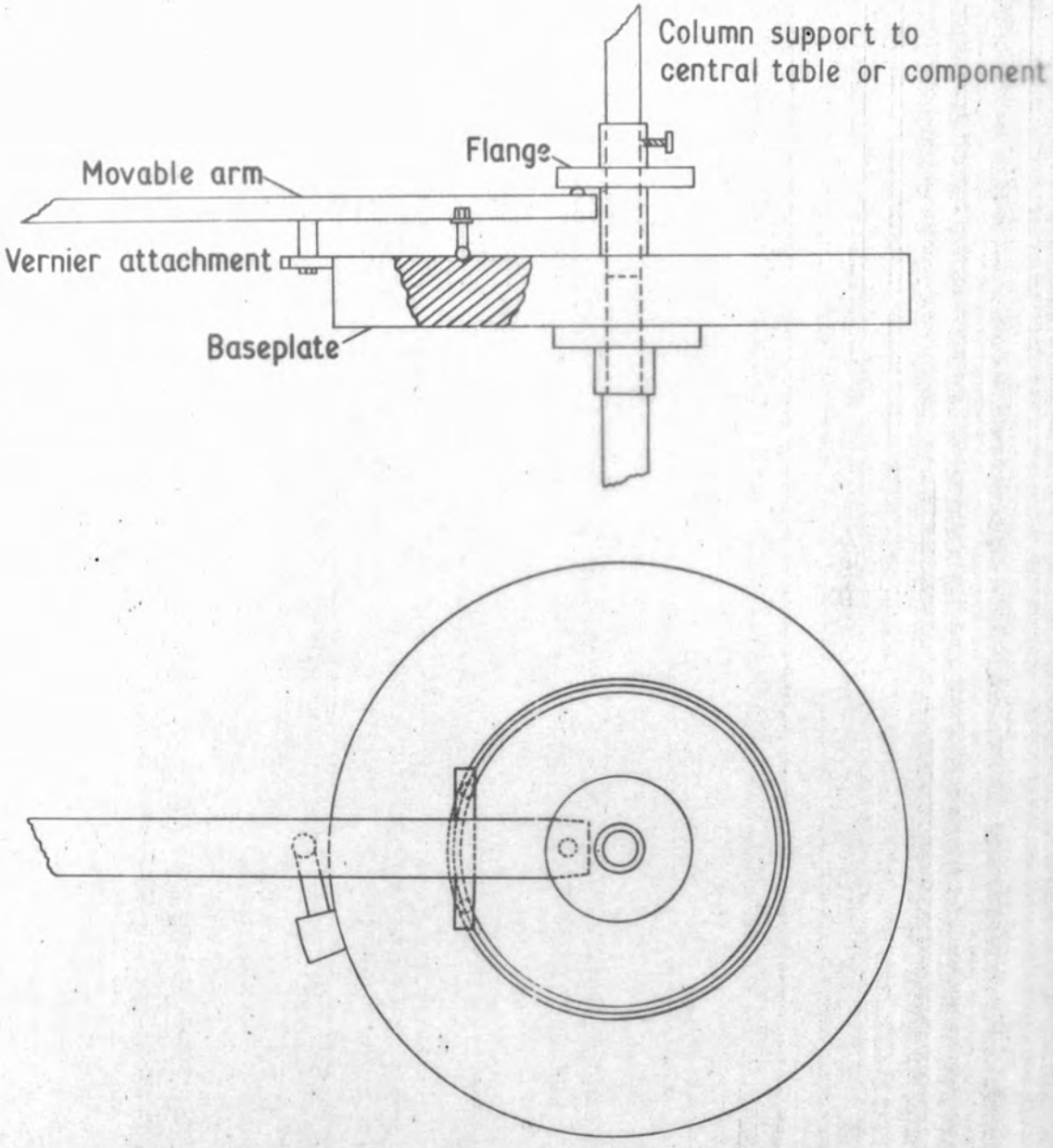

Fig.3.8.
Kinematically Designed 'Spectrometer Table'

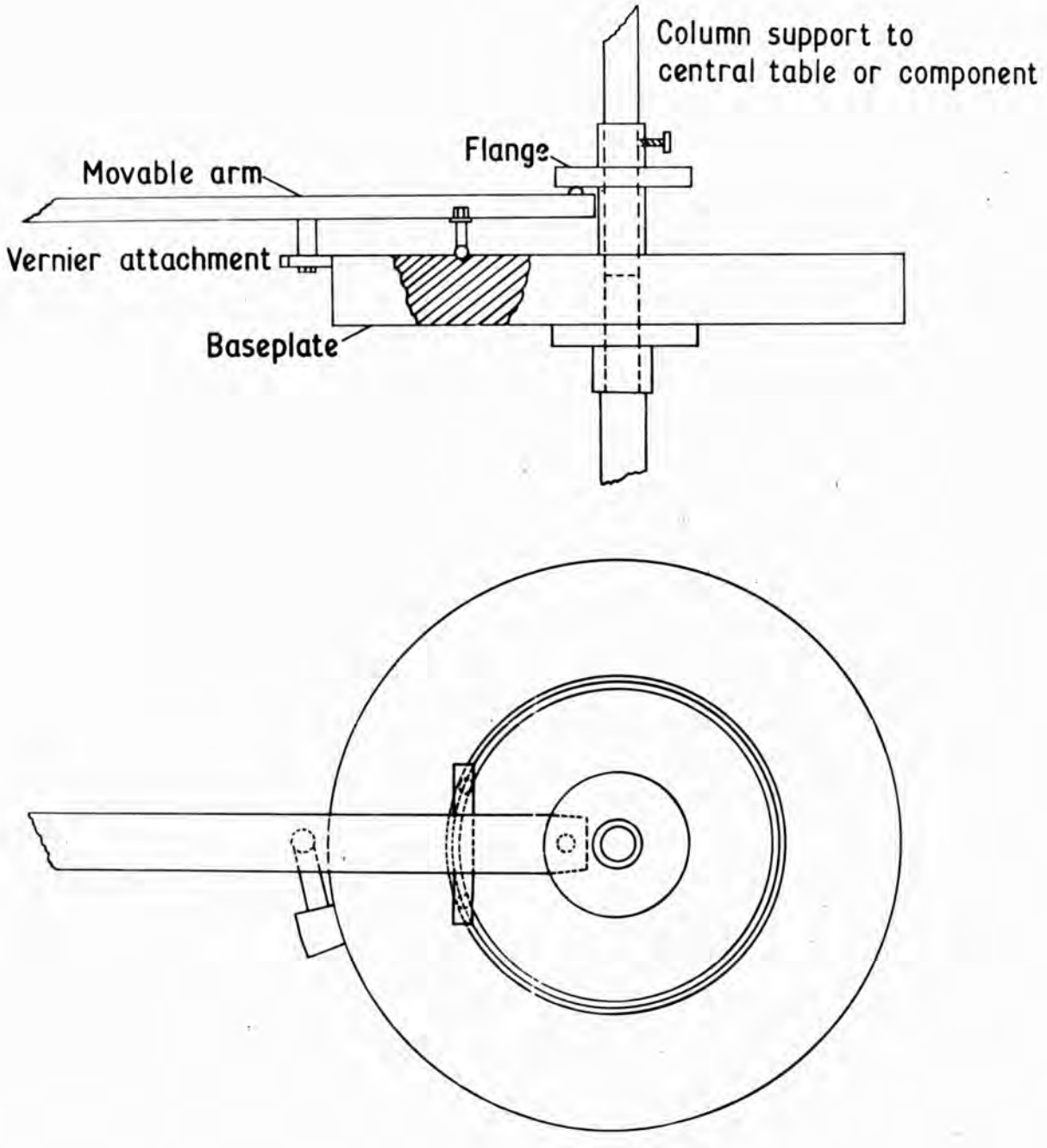
Column support to
central table or component
Flange
Movable arm
Vernier attachment
Baseplate

circular groove of V shaped cross-section in the base-plate. The ball on the upper surface of the arm rested against a flange on the centre column which was rigidly fixed to the base-plate. The five points contact provided by this arrangement allowed one degree of freedom which was of course rotation around the axis of the table. So long as the centre of gravity of the arm and supported components lay outside the circular groove, this arrangement was kept perfectly stable by gravity though the arm could be easily removed as shown in Fig.3.7. A vernier attachment showed the angular position to one tenth of a degree while incremental adjustments of as little as ·1 m.rad. could be accurately made using the micrometer adjustment.

The probe scattering cell was mounted on the carriage on the central table. Two balls on the underside of this carriage rested in the straight groove in the central table while a third rested on its plane surface. This allowed linear movement of the cell along the ruby laser beam.

Angles between light beams within the liquid in the cell could be directly measured. This was achieved by mounting a horizontal bar on a vertical rod supported by one of the moveable arms. The horizontal bar crossed the axis of the arm's rotation and at this point an optical table was mounted on its underside. A one inch square of beam splitter was stuck by its edge to the surface of the table. This beam splitter was thus in the vertical plane containing the axis of the system and could be rotated about that axis. It could be lowered into the liquid or raised and removed when not in use. The angle between two light beams was simply the angle by which the arm was rotated to move the beam splitter between positions normal to each beam.

The base-plate of the system, itself had three grooves on the underside which rested on three adjustable thumb screws in the lower base-plate.

The plane of rotation of the movable arms could thus be made parallel to the plane containing the argon and ruby laser beams (i.e. the horizontal plane).

3.5 THE FABRY-PEROT SYSTEM

In the early experiments a simple 1 cm Fabry-Perot system was used to monitor the spectrum of the ruby laser beam. Later when more accurate knowledge of the mode structure of the beam was wanted a new system was constructed which could take a spacer of up to 5 cms. The use of this instrument confirmed that a single mode could be obtained but was inconvenient because when a second mode does occur it is usually shifted by the frequency of the stimulated Brillouim shift which is very nearly equal to the free spectral range of a 5 cm Fabry-Perot. For this reason the spectrum was usually monitored with the 1 cm instrument.

In the experiments of Chapter VIII, it was necessary to monitor separately the forward and backward travelling ruby laser beams. For this reason the system shown in Figs.3.9, 3.10 and Frontispiece were developed[197].

Fig.3.9 shows schematically the principle of the system. The forward (left to right) and backward going beams were both polarized in a plane perpendicular to the paper. The backward beam was reflected by the beam splitter directly into the Fabry-Perot. The forward beam, reflected in the opposite direction passed through a quarter wave plate, was reflected from a 100% mirror and passed again through the quarter wave plate. This beam was thus polarized in the plane of the paper and most of it passed through the beam splitter into the Fabry-Perot. Cones of light of each polarization were created by inteference in the usual way and these were focused by the camera to form rings on the photographic film. A composite polaroid disc was placed just in front of the film

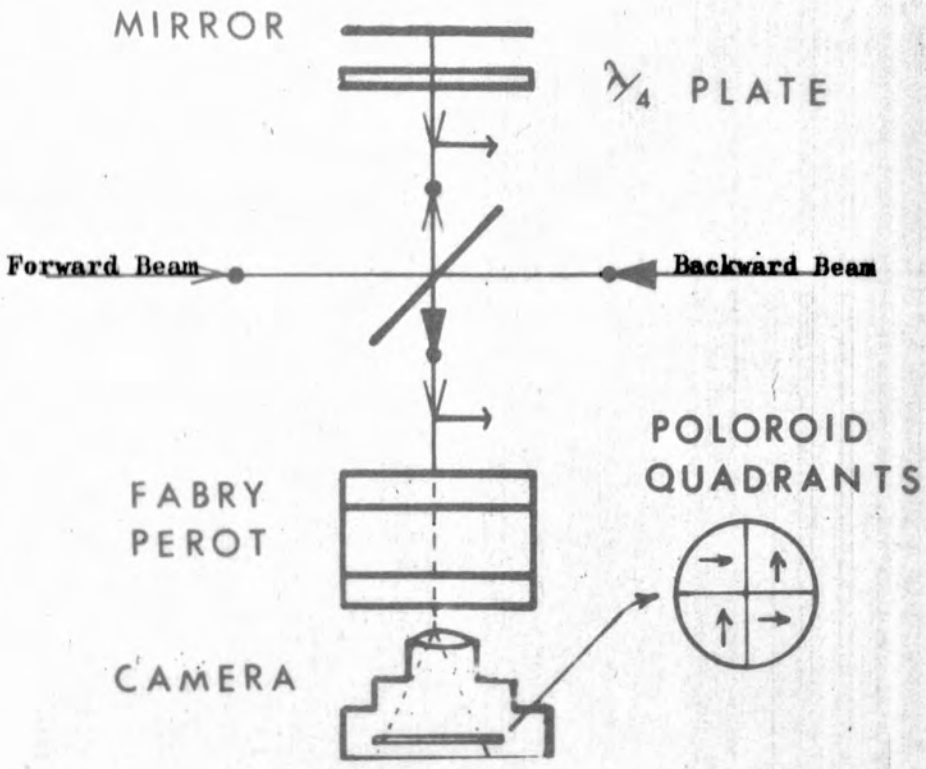

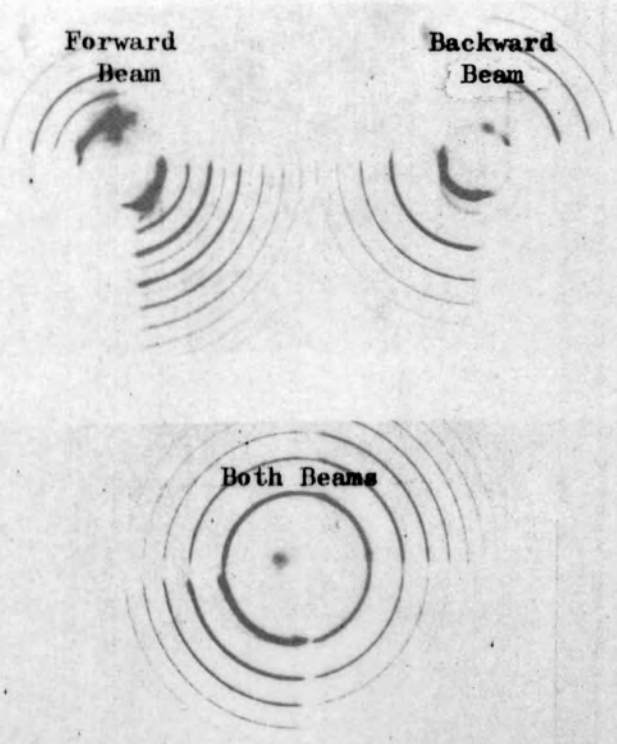

Fig.3.9
The Fabry-Perot System

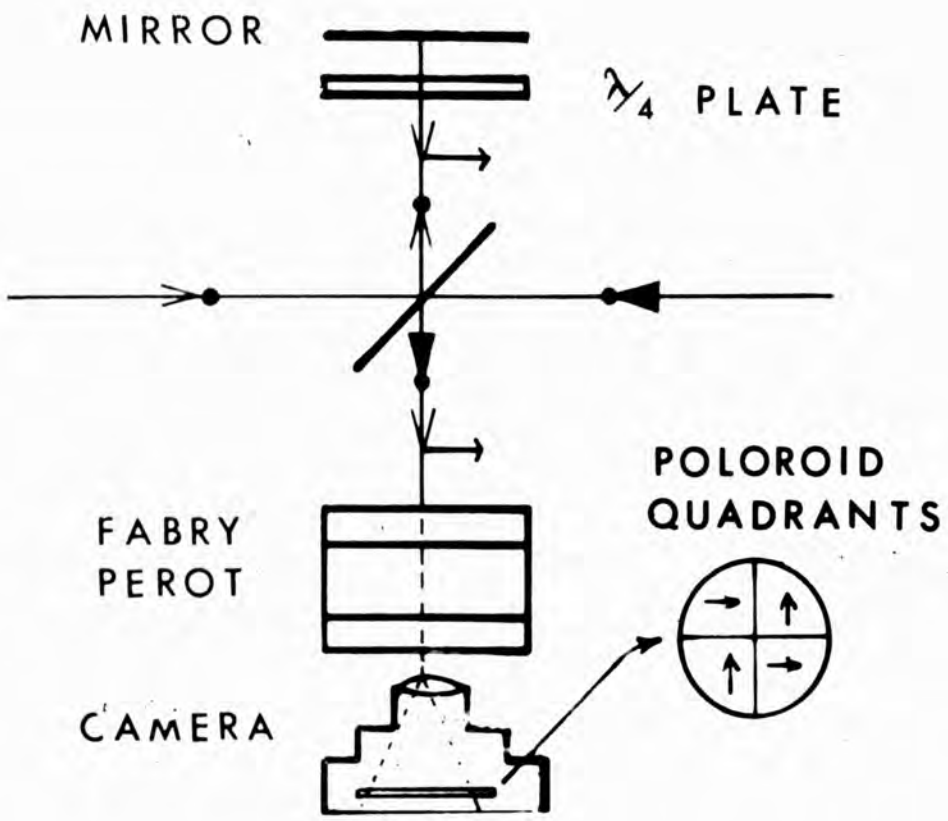
MIRROR
λ/4 PLATE
POLOROID
QUADRANTS
FABRY
PEROT
CAMERA

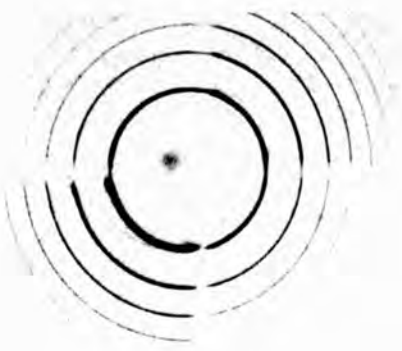

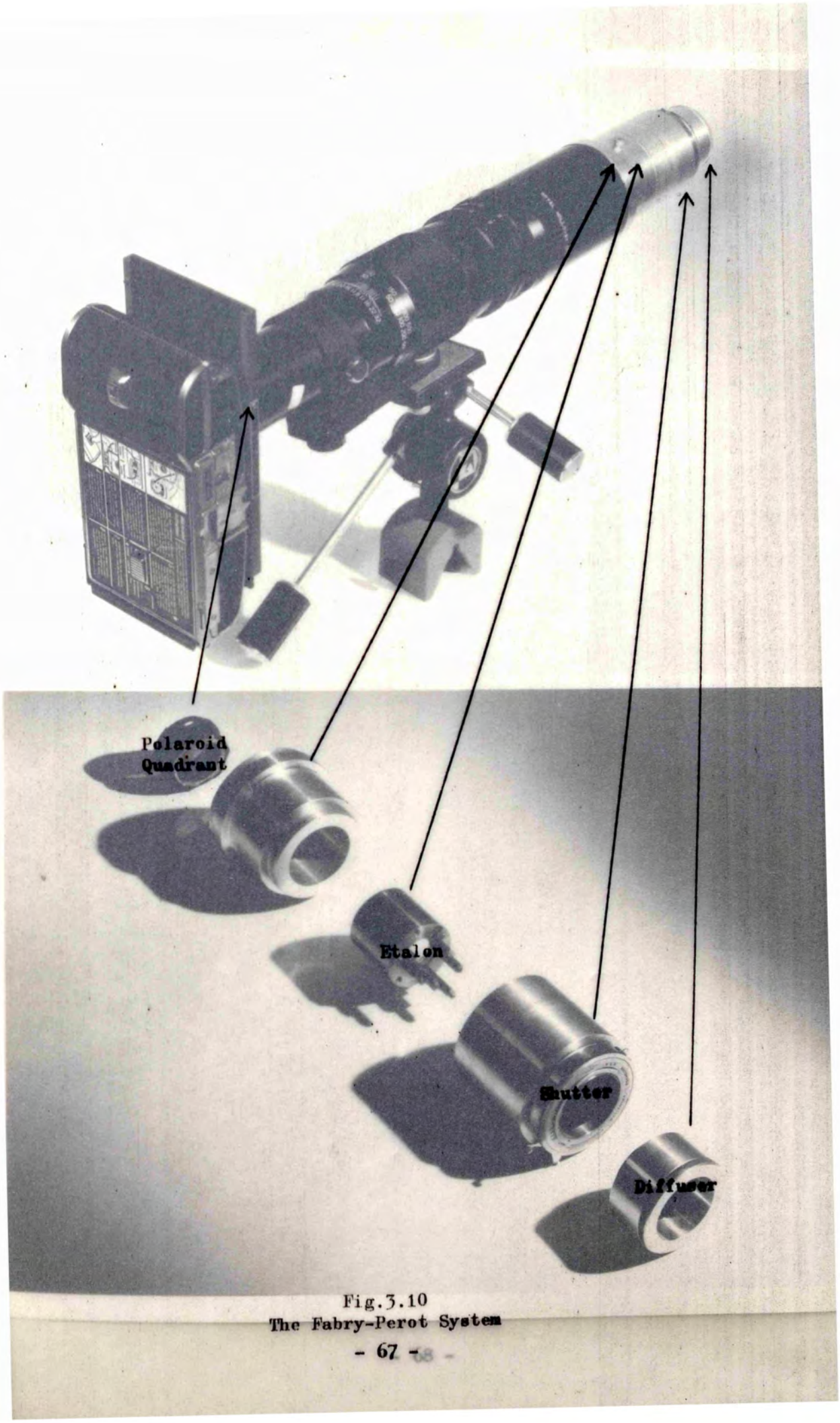

Fig.3.10
The Fabry-Perot System

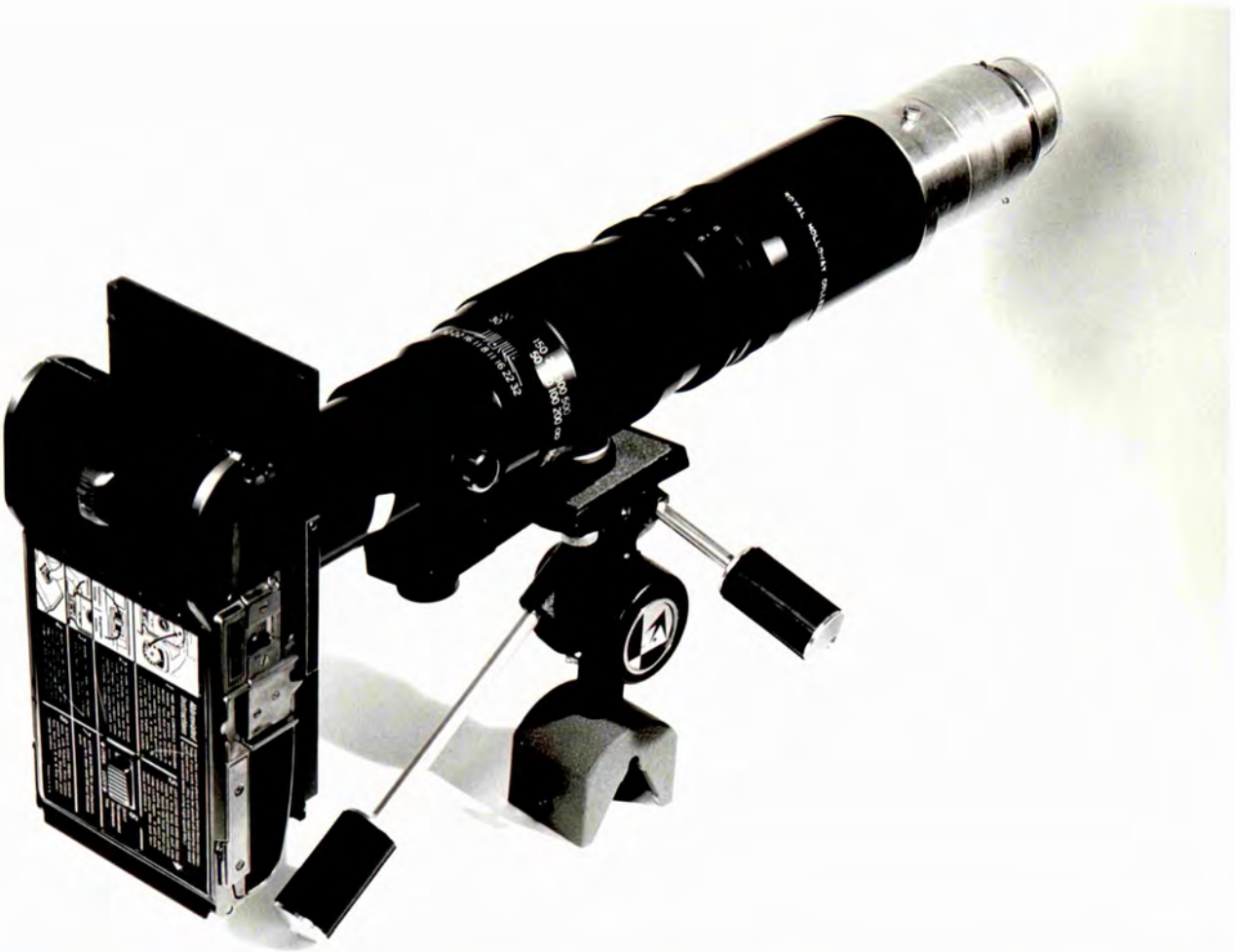

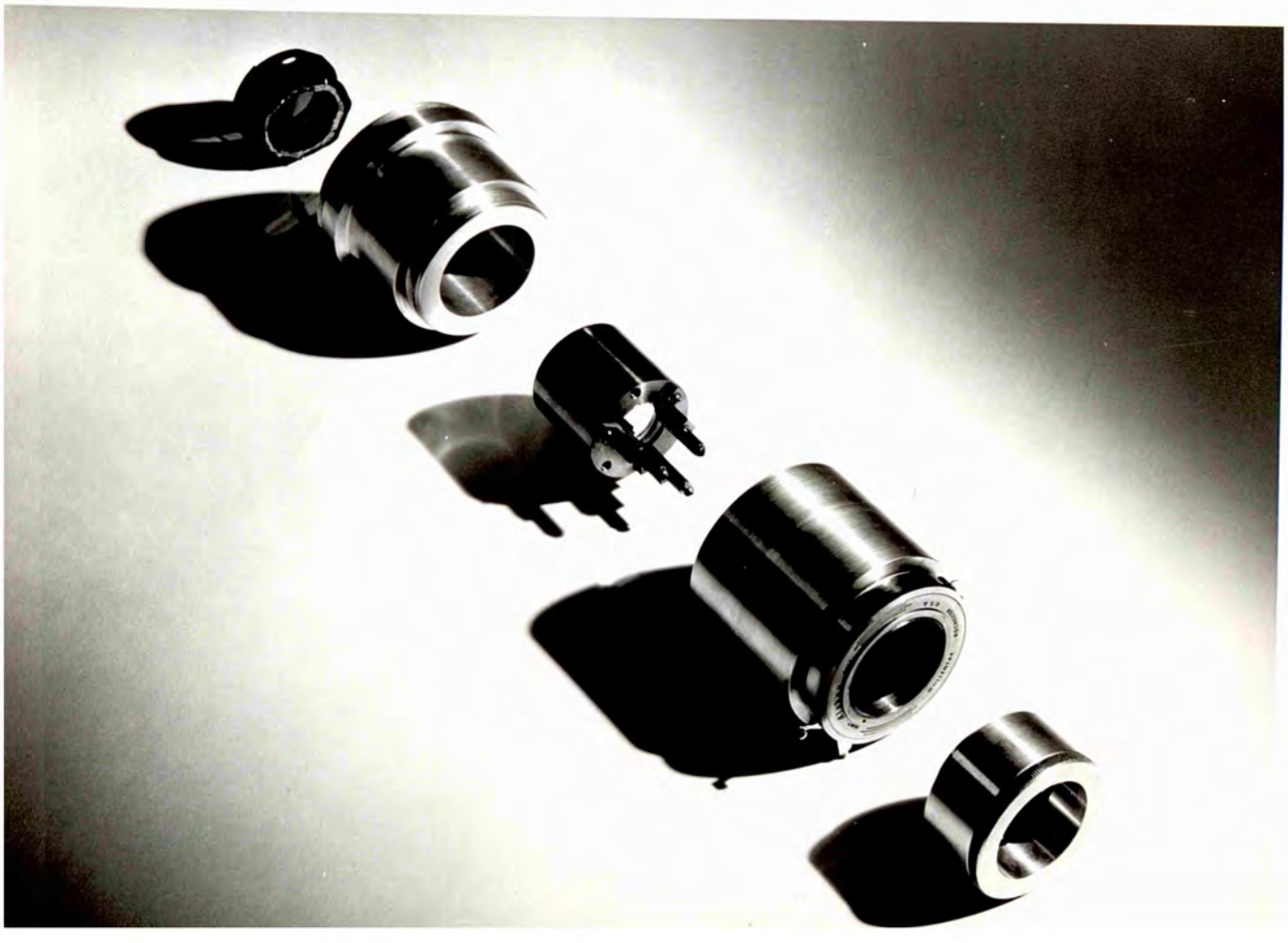

so that ajacent quadrants of the disc transmitted light of perpendicular polarizations. The disc was adjusted so that the light from the forward and backward going beams appeared in separate quadrants. The photographs in Fig.3.9 show the pictures obtained for the forward beam alone, backward beam alone and for the two together. The separation of the two beams is obviously very effective.

The Fabry-Perot system was attached directly to the end of a 76 cm telephoto lens in the manner shown in Fig.3.10. At the other end of the lens were the polaroid quadrants and a camera using polaroid 410 film. The whole arrangement allowed Fabry-Perot photographs to be taken very conveniently and the use of polaroid 410 film, while causing a slight loss of resolution, meant that pictures were immediately available. This was very important since the main purpose of the Fabry-Perot system was to check the mode structure of the laser output rather than to take quantitative measurements.

CHAPTER IV

PRELIMINARY EXPERIMENTS

4.1 RUBY LASER SELF-FOCUSING

At the time that the experiments described in Chapters 6 and 7 of this thesis were being prepared the phenomenon of self-focusing was widely discussed in the literature[133-144]. Advantage was taken of the usual hold-ups due to experimental and equipment difficulties in the main programme to make a brief investigation of self-focusing, with particular reference to the scattering properties of self-focused beams[245]

Fig.4.1(i) shows a self-trapped filament produced when a 20 nsec ruby laser pulse of about 100 MW was focused (from left to right) in a cell of water. The high light intensity at the focal point increases (by electrostriction and the Kerr effect) the refractive index in that region to such an extent that the light is totally internally reflected and propagates as a thin pencil.

The first unusual feature of self-trapping in water that was noticed was that the photographs (taken in light scattered normally to the beam in the plane of its polarization) appeared very different in different samples of water. This is clearly seen by comparison of Figs. 4.1(ii) and 4.1(iii). Each of these photographs shows two crossing self trapped beams generated as shown in Fig.4.2. The conditions under which each was taken were identical except that the water used when Fig.4.1(ii) was taken was freshly distilled while that used for Fig.4.1(iii) had stood in the laboratory for some days. The reason for the dramatically different scattering in these two cases is probably that in the freshly distilled water the very high light intensity caused dissolved air to be released as tiny bubbles with consequent intense

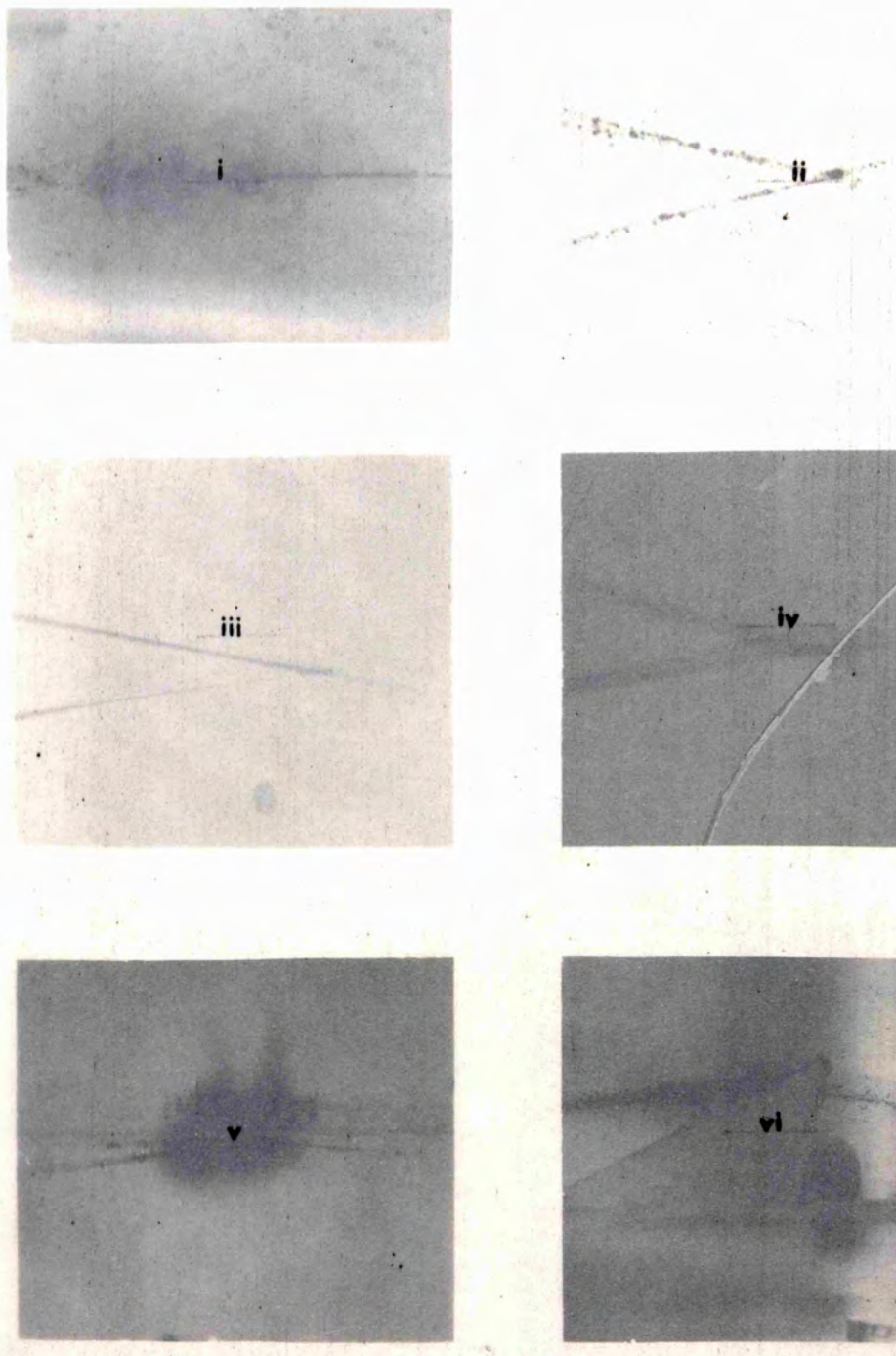

Fig.4.1
Self Trapped Ruby Laser Beams in Water

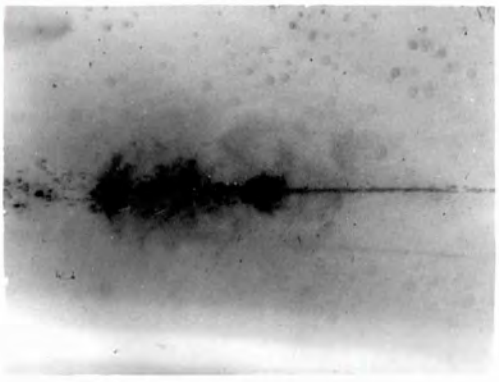

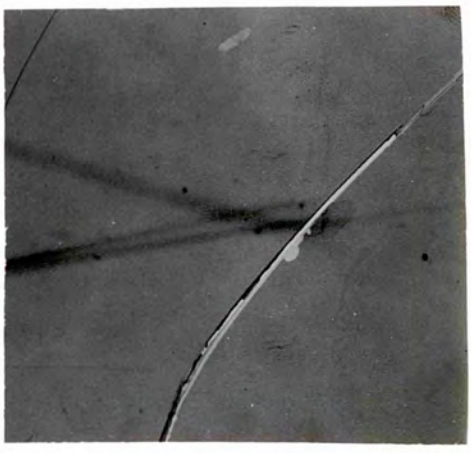

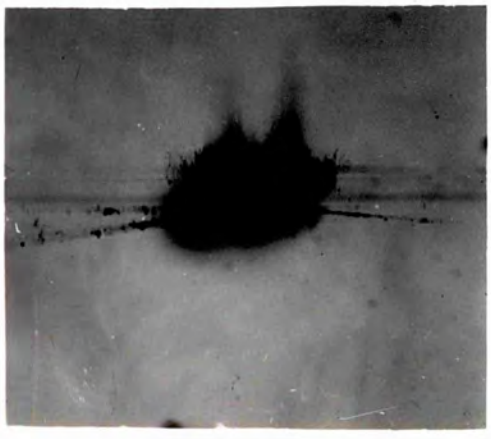

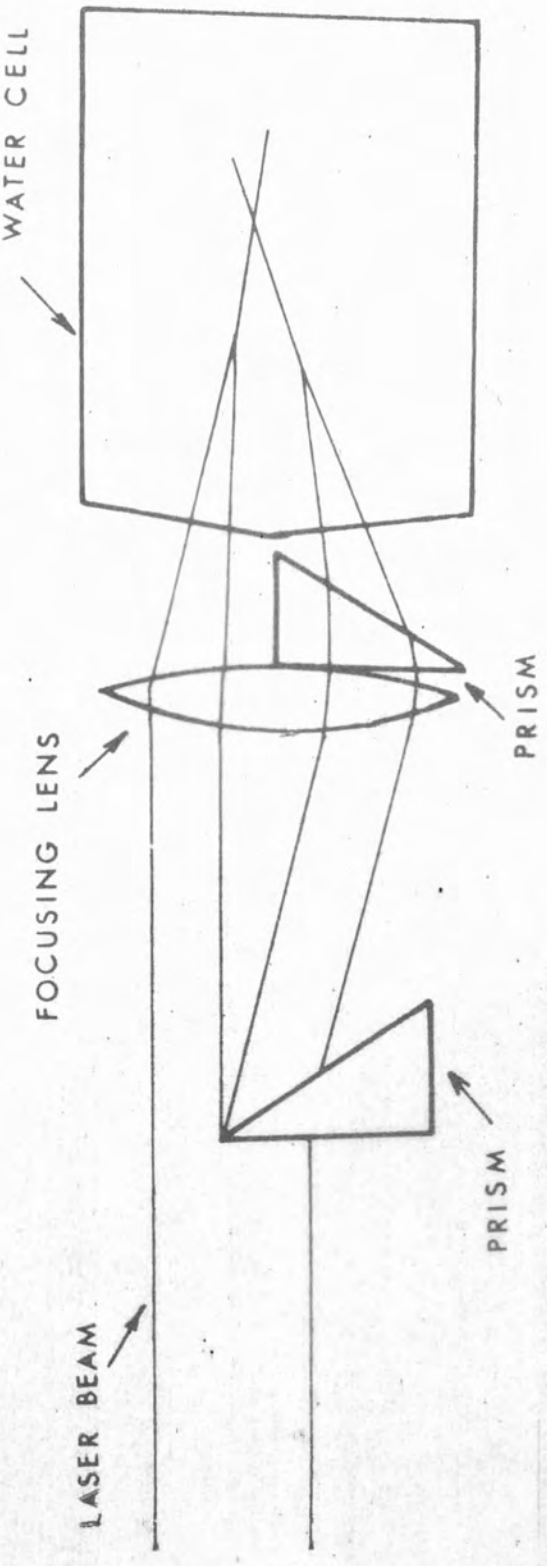

Fig.4.2
Generation of Intersecting Self Trapped Beams

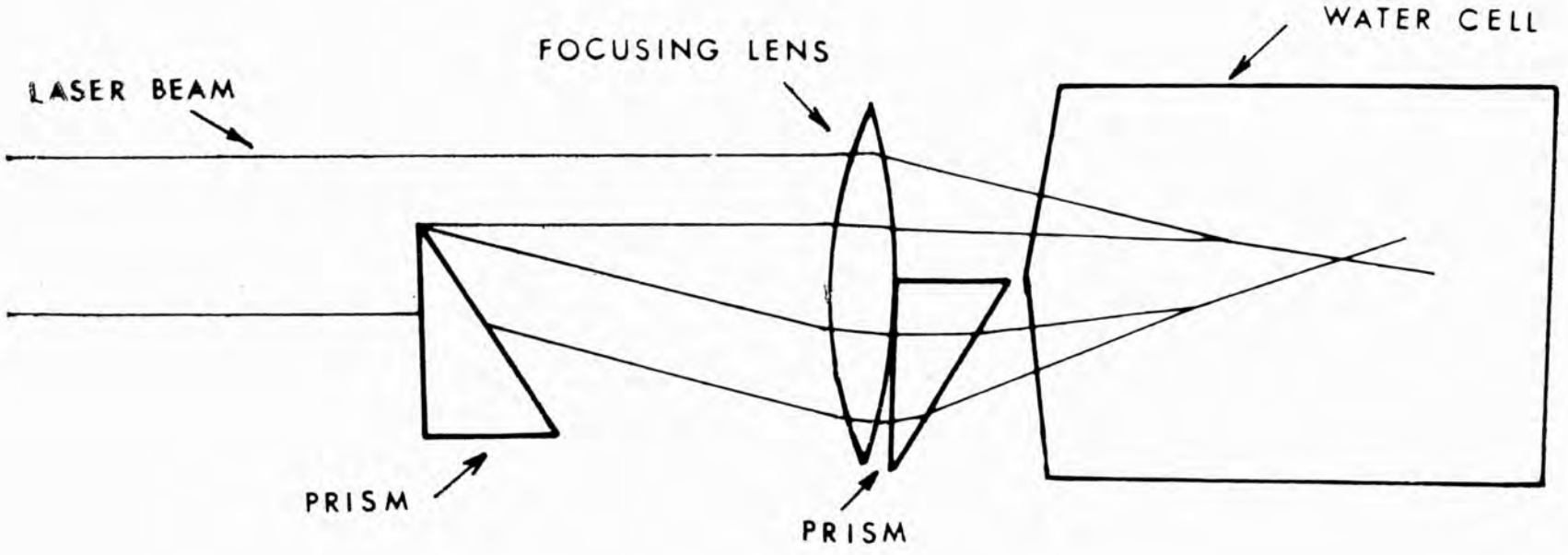
WATER CELL
FOCUSING LENS
LASER BEAM
PRISM
PRISM

localised scattering[178]. The water which had stood for some days contained less air (the air dissolved in distillation tended to be released as bubbles on the sides of a vessel containing the water) and gave a uniform diffuse scattering.

When the two diffusely scattering beams of Fig.4.1(iii) intersected there was a distinct loss of intensity from the upper, more powerful, beam. (A similar loss probably occured in Fig.4.1(ii) but is not obvious because of the non-uniform scattering.) Chaban has shown[211] that when two high intensity light beams overlap a phase grating is produced in such a way that the beams reflect light into each other. The percentage of light reflected from each beam is the same so there is a nett loss of power from the more powerful beam. The accompanying increase in power of the weaker beam is not obvious in the photograph. This is probably because other losses, such as stimulated scattering and reflection from the increased refractive index in the intersection region, accentuate the loss from the more powerful beam while counteracting any power increase in the weaker-beam.

In the focal region the lower beam split into two parts, (Figs. 4.1(iii) and 4.1(iv))the weaker of which bends back towards the stronger (The light streak in Fig.4.1(iv) is due to a damaged plate). The reason for this is probably the very non-uniform intensity distribution of the lower beam generated by the apparatus of Fig.4.2. It is known[149,150] that such a distribution can cause self bending due to the generation of a non-uniform refractive index distribution across the beam.

Figs.4.1(v) and 4.1(vi) show reflection and refraction of self trapped beams. In Fig.4.1(v) the ruby laser beam is focused just before it is incident on the underside of the water surface. The angle of incidence is sufficient to give total internal reflection and a distinct

reflected self-trapped filament can be seen. (The splash seen at the surface is illuminated by the ruby laser flashlamp. It could not move so far during the 20 nsec ruby laser pulse.) The filament shown in Fig.4.1(vi) passed right through the glass prism, being refracted in the usual way. There was severe damage to the prism, a series of concentric rings on the surface indicating the effect of a powerful shock wave. This could easily have been caused by electrostriction showing that this is a powerful effect in self-trapped filaments though the Kerr effect may be more important as their cause[136-142].

4.2 ARGON LASER DEFOCUSING

While the electrostriction and Kerr effect due to a laser giant pulse cause self focusing the decrease in density due to absorption of a continuous laser beam has the opposite effect of defocusing[145-148].

The far field pattern of the argon laser beam, after transmission through a 5 cm cell of a solution of iodine in nitrobenzine with an absorption coefficient of about ·05 cm^{-1} is shown in Figs.4.3 and 4.4.

The photographs in Fig.4.3 show the stable pattern set up after some time when the argon laser beam had the powers shown in the diagram. At low powers defocusing was insignificant and good collimation was retained. As the power was increased the spot became a diffraction pattern of increasing size and complexity, retaining an almost circular shape in the lower half and becoming increasingly flattened at the top.

Fig.4.4 shows the time development of the pattern when a ·6 W beam was suddenly incident on the cell. As the liquid in the beam path was heated the transmitted spot spread into an increasing number of circular fringes until convection of the heated liquid began to occur in the cell. When this happened the rings no longer increased in size and number but

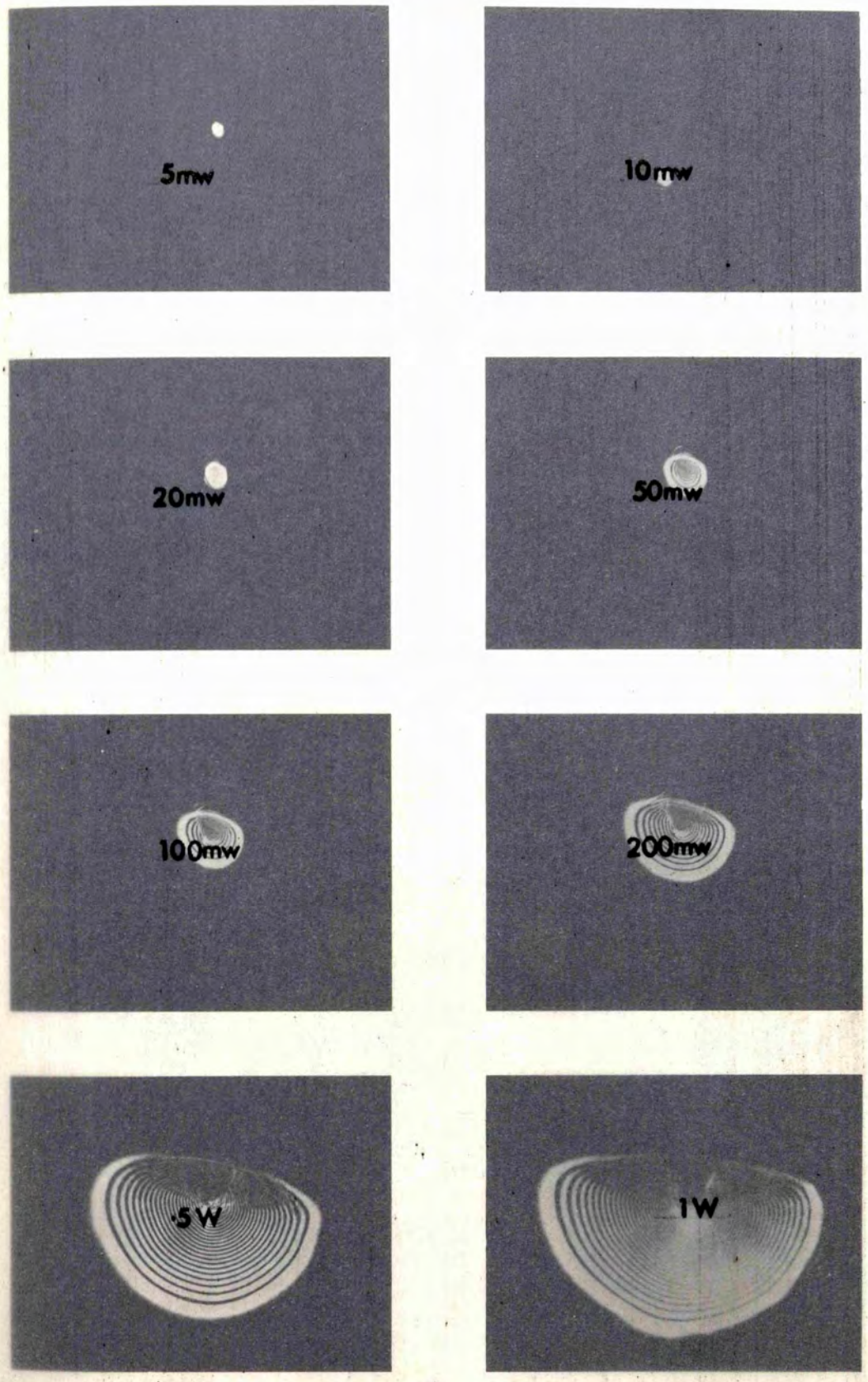

< 1° >

Fig.4.3
Defocusing of the Argon Laser Beam

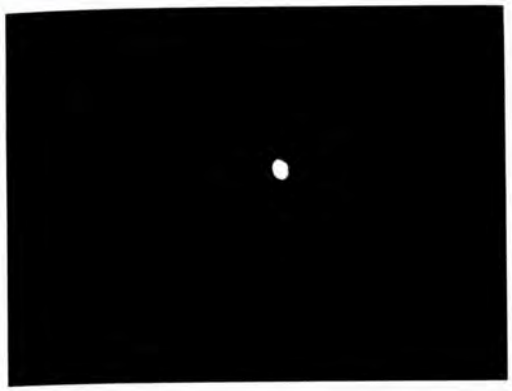
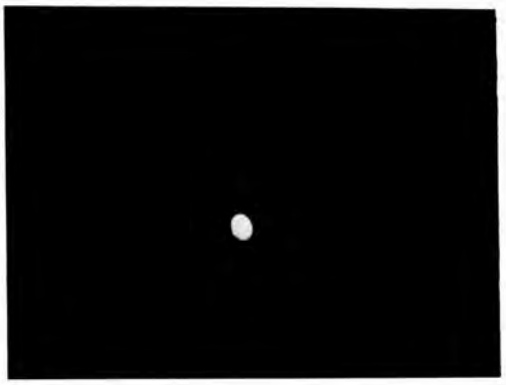
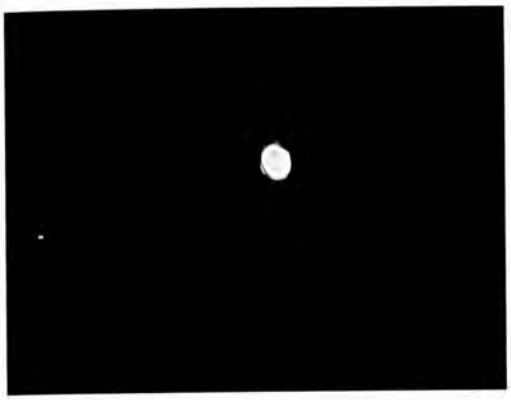
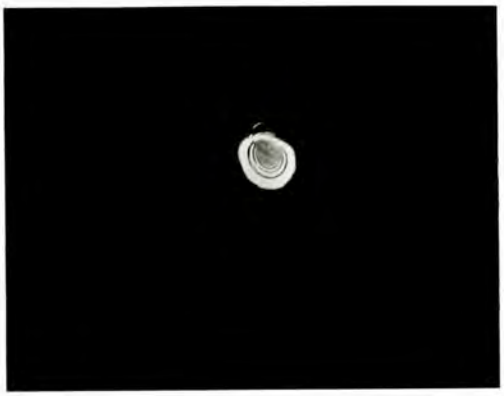
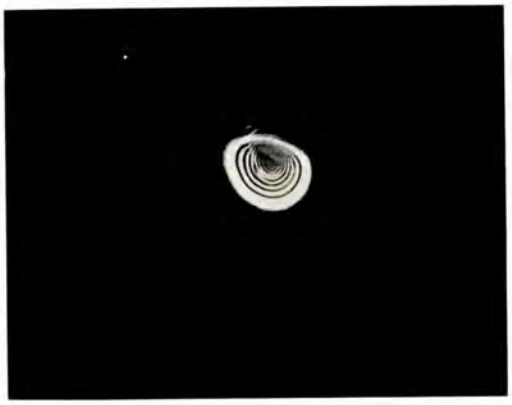

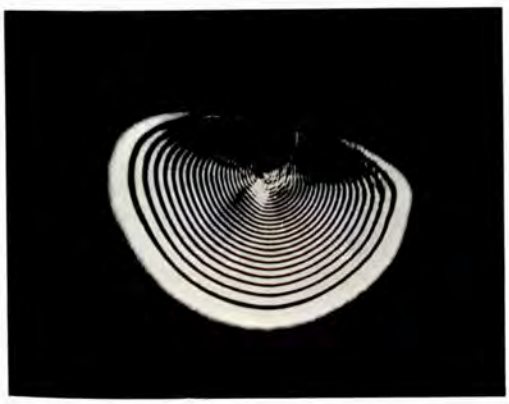


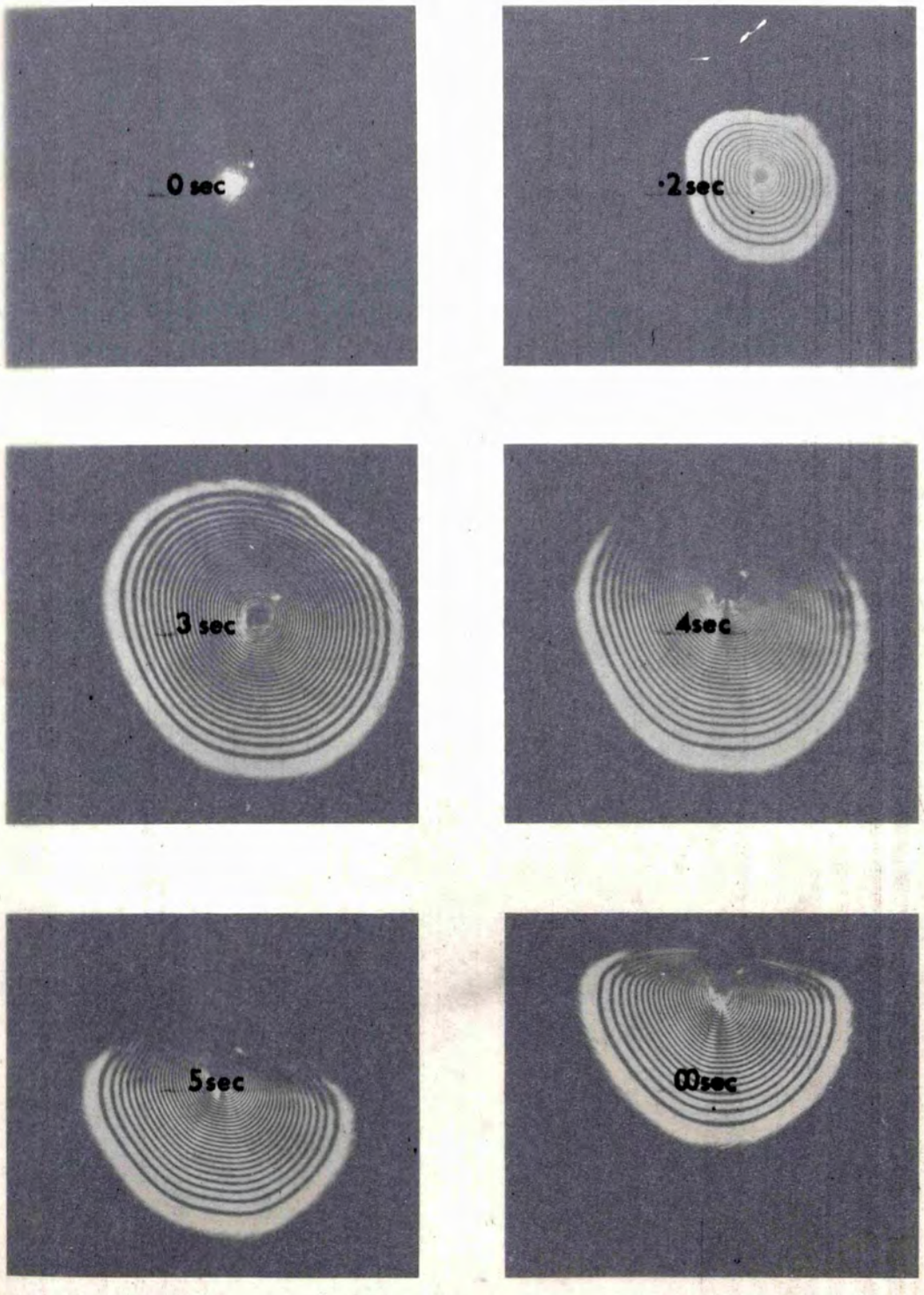

< 1° >

Fig.4.4
Temporal Development of Defocusing

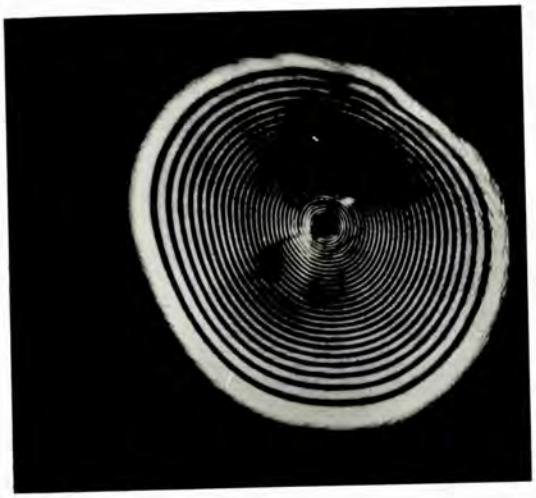

became distorted as there was a refractive index gradient in the lower part of the beam, where cool liquid was drawn in, but much less gradient in the upper part, where the heated liquid flowed away.

4.3 RESIDUAL RUBY GAIN AND MULTIPLE STIMULATED SCATTERING

In stimulated scattering processes laser light is reflected from a disturbance caused by its own wave front. For this reason the scattered light forms a beam in precisely the reverse direction to the incident beam. Any divergence in the incident beam is replaced by convergence in the scattered beam which thus enters the laser with the same diameter as the initial beam[171,172,174,178].

In the experiment illustrated in Fig.4.5 the distance of the cell (which contained ether) from the laser was such that the light beam scattered from the cell arrived at the ruby after the end of the initial giant pulse. (As the velocity of light is about one foot per nanosecond and the pulse duration about 20 nsec the cell had to be at least ten feet from the laser.) This light incident on the ruby rod immediately after the end of the giant pulse served as a measure of the residual gain left in the rod. The residual gain in the rod is proportional to the residual population inversion which can be shown to be given by the equation[232]:

$$e^{n_f/n_p} = e^{n_i n_p} .$$

This, as shown in Fig.4.6 has the trivial solution $n_f = n_i$ which holds so long as lasing has not been initiated and a real solution where n_f is a sharply decreasing function of n_i. (n_f cannot be greater than n_i so $n_f = n_i$ is the only real solution when $n_i < n_p$, i.e. no lasing can occur. This is of course physically obvious.)

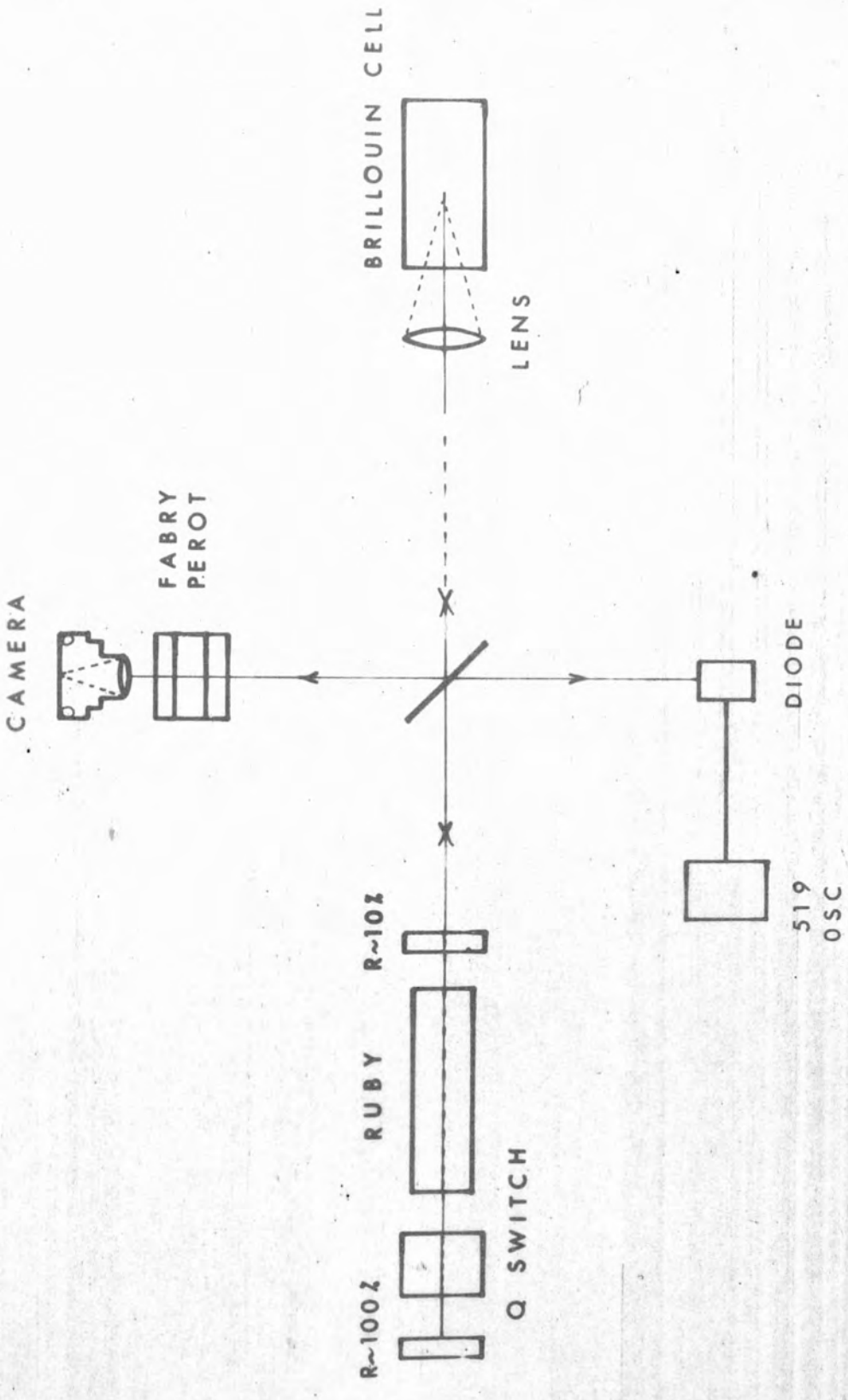

Fig.4.5
Multiple Scattering Apparatus

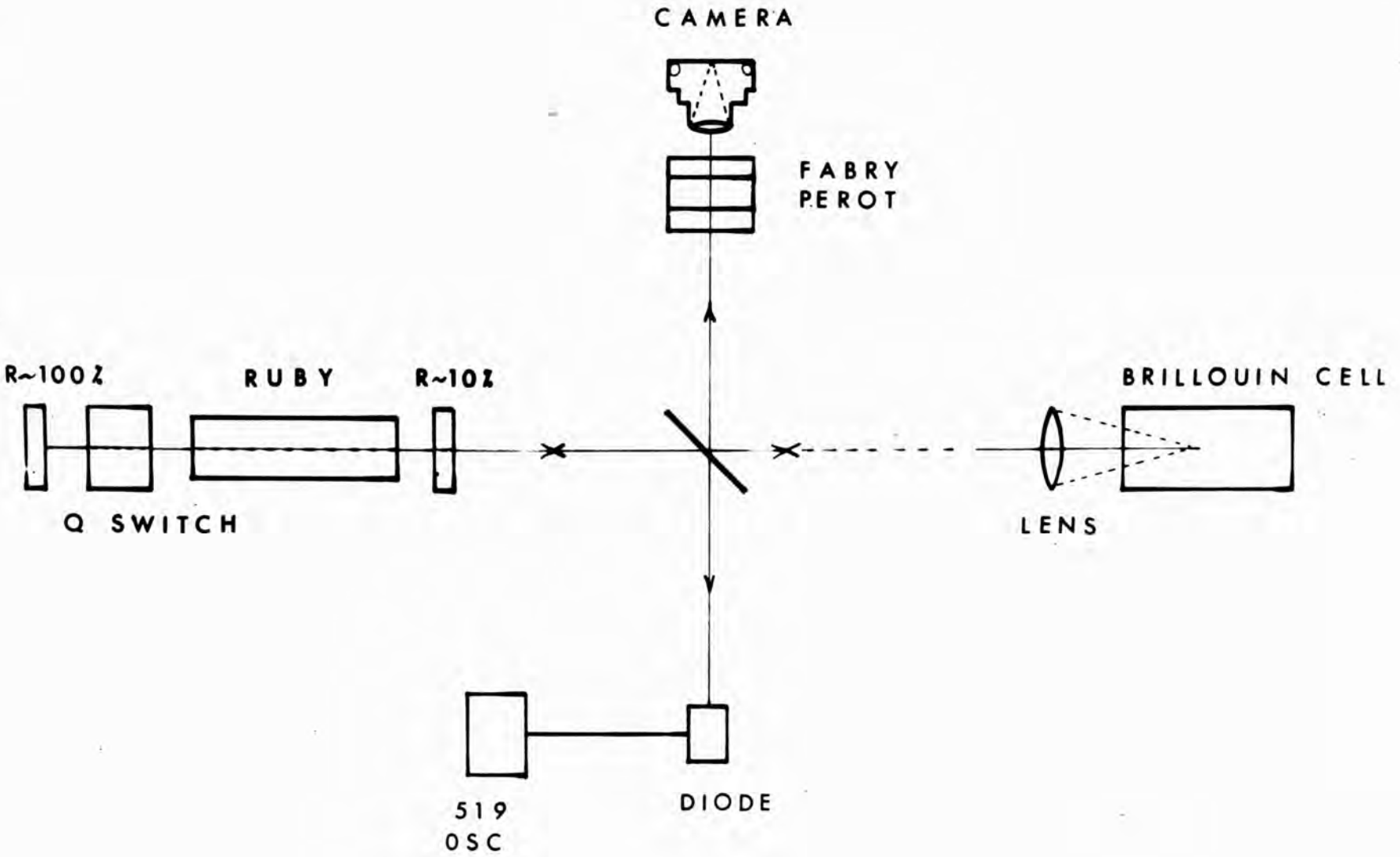
CAMERA
FABRY
PEROT
R~100%
RUBY
R~10%
BRILLOUIN CELL
Q SWITCH
LENS
519
OSC
DIODE

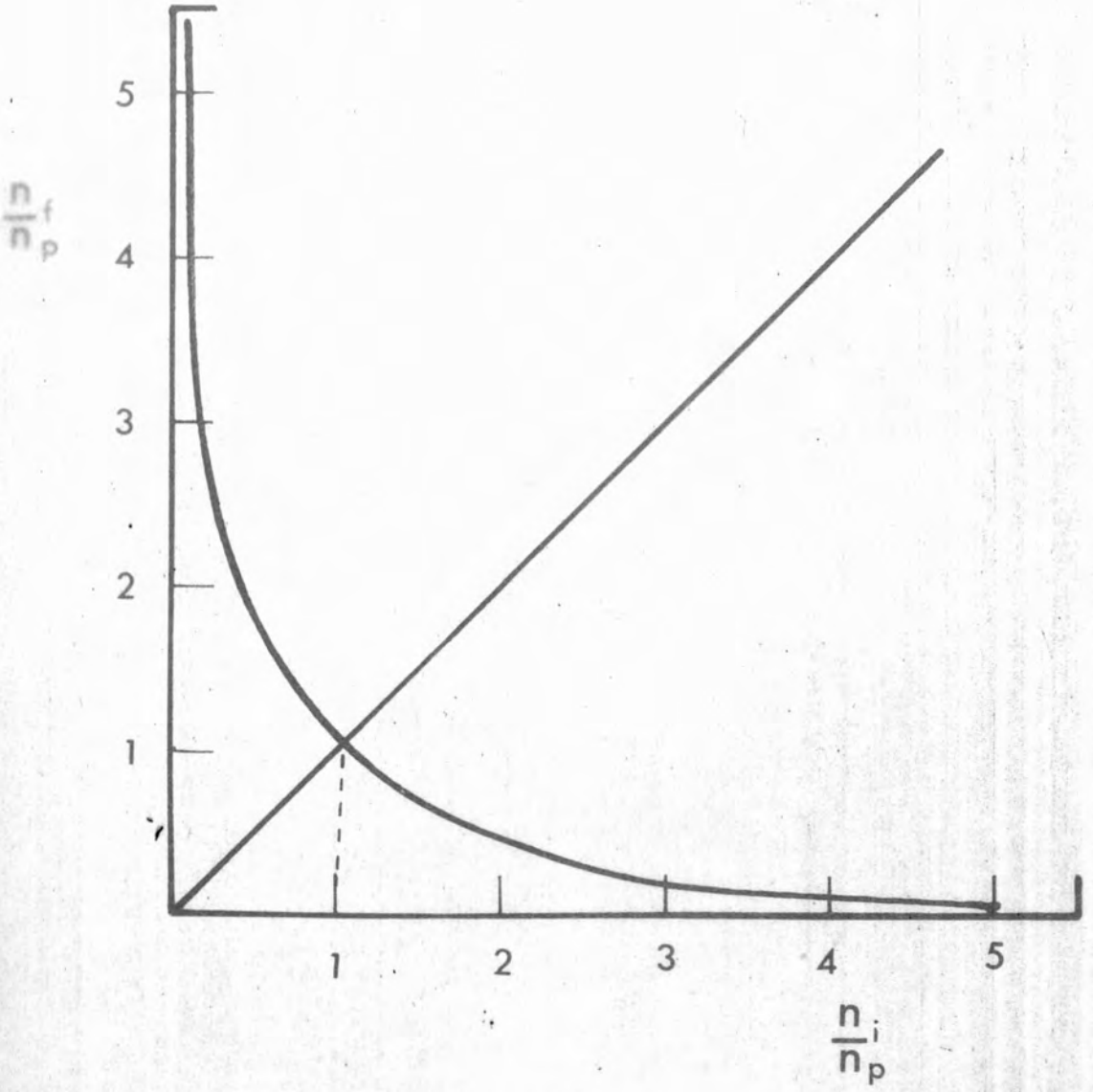

Fig.4.6
Residual, as a Function of Initial Gain

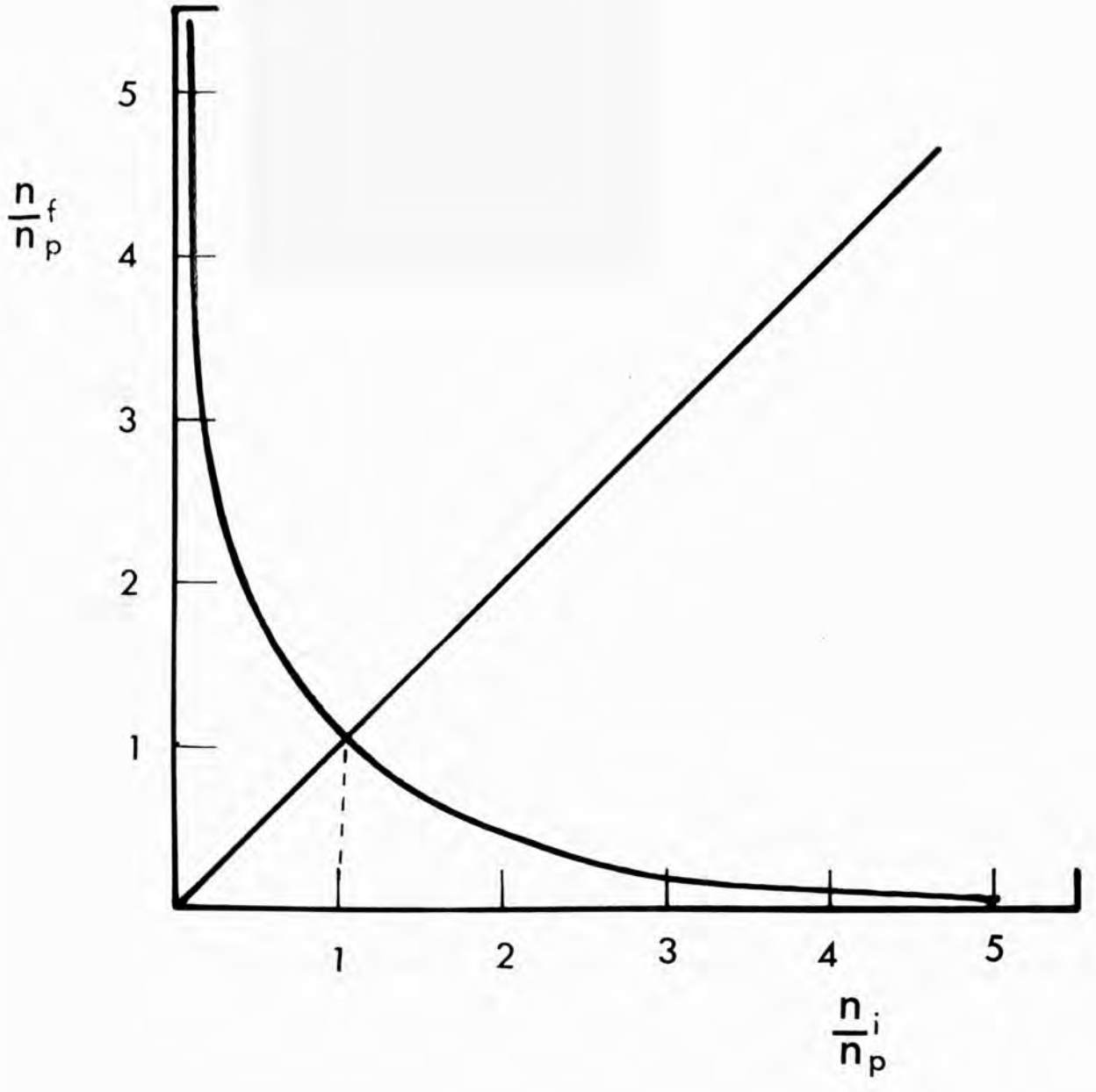
$\frac{n}{n_p}_f$
5
4
3
2
1
1
2
3
4
5
$\frac{n}{n_p}_i$

Figs.4.7 and 4.8 show the results of an experiment to check this prediction, (the short trace is that of the Tektronix 551, not shown in Fig.4.5, which checks that a single giant pulse occurs). When the gain in the rod was greater than the losses in the rest of the system the scattered pulse was re-amplified and re-scattered with increased power. Each re-amplification decreased the inversion left in the rod so that eventually the power decreased till the Brillouin threshold was reached and the process ceased.

In Fig.4.7 the results obtained with a very strongly and very weakly Q-switched giant pulse are shown. With the strongly Q-switched pulse there was very high initial and consequently very low final population inversion. The gain in the ruby rod was thus small while the loss in the Q-switch was large. As a result only one stimulated Brillouin pulse occurred. In the weakly switched case there was enough residual inversion to give a gain between successive pulses of about $2\frac{1}{2}$ times even after all the losses in the system. A large number of pulses occurred before the gain in the ruby rod was reduced and the pulses faded away. (The later pulses are obscured by electronic ringing the full number being about fifteen.)

In Fig.4.8 the results at intermediate Q-switching levels are shown. A steady decrease in gain and number of pulses produced is observed with increasing initial inversion.

Feedback of this kind can occur in all stimulated scattering experiments and can be most confusing. It should in principle always be eliminated but the only reliable way to do this is to use a Faraday isolator[194,233] which is technically difficult and introduces problems of its own such as beam degradation, damage etc. In the more important experiments described in this thesis a compromise system was used. A

519 traces

Transmission of Q-switch

551 traces

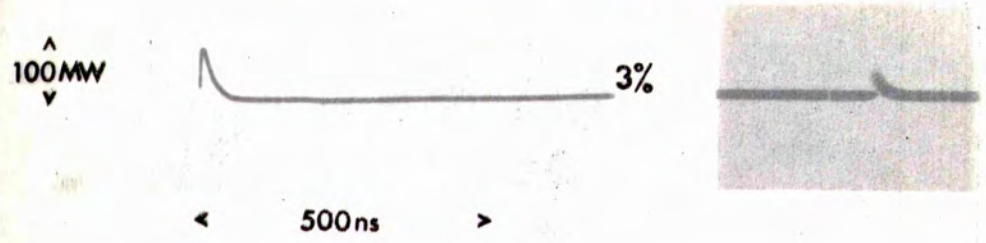

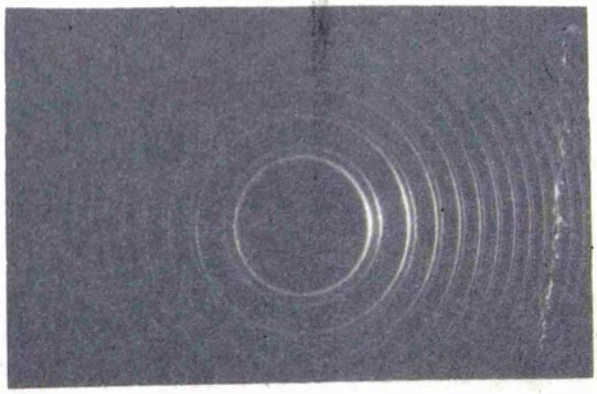

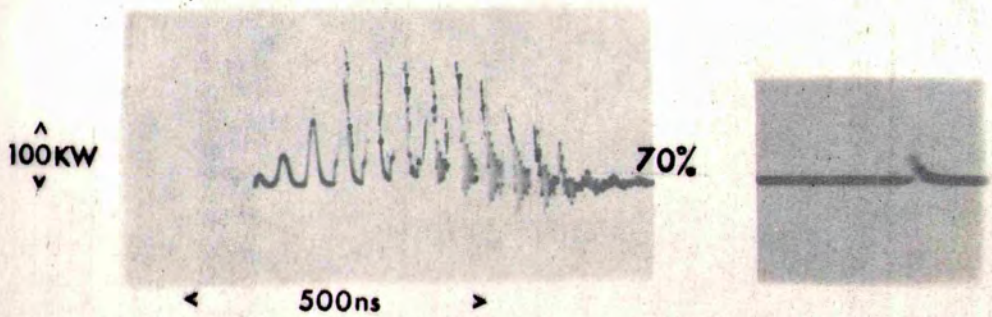

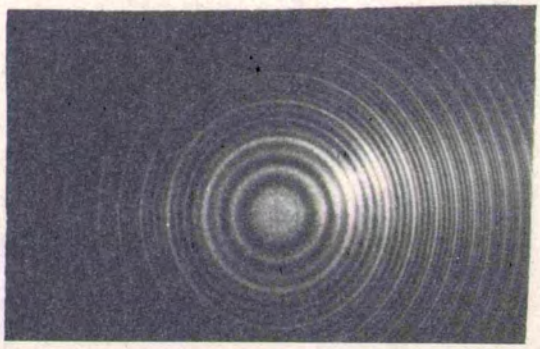

Fig.4.7
Multiple Scattering with Strong and Weak Q-switching

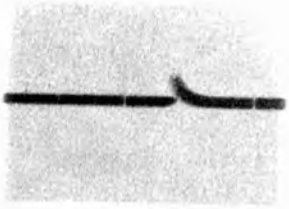

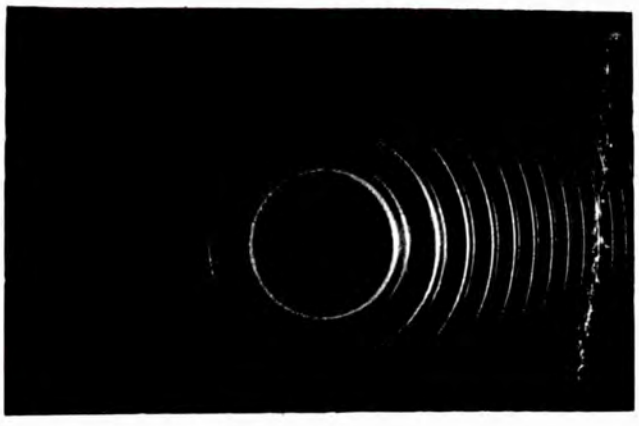

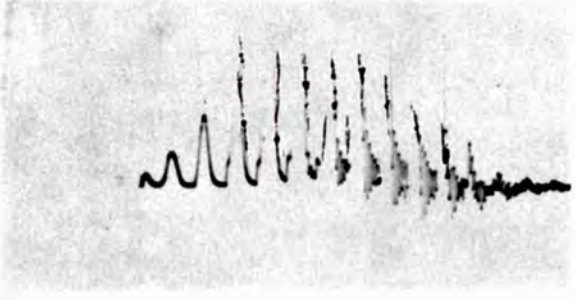

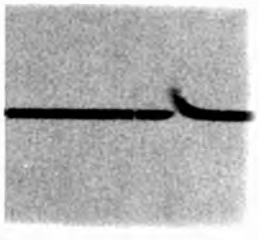

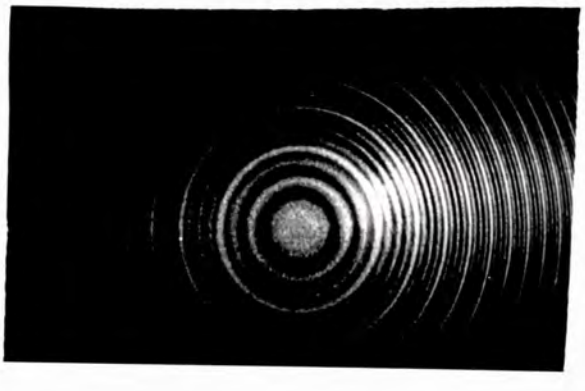

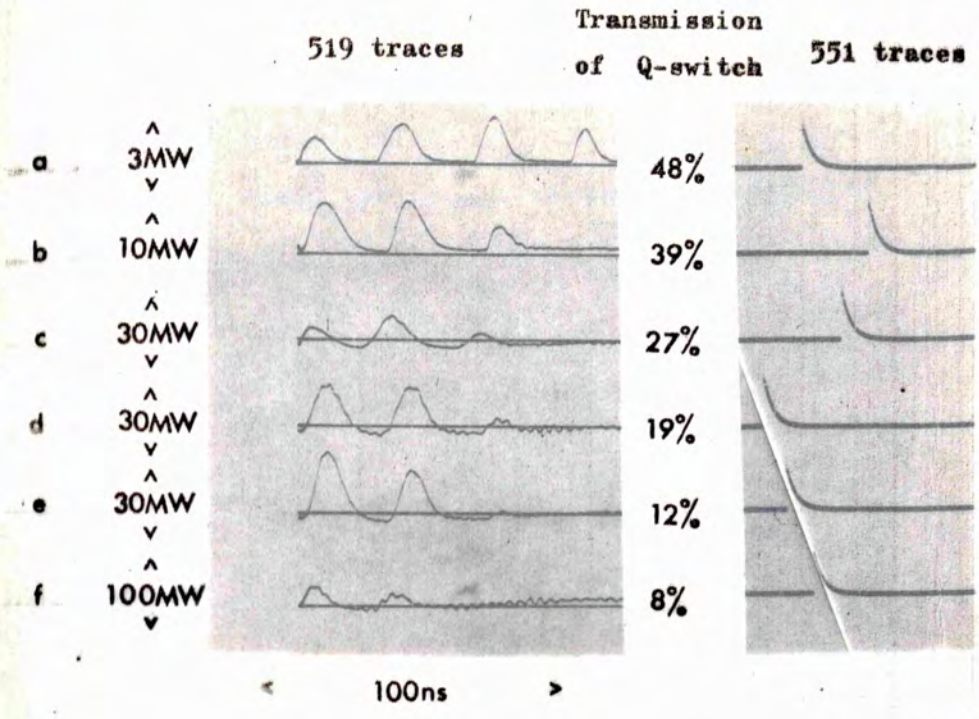

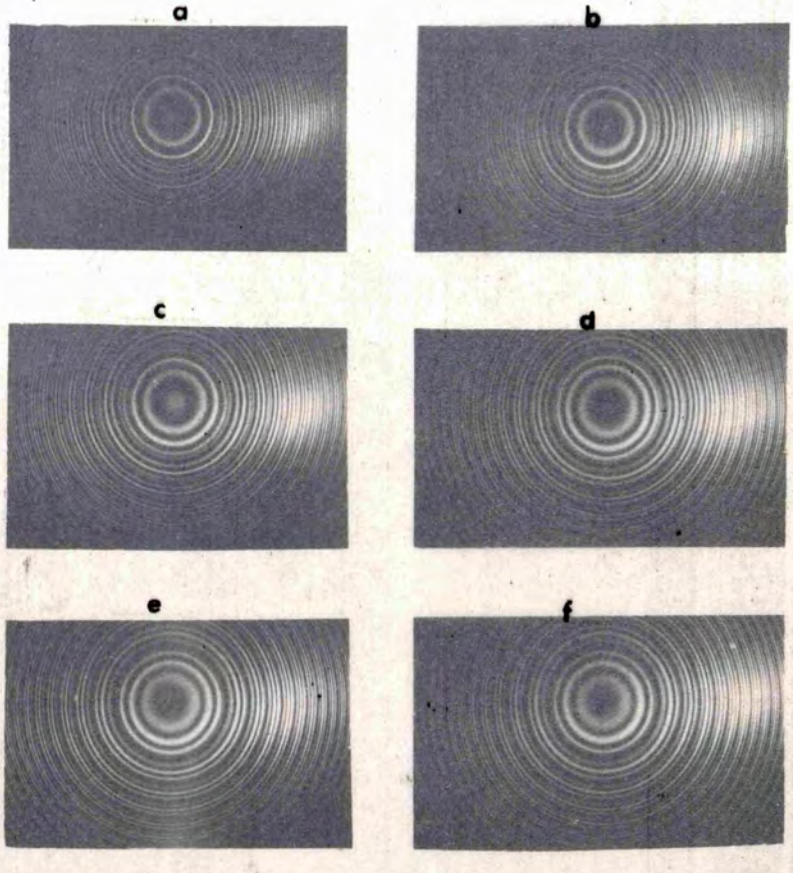

Fig.4.8
Multiple Scattering with Intermediate Q-switching

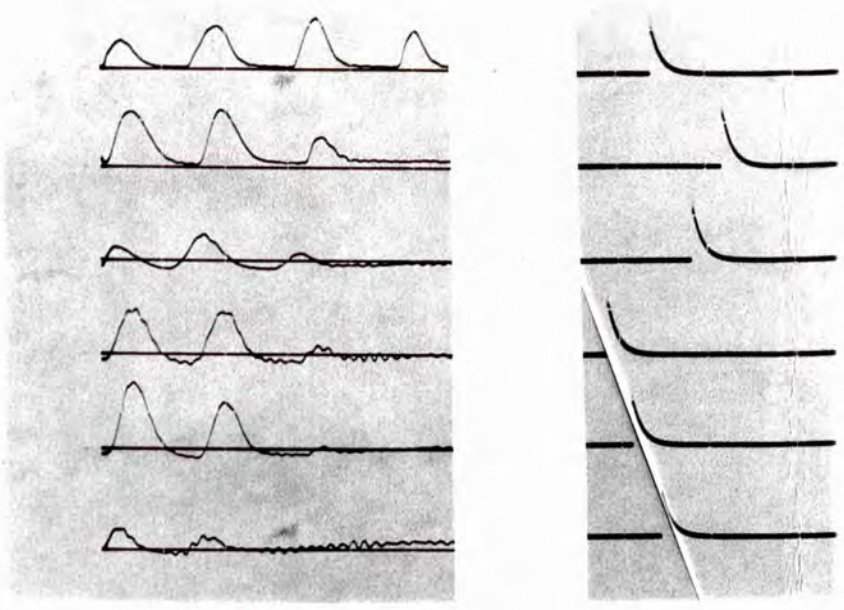

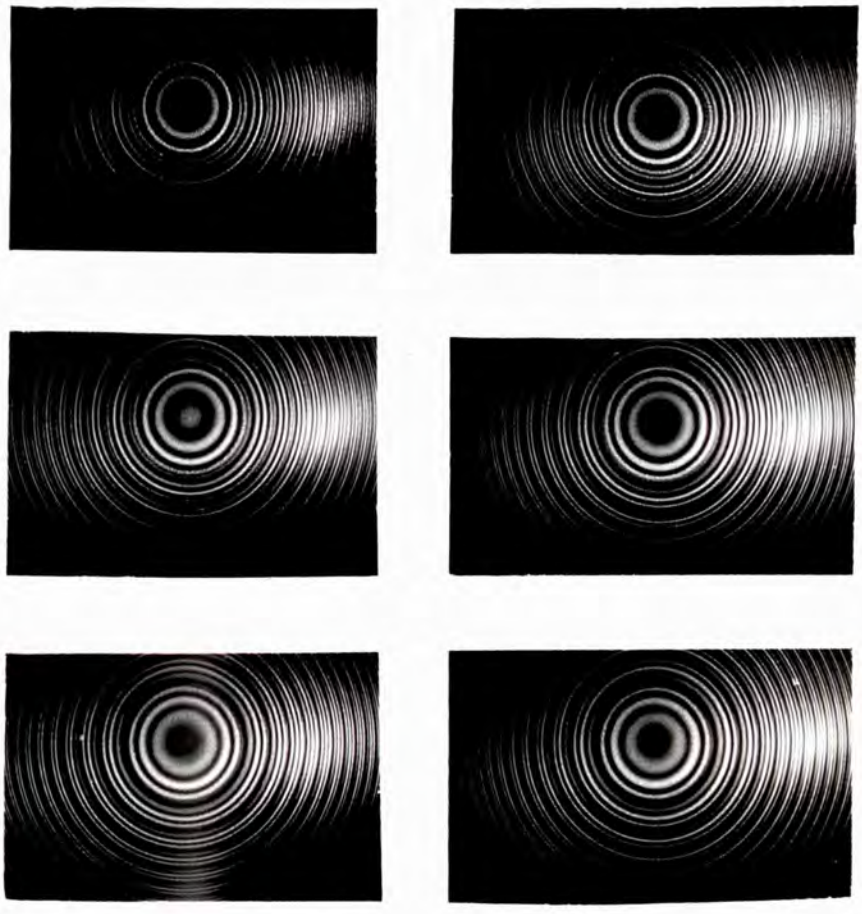

cell with an absorbing solution transmitting up to 20% of light at 6943 Å was placed in front of the laser. This of course wasted much of the beam power but, while not totally excluding feedback, cut it down by a factor of at least twenty-five.

4.4 REFLECTIONS WITHIN THE Q-SWITCH CELL

In the Q-switch of a ruby laser two beams of light of the same frequency traverse an absorbing medium in opposite directions. More energy is absorbed at the antinodes of the resulting field than at the nodes thus creating a temperature modulation in the medium. This in turn caused a refractive index modulation or phase grating from which the light can reflect. (This may be regarded as a form of stimulated thermal Rayleigh scattering[197-200] with external feedback of unshifted frequency provided by the laser mirror).

It has been suggested that such reflections within the Q-switch cell can have an important effect on Q-switch dynamics particularly when using pure, slightly absorbing solvents[234].

Beam splitters were placed in front of and behind the Q-switch cell of the ruby laser and the incident and transmitted powers were measured in the forward and backward directions, (Fig.4.10). Unfortunately at this time only two detectors were available so the measurements could not be taken simultaneously. However only the ratios of transmitted to incident beam powers in each direction are important so this should not have caused much error. Fig.4.9 shows these beam powers with (lower four photos) and without (upper four photos) dye in the Q-switch. Assuming that no non-linear processes can occur at the low powers involved in the latter case these photographs can be used to calibrate the detection systems for finding the reflectivity in the former case.

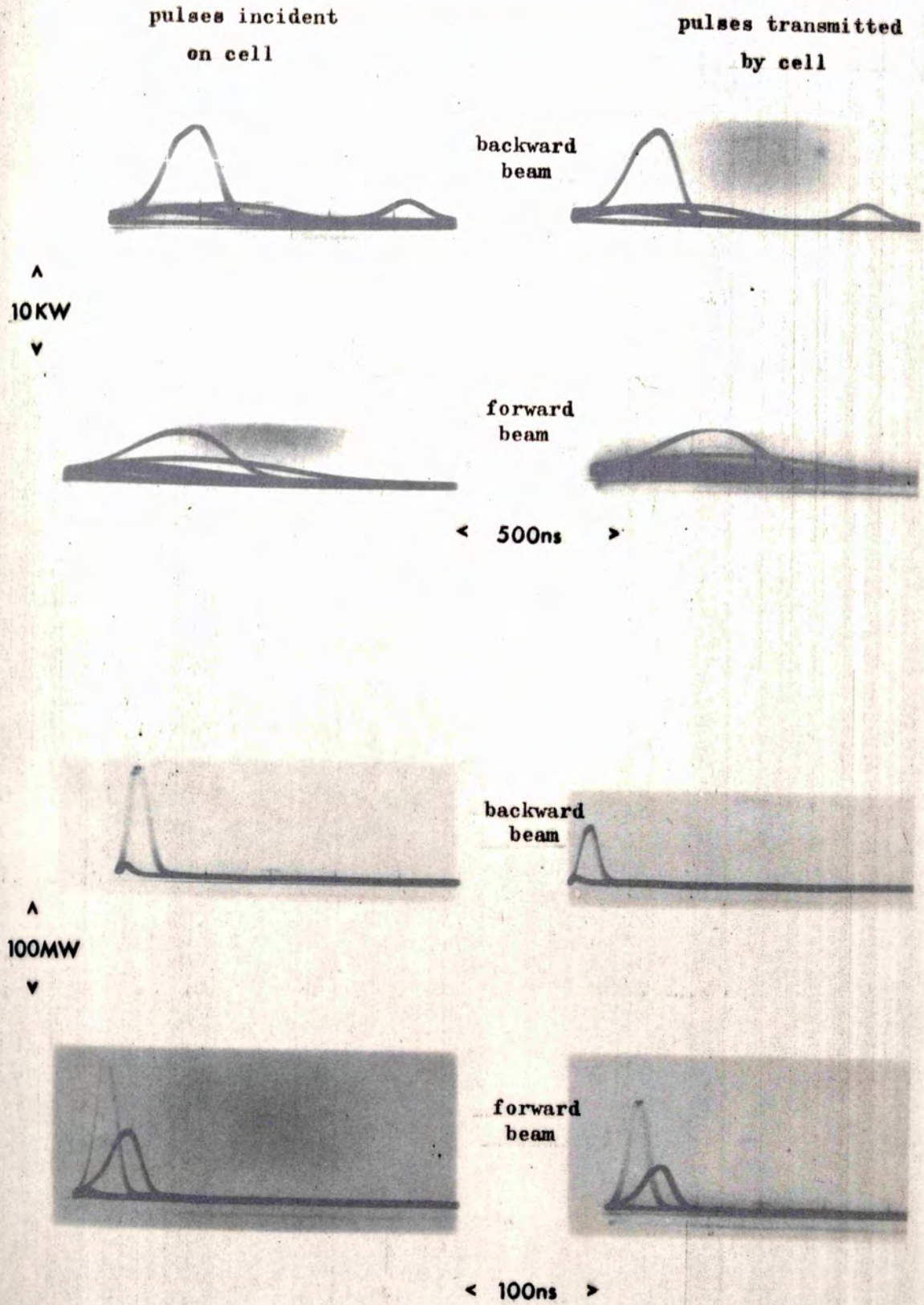

Fig.4.9
Pulses incident on and transmitted by Q-switch cell

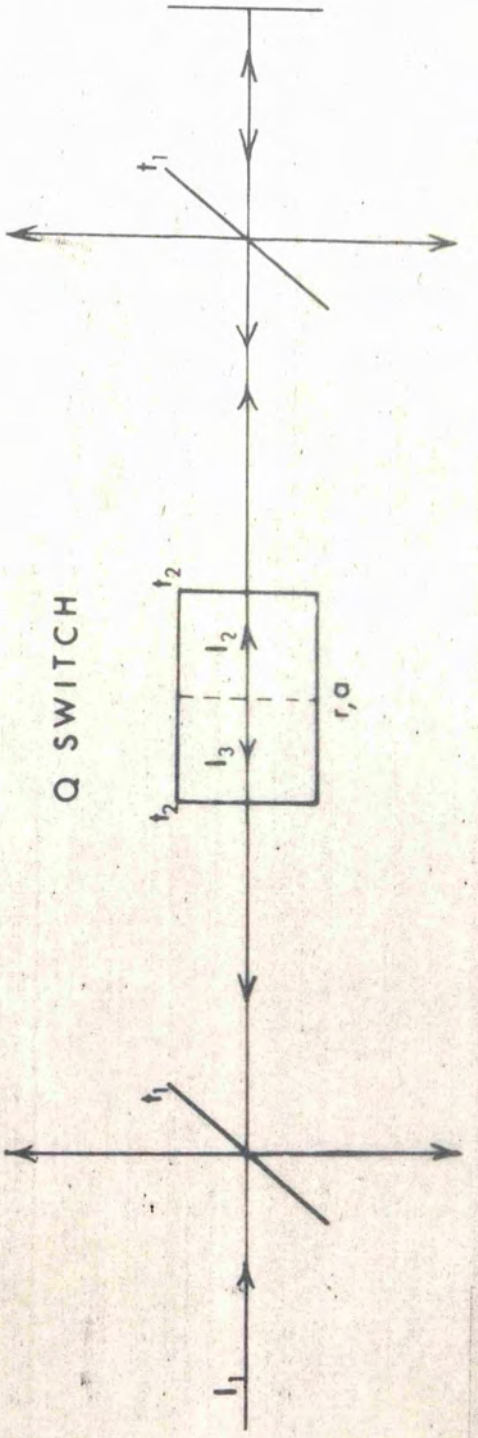

Fig.4.10
Reflections within the Laser Q-Switch

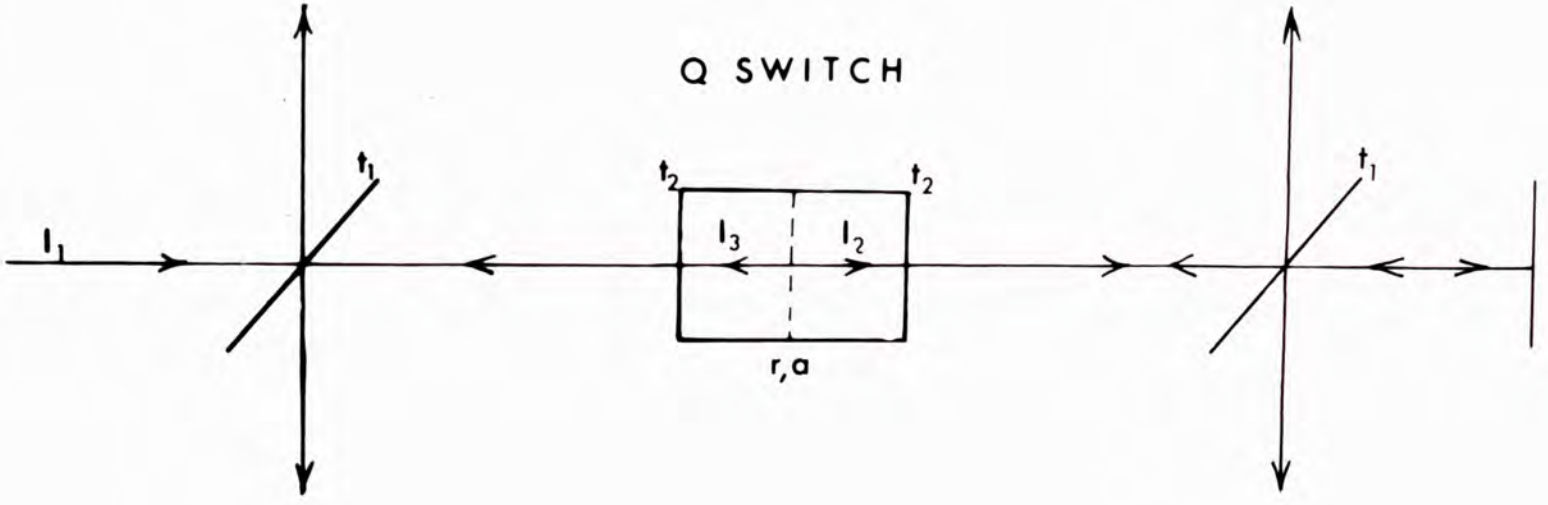
Q SWITCH
t_1
t_2
t_2
t_1
I_1
I_3
I_2
r, a

The induced reflectivity and absorption of the cell may be considered as a localised layer between the lossy walls of the cell, which is itself between two lossy beam splitters, the whole system being in front of the 100% rear laser mirror (Fig.4.10). We may write for the light travelling away from the layer in each direction

$$I_2 = I_1 t_1 t_2 (1 - r)(1 - a) + I_2 t_1^2 t_2^2 r$$

$$I_3 = I_2 t_1^2 t_2^2 (1 - r)(1 - a) + I_1 t_1 t_2 r \quad .$$

Hence:

$$r = \frac{t_1^2 t_2^2 \left(\frac{R_1}{R_{1,0}} \cdot \frac{R_2}{R_{2,0}} - 1 \right)}{\left(\frac{R_1}{R_{10}} \right) - t_1^4 t_2^4} \quad .$$

For the photographs in Fig.4.9

$$R_{1,0} = 1{\cdot}05 \qquad R_1 = 1{\cdot}90$$

$$R_{2,0} = {\cdot}95 \qquad R_2 = {\cdot}80$$

but $t_1 \sim {\cdot}95$, $t_2 \sim {\cdot}85$,

thus $r \sim {\cdot}13$.

Owing to the elementary theoretical analysis (which took no account of interference or the extended region of reflection and absorption) and the practical difficulties (measuring R_1 and R_2 for different laser shots when α and r could be different) this can only be taken as a crude estimate. Repetition of the experiment showed a variation in the estimate of r of about 50% .

CHAPTER V

STUDY OF FLUORESCENCE DUE TO EXCITED STATE ABSORPTION

5.1 EXPERIMENTAL ARRANGEMENT:

During one of the experiments described in Chapter 8, a solution of cryptocyanine in methanol was used in the probe scattering cell. Under these conditions the Bragg reflection of the argon laser light was obscured as an intense blue fluorescence at approximately the same frequency. The high degree of collimation of the Bragg reflected beam allowed this difficulty to be overcome by placing the detectors at a greater distance from the cell. The nature of the fluorescence however remained of some interest and was investigated for a variety of dyes and solvents[248].

In these investigations the ruby laser was strongly Q-switched to give a 200 MW, 15 nsec pulse which was passed through a cell containing a solution of copper sulphate of which the concentration was varied in order to vary the transmitted power. This method of varying the power was preferable to that of varying the concentration of dye in the Q-switch as the beam divergence, pulse duration and spectral composition of the resulting beam were less affected.

The beam obtained in this way was passed through a cell containing the solution to be investigated. A dilute solution in a thin cell was used so that intensity variations within the solution should be minimized. The use of a thin cell, misaligned with respect to the ruby laser beam also helped to avoid the occurrence of stimulated effects within the liquid. The resulting fluorescence was detected with a Mullard 56 AVP photomultiplier, red light being excluded by Jena BG 18 green filters and blue light, from the laser flash tube, by a Wratten 29 filter placed after the copper sulphate attenuator. (This filter itself produced some blue, two photon, fluorescence but the effect of this on the detector was

negligible providing the cell was placed at a considerable distance from the filter.) The incident laser power was monitored with a photodiode and, using a delay line, the diode and multiplier signals were displayed on the same trace of Tektronix 454 oscilloscope.

5.2 TWO PHOTON ABSORPTION

In order to check the experimental technique fluorescence was first investigated using a solution of Rhodamine 6G in methenol, a well known two photon absorber[135]. In this case there is no real intermediate energy level to saturate and the fluorescence should be proportional to the square of the incident intensity for all accessible power levels[105,140].

The experimental dependence of fluorescence on incident intensity shown in Fig.5.1, is in excellent agreement with the theoretical line indicating a square law.

The absorption spectrum of chloronapthalene, shown in Fig.5.2, reveals high absorption at twice the ruby laser frequency. Two photon absorption is therefore possible in this solvent without any added solute. The dependence of the fluorescence on the incident intensity for chloronapthalene is shown in Fig.5.3. This dependence is a square law for fairly low incident intensities but this law breaks down for intensities greater than about 3×10^6 W/cm^2. At the same power level the duration of the fluorescent pulse changes from approximately that of the laser pulse to one considerably longer. The reason for this change is probably chemical breakdown in the liquid[235] and may be connected with the fact that chloronapthalene is very difficult to purify and particularly to keep dry.

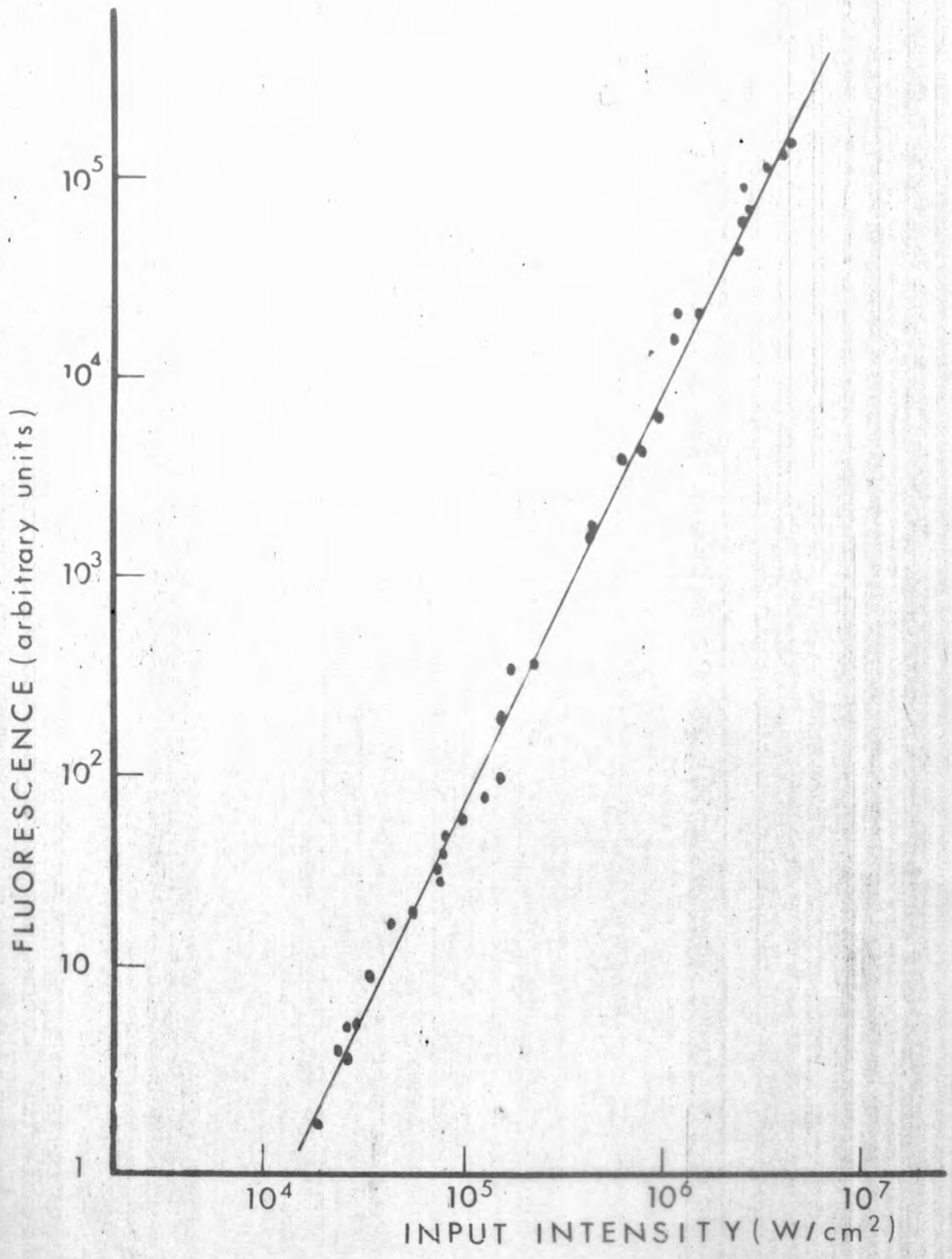

Fig.5.1
Two Photon Fluorescence from Rhodamine 6G

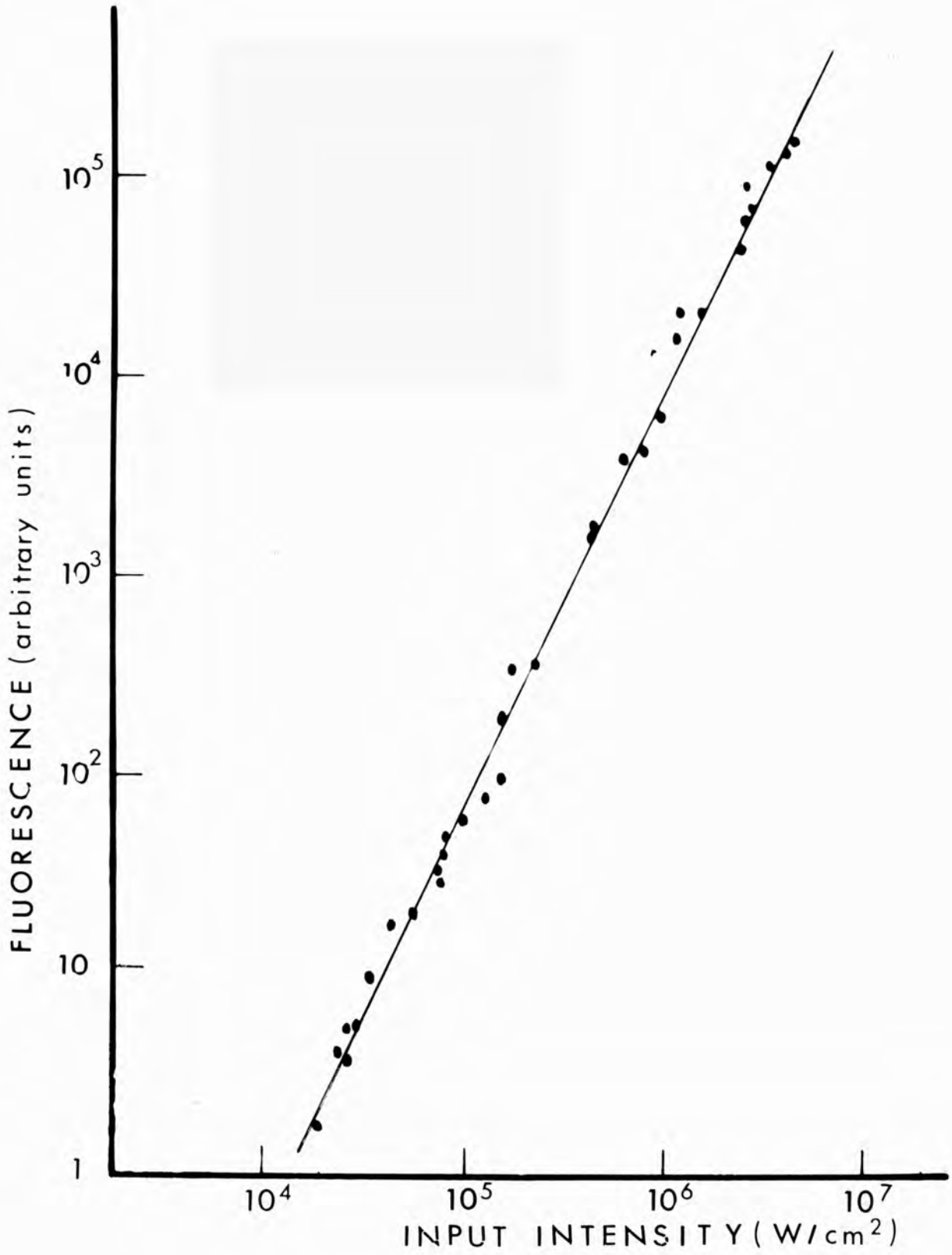
FLUORESCENCE (arbitrary units)
10^5
10^4
10^3
10^2
10
1
10^4
10^5
10^6
10^7
INPUT INTENSITY (W/cm^2)

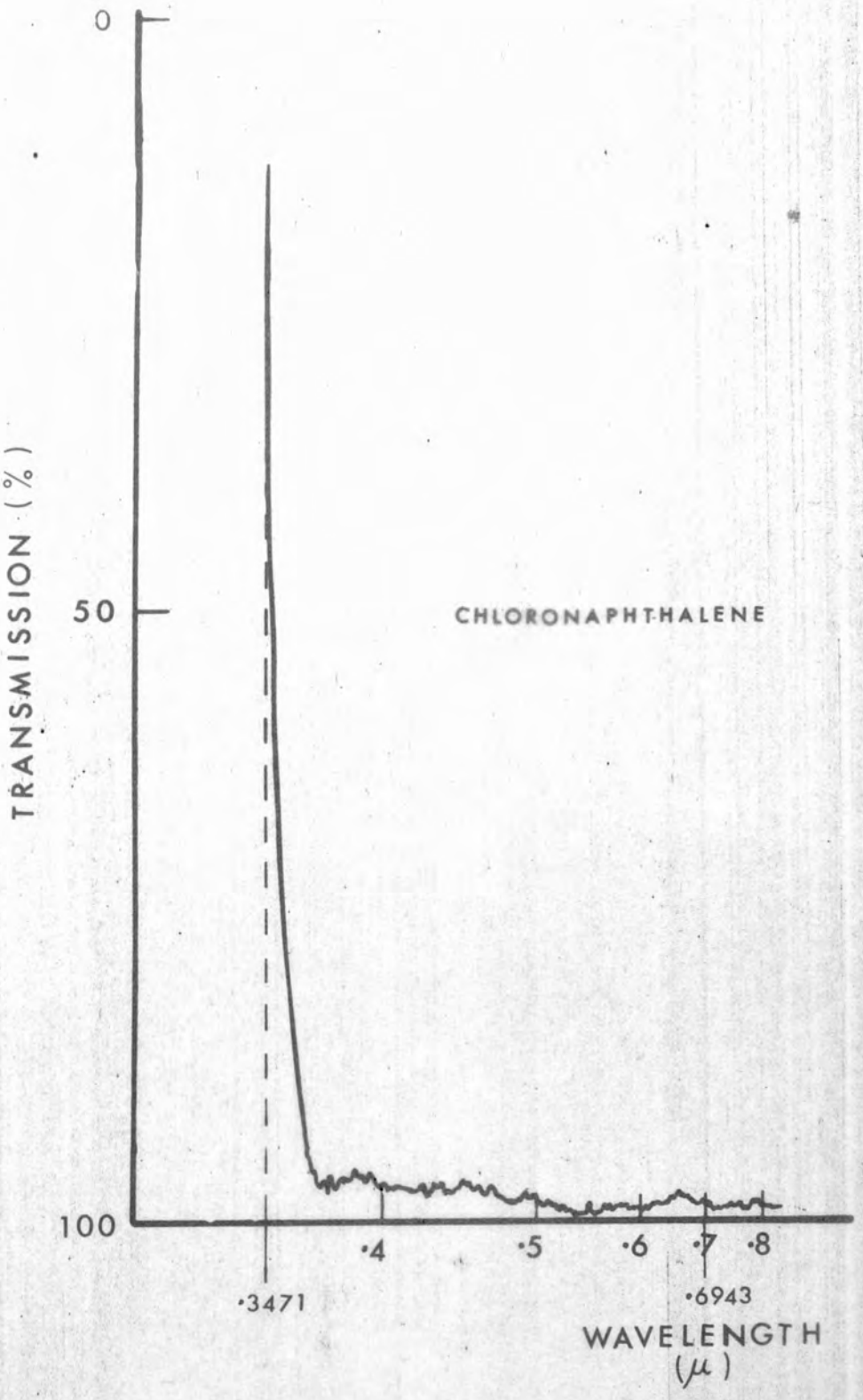

Fig.5.2
Absorption Spectrum of Chloronapthalene

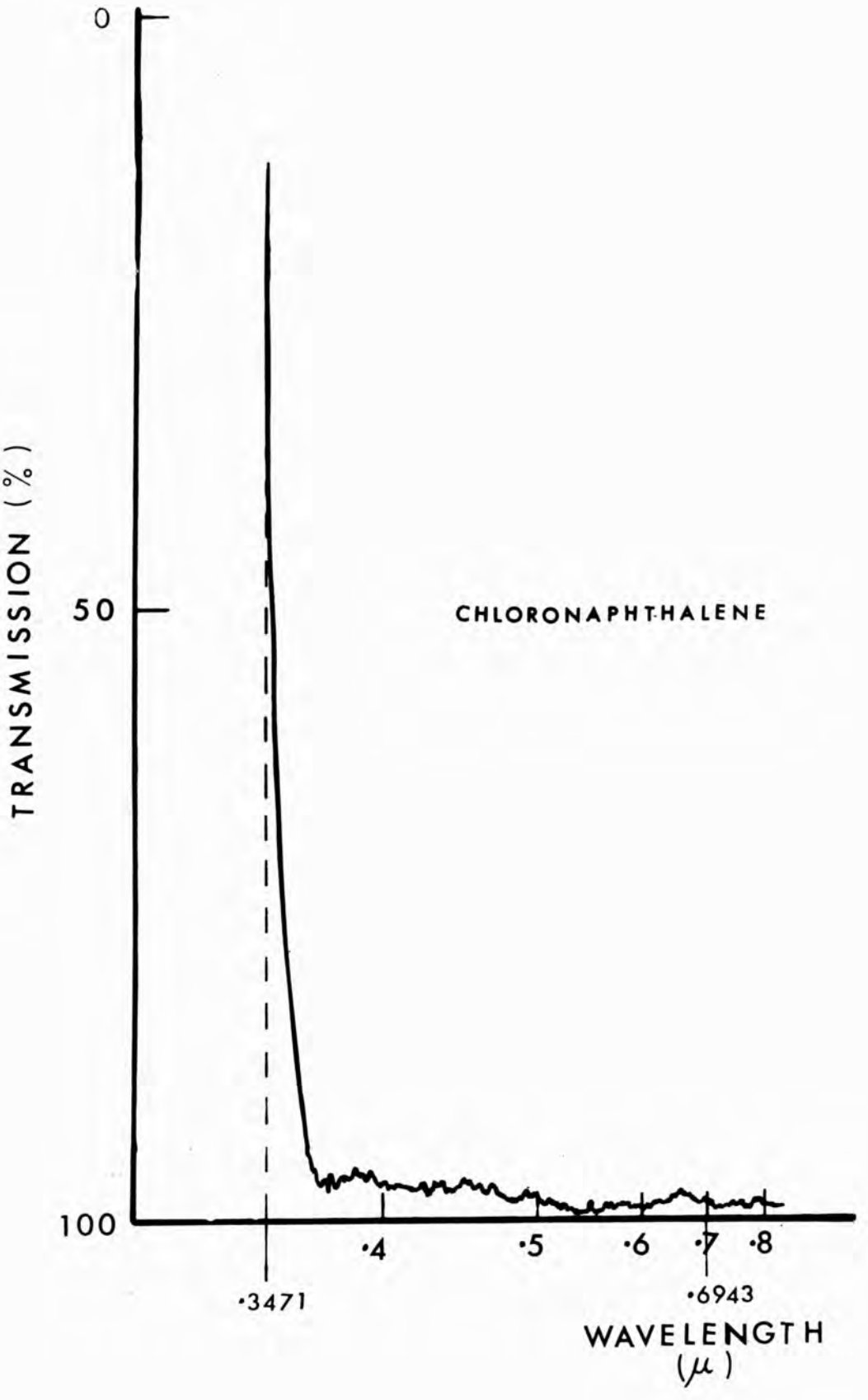
0
50
100
TRANSMISSION (%)
CHLORONAPHTHALENE
·4
·5
·6
·7
·8
·3471
·6943
WAVELENGTH
(μ)

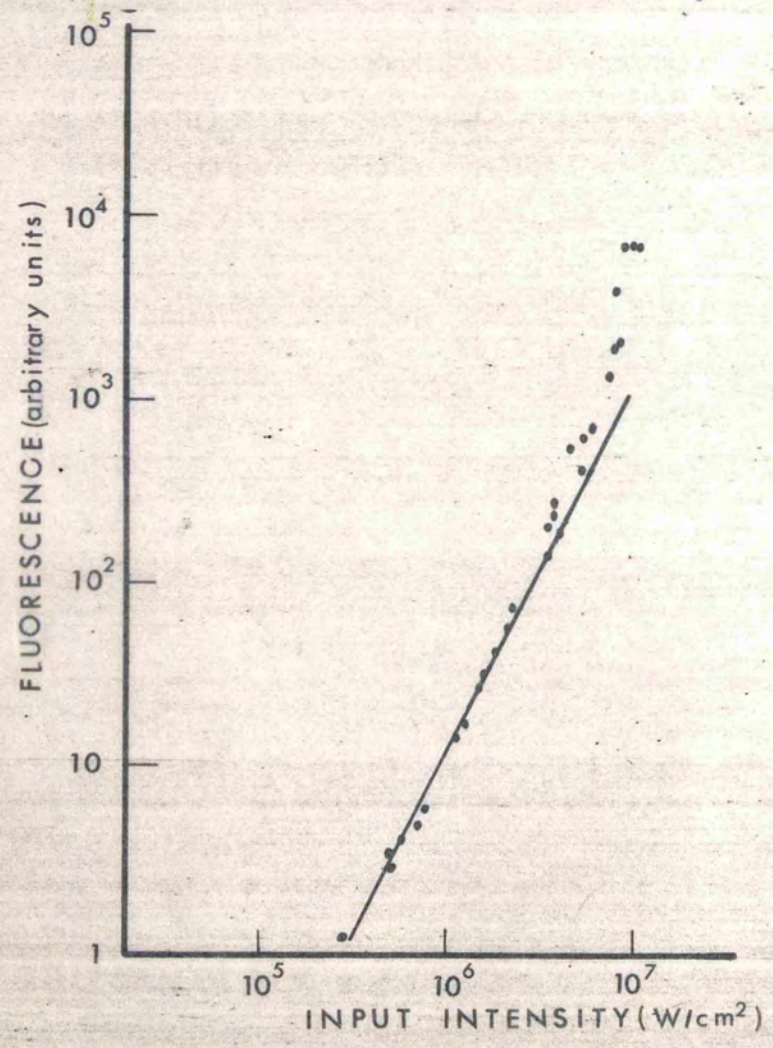

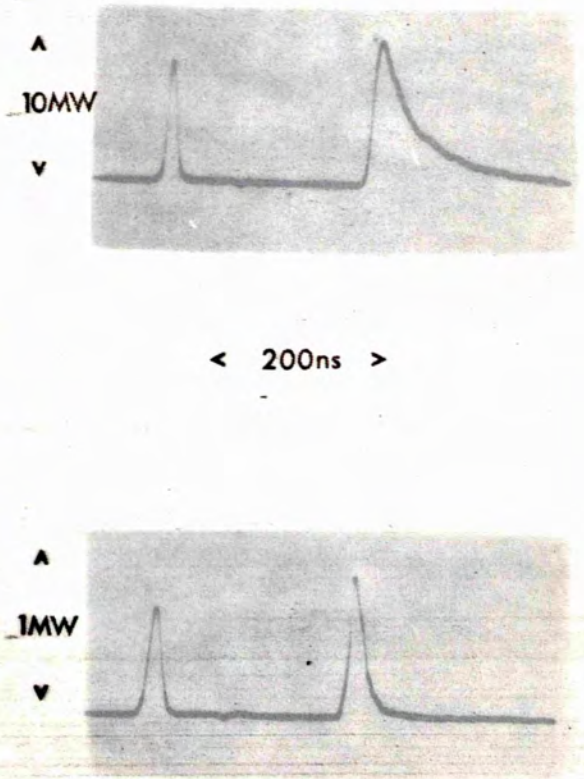

Fig.5.3
Two Photon Fluorescence from Chloronapthalene

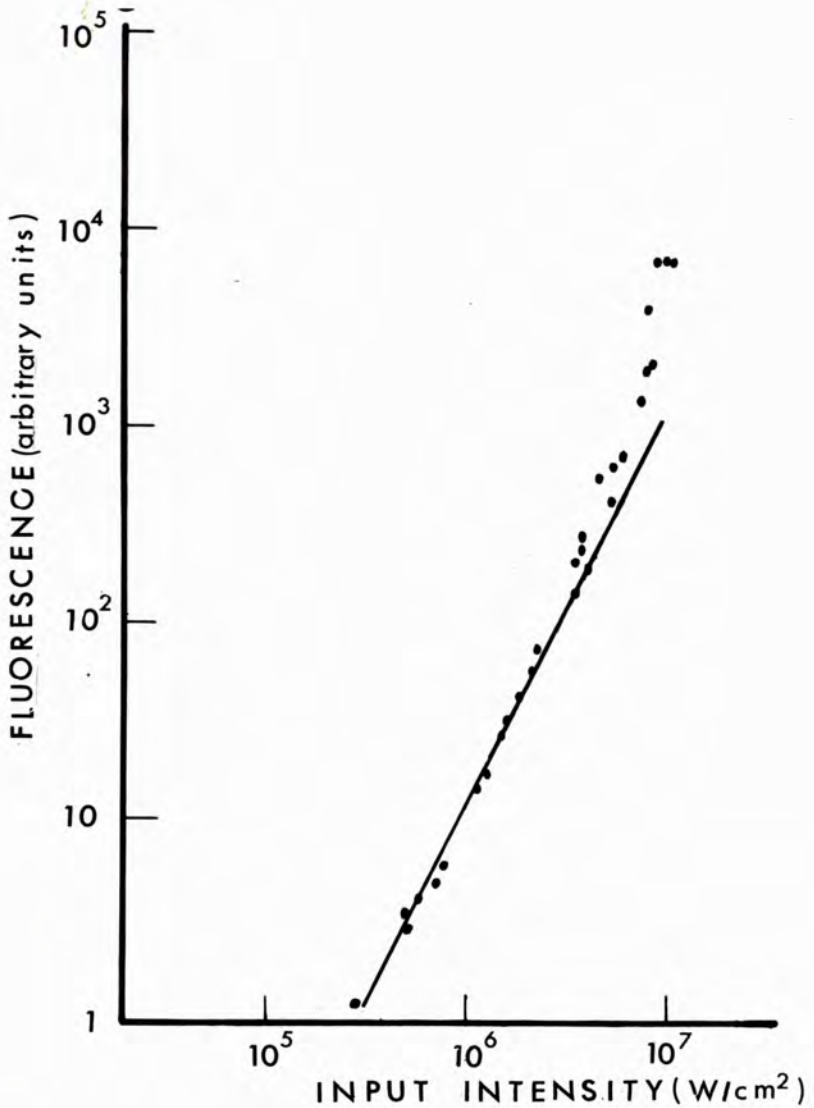
FLUORESCENCE (arbitrary units)
10^5
10^4
10^3
10^2
10
1
10^5
10^6
10^7
INPUT INTENSITY (W/cm^2)

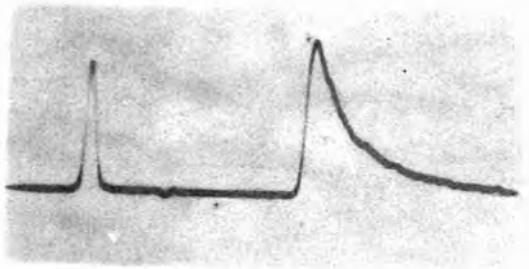

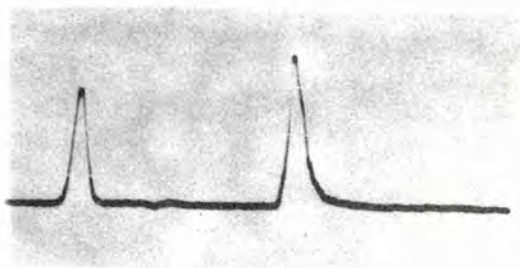

5.3 INTENSITY DEPENDENCE OF FLUORESCENCE DUE TO EXCITED STATE ABSORPTION

The blue fluorescence excited in saturable absorbers is due to excited state absorption[108]. It has been shown that the saturation of the first excited state leads to a dependence of fluorescent on incident intensity of the form:

$$\text{fluorescence} \propto \frac{I^2/I_c^2}{1 + 2\,I/I_c} \qquad \text{(Chapter 2.1)}$$

where

$$I_c \propto \sigma_1^2 T_1^2$$

and is an intensity characteristic of saturation of the first excited state. σ_1 is the absorption cross-section for excitation from the ground to the first excited state and T_1 is the lifetime of that state.

The values of σ_1 , T_1 and the relative values of I_c calculated from them are listed below for various solutions[224,237].

Solution	$\sigma_1 \times 10^{16} cm^2$	$T_1 \times 10^9$ secs	Relative values of I_c
Chloroaluminium Phthalocyanine in chloronapthalene	3	5	1
Vanadium phthalocyanine in nitrogen	4·1	2	2
Cryptocyanine in methanol	8·1	·1	20

Curves A and B of Fig.5.4 show the dependence of fluorescence on incident intensity for solutions of CAP in chloronaphalene and methanol respectively. Both curves indicate a square law dependence at low input intensities and a linear dependence for high intensities. The value of I_c characteristic of the transition between these two parts of the curve is clearly greater for the solution in methanol. While values of σ_1

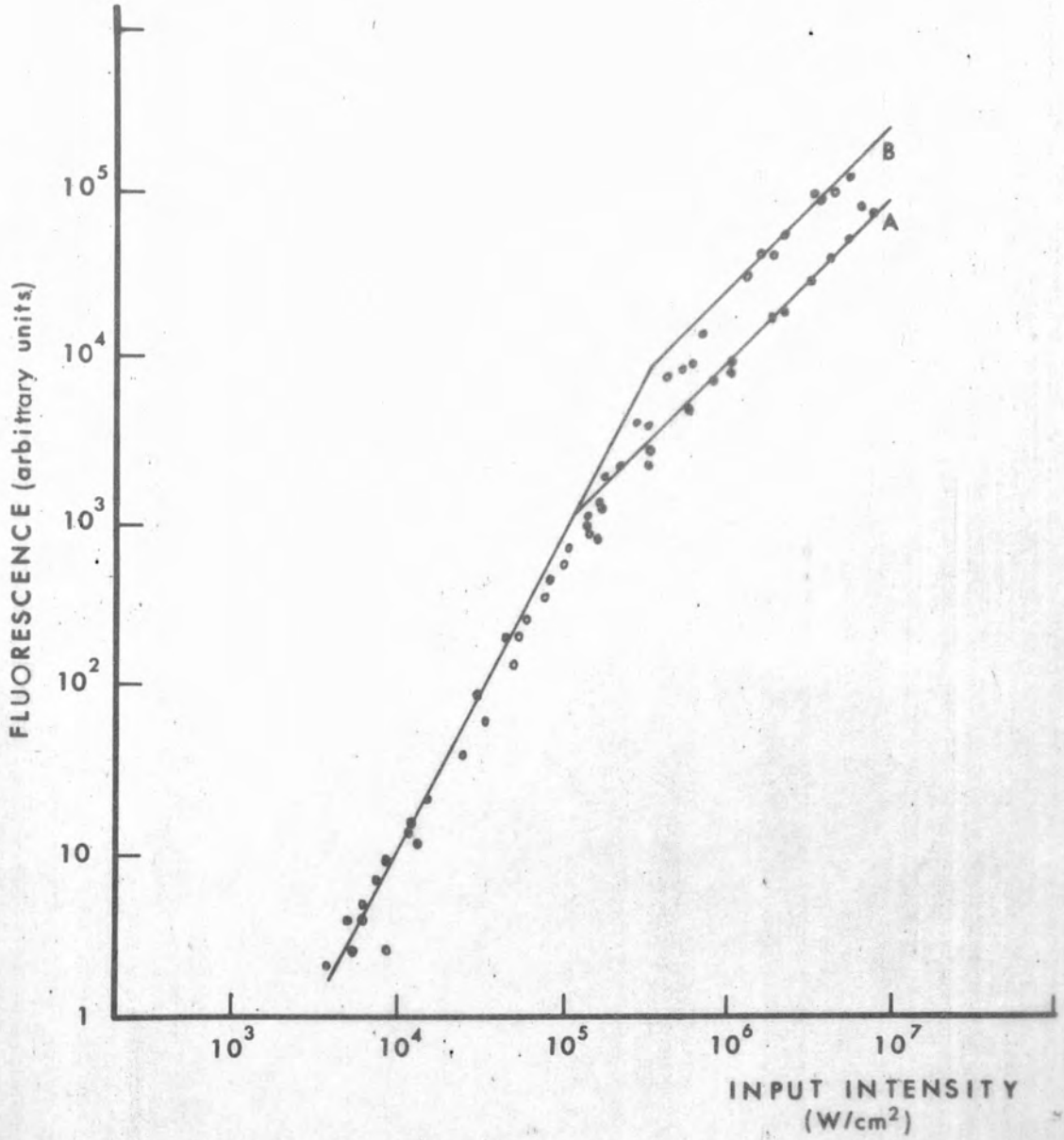

Fig.5.4
Fluorescence due to Excited State Absorption in CAP

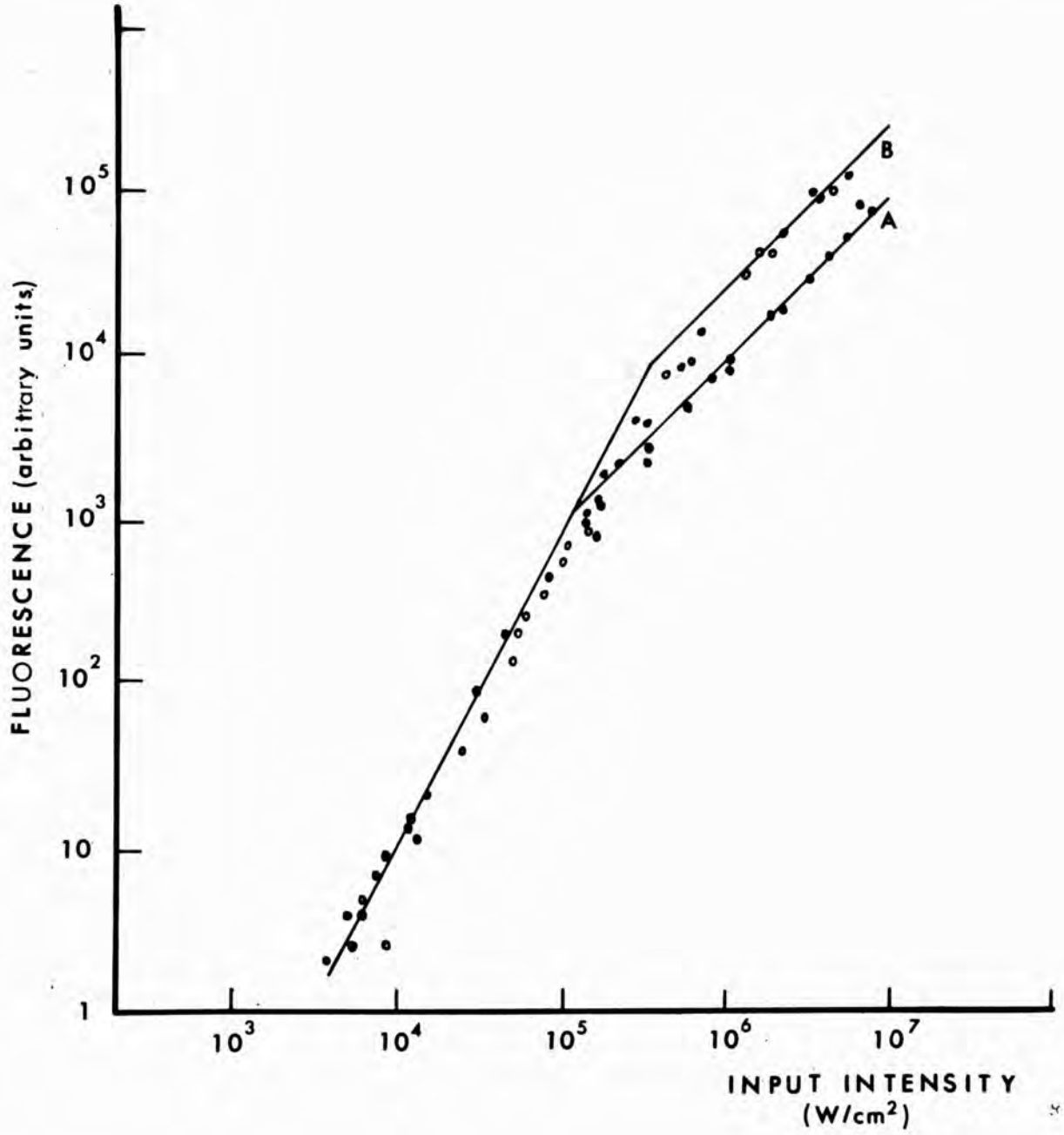
FLUORESCENCE (arbitrary units)
10^5
10^4
10^3
10^2
10
1
B
A
10^3
10^4
10^5
10^6
10^7
INPUT INTENSITY
(W/cm^2)

and T_1 for this solution are not given in the literature it is known that the absorption spectrum of CAP in methanol has its peak much further from 6943 Å than that of CAP in chloronapthalene. This indicates a lower value of σ_1 for the solution in methanol and explains the higher value of I_c in this case.

The value of I_c, indicated by curve A, for the CAP in chloronapthalene solution is about $10^5 W/cm^2$ while that for vanadium phthalocyanine in nitrobenzene (Fig.5.5) is about 3×10^5 W/cm^2. (The non-linear dependence of the fluorescence at very high powers in this graph is due to chemical breakdown of the solvent.) The ratio between them is in reasonable agreement with the theoretical estimate above.

The value of I_c for a solution of cryptocyanine in methanol can be estimated from Fig.5.6. The much shorter lifetime of the excited state of this dye leads to the very high saturation power $I_c \sim 2 \times 10^6 W/cm^2$ which is also in agreement with the theoretical ratio above.

All these values of I_c are in agreement with those obtained by other workers using transmission and single photon fluorescence measurements[106,224,238].

5.4 SPECTRUM OF FLUORESCENCE FROM EXCITED STATE ABSORPTION

The second excited state causes a weak peak in the absorption spectrum of cryptocyanine at about 4000 Å (Fig.5.7). The fluorescence spectrum due to decay of this state would be expected to be a band with its peak intensity at a slightly longer wavelength than the absorption peak[108].

A simple diffraction spectrometer was constructed to observe the spectrum of the fluorescence from the solution of cryptocyanine in methanol. The observed spectrum, shown in Fig.5.8, had the expected peak

intensity at about 4600Å . The resolution of the instrument was not sufficient to permit detailed analysis of the spectrum but an asymmetry of the spectrum, probably due to self absorption is clearly visible.

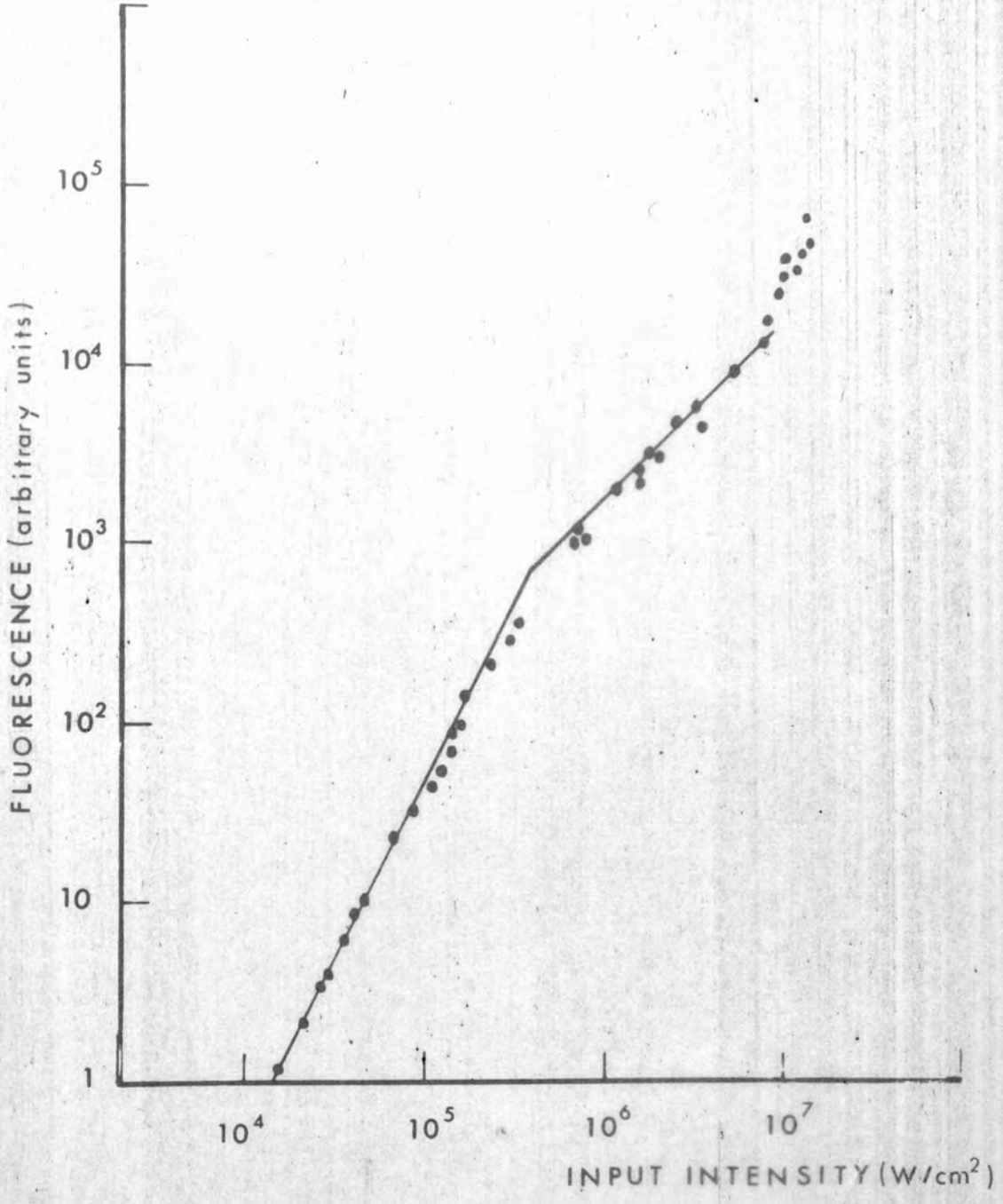

Fig.5.5
Fluorescence due to Excited State Absorption in VnOPc

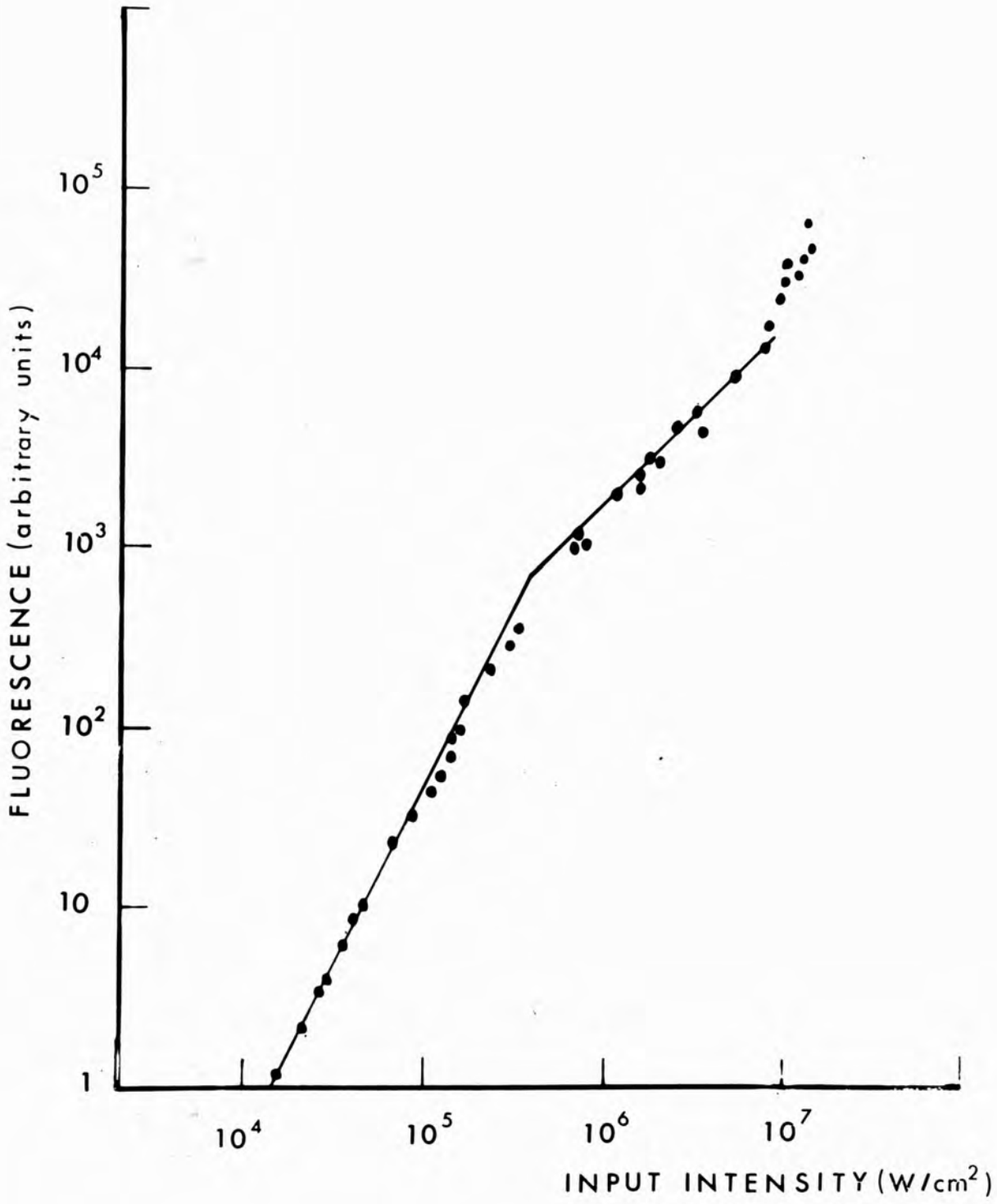
FLUORESCENCE (arbitrary units)
10^5
10^4
10^3
10^2
10
1
10^4
10^5
10^6
10^7
INPUT INTENSITY (W/cm^2)

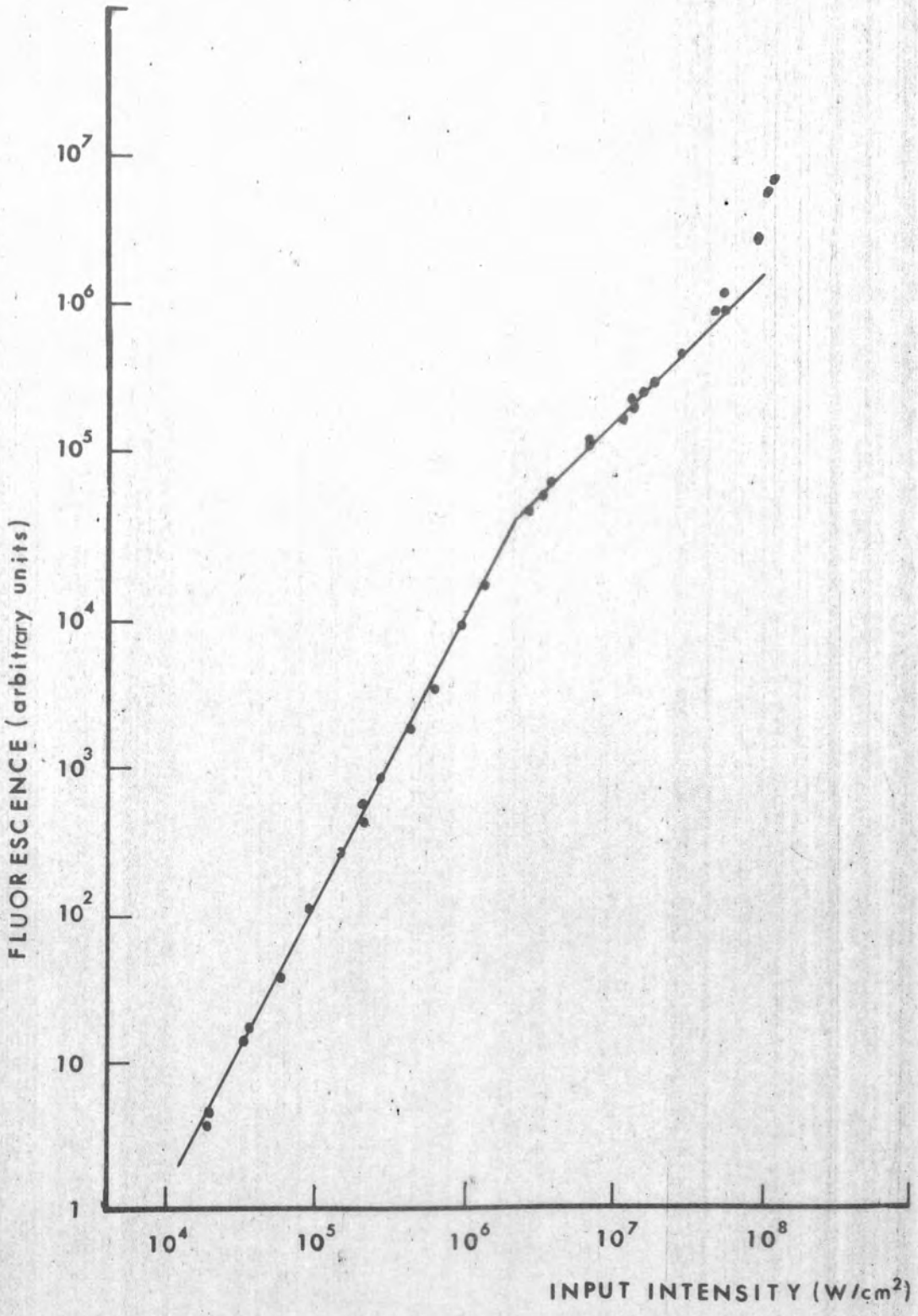

Fig.5.6
Fluorescence due to Excited State Absorption in Cryptocyanine

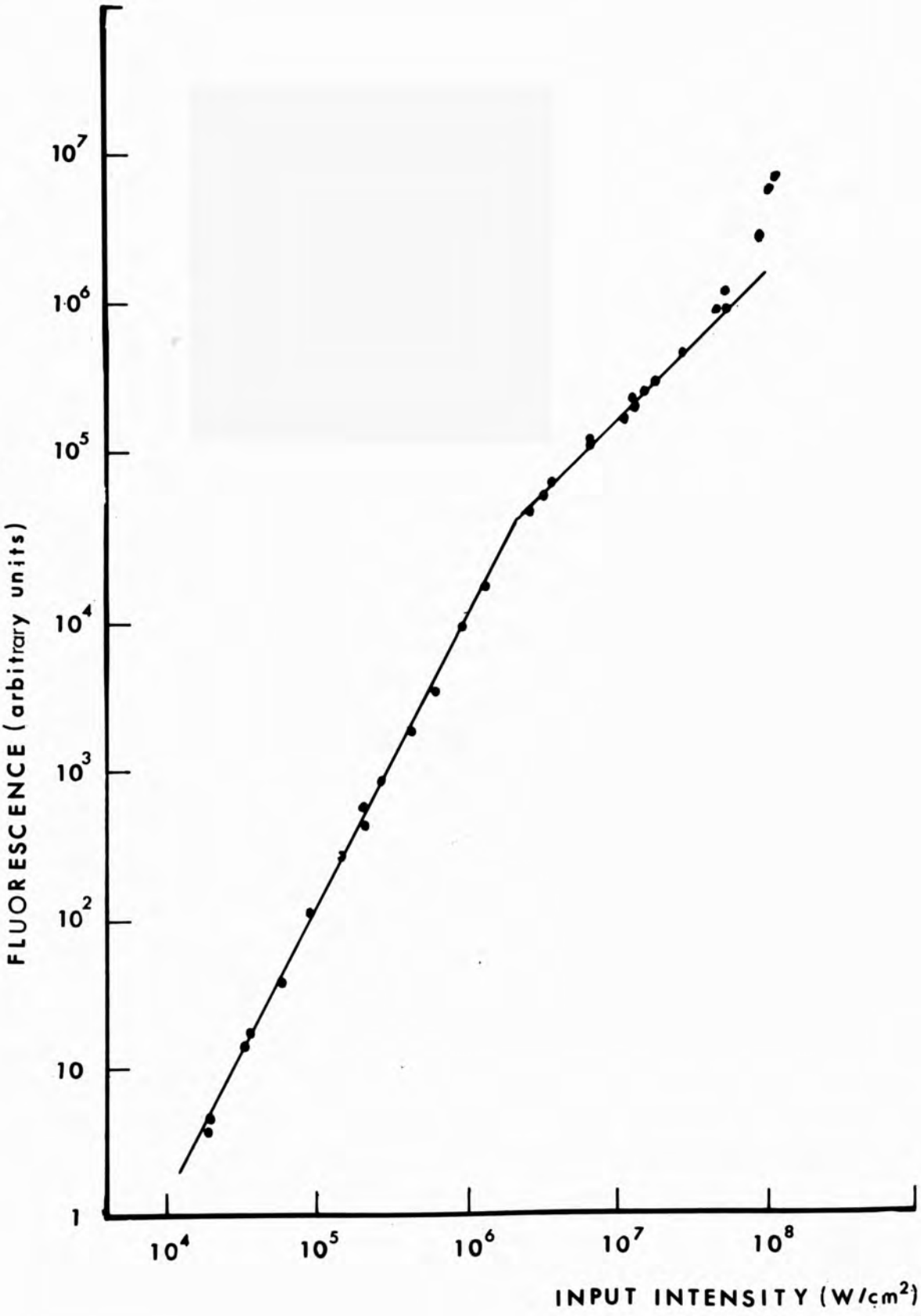
FLUORESCENCE (arbitrary units)
10^7
10^6
10^5
10^4
10^3
10^2
10
1
10^4
10^5
10^6
10^7
10^8
INPUT INTENSITY (W/cm^2)

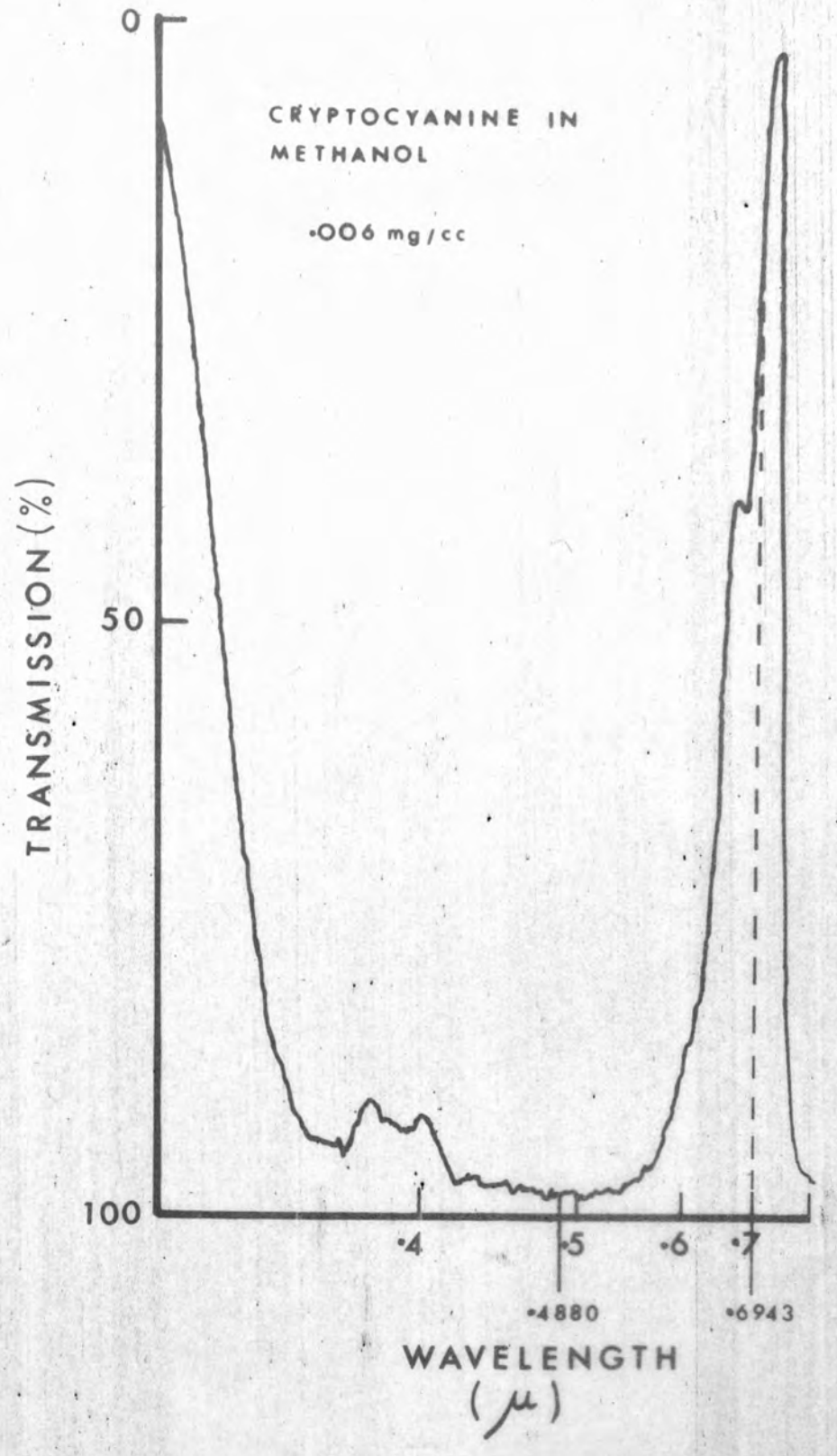

Fig.5.7
Absorption Spectrum of Cryptocyanine

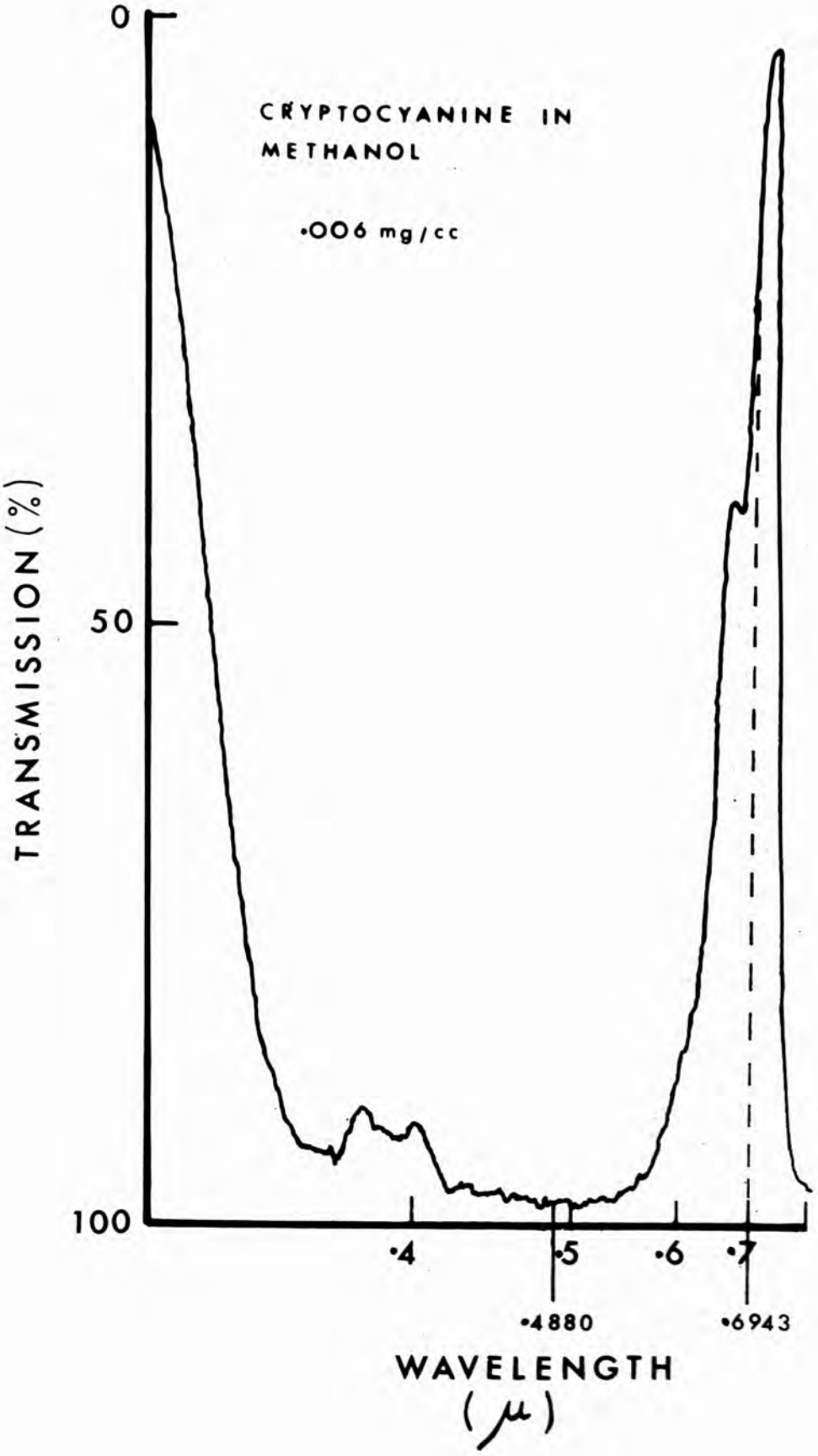
0
50
100
TRANSMISSION (%)
CRYPTOCYANINE IN METHANOL
·006 mg/cc
·4
·5
·6
·7
·4880
·6943
WAVELENGTH (μ)

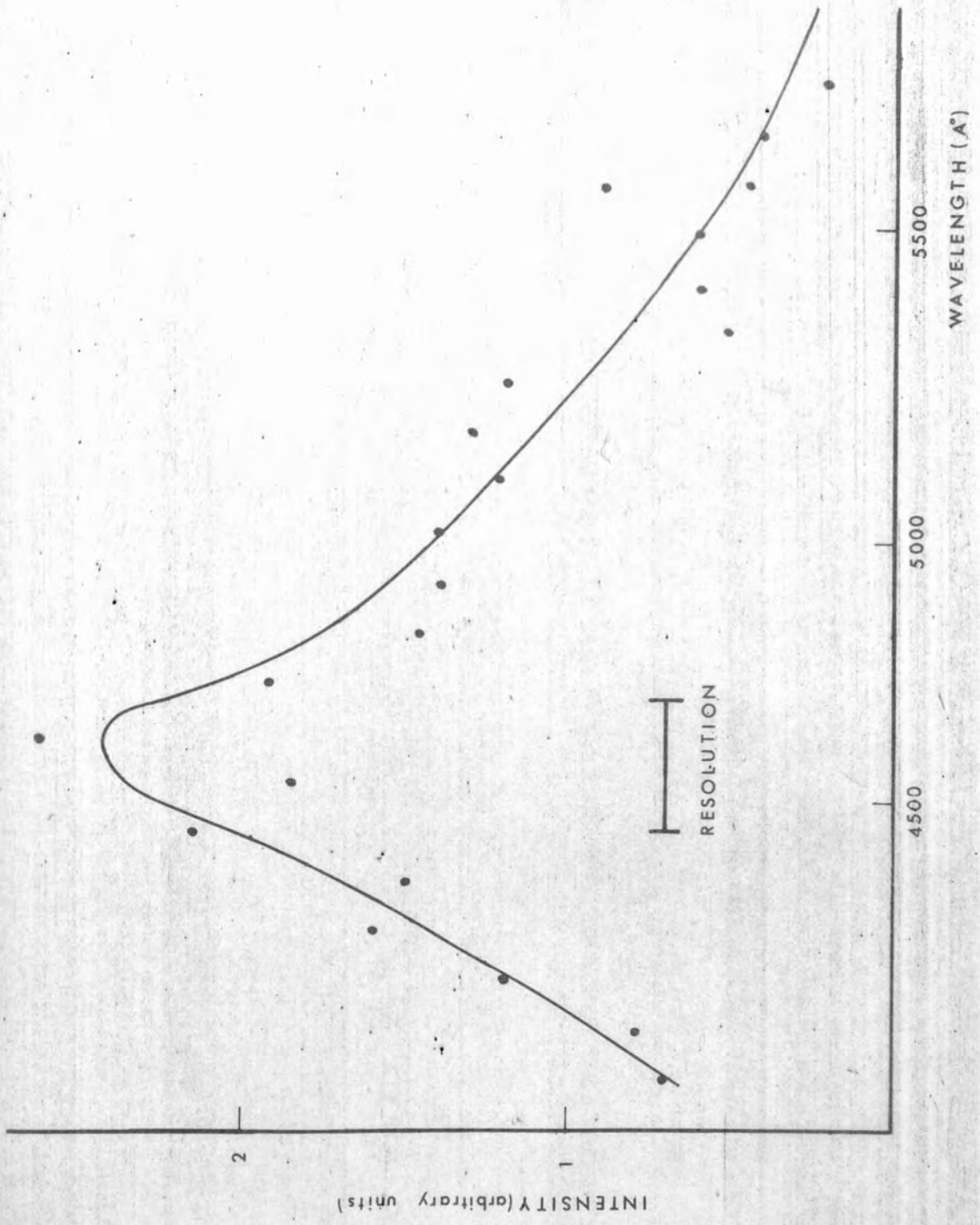

Fig.5.8
Two Photon Fluorescence Spectrum of Cryptocyanine

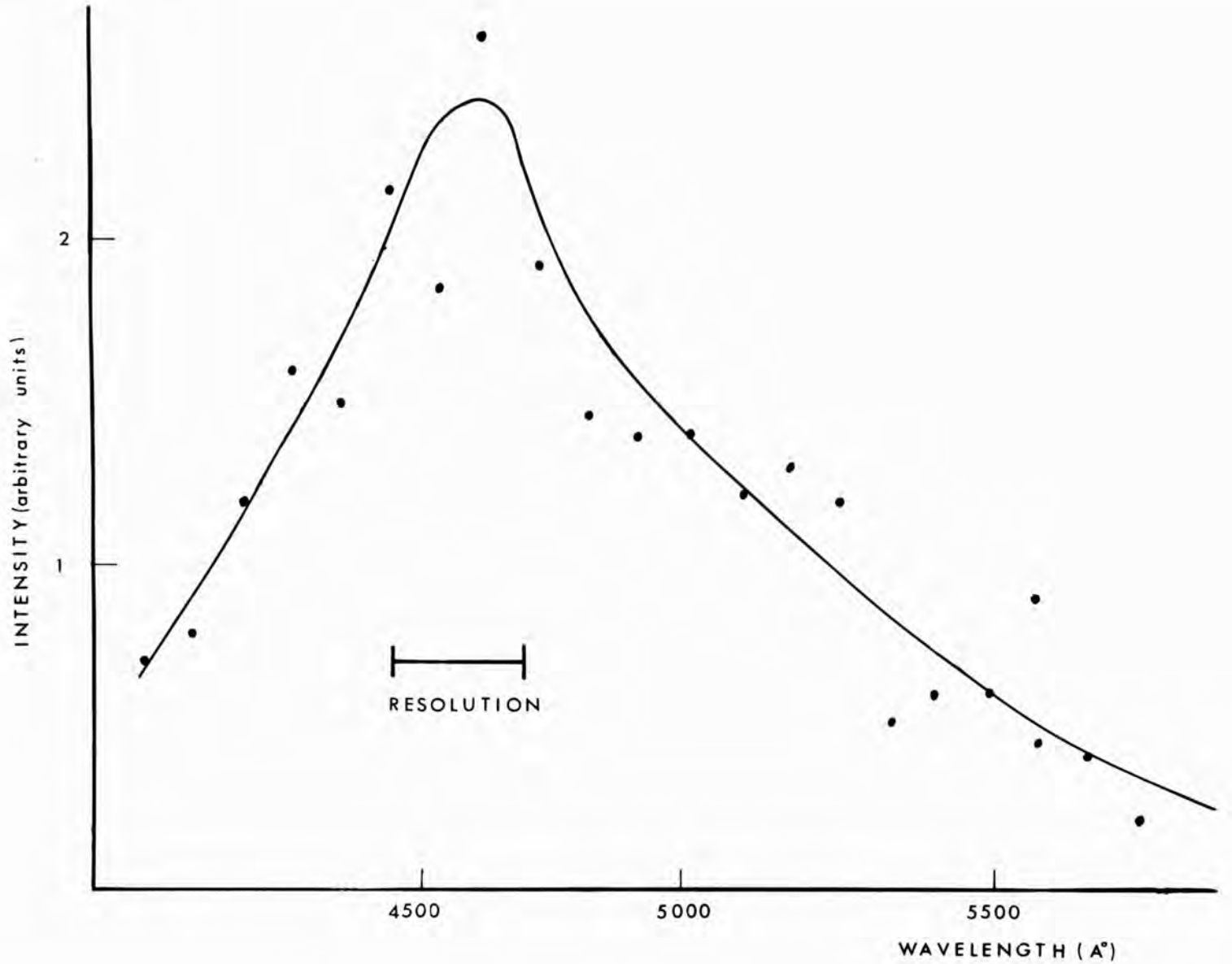
INTENSITY (arbitrary units)
2
1
RESOLUTION
4500
5000
5500
WAVELENGTH (A°)

CHAPTER VI

SCATTERING OF A FREQUENCY DOUBLED PROBE BEAM

6.1 FREQUENCY DOUBLING

The angle of incidence, for maximum interaction, between a probe and scattering beam is given by (Section 2.5).

$$\theta_{max} = \cos^{-1} \frac{\lambda_{probe}}{\lambda_{ruby}} \cdot \frac{n_{ruby}}{n_{probe}} \quad .$$

For this angle to be real:

$$\lambda_{probe} < \lambda_{ruby}.$$

A beam of shorter wavelength may easily be obtained from a ruby laser beam by frequency doubling[109,112]. In this case $\lambda_{probe} = \frac{1}{2} \lambda_{ruby}$ and $\theta_o = 60^o$ neglecting dispersion.

The frequency doubled beam was generated by passing the ruby laser beam through a crystal of ammonium dihydrogen phosphate (ADP) cut to a cuboid $1" \times \frac{1}{2}" \times \frac{1}{2}"$. The cuboid was cut with its axis at $42\frac{1}{2}^o$ to the optic axis of the crystal and the two square faces were polished flat to $\lambda/10$.

In order to generate a significant amount of frequency doubled light phase matching must be achieved[110,112]. Fig.6.1 shows the wave fronts of an ordinary fundamental and an extraordinary second harmonic wave in Potassium Dihydrogen Phosphate (KDP). (The situation in ADP, used here because it is less hygroscopic then KDP, is essentially similar but the information available is not so detailed.) The angle between the optic (z) axis and O, the line of intersection of the wavefronts indicates the direction in which phase matching is achieved. (In A.D.P. this angle[239] is 42^o allowing phase matching for light incident normally on the crystal cuboid described.) Any deviation from this direction gives the very sharp decrease of frequency doubled power indicated in the graph of that

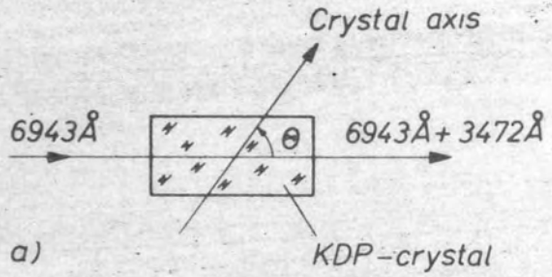

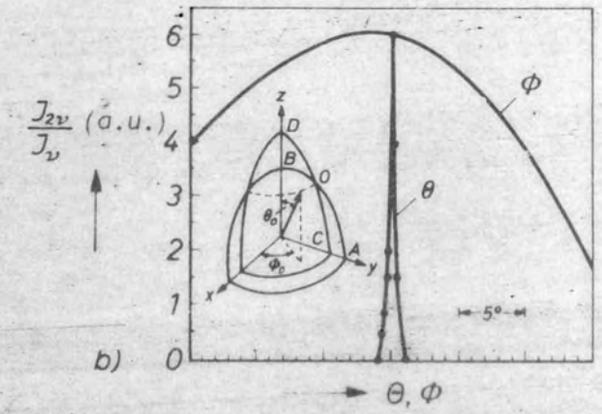

Fig. 6.1
Frequency Doubling

Frequency doubling and Phase Matching in KDP

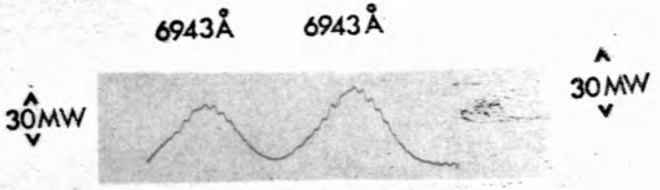

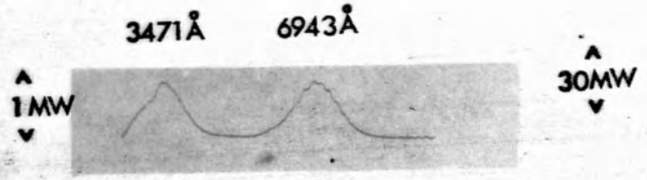

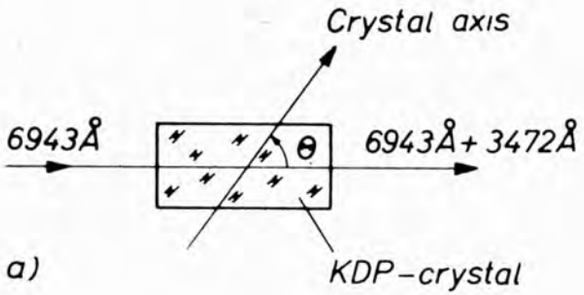

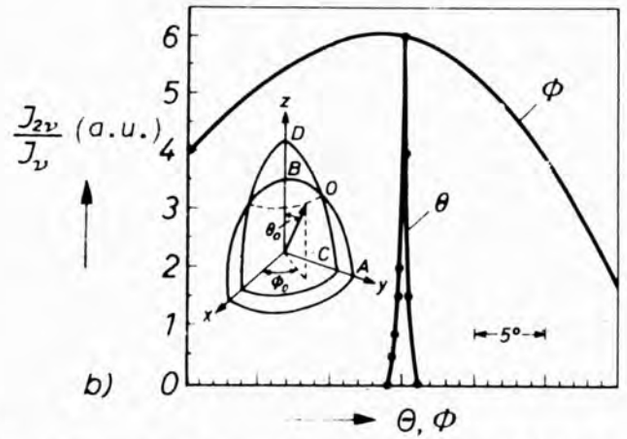

Frequency doubling and Phase Matching in KDP

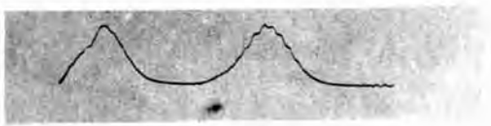

power as a function of the angle θ. The power also depends on the angle φ but much less critically. A kinematically designed optical stand allowed very accurate micrometer adjustment of the angle θ so phase matching was easily achieved. (This was made easier by the fact that when there is slight mismatch the frequency doubled light appears as a series of 'Giordmaine rings' whose radius and position indicate the amount and direction of mismatch[240].)

It was not necessary to know the exact output of frequency doubled light as only the fraction reflected was of experimental significance Nevertheless the approximate amount of conversion was of interest and was measured by allowing the red and blue output from successive laser shots through the crystal to fall on a photodiode while a time delayed reference beam of red light fell on the same diode to indicate the incident power level for each shot.

The oscillograms obtained, shown in Fig.6.1 indicated a typical conversion of about 3% for an incident power of about 30 MW.

6.2 EXPERIMENTAL ARRANGEMENT FOR THE SCATTERING OF A FREQUENCY DOUBLED PROBE

The experimental lay-out is shown schematically in Fig.6.2. In this experiment the usual Q-switch cell was replaced by a hexagonal one so that the probe scattering could take place within the Q-switch cell[246]. The probe scattering could in fact be more easily investigated in a separate cell but this arrangement was used because it had been suggested that a phase grating within the Q-switch cell could be responsible for certain features of Q-switched laser operation[234].

The Q-switch and pumping levels of the ruby laser were such as to give a 30 MW, 20 nsec, single pulse output. The occurrence of only one pulse was checked with a Tektronix 551 oscilloscope, not shown in the

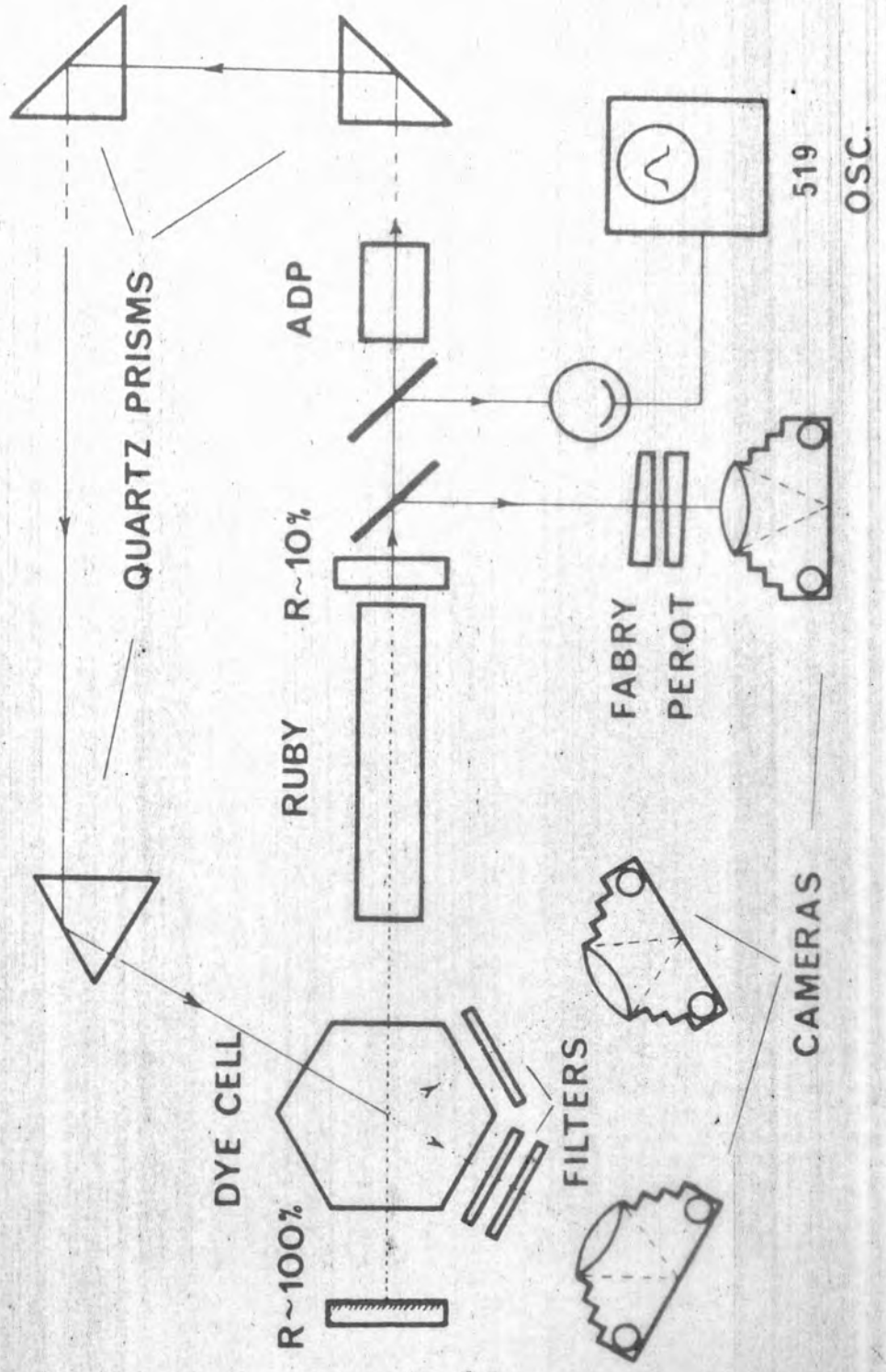

Fig.6.2

FIG. 6.2. **Experimental Arrangement for Bragg Reflection of Frequency Doubled Light**

FIG. 6.2.

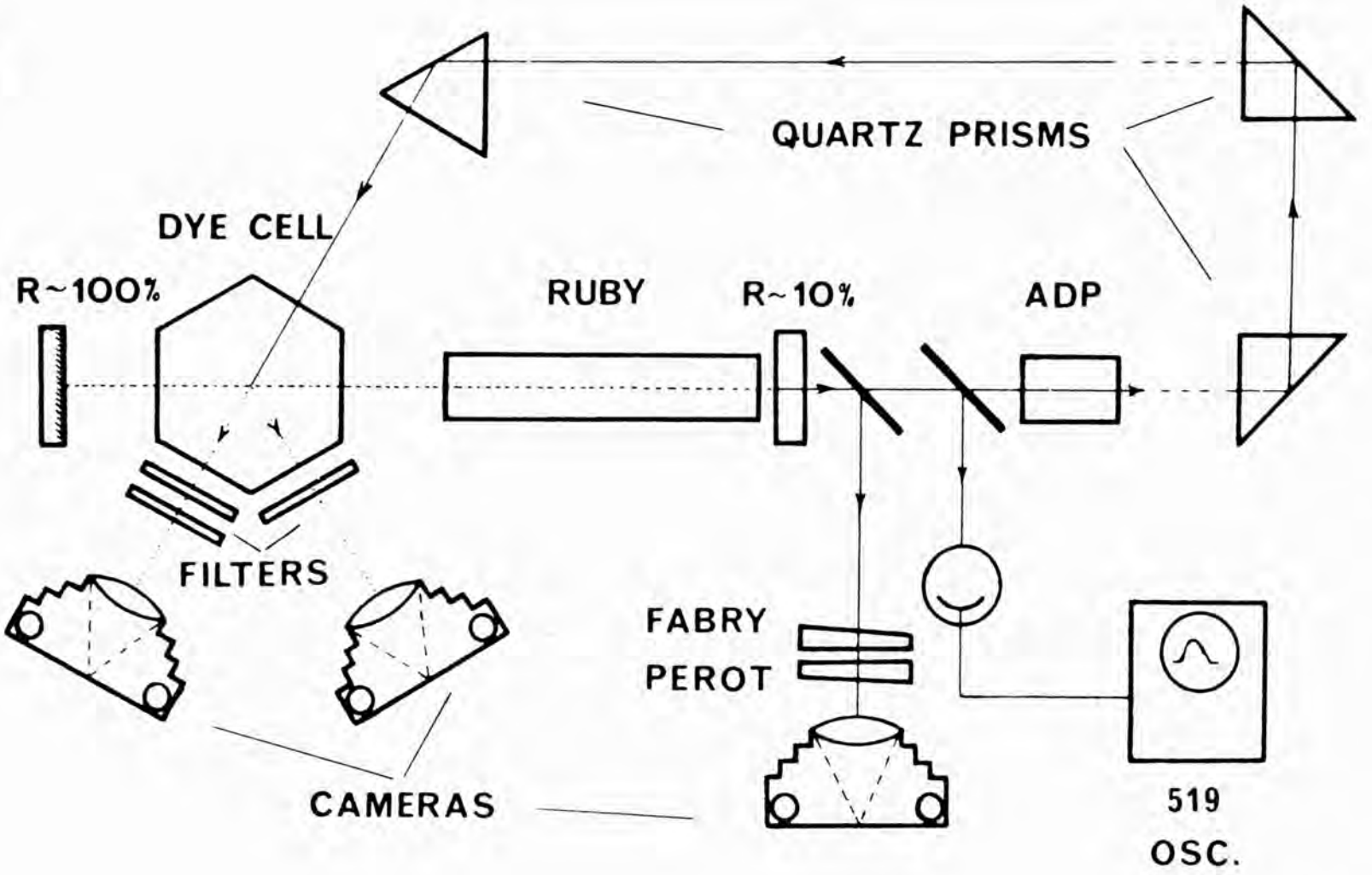
QUARTZ PRISMS
DYE CELL
R~100%
RUBY
R~10%
ADP
FILTERS
FABRY
PEROT
CAMERAS
519
OSC.

diagram, while the power of that pulse was monitored using the Tektronix 519 oscilloscope. The spectrum of the output was monitored with a Fabry-Perot interferometer in order to ensure that the stimulated Brillouin effect did not occur within the Q-switch cell.

The ruby laser beam, polarized in the plane of the diagram passed through the ADP crystal at the phase matching angle generating about 1 MW of light at 3471 Å, polarized perpendicular to the diagram. This light passed round a delay path of variable length and was then reflected into the Q-switch cell, at 60° to the direction of the ruby laser beam, by a quartz prism supported on an arm of the 'spectrometer table' described in Section 3.4.

The ruby laser light formed an intense standing wave of electric field within the Q-switch cell. Although the Q-switching dye was a saturable absorber there was still some absorption in the dye cell which caused a greater temperature rise at the antinodes of the field than at the nodes. The temperature rise caused thermal expansion, reducing the density and refractive index at the antinodes of the field. In this way a phase grating was set up which could Bragg reflect light incident at the appropriate angle[213,214].

The light beams transmitted, and reflected, by this grating were recorded photographically after passing through filters to remove any red light and to attenuate the blue beam to a suitable intensity.

6.3 BRAGG REFLECTION OF PROBE LIGHT

Fig.6.3 shows the transmitted and reflected beams when the angle between the frequency doubled probe beam and the ruby laser beam was slightly varied about 60°. The reflected beams disappeared when:

(a) The angle between the beams in the cell differred from 60° by more than 10 m.rad.

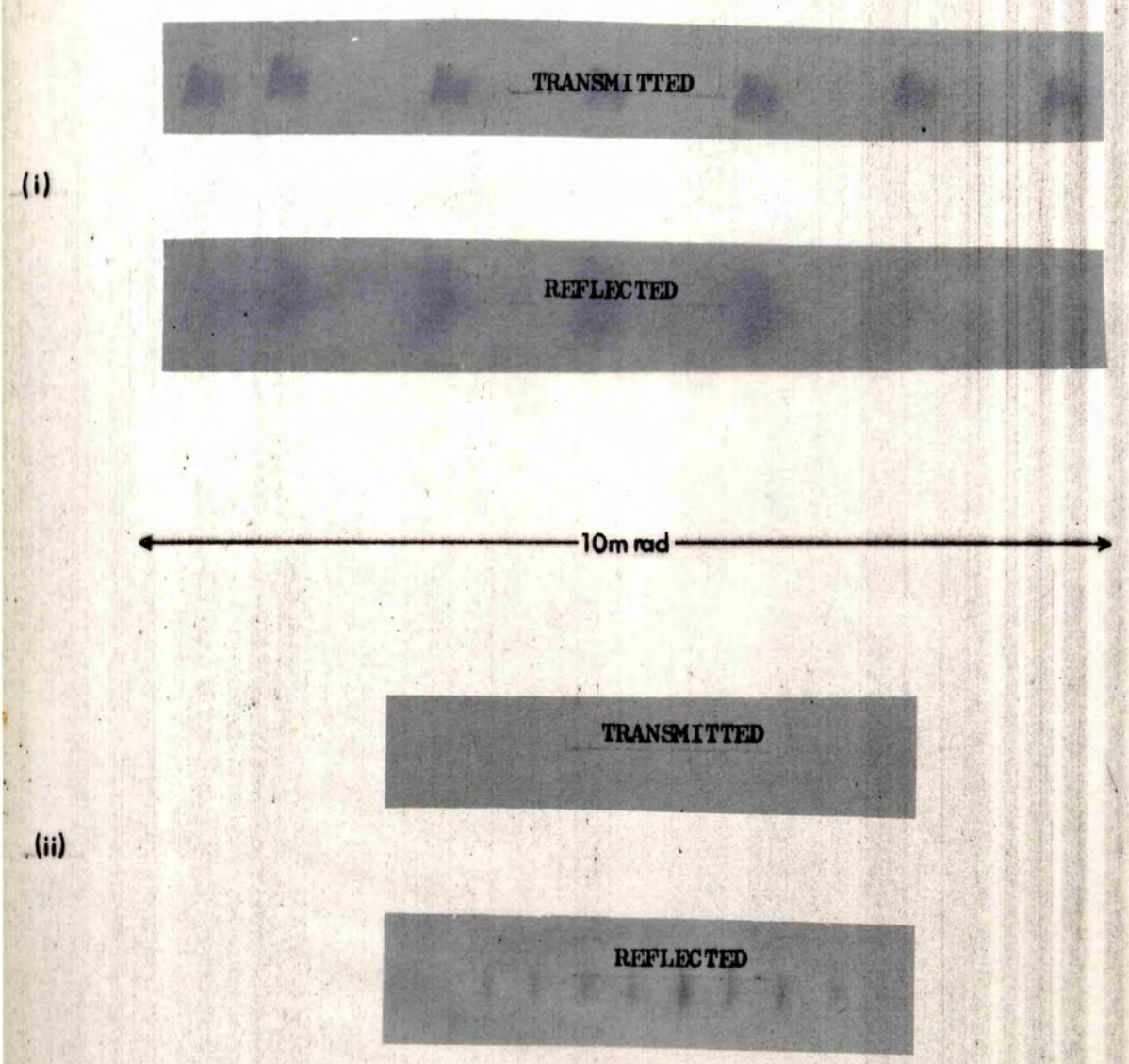

Fig. 6.3
Bragg reflection of Probe Light

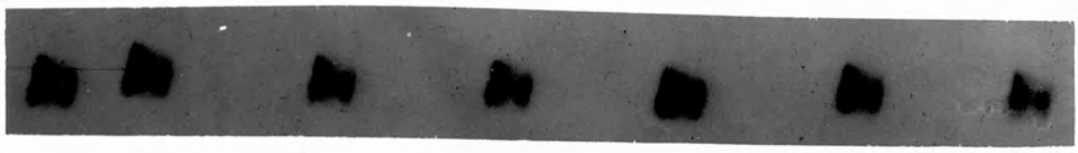

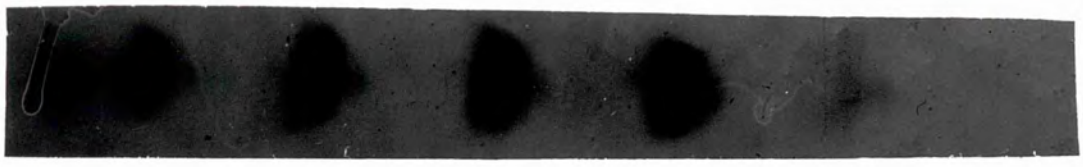

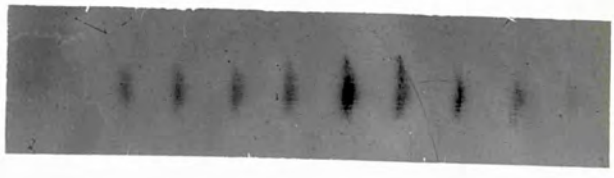

(b) A red filter was put in front of the camera and the green ones removed.

(c) The frequency doubling crystal was misaligned from the phase matching angle.

(d) the back mirror of the laser was put in front of the hexagonal cell and another Q-switch was provided.

These facts imply that the photographs show genuine Bragg Reflection not an artefact due to spurious light.

Fig.6.3(ii) was obtained when the divergence of the probe beam was cut to 2 m.rad. by the use of two small apertures while in Fig.6.3(i) the probe had its natural divergence of about 5 m.rad. The width of the angle between positions at which the scattering had half its maximum value is seen to correspond approximately to the divergence of the probe beam. This is to be expected because the width of the Bragg angle (calculated in Chapters II and VIII) is exceedingly small and the reflected light is a fixed proportion of the incident light falling within this width. (The divergence of the ruby laser-beam is less significant because the nodes of the field are parallel to the mirror for any angle of incidence.)

The intensities of the transmitted and Bragg reflected beams imply a maximum reflectivity of the phase grating of about 1% for the 5 m.rad. probe beam and 3% for the 2 m.rad. beam.

An attempt was made to measure the decrease of Bragg reflection when the length of the delay path of the probe beam was increased. No decrease was observed for delay paths of up to thirty feet, which was the longest practicable length with our apparatus, but these measurements were complicated by a number of factors. In the first place thirty feet, which gave about thirty nanoseconds delay was not long enough to allow much decay of the phase grating induced by a pulse of 20 nsec duration between the half intensity points. Also the divergence of the beam was such that only a

part of it entered the cell after a long delay path. The divergence of the light actually entering the cell was thus a function of the delay path and the Bragg reflection depends strongly on the divergence. This problem was partially solved by the use of apertures and focusing the beam but it became obvious that much better results could be obtained using a continuous probe beam from an independent laser.

CHAPTER VII

SCATTERING OF AN ARGON LASER PROBE BEAM

7.1 EXPERIMENTAL ARRANGEMENT

The arrangement for the argon laser probe scattering experiments is shown schematically in Figs.7.1 and 7.2 and a photograph of the experiment is shown in the Frontispiece[249].

Fig.7.1 illustrates the electrical detection and display system while Fig.7.2 is a more complete diagram of the optical arrangement. The forward and backward going ruby light beams were detected by the diodes D_1 , D_2 and D_3 and displayed via channel 1 of the 454 oscilloscope while the Bragg reflected argon beam was detected by the photomultiplier P and displayed with different gain, via channel 2 on the same trace of the 454. The signal detected by D_1 was calibrated against a calorimeter in the usual way (Chapter 3.2 and Fig.7.3) and those detected by D_2 , D_3 were calibrated against D_1 knowing the losses in the cell, beam splitters etc.

The output of the ruby laser, as described in Section 3.2 was a pulse of up to 100 MW/cm^2 intensity and about 15 nsec duration, while that of the argon laser was a continuous beam with a power of about 1 W and wavelength of 4880 Å. The output of both lasers was polarized in a plane perpendicular to the plane of Fig.7.2.

The backward going light beam was generated by reflecting the forward going one either by a plane mirror normal to the beam or else by generating stimulated scattering by focusing the light into cell 2 (Fig.7.2). Reflection by a mirror gave a beam of the same frequency as the forward going one while stimulated scattering gave one of slightly shifted frequency.

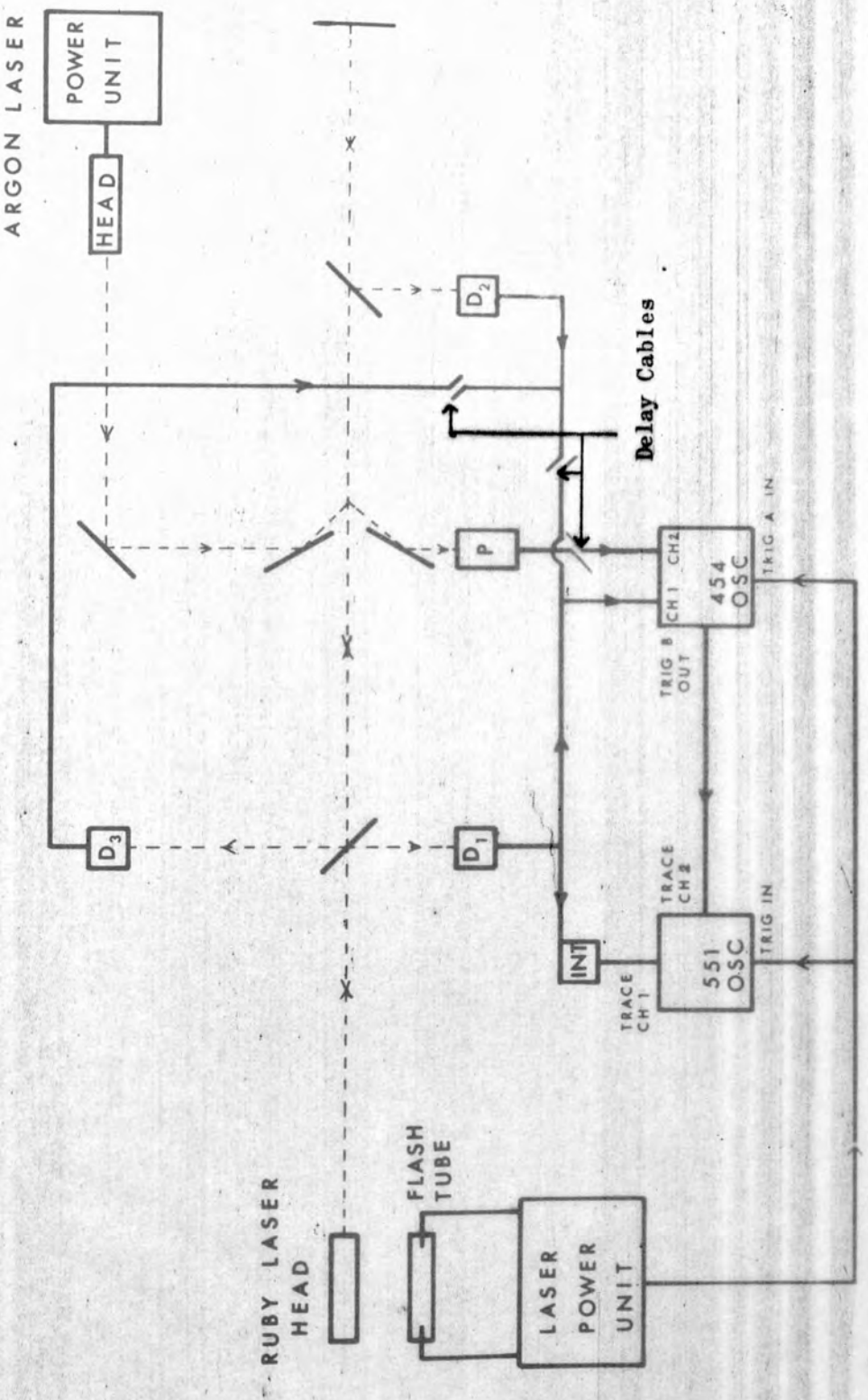

Fig.7.1
Detection Electronics

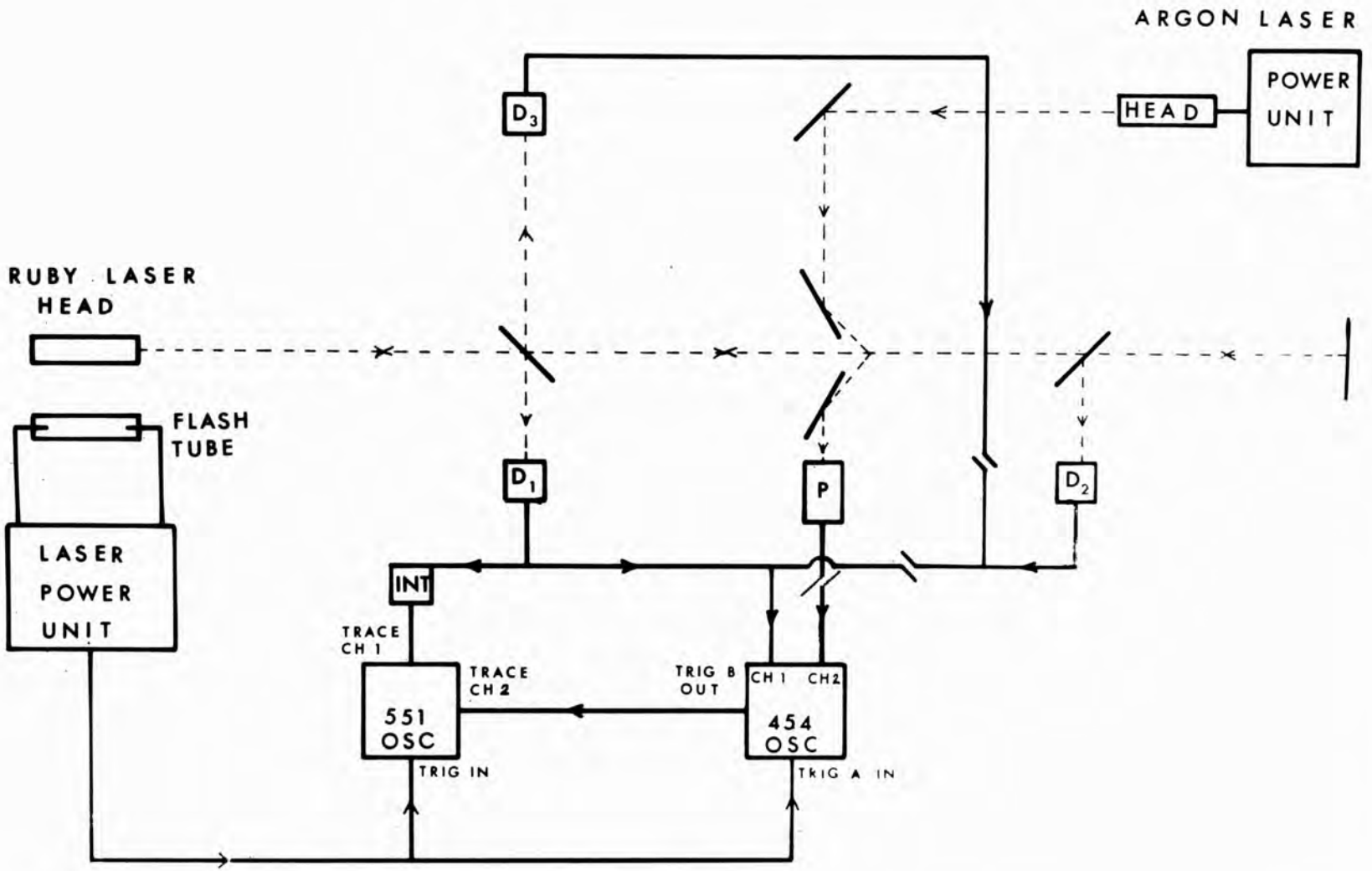
ARGON LASER
POWER UNIT
HEAD
D_3
RUBY LASER HEAD
FLASH TUBE
D_1
P
D_2
LASER POWER UNIT
INT
TRACE CH 1
TRACE CH 2
TRIG B OUT
CH 1 CH2
551 OSC
454 OSC
TRIG IN
TRIG A IN

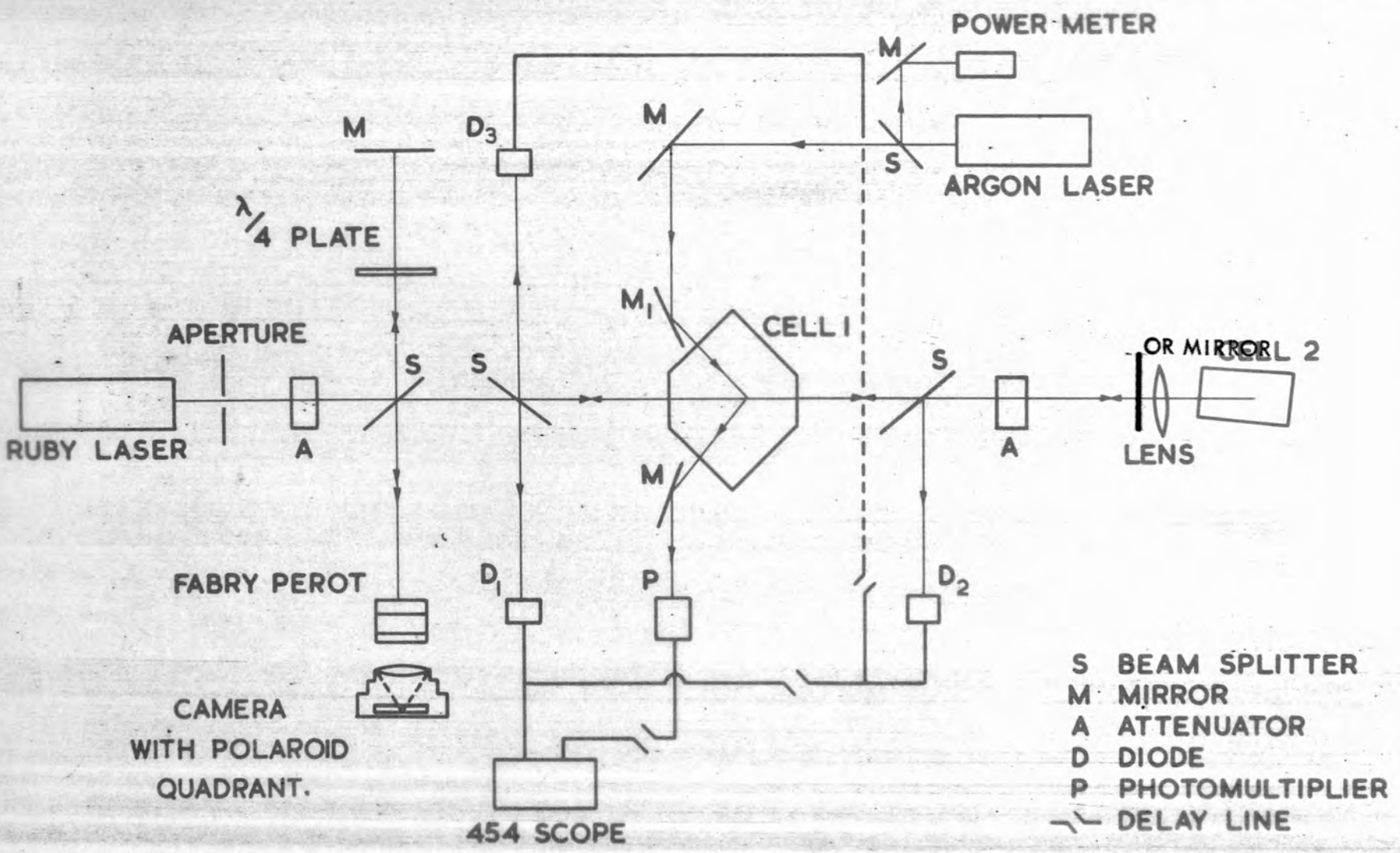

Fig.7.2

Fig.7.2.Experimental arrangement

CLM-P224

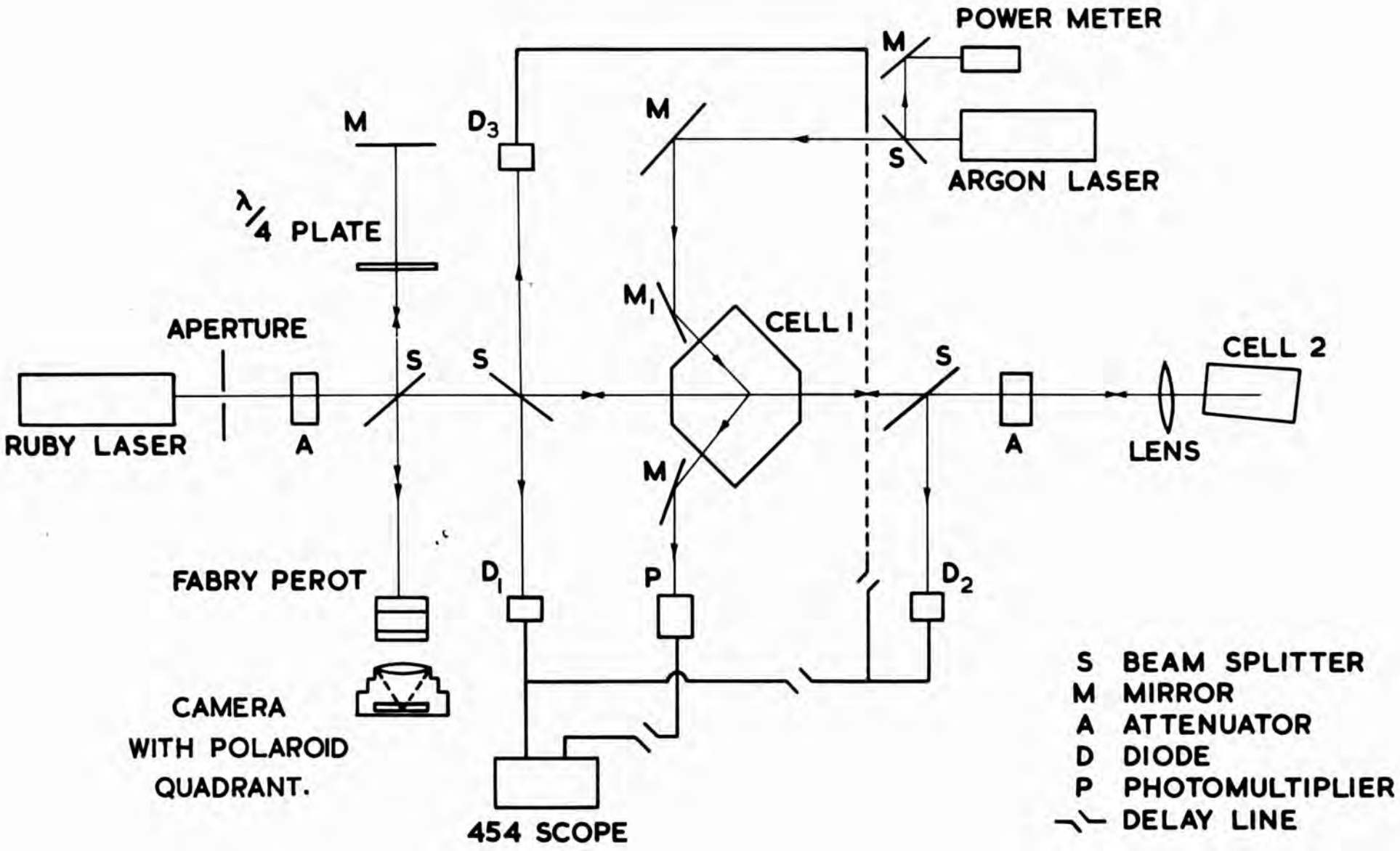

Fig.7.2.Experimental arrangement

CLM-P224

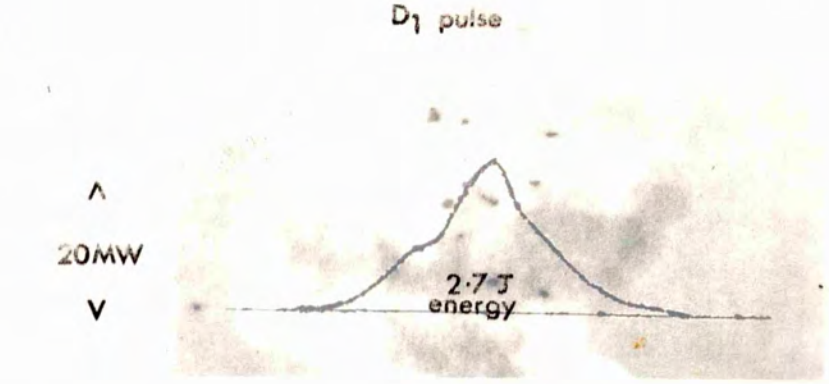

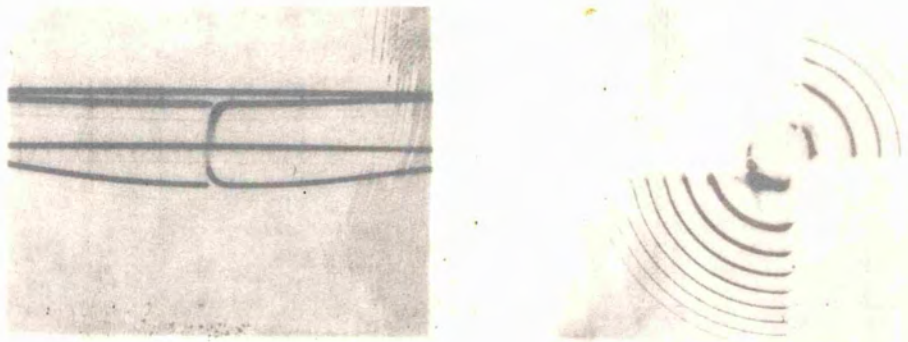

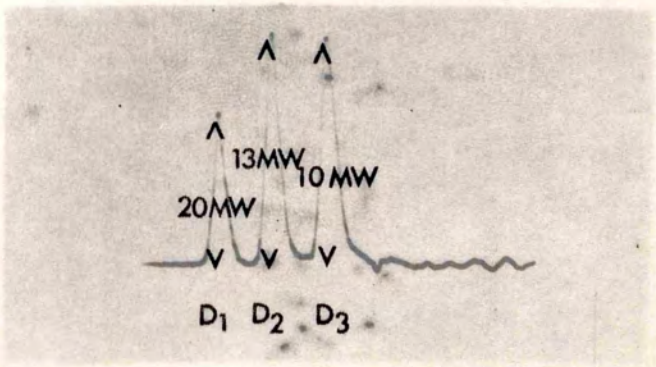

Fig.7.3
Diode Calibration

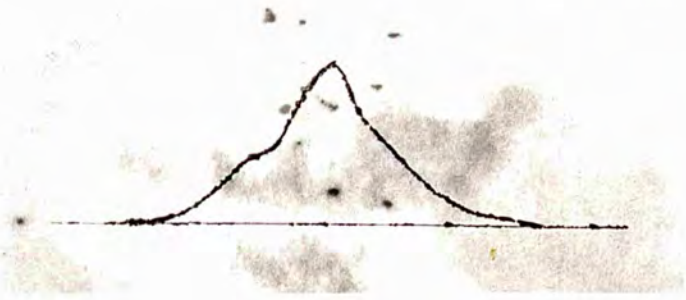

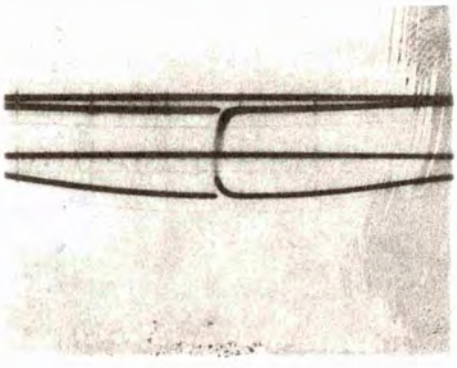

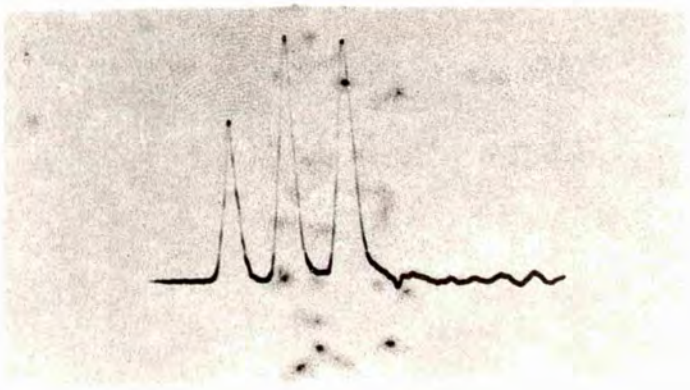

The power of the forward and backward going ruby light beams was controlled by copper sulphate solution attenuation. The shift in frequency of the backward going beam was measured on the Fabry-Perot, which also checked the single mode output of the ruby laser (Section 3.5)

The forward and backward going beams produced a refractive index modulation in the cell 1 (Fig.7.4) which could Bragg reflect the argon laser beam (Section 2.5) when it was incident at the appropriate angle. This angle is 45·5° for Bragg reflection of argon by ruby laser light and permitted convenient, nearly normal, incidence on the walls of the geometrically simple cell 1 (Fig.7.2). The angle between the ruby and argon laser beams could be measured to ·1° and much smaller incremental adjustments (·1 m.rad) could be accurately made using the 'spectrometer table' described in Section 3.4.

7.2 PROBE SCATTERING MECHANISMS

Two oppositely directed light waves in a medium may, as discussed in Chapter II, modulate the refractive index of that medium by a number of mechanisms[191]. The principal mechanisms involved are:-

(a) Absorption, which affects the temperature and hence the density of the medium.

(b) Electrostriction which directly affects the density of the medium.

(c) The Kerr effect which is a change in the polarizability of the medium due either to molecular re-orientation or to the non-linear polarizability of the molecules themselves.

Each of these mechanisms gives rise to an associated stimulated scattering process, these being:

(a) Stimulated thermal Rayleigh scattering[196], and the thermal modification of stimulated Brillouin scattering.

(b) Stimulated Brillouin scattering[170],

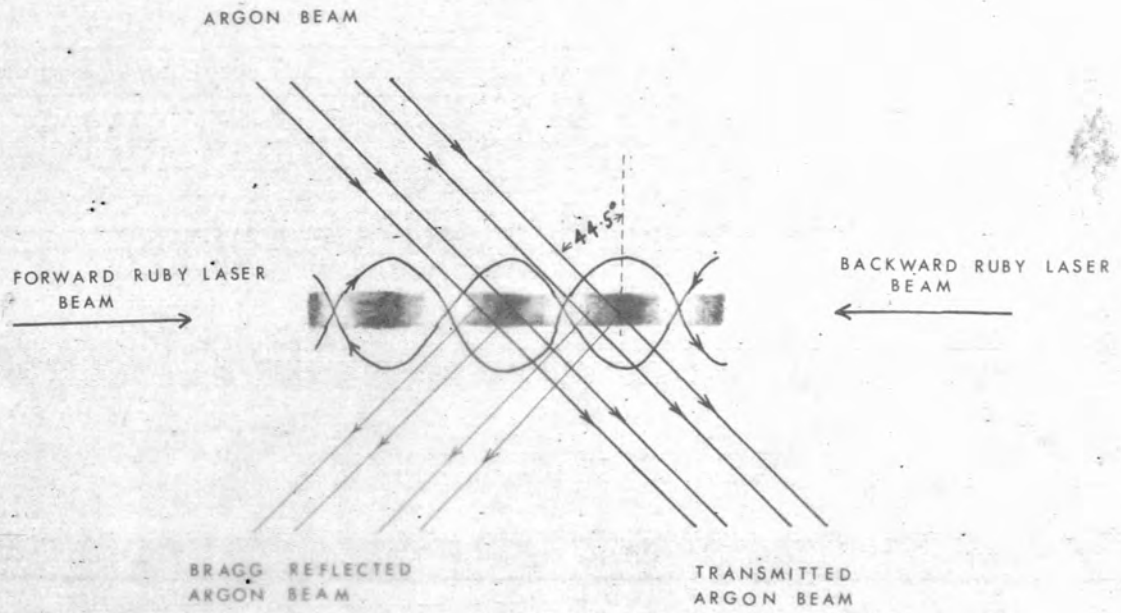

Fig. 7.4 Illustrative diagram showing Bragg reflection of a continuous argon beam from a periodic structure induced in a liquid by the standing wave of a ruby laser beam.

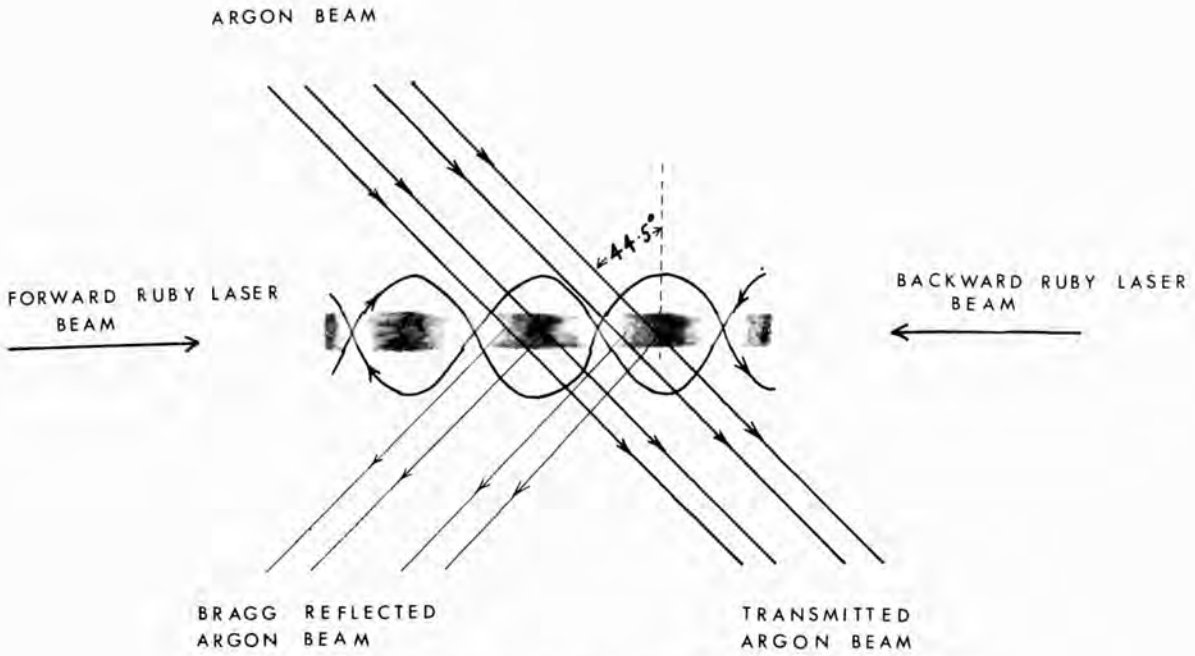

Fig.7.4. Illustrative diagram showing Bragg reflection of a continuous argon beam from a periodic structure induced in a liquid by the standing wave of a ruby laser beam.

(c) Stimulated Rayleigh wing scattering[184] and stimulated Raman scattering[156] due to molecular re-orientation and non-linear molecular polarizability respectively.

The refractive index modulation due to each mechanism also results in a corresponding probe scattering of the argon laser beam.

7.3 PROBE SCATTERING DUE TO ABSORPTION

The easiest of these mechanisms to identify positively is that of absorption. The resulting Bragg reflection has a maximum when the backward going and forward going beams are of the same frequency (Section 2.5) and, while absent when the beams intersect in a pure non-absorbing solvent, will appear when a small amount of an absorbing substance is dissolved in that solvent.

Fig.7.5 shows the signals on the diodes and photomultiplier when the backward beam was generated by a mirror and pure methanol (upper trace) or a solution of copper acetate in methanol (lower trace), were used in the scattering cell. [A solution of copper acetate in methanol with an absorption coefficient of $\bar{\cdot}15$ and an absorption spectrum as in Fig.7.6 is used in all these experiments unless otherwise stated.] The signal on the photomultiplier disappeared if either ruby light beam or the argon laser beam was cut off and was critically dependent on the angle between the beams.

These facts, and the absence of photomultiplier signal on the upper trace imply that the signal on the photomultiplier, displayed on the lower trace of Fig.7.5, was due to Bragg reflection of the argon laser from a phase grating produced by absorption of the ruby laser light.

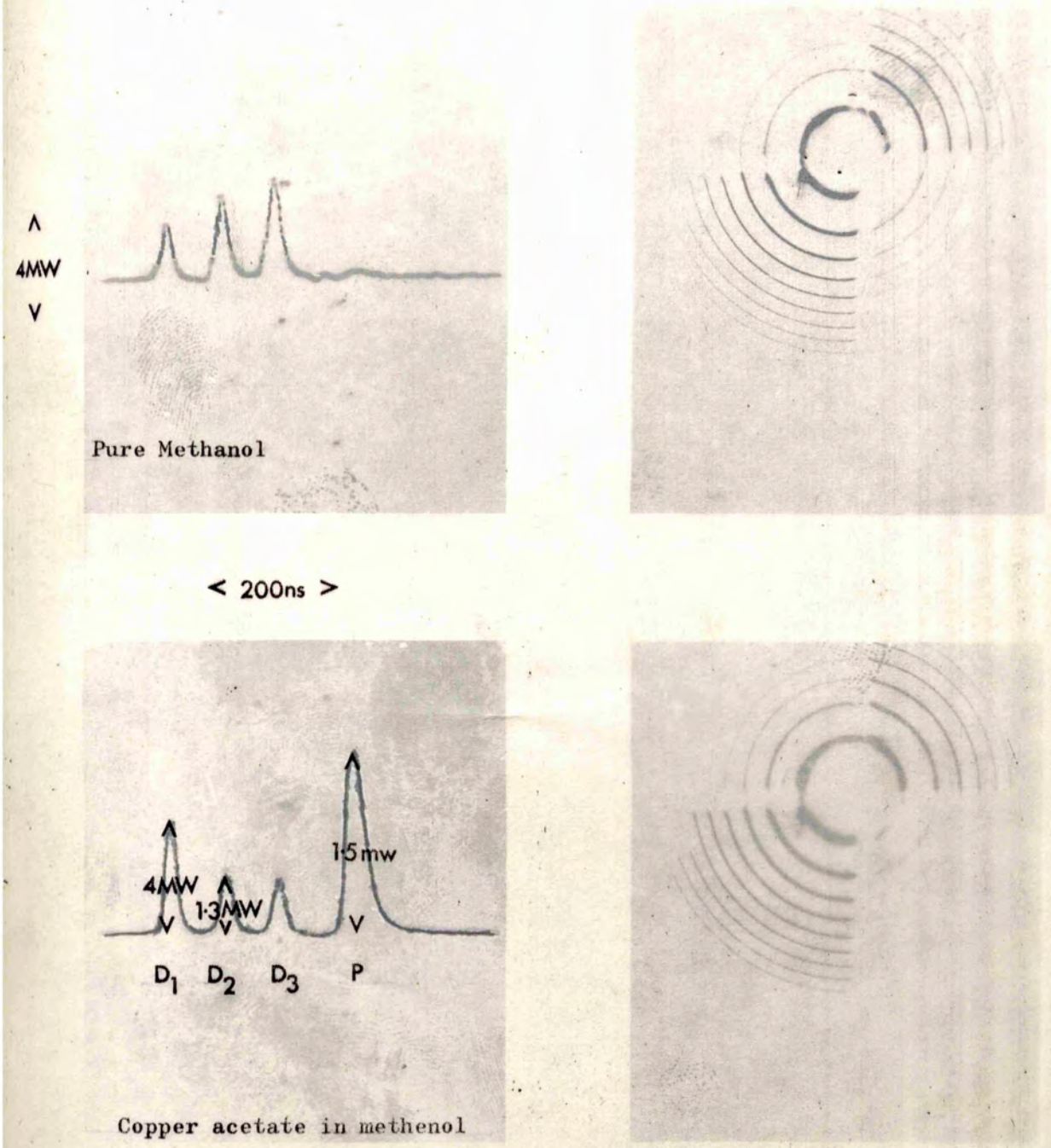

Fig.7.5
Bragg Reflection due to **Absorption**

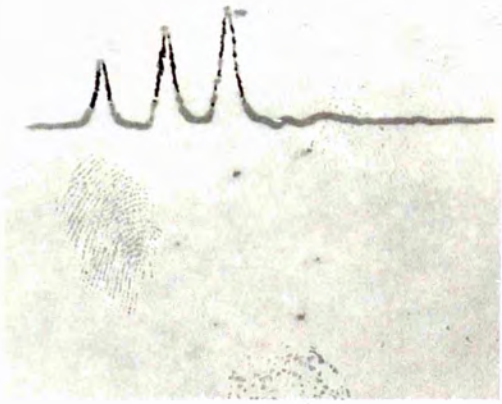

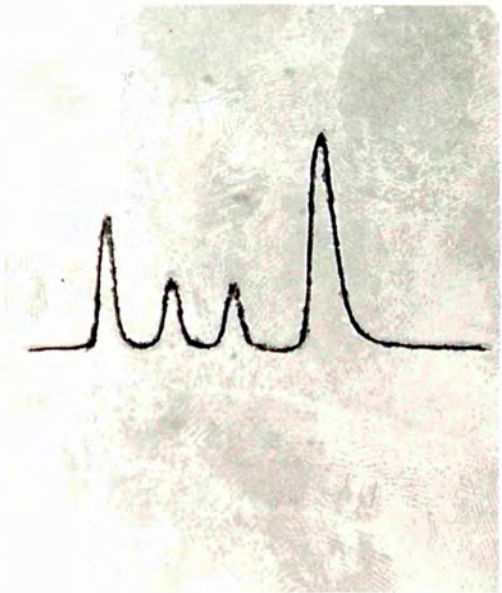

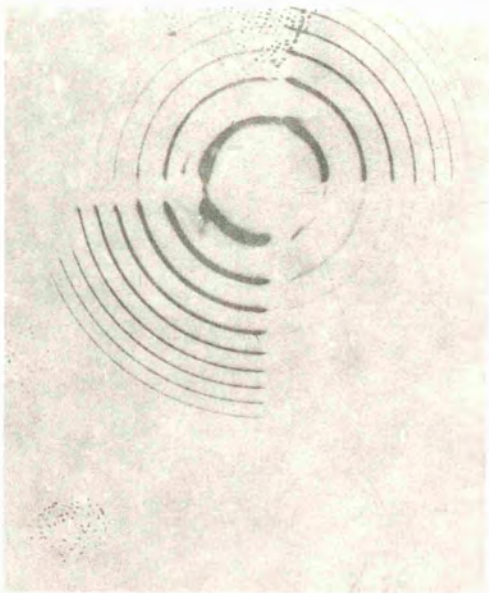

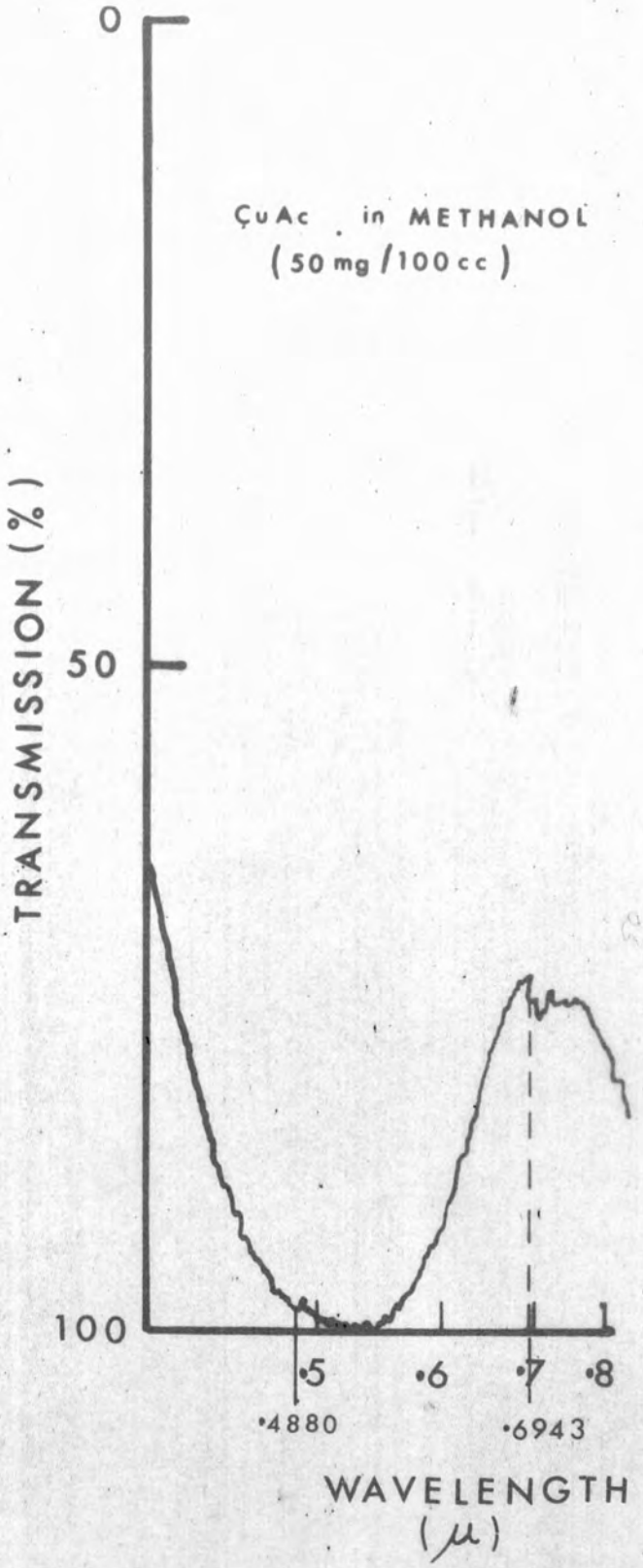

Fig. 7.6.
Absorption Spectrum of Copper Acetate in Methanol

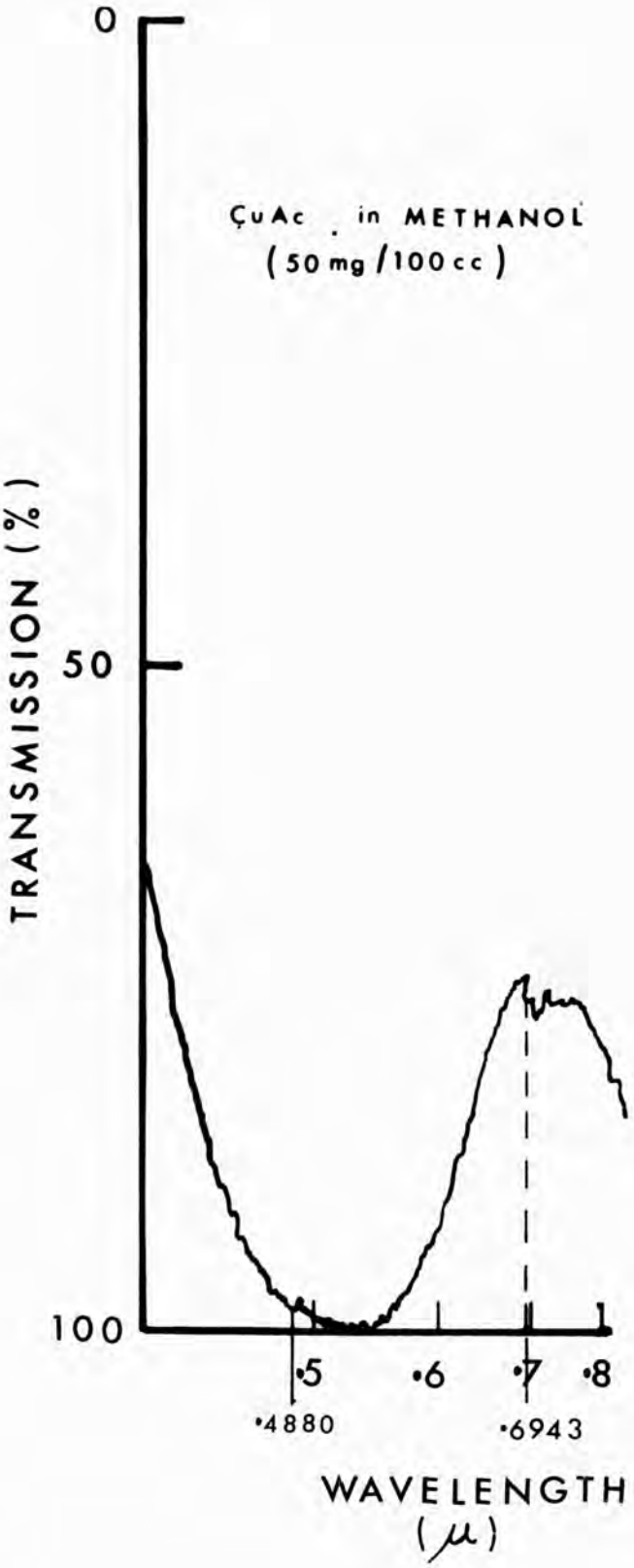
0
CuAc . in METHANOL
(50 mg/100 cc)
TRANSMISSION (%)
50
100
·5
·6
·7
·8
·4880
·6943
WAVELENGTH
(μ)

7.4 PROBE SCATTERING DUE TO ELECTROSTRICTION

The refractive index modulation induced by electrostriction is negligible unless the backward going beam contains light of a frequency shifted from that of the forward going beam by an amount close to the Brillouin frequency shift (Section 2.5). To obtain the photographs in Fig.7.7 the light of shifted frequency was generated by stimulated Brillouin scattering in the laser Q-switch and the backward beam was generated by the use of a mirror normal to the ruby laser beam rather than by focusing into cell 2. The spectra shown are those of the forward beam and were photographed with a simple Fabry-Perot interferometer not using the polaroid quadrant technique (Section 3.5). This system, used before the development of the more sophisticated arrangement of Fig.7.2, was adequate to demonstrate probe scattering due to electrostriction in pure methanol.

It can be seen in Fig.7.7 that when the frequency shifted light component was absent (top photo) there was no Bragg reflected signal on the photomultiplier. As the intensity of the light of shifted frequency increased (top to bottom photographs) the intensity of the Bragg reflected pulse also increased. The duration of the Bragg reflected pulse in this case is shorter than that in the case of thermal scattering since the latter was lengthened by the slow relaxation of the thermal grating whereas the former only exists while both the fundamental and Brillouin shifted beams exist.

7.5 PROBE SCATTERING DUE TO THE KERR EFFECT

The major part of the Kerr effect (that due to re-orientation) causes the greatest refractive index modulation when there is no shift in frequency of the backward going beam, (Section 2.5). This effect

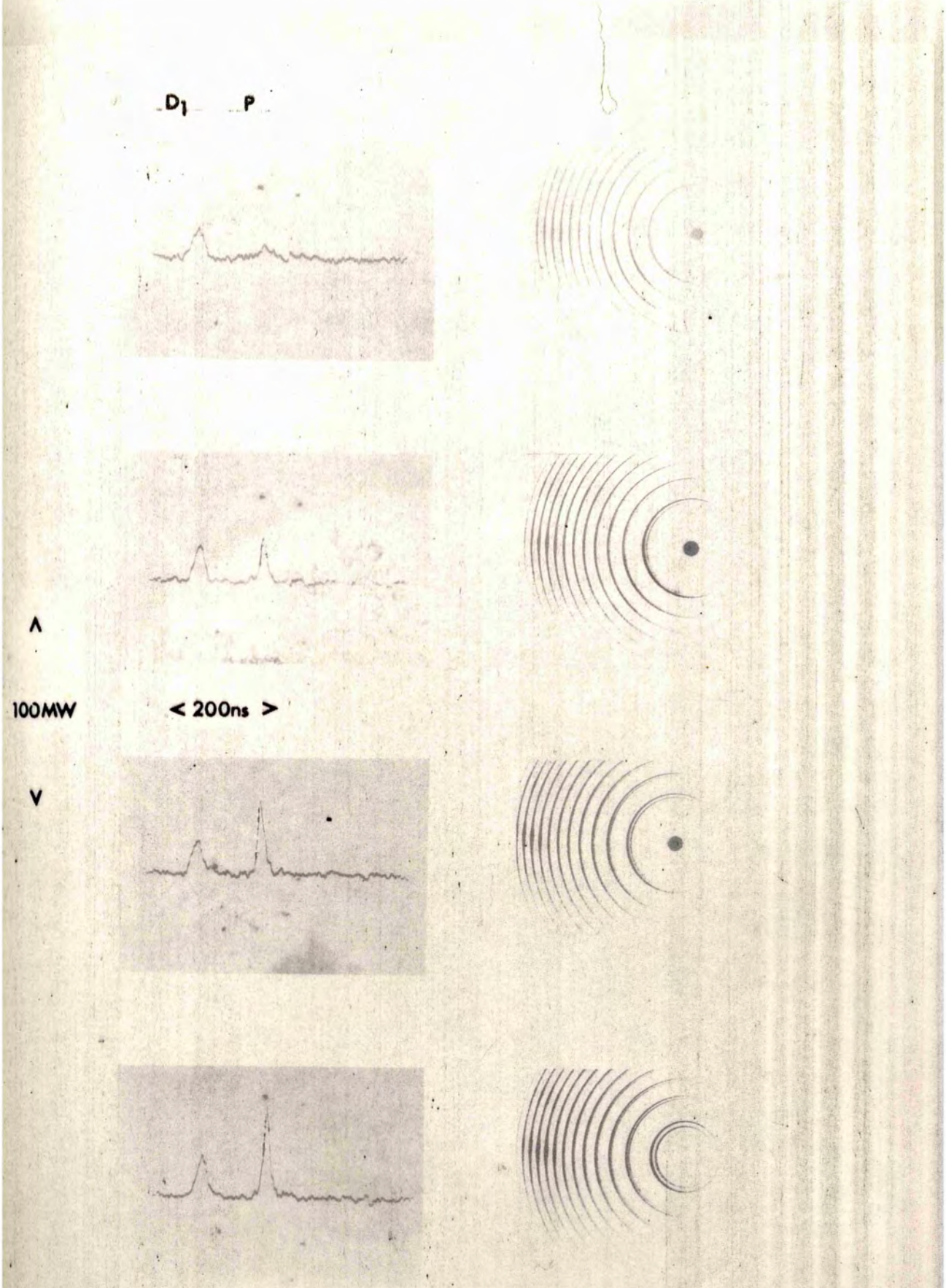

Fig.7.7
Bragg Reflection due to Electrostriction

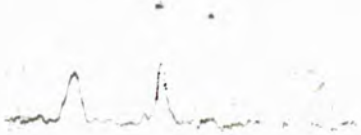

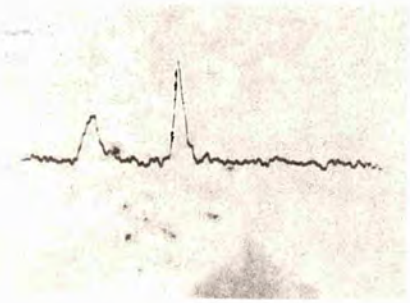

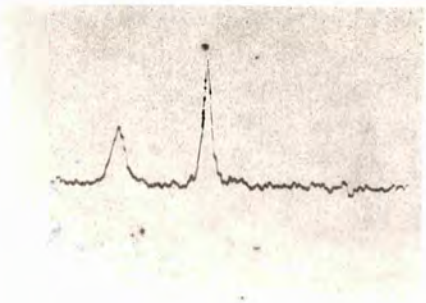

can therefore cause Bragg reflection in a pure non-absorbing medium when the backward and forward beams have the same frequency. This Bragg reflection is very weak in methanol and was not detectable under the experimental conditions of Fig.7.5. It is important to distinguish this weak Bragg reflection from that due to residual absorption in the medium or to a light component of shifted frequency too weak to detect on the Fabry-Perot. This can be done by taking into account their different polarization properties. The absorptive and electrostrictive mechanisms act on the density of the medium and have no directional properties. The Kerr effect however causes a refractive index change which has a value in the direction of the electric field of about twice that in a direction perpendicular to that field (Havelock's Law)[242].

The upper trace of Fig.7.8 shows the signal due to Bragg reflection from pure methanol with forward and backward beams of the same frequency. (A liquid of high Kerr effect, such as nitrobenzene could not be used because of the low self-trapping (Section 4.1) threshold in these liquids.) The middle trace was obtained when a disc of fused silica was placed in the path of the ruby laser beam to simulate the losses introduced in obtaining the lower trace. This caused no significant change in the Bragg reflection. To obtain the lower trace a disc of crystal quartz, with faces perpendicular to its optic axis, was placed in the ruby laser beam so that the polarization of that beam was rotated through 90^{o}. The marked reduction of the photomultiplier signal implies that the Kerr effect was the mechanism responsible for the Bragg reflection indicated by the traces of Fig.7.8.

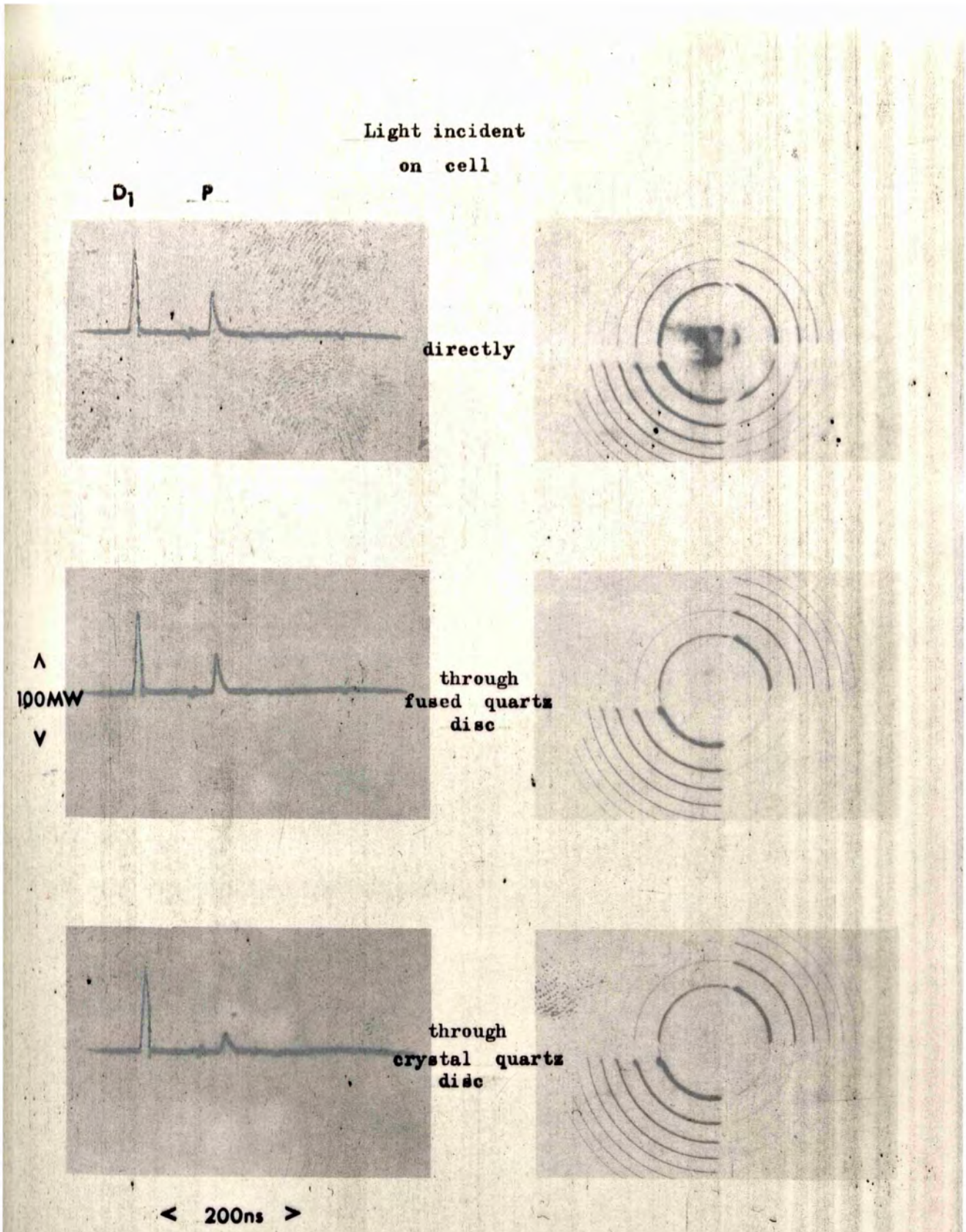

Fig.7.8
Bragg Reflection due to the Kerr Effect

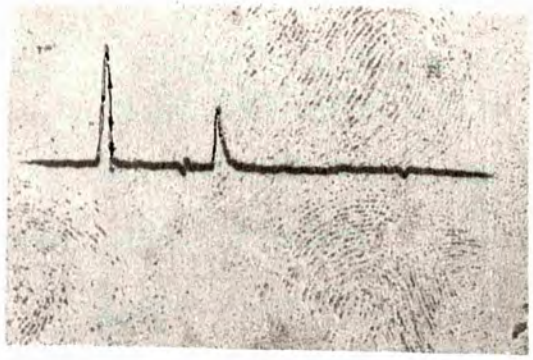

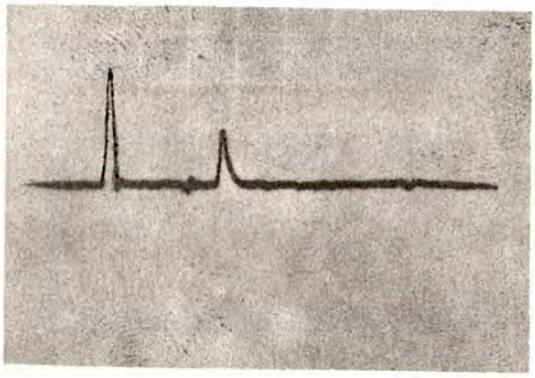

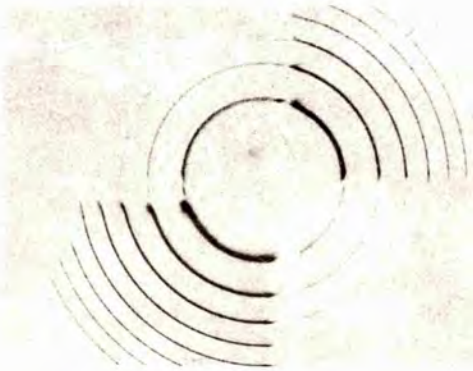

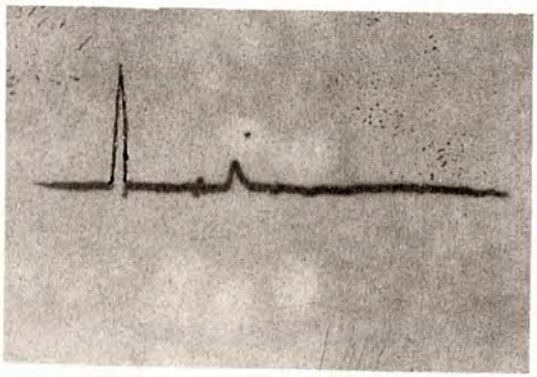

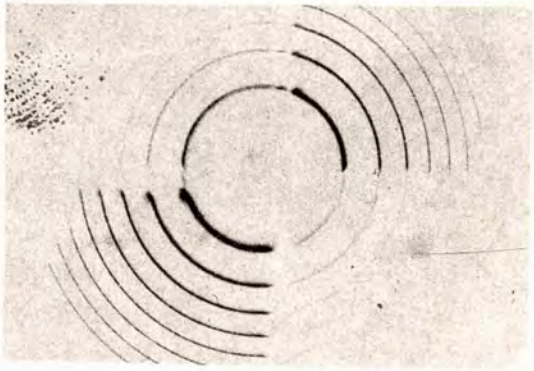

CHAPTER VIII

QUANTITATIVE STUDY OF PROBE SCATTERING DUE TO ABSORPTION

8.1 APPLICATION OF THEORETICAL CONCLUSIONS TO THE EXPERIMENTAL SITUATION

The probe scattering due to absorption was chosen for further study for a number of reasons.

First, in probe scattering experiments (in contrast to the situation in conventional stimulated scattering experiments[74,164]), absorption is the mechanism most easily studied experimentally. It results in a much stronger Bragg reflection than that due to the Kerr effect and is more easily induced than electrostriction.

Secondly, the build-up and decay of the thermal grating induced by absorption is a relatively slow process (10^{-8} secs) and can be conveniently studied by probe scattering whereas the density grating induced by electrostriction and the molecular orientations responsible for the Kerr effect have much shorter lifetimes (10^{-10} and 10^{-12} secs respectively) more easily studied by the broadening of the associated spontaneous scattering lines.

Thirdly, this mechanism has previously undergone considerably less investigation.

Let us consider the equation for absorptive probe scattering derived in Section 2.5.

$$\left(\frac{I_R}{I_I}\right)_{max} = \left(\frac{\pi N \alpha \beta \gamma}{8k_r^2 \; n_r^2 \cos^2\theta_{max} \; K \; n_a^2}\right)^2 \; \frac{1}{1+\left(\frac{\omega}{\Gamma_R}\right)^2} I_1 I_2 .$$

In the experiment a mirror was used to generate the backward going beam so $\omega = 0$ and the equation becomes

$$\left(\frac{I_R}{I_I}\right)_{max} = \left(\frac{\pi N \alpha \beta \gamma}{8k_r^2 \; n_r^2 \cos^2\theta_{max} \; K \; n_a^2}\right)^2 \; I_1 I_2 .$$

Now $\left(\frac{I_R}{I_I}\right)_{max}$ is the reflectivity of the grating for probe light incident at the angle θ_{max}. This reflectivity falls off sharply with any change in angle the angular width at half reflectivity being:

$$\delta\theta = \frac{4 \times 1{\cdot}39}{\pi\ N \tan \theta_{max}} \quad .$$

Since N the number of refractive index modulations in the scattering region was about 10^5 this angle is much less than $\Delta\theta$ the divergence of the argon laser beam which was about two milliradians. The maximum reflectivity for the whole argon laser beam was therefore approximately:

$$\frac{\delta\theta}{\Delta\theta} \cdot \left(\frac{I_R}{I_I}\right)_{max}$$

while the angular dependence of the reflectivity was the same as the angular distribution of the argon laser beam intensity.

Now the values of $\left(\frac{I_R}{I_I}\right)_{max}$ and $\delta\theta$ were calculated in Section 2.5 for a region of length L (along the ruby beam direction) in which constructive interference of the increments of light amplitude reflected from each modulation could occur. In the experimental situation where the narrow argon laser beam crosses the much wider ruby laser beam the dimensions of such a region would be approximately the diameter of the argon laser beam $\mathcal{L}_a$. The number of such regions, which may be considered as scattering independently, would be $\frac{\mathcal{L}_r}{\mathcal{L}_a}$.

The overall reflectivity for the argon laser beam crossing the phase grating induced by the ruby laser beam at the angle giving maximum reflection is thus R where:

$$R \sim \frac{\mathcal{L}_r}{\mathcal{L}_a} \cdot \frac{\delta\theta}{\Delta\theta} \cdot \left(\frac{I_R}{I_I}\right)_{max} ,$$

therefore

$$R \sim \frac{\mathcal{L}_r}{\mathcal{L}_a} \cdot \frac{4 \times 1{\cdot}39}{\pi\ N \tan \theta_{max}\ \Delta\theta} \cdot \left(\frac{\pi\ N\ \alpha\ \beta\ \gamma}{8\ k_r^2\ n_r^2 \cos^2 \theta_{max}\ K\ n^2}\right)^2 I_1\ I_2$$

but:

$$\pi N = \frac{2 \pi n_r \mathcal{L}_a}{\lambda_r} = k_r n_r \mathcal{L}_a \quad ,$$

therefore:

$$R \sim \mathcal{L}_r \cdot \frac{4 \times 1{\cdot}39}{k_r n_r \tan \theta_{max} \Delta\theta} \cdot \left(\frac{\alpha \beta \gamma}{8 k_r n_r \cos^2 \theta_{max} K n_a^2} \right)^2 I_1 I_2 .$$

8.2 ABSOLUTE VALUE OF THE BRAGG REFLECTIVITY

The lower trace of Fig.7.5 was obtained when the intensity of the forward going beam was 20 MW/cm^2 (power 3·7 MW, diameter $\frac{1}{2}$ cm) and that of the backward going beam was a third of this value. The height of the photomultiplier pulse indicates a reflectivity of about ·15%.

The liquid in the scattering cell was a solution of copper acetate in methanol with an absorption coefficient of $\bar{\cdot}15$ cm^{-1}. The values of the parameters, appropriate to this solution, appearing in the reflectivity equation are given at the end of the Appendix. Using these parameters we find, under the experimental conditions:

$$R \sim 10^{-3}$$

A more accurate calculation of the absolute value is not justified in view of the unknown intensity distributions of the three beams involved and the inaccuracy introduced in the calibration of the Bragg reflected pulse (Section 3.1). For these reasons the variation of reflectivity with the relevant experimental parameters provides a better test of theory than its absolute magnitude.

8.3 VARIATION OF REFLECTIVITY WITH THE ANGLE BETWEEN THE BEAMS

Fig.8.1 shows the oscilloscope traces obtained when the angle between the beams was varied in the region of $\bar{45}{\cdot}5^0$. The results shown confirm this estimate of θ_{max}. In the graph the fact that $R \propto I_1 I_2 \propto I_1^2$ has been used to calculate the value of reflectivity

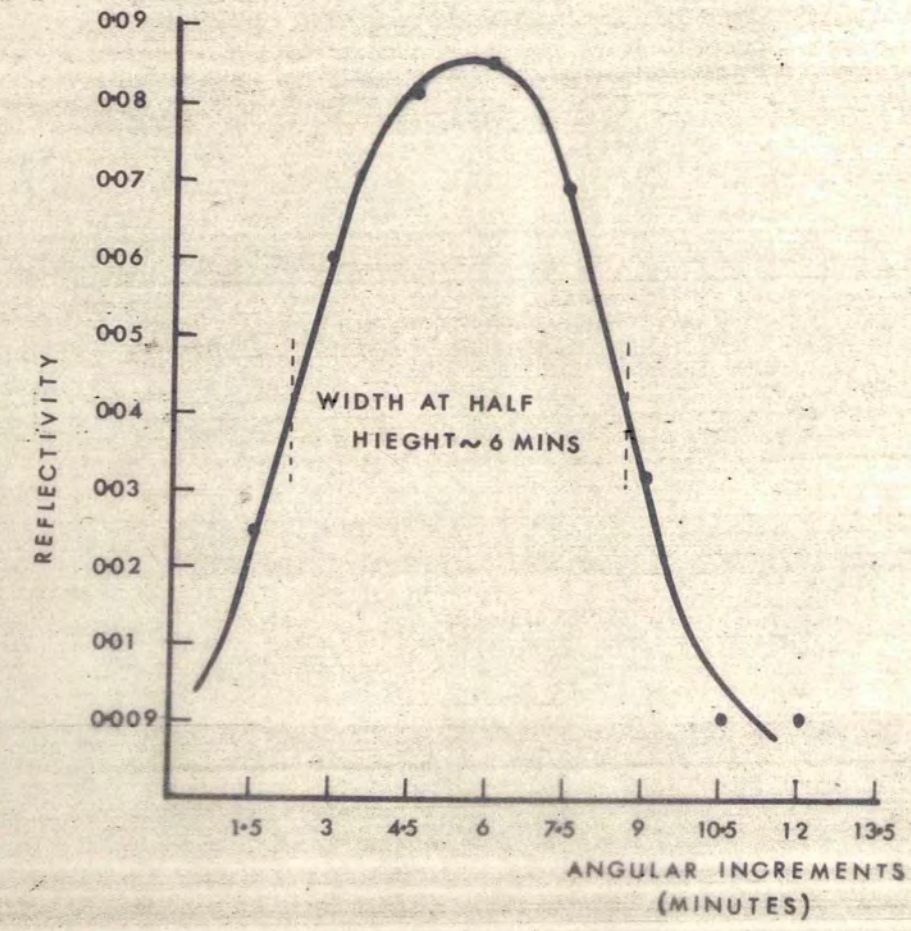

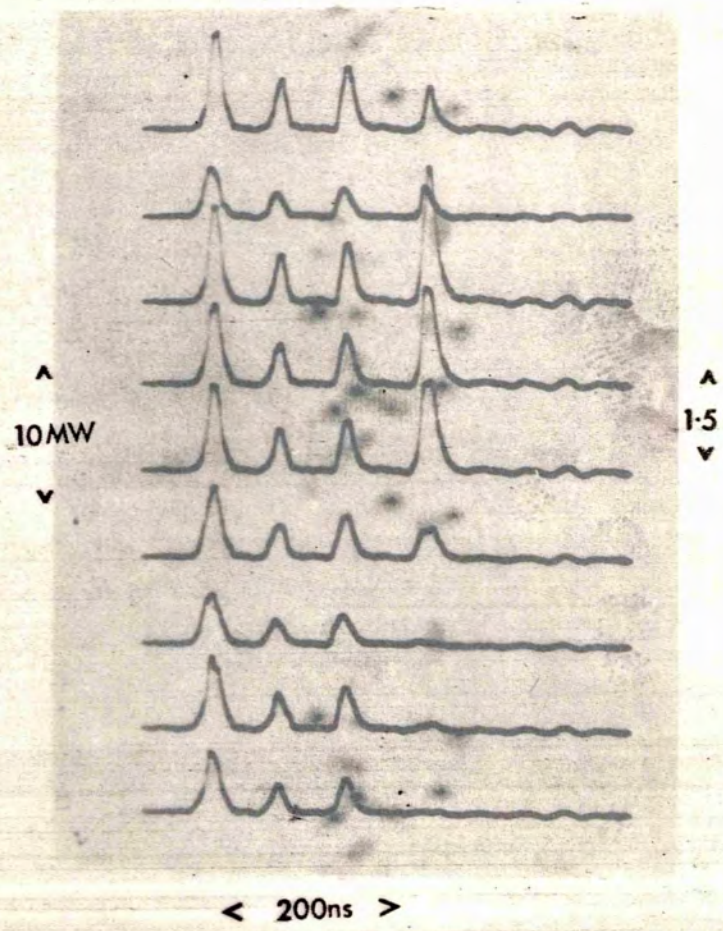

Fig.8.1
Variation of Reflectivity with the Angle between the Beams

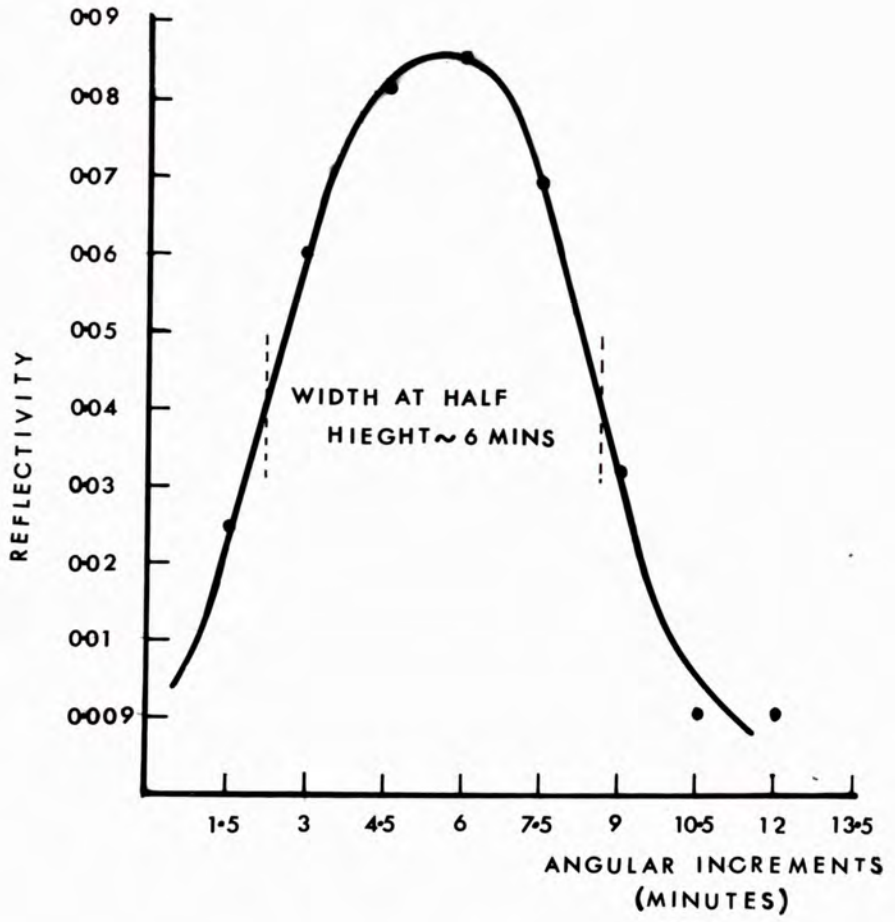
0·09
0·08
0·07
0·06
0·05
0·04
0·03
0·02
0·01
0·009
REFLECTIVITY
WIDTH AT HALF
HIEGHT ~ 6 MINS
1·5
3
4·5
6
7·5
9
10·5
12
13·5
ANGULAR INCREMENTS
(MINUTES)

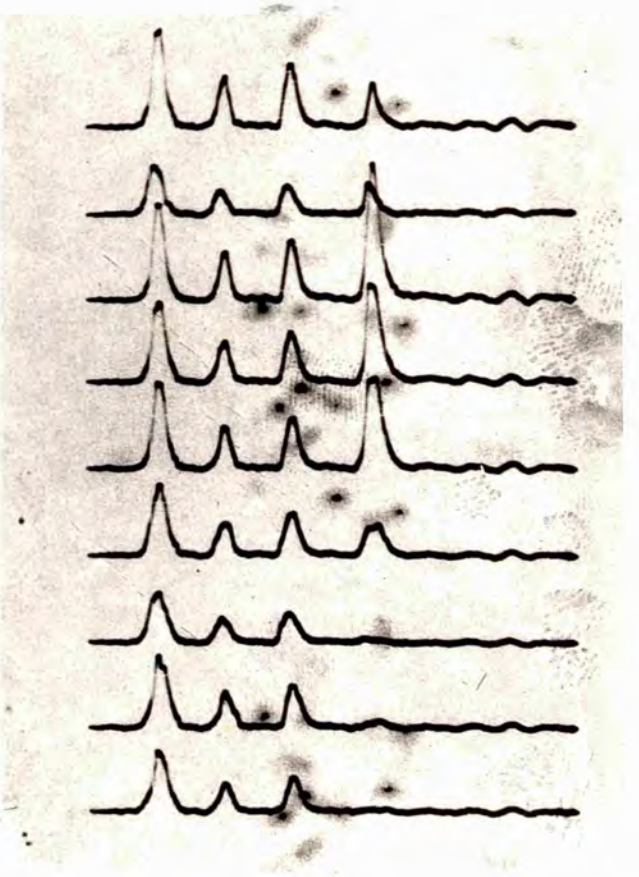

which would have been observed had I_1 been constant. This graph shows an angular distribution of reflectivity with a width at half height of six minutes. As expected this is approximately equal to the 2 m.rad. divergence of the argon laser beam.

8.4 VARIATION OF REFLECTIVITY WITH INCIDENT POWERS

In practice it was difficult to keep I_2 constant when I_1 was varied as this involved varying the absorption in both attenuators simultaneously. Instead Fig.8.2 shows the reflectivity for various values of I_1 when $I_2 = \frac{I_1}{3}$. Clearly the results fit the line showing $R \propto I_1^2$. This relationship has been used to correct for fluctuations in the laser output in graphs where the effect of other parameters was being investigated.

Fig.8.3 shows that $R \propto I_2$ when I_1 is constant. Together these results confirm the theoretical relationship $R \propto I_1 I_2$.

The absolute magnitudes of reflectivity in these and subsequent graphs were not rigourously calibrated as were those in Section 8.2. The vertical scale must therefore be regarded as arbitrary but this does not affect any conclusions as only the relative values are of importance here. The considerable errors shown in the graphs were probably due mainly to the lask of transverse mode control in the ruby laser. This would have resulted in large and varying differences in intensity over the area of the beam.

Fig.8.4 shows the variation of reflected with incident argon laser power. The linear law indicated shows that the reflectivity of the grating is independent of the argon laser power, confirming that the argon laser itself is a passive probe not contributing non-linear effects of its own. (This is not true in media which absorb at 4880Å.

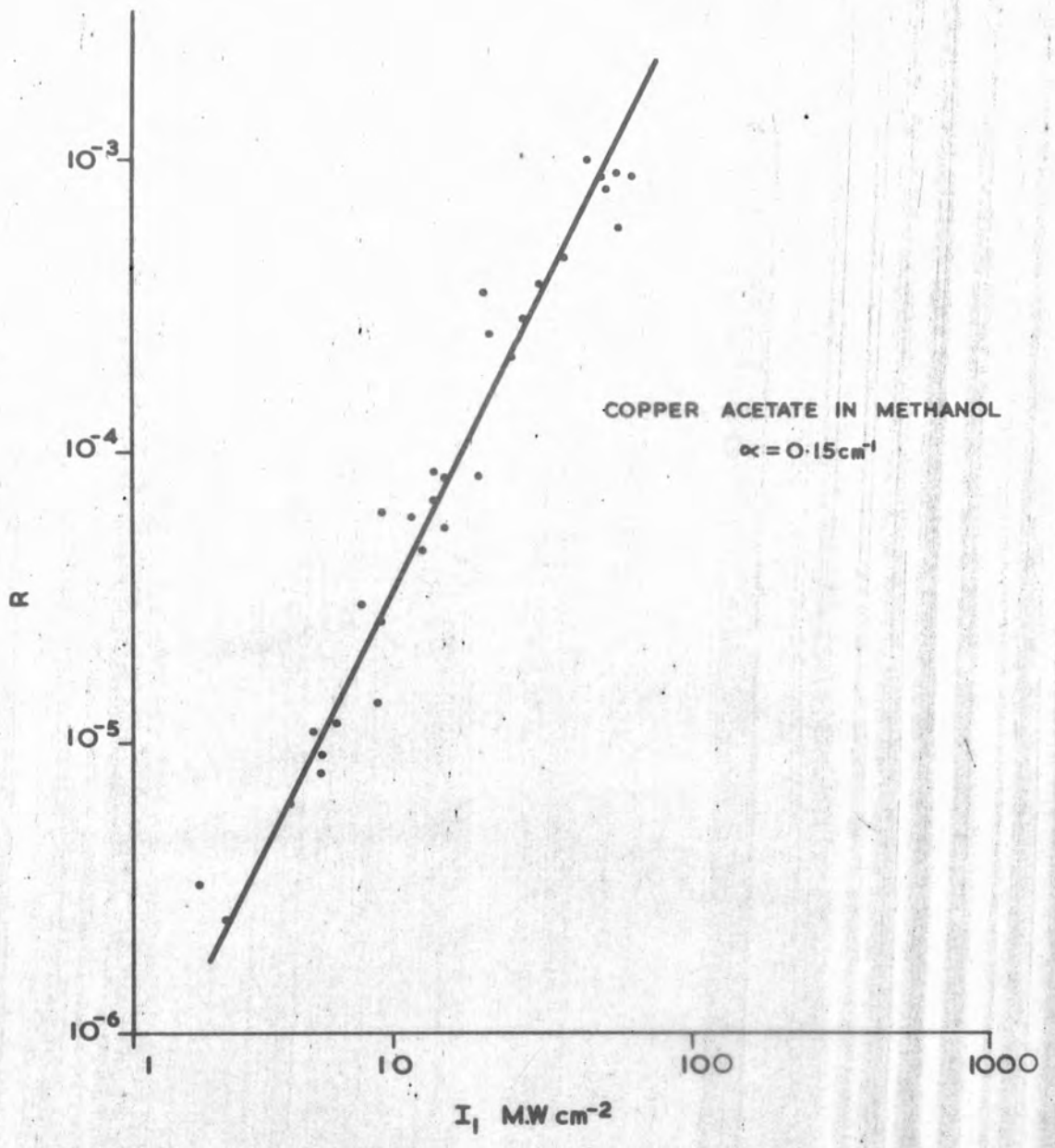

Fig.8.2.
Reflectivity (R) of the phase grating as a function of the intensity (I_1) of the forward-going beam with $I_2 \propto I_1$. The line shows the theoretical square law.

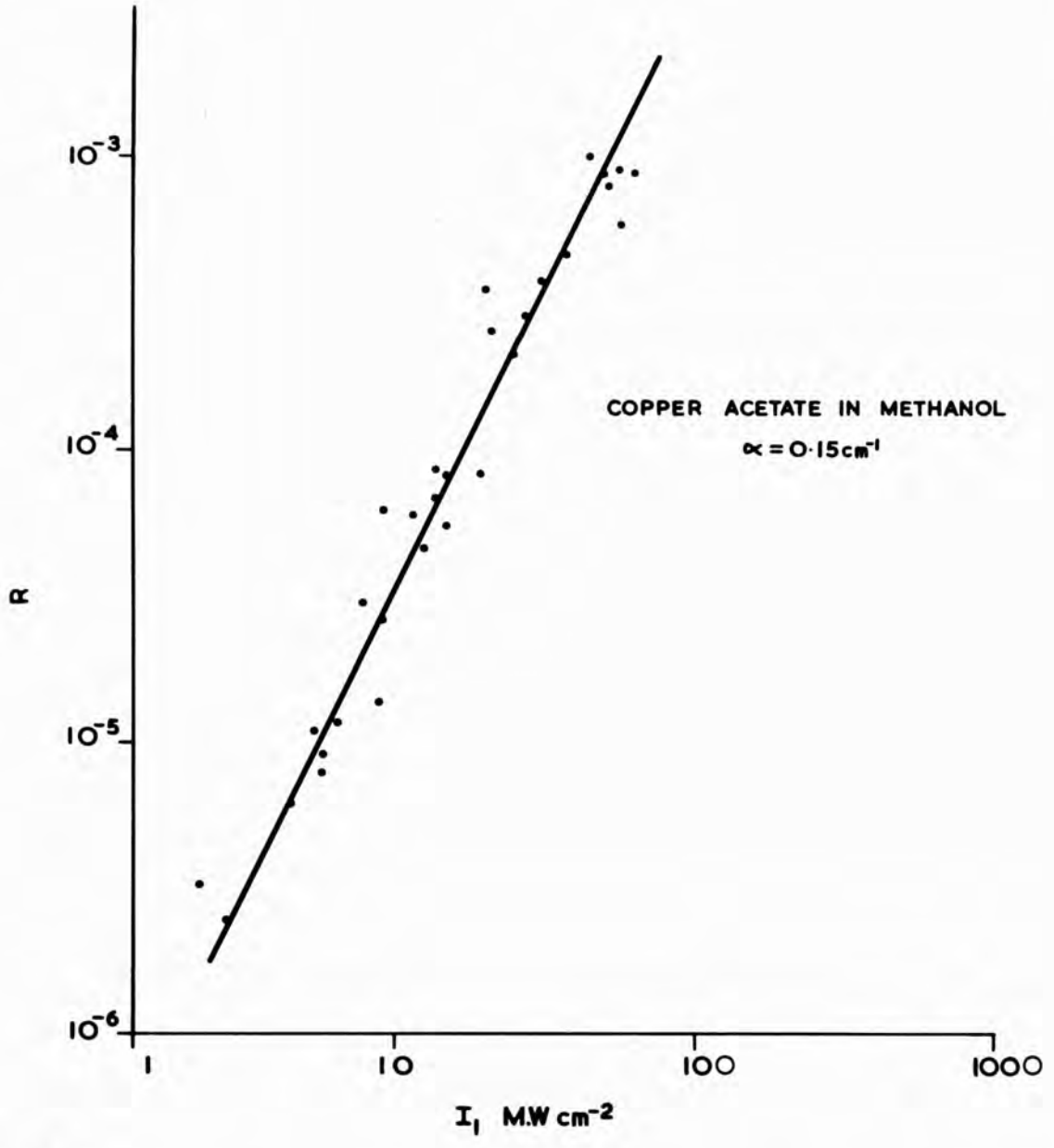

Fig.8.2.

Reflectivity (R) of the phase grating as a function of the intensity (I_1) of the forward-going beam with $I_2 \propto I_1$. The line shows the theoretical square law.

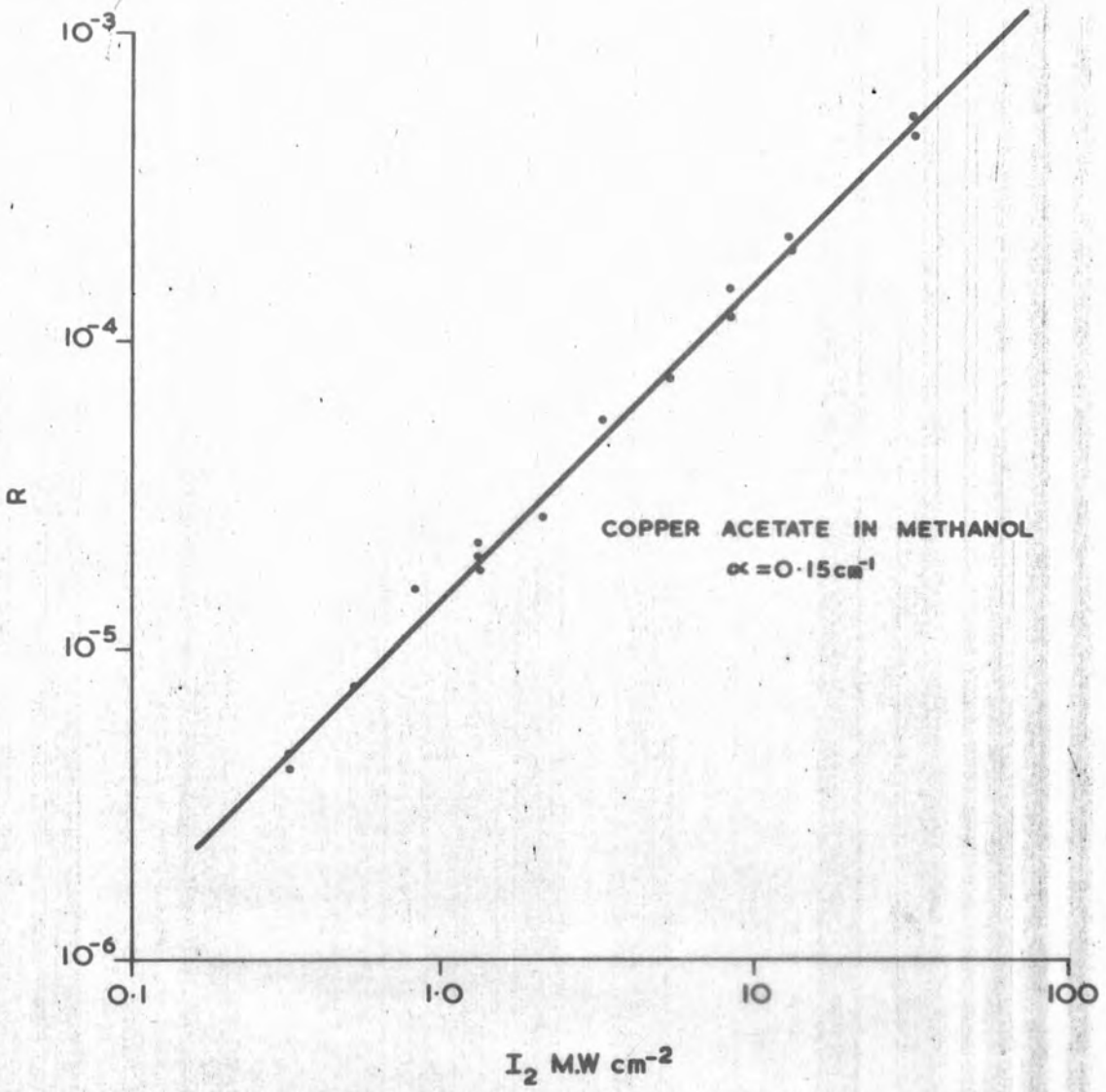

Fig. 8.3.
Reflectivity (R) of the phase grating as a function of the intensity (I_2) of the backward-going beam with I_1 constant at 71 MW cm^{-2}. The line shows the theoretical linear law.

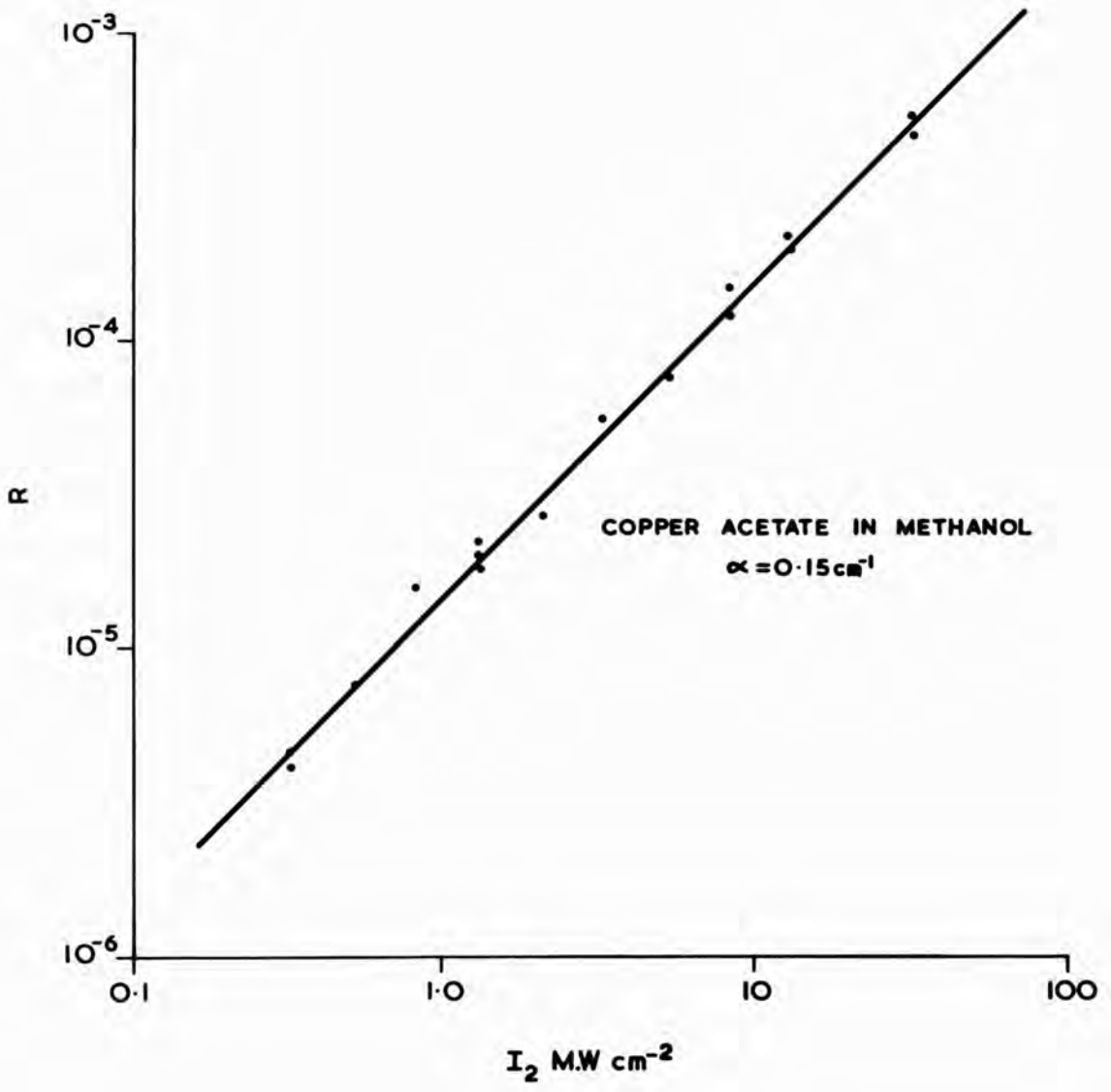

Fig. 8.3.
Reflectivity (R) of the phase grating as a function of the intensity (I_2) of the backward-going beam with I_1 constant at 71 MW cm^{-2}. The line shows the theoretical linear law.

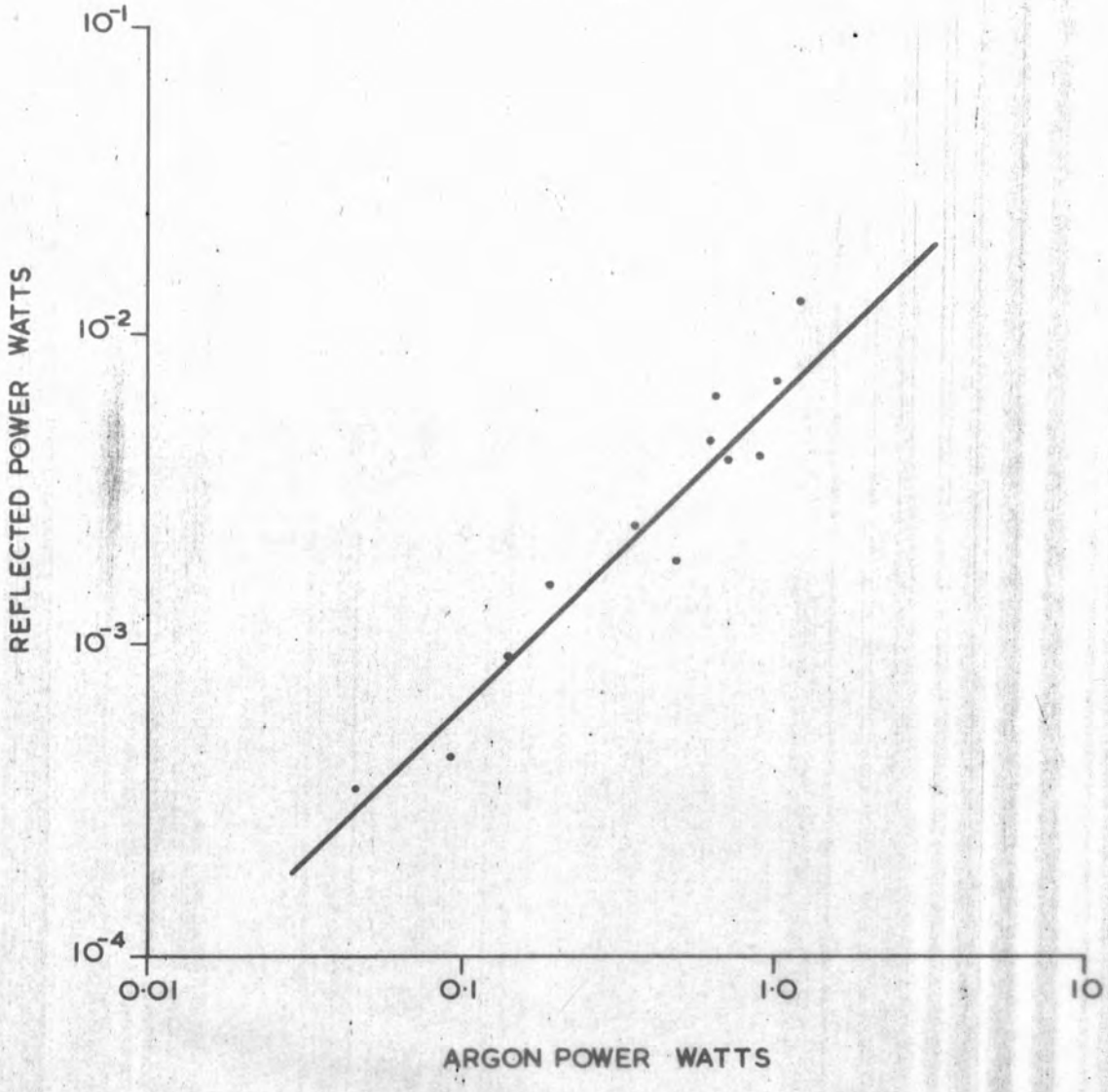

Fig.8.4.
Reflected power as a function of incident argon laser power.

CLM-P224

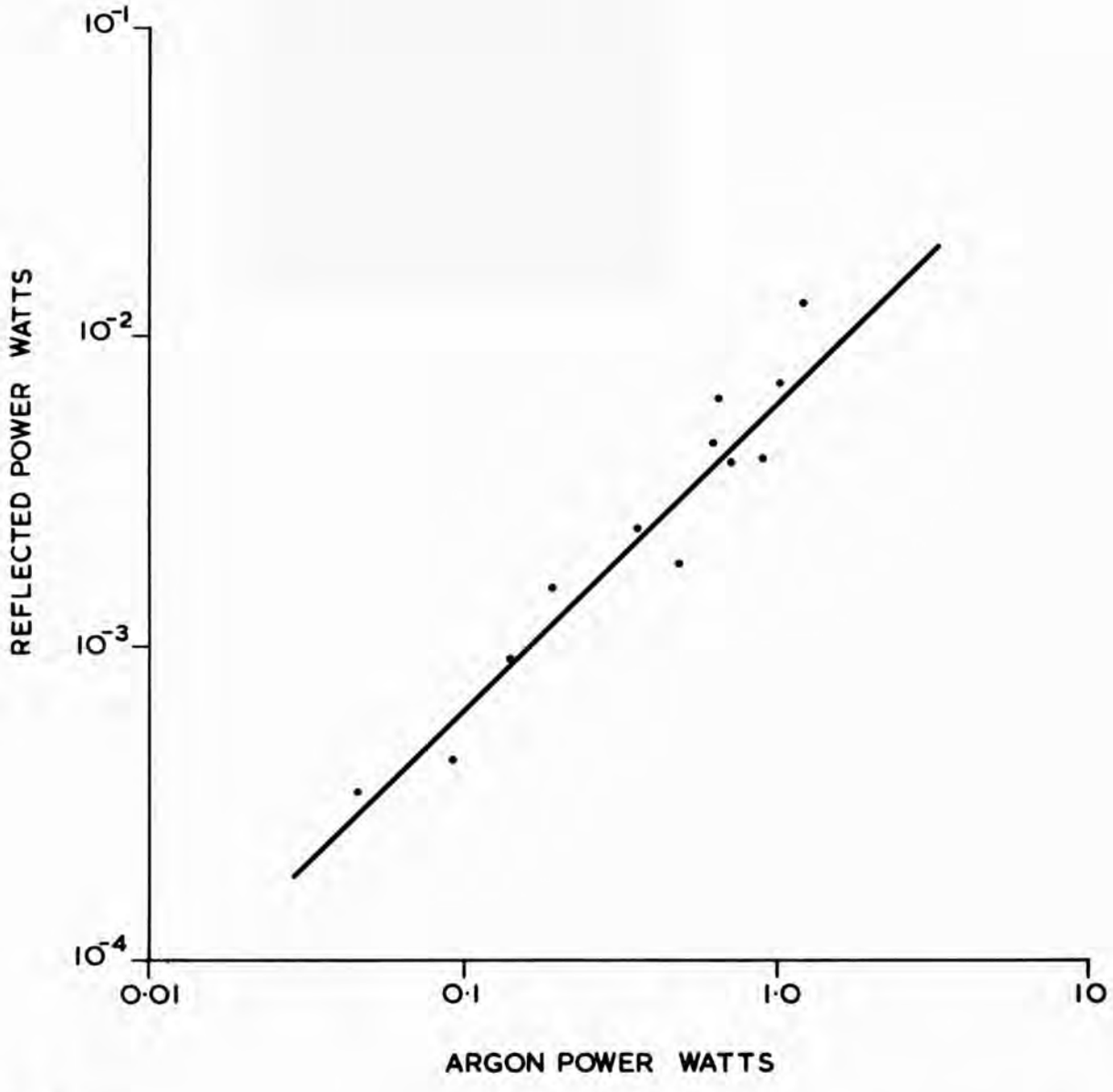

Fig.8.4.
Reflected power as a function of incident argon laser power.

CLM-P224

In such media there is a marked decrease in reflectivity with argon laser power due to defocusing (Section 4.2).)

Fig.8.5 indicates the reflectivity observed using a solution of cryptocyanine in methanol with $I_2 \propto I_1$. This reflectivity is also proportional to I_1^2 for intensities below 10 MW/cm. At higher intensities the reflectivity is less that that predicted by the square law because of saturation of the absorption of the dye.

8.5 VARIATION OF REFLECTIVITY WITH ABSORPTION COEFFICIENT

Fig.8.6 shows the variation of reflectivity with the absorption coefficient of the solution.

To obtain these results a thin cell containing the absorbing solution was inserted in the main cell in such a position as to contain the region of intersection of the ruby and argon laser beams. This arrangement, which did not interfere with the beam alignment, was necessary to avoid too great attenuation of the backward beam. Such attenuation occurs in any case and the points in the graph have been corrected to show the reflectivity that would have occurred had $I_1 I_2$ been constant. The graphs confirms the theoretical relationship $R \propto \alpha^2$.

8.6 VARIATION OF REFLECTIVITY WITH POSITION OF INTERACTION REGION

Fig.8.7 shows the reflectivity observed with the interaction region at a distance z from the back face of the scattering cell. Absortion in the cell results in the relationships $I_1 \propto e^{\alpha z}$, $I_2 \propto e^{-\alpha z}$. Thus $I_1 I_2$ is constant in the absence of non-linear effects. Any variation in the reflectivity is therefore due to gain in the backward beam caused by stimulated thermal Rayleigh scattering.

The gain indicated by the graph is about $\cdot 2\ cm^{-1}$. The laser

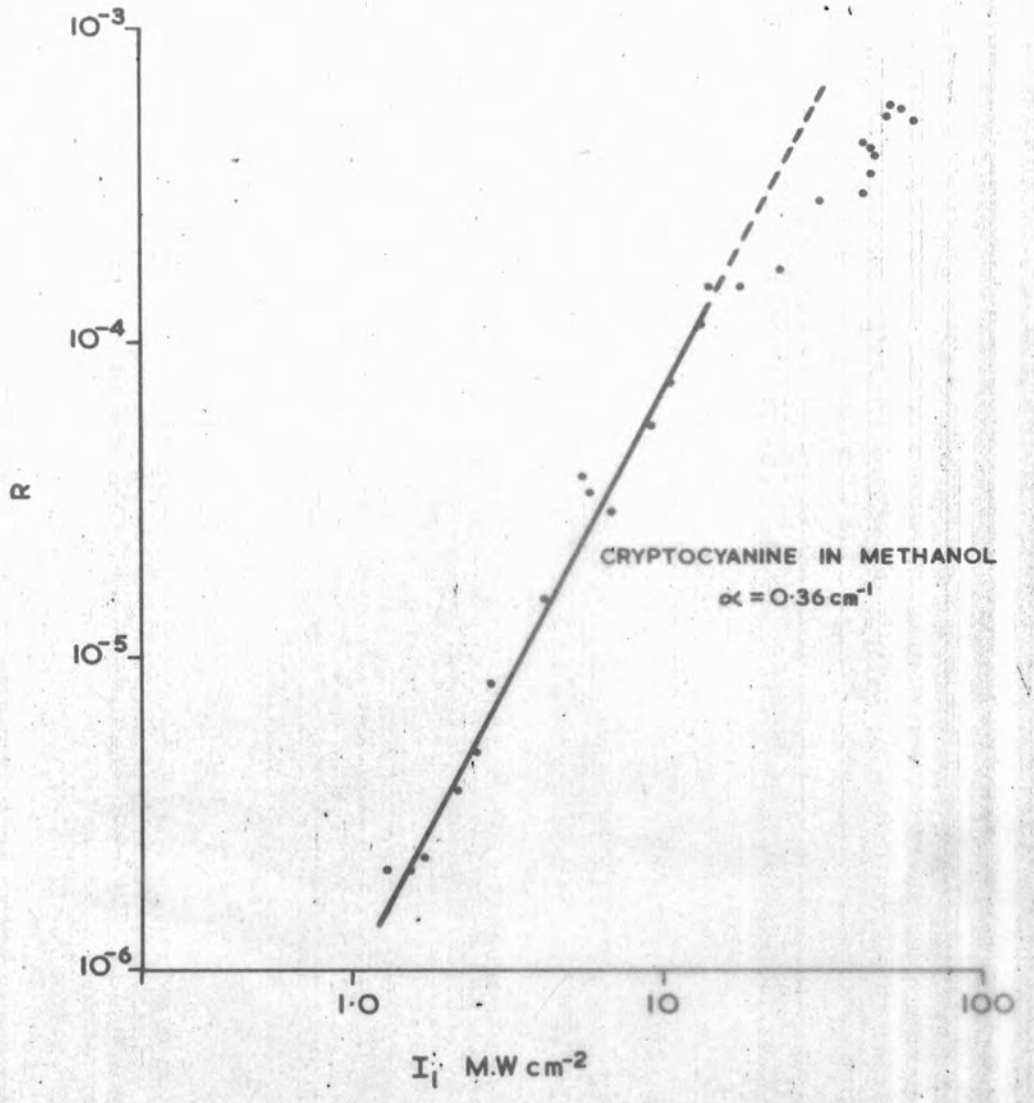

Fig.8.5
Reflectivity of phase grating as a function of I_1 for a saturable absorber.

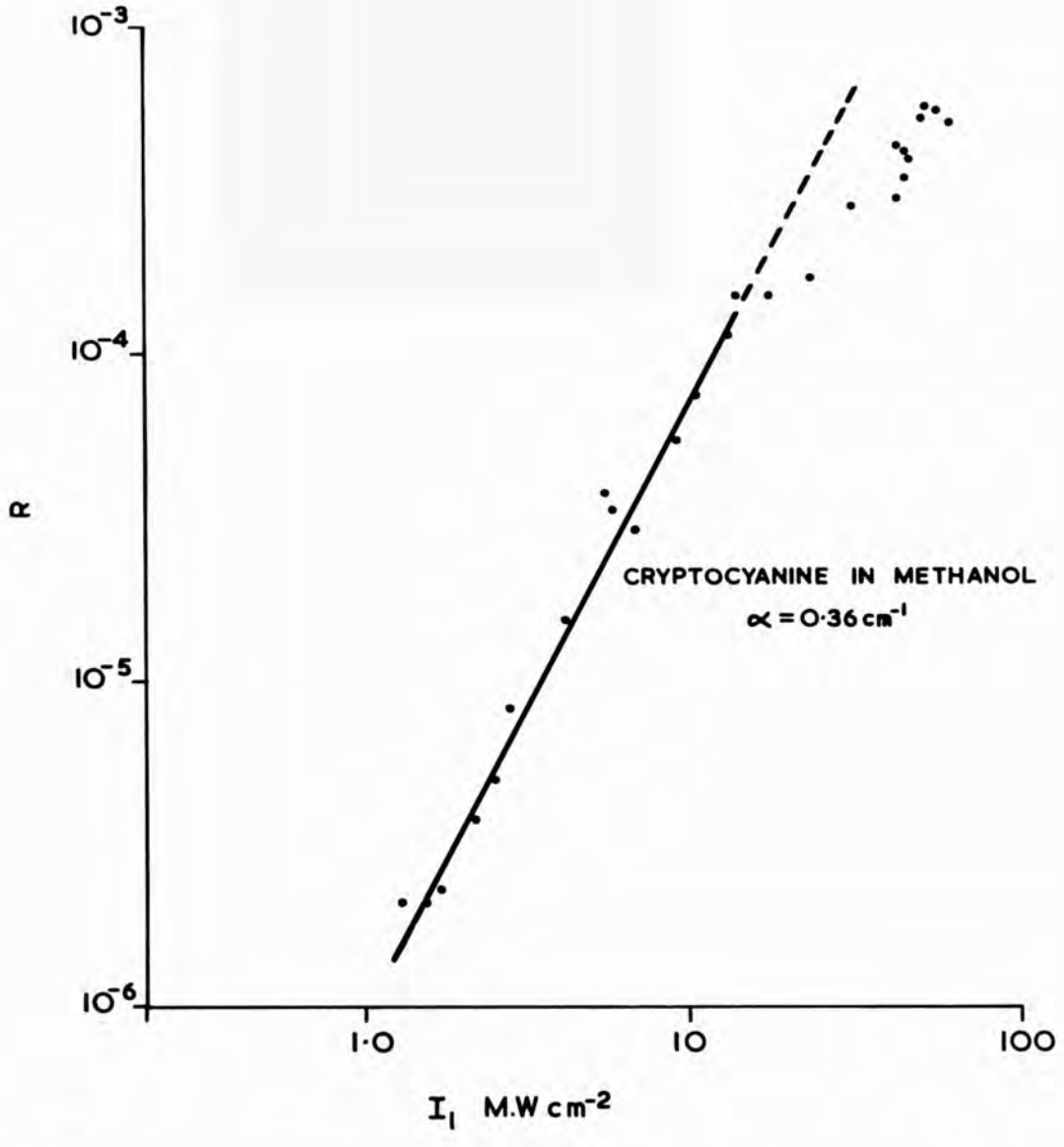

Fig.8.5
Reflectivity of phase grating as a function of I_1 for a saturable absorber.

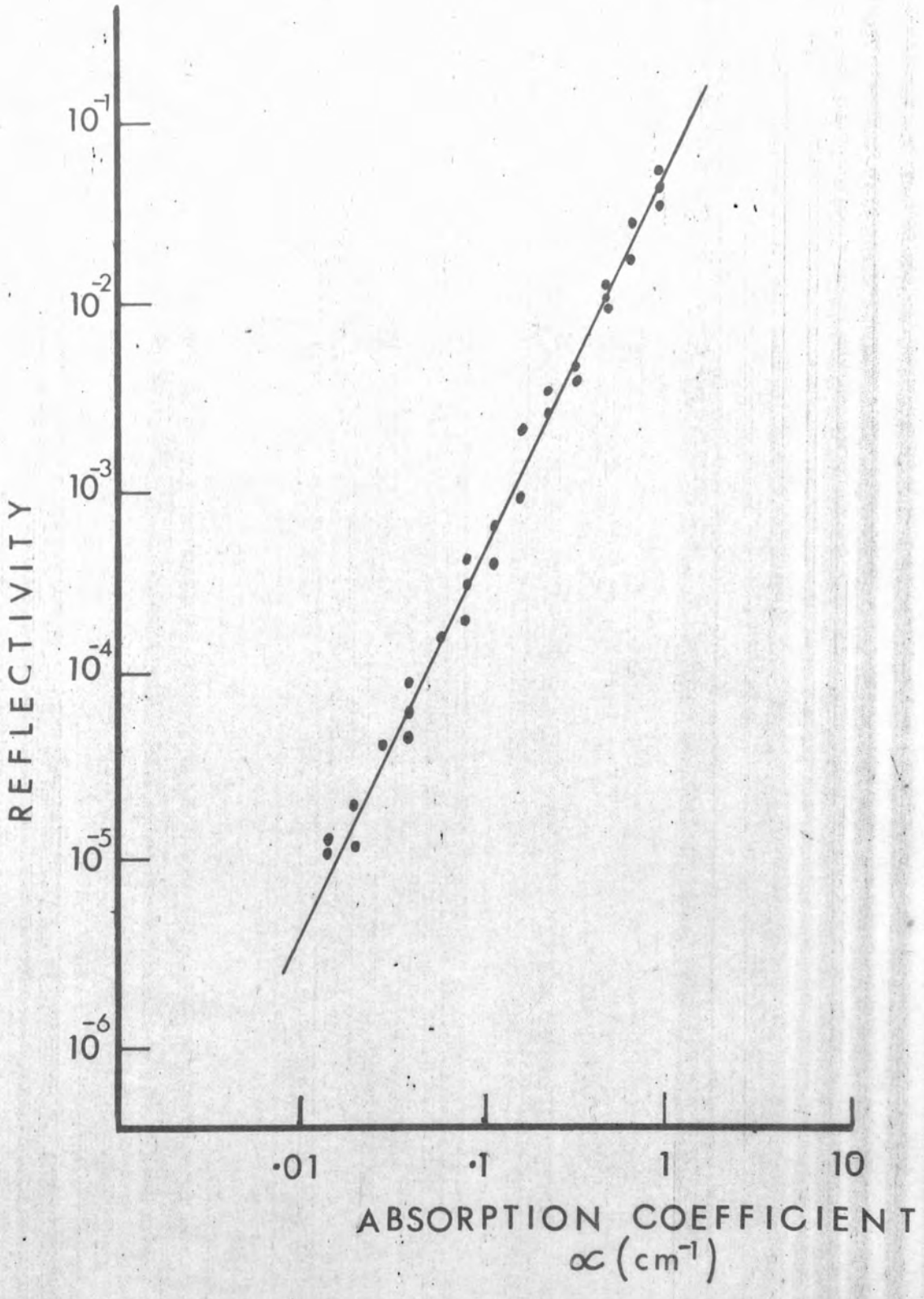

Fig.8.6

Variation of Reflectivity with Absorption Coefficient

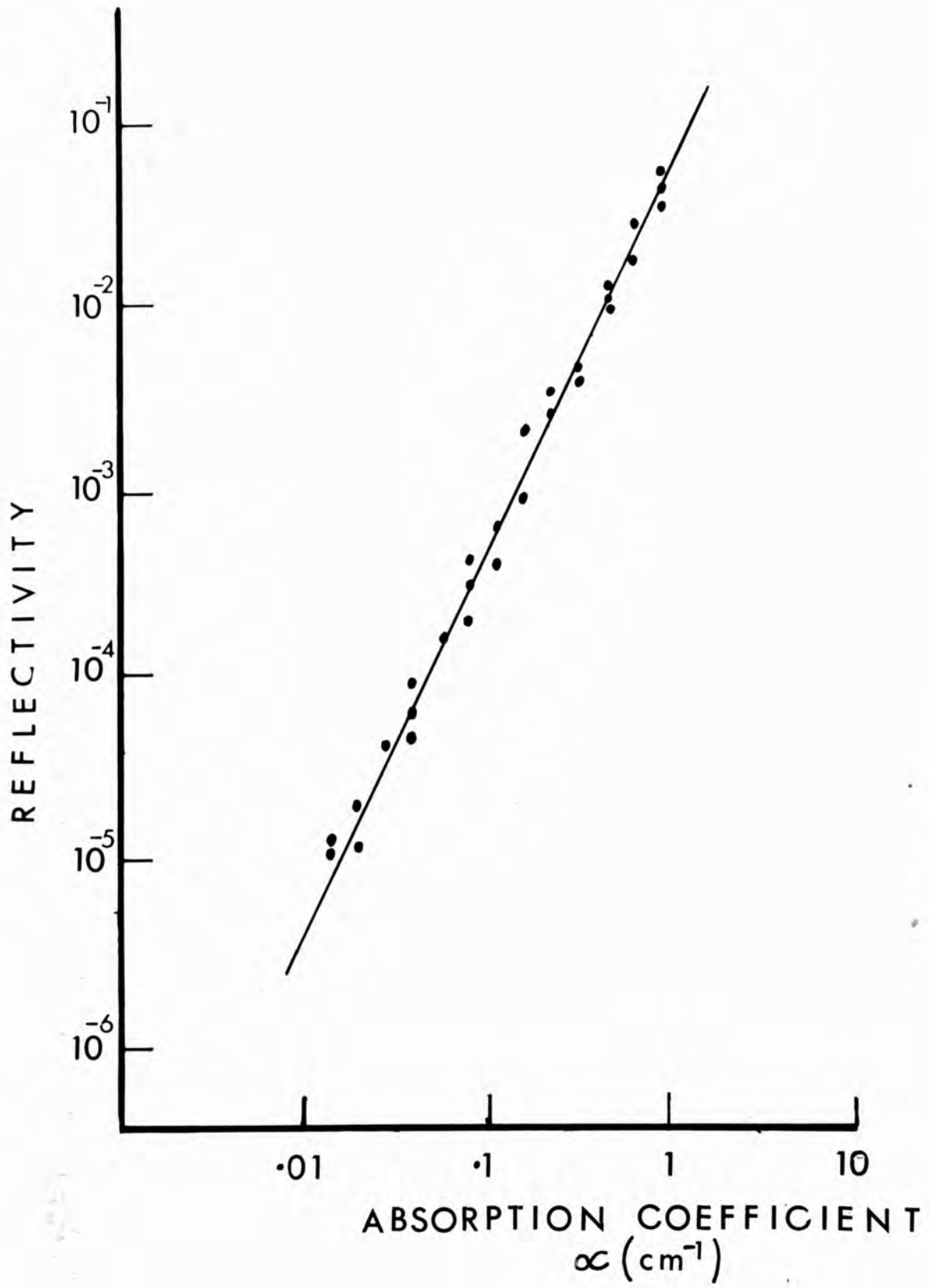
REFLECTIVITY
10^{-1}
10^{-2}
10^{-3}
10^{-4}
10^{-5}
10^{-6}
·01
·1
1
10
ABSORPTION COEFFICIENT
α (cm^{-1})

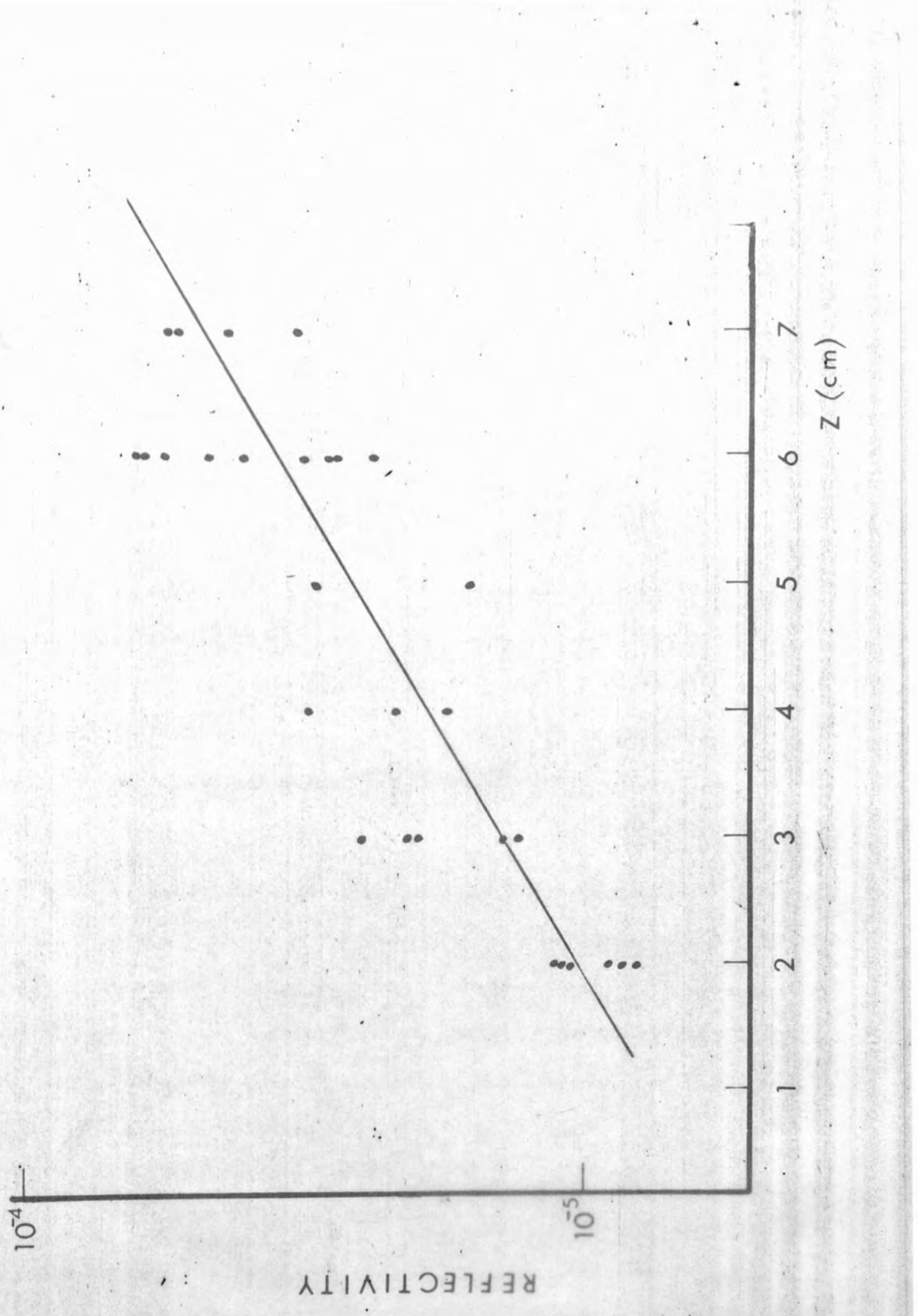

Fig.8.7

Variation of Reflectivity with Position of the Interaction Region

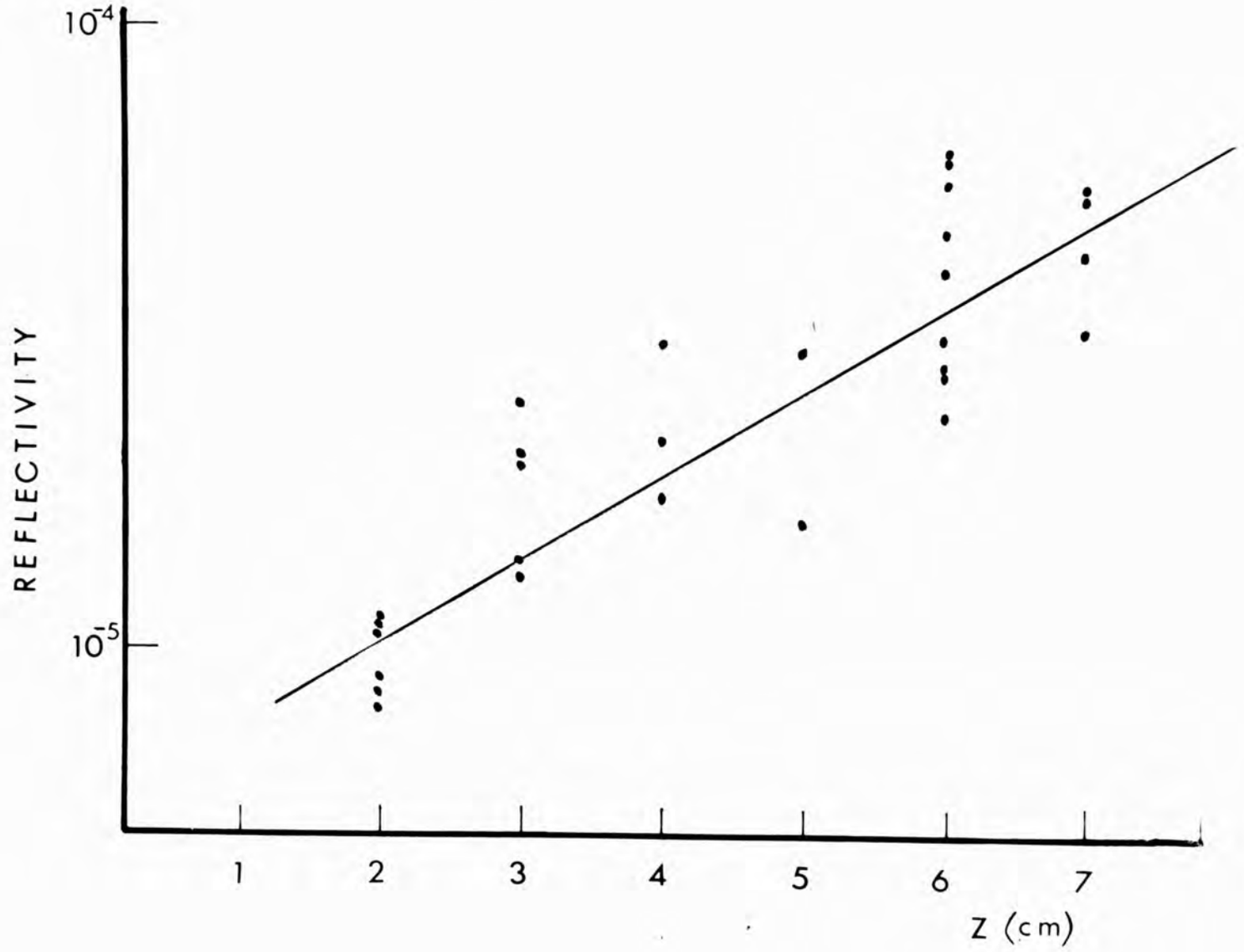
10^{-4}
10^{-5}
REFLECTIVITY
1
2
3
4
5
6
7
Z (cm)

linewidth Γ_L is in fact greater than Γ_R reducing the theoretical estimate of the gain (Section 2.5) by a factor of about $\frac{\Gamma_R}{\Gamma_L}$. This linewidth also implies that the higher frequency parts of the laser line will experience gain while the lower parts suffer a loss. The overall gain is difficult to calculate exactly but will be about $\frac{\Gamma_R}{\Gamma_L}$ times the gain calculated in Section 2.5 provided this gain is sufficient to make $e^{gz} \gg e^{-gz}$. These assumptions imply a gain under the experimental conditions of about 10^{-1}cm in reasonable agreement with the experimental estimate.

8.7 DECAY OF THE THERMAL MODULATION INDUCED IN A LIQUID

When two oppositely directed light beams of the same frequency traverse an absorbing medium more energy is absorbed at the antinodes, than at the nodes, of the resulting standing wave. It is the temperature modulation caused by such absorption which is responsible for the modulation in density and refractive index discussed in Sections 2.4 and 2.5.

Such a temperature modulation does not arise or disappear instantly with the electric field of the light wave but tends exponentially towards an equilibrium value for any constant field amplitude. In general when the field amplitude is a function of time the behaviour of the temperature modulation may be deduced by consideration of the heat continuity equation:

$$\rho_o C_v \frac{\partial \Delta T}{\partial t} - K \frac{\partial^2 \Delta T}{\partial x^2} - \frac{(C_p - C_v)}{\beta} \frac{\partial \Delta \rho}{\partial t} = \frac{1}{4\pi} n c \alpha E^2$$

(Section 2.4)

Since the frequencies of the forward and backward beams are in this case equal the temperature modulation is stationary and there can be no out of phase component of ΔT.

$$\Delta T' = |\Delta T| \quad \text{and} \quad \Delta T'' = 0.$$

Also, providing the fields are varying slowly compared with the time required for sound to propagate over a wavelength of the modulation ($\sim 10^{-10}$ secs):

$$\frac{\partial \Delta \rho}{\partial t} = \rho_o \beta \frac{\partial \Delta T}{\partial t} \quad .$$

Thus

$$\rho_o C_p \frac{\partial \Delta T}{\partial t} - K \frac{\partial^2 \Delta T}{\partial x^2} = \frac{1}{4\pi} n c \alpha A_1 A_2 \cos 2 k_r n_r x$$

(contributions to ΔT with no spatial variation have been ignored)

therefore:

$$\frac{\partial^2 |\Delta T|}{\partial t} + 4 \frac{K k_r^2 n_r^2}{\rho_o C_p} |\Delta T| = \frac{1}{4\pi} \frac{n c \alpha}{\rho_o C_p} A_1 A_2 .$$

Thus

$$\tau = \frac{\rho_o C_p}{4 K k_r^2 n_r^2}$$

is the relaxation time of the thermal grating(242).

In the experiment the light path behind the cell was short so at any time during the pulse:

$$I_1 \propto I_2$$

and

$$A_1 A_2 \propto I_1 ,$$

thus

$$\frac{\partial |\Delta T|}{\partial t} + \frac{1}{\tau} |\Delta T| \propto I_1$$

and

$$\frac{\partial \Delta n}{\partial t} + \frac{1}{\tau} \Delta n \propto I_1 ,$$

therefore:

$$\Delta n \propto e^{-t/\tau} \int_{t'=o}^{t} I_1 e^{+t'/\tau} \, dt' \quad ,$$

(where the origin of time is taken before the beginning of the laser pulse).

The integral may be replaced by a summation over N intervals of duration δt, short compared to either τ or the time over which I_1 changes significantly.

$$\Delta n_{(N\delta t)} - e^{-\delta t/\tau} \Delta n_{((N-1)\delta t)} \propto I_1(N\delta t) \frac{\delta t}{\tau} \quad .$$

The diode-detected laser pulses in Figs.8.8, 8.9 indicate the values of I_1 to be used in this equation. The formula allows a numerical calculation of the time profile of Δn for the observed pulse I_1 and any assumed value of τ. Now the grating reflectivity is proportional to $(\Delta n)^2$ so the assumed value of τ allows calculation of the time dependence of the resulting Bragg reflected pulse. The value of τ giving the best fit to the observed Bragg reflected pulse is the best estimate of the relaxation time of the thermal modulation in the liquid.

In fitting the calculated to the observed profile of the Bragg reflected pulse the finite instrumental relaxation time must also be taken into account. If the calculated signal at any time t is P_c then the observed signal, P_o is given by the equation:

$$\tau_i \frac{\partial P_o}{\partial t} + P_o = P_c \quad .$$

The relaxation time of the electrostrictive Bragg reflection process (causing the top trace of Fig.8.9 and the lower trace of Fig.8.8) is very short (about 10^{-10} secs - the lifetime of the phonons generated in this process) so $P_c \propto I_1^2$ in this case.

The equation above thus allows estimation of τi in a manner analogous to the estimation of τ described. A good fit to the falling part of the lower curve of Fig.8.9 is obtained assuming $\tau i = 7$ nsec. (NOTE: A fit to the rising part cannot be expected since the time of initiation of the stimulated Brillouin scattering causing the electrostriction is unknown.) Significant misfit occurs for $\tau i < 6$ nsec or $\tau i > 8$ nsec.

Given I_1 and assuming values for τ we may now calculate the

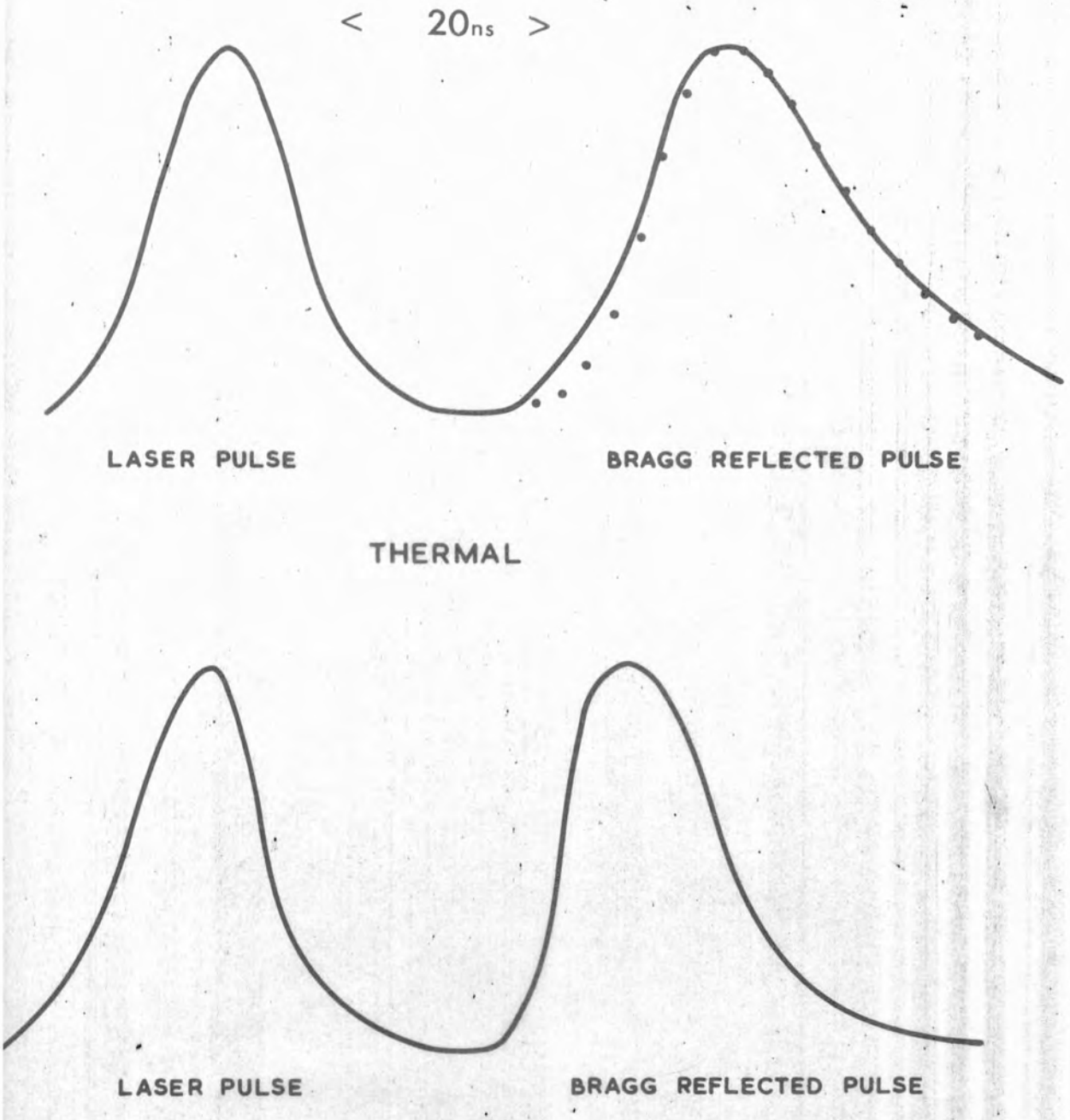

Fig. 8.8. Time profile of the ruby laser pulse and the resulting Bragg reflected pulse in the thermal and electrostrictive cases. The points marked are those calculated given the theoretical relaxation time.

CLM-P224

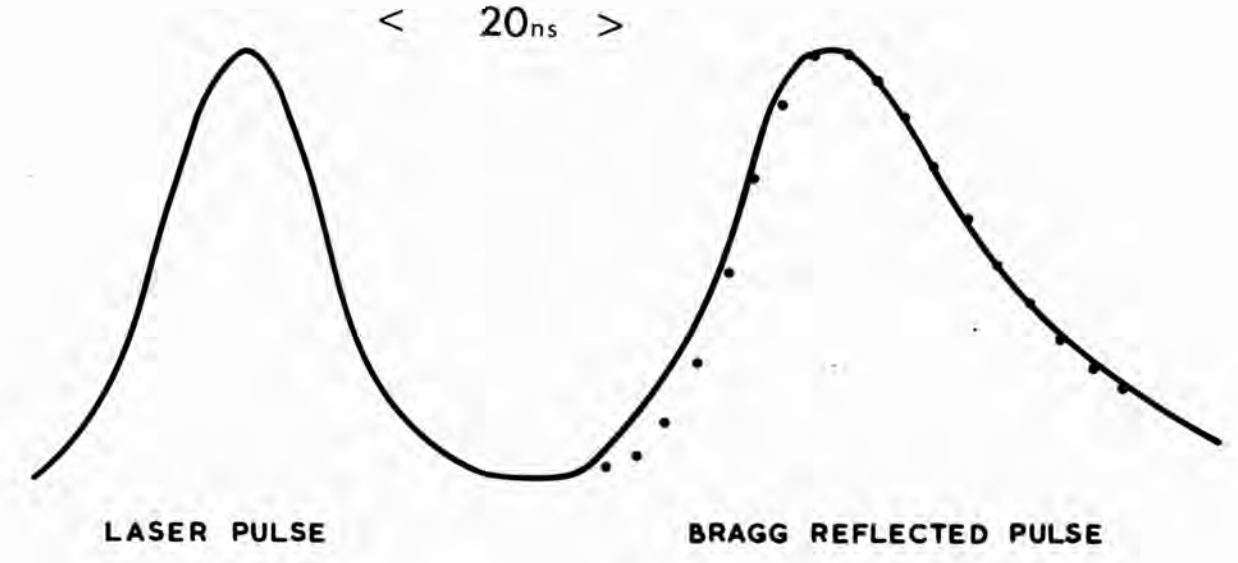

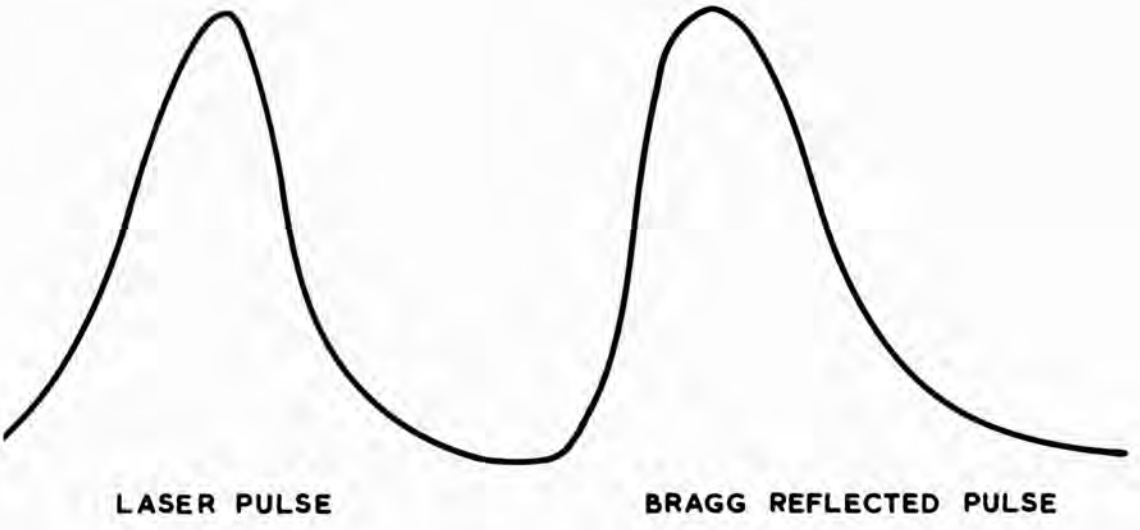

Fig. 8. Time profile of the ruby laser pulse and the resulting Bragg reflected pulse in the thermal and electrostrictive cases. The points marked are those calculated given the theoretical relaxation time.

CLM-P224

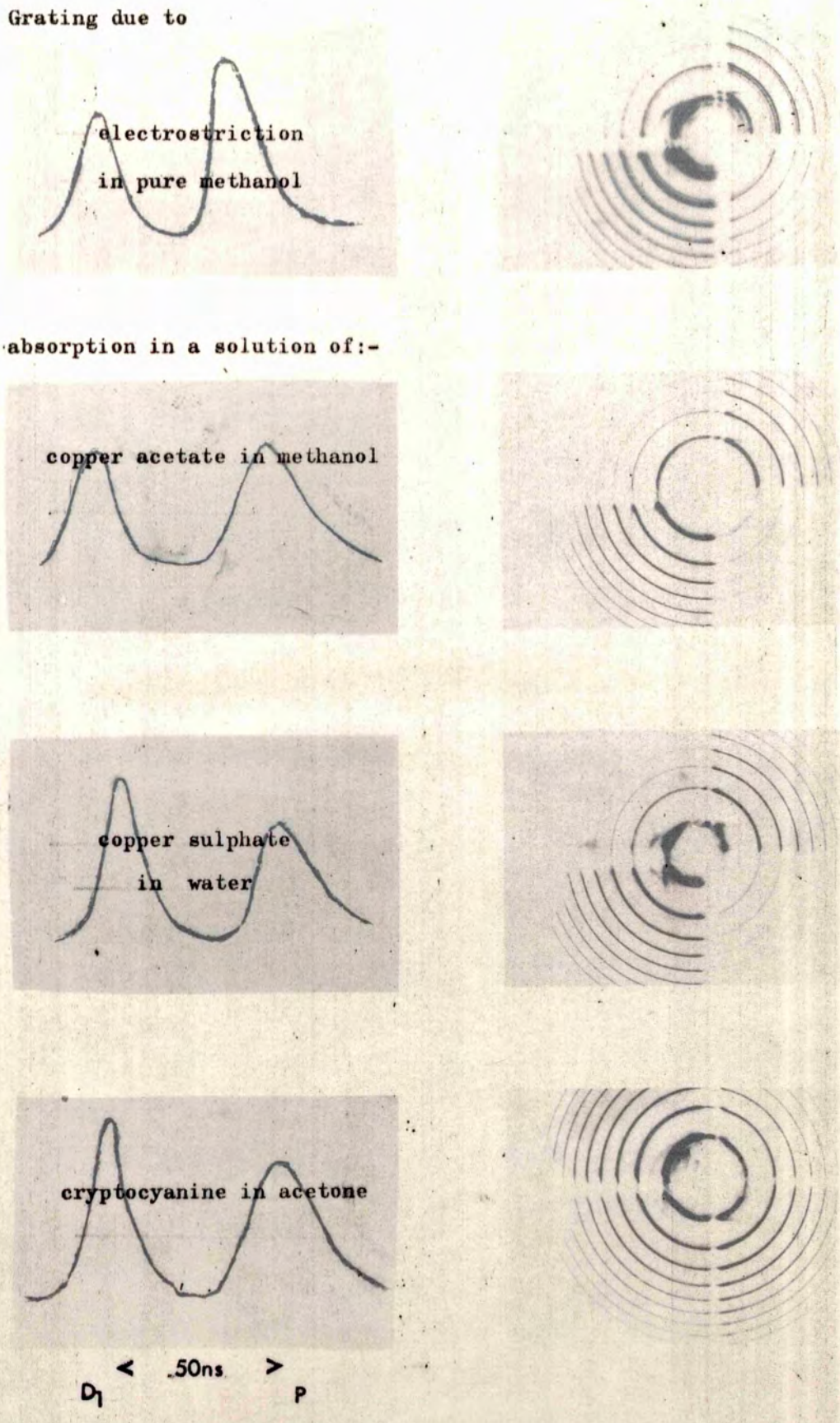

Fig.8.9
Decay of Phase Grating in Various Solvents

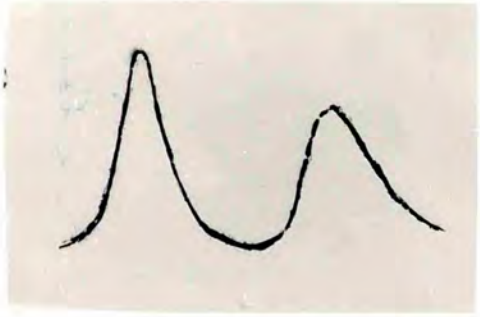

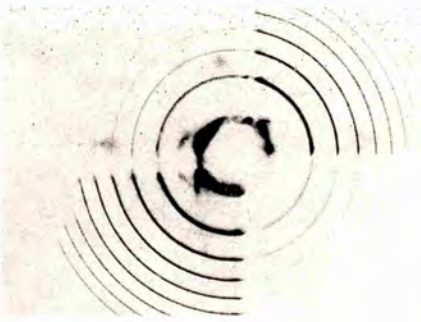

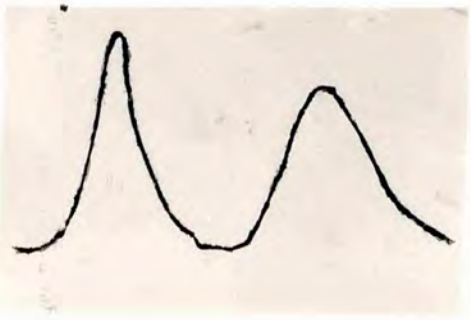

value of P_c and hence, using $\tau i = 7$ nsec, the value of P_o for the pulses Bragg reflected from thermal modulations, displayed on the other traces of Figs.8.8 and 8.9. The points shown with the upper trace of Fig.8.8 are the results of such a calculation taking $\tau = 16.5$ nsec.

These points are in good agreement with the experimental trace which was obtained using a solution of copper acetate in methanol in the scattering cell. Significant misfit occurs when it is assumed that $\tau < 14$ nsec or $\tau > 18$ nsec.

Similar curve fitting calculations for the other traces of Fig.8.9 indicate the values in the table below which also shows the values calculated theoretically for each solvent using the equation:

$$\tau = \frac{\rho_o C_p}{4 K k_r^2 n_r^2}$$

(The values of these parameters are given at the end of the Appendix.)

SOLVENT	τ nsec	
	theoretical	experimental
Methanol	17.0	16.5 ± 2
Water	12.1	12 ± 2
Acetone	17.9	17 ± 2

The method described in this section can in principle be used to investigate the build-up and decay of any non-linear disturbance of the refractive index of a medium. The measurements here have been confined to thermal relaxation rates because of the length of the ruby laser pulses and the rise time of the photodetection. The use of mode locked pulses and very fast photomultipliers, now becoming available, should allow direct measurement of the lifetimes of the phonons generated in stimulated Brillouin scattering (10^{-10} - 10^{-9} secs) and even of molecular orientations responsible for stimulated Rayleigh wing scattering (10^{-12} - 10^{-11} secs)[168].

APPENDIX

DEFINITIONS OF SYMBOLS AND MAGNITUDES OF PARAMETERS USED IN THIS THESIS

DEFINITIONS OF SYMBOLS

CHAPTER I

Section 1.4

I is the intensity at a particular frequency, of spontaneously scattered light.

$\Delta\omega$ is the difference in frequency between the incident and scattered light.

Ω is a frequency (shift) characteristic of a particular stimulated scattering process and scattering medium.

Γ is a frequency (width), characteristic of a particular stimulated scattering process and scattering medium.

Section 1.6

G is the gain coefficient for a beam of light travelling in the opposite direction to the laser beam.

$\Delta\omega$ is the difference in frequency between the laser and oppositely directed beams.

Ω and Γ are the same constants as in Section 1.4.

CHAPTER II

Section 2.1

N is the total number of dye molecules in the interaction region.

N_0 is the number of those molecules in the ground state.

N_1 is the number of those molecules in the first excited state.

N_2 is the number of those molecules in the second excited state.

A_{10} is the number of spontaneous transitions, per unit population of the first excited state, per unit time, from the first excited, to the ground state.

A_{20} is the number of such transitions from the second excited, to the ground state.

Section 2.1 (continued)

A_{21} is the number of such transitions from the second to the first excited state.

B_{01} is the number of stimulated transitions, per unit population of the ground state, per unit time, per unit incident intensity, from the ground to the first excited state.

B_{10} is the number of such transitions from the first excited, to the ground state.

B_{12} is the number of such transitions from the first to the second excited state.

B_{21} is the number of such transitions from the second to the first excited state.

σ_1 is the absorption cross-section of the transition from the ground to the first excited state.

T_1 is the lifetime of the first excited state.

$I_c = \frac{A_{10}}{B_{01}} \propto \frac{1}{\sigma_1 T_1}$ is an intensity characteristic of saturation of the first excited state.

Section 2.2

λ_s is the wavelength of a sound wave within the medium.

λ_L is the wavelength of the light wave in vacuo.

n is the refractive index of the medium when undisturbed

θ is the angle through which the light is scattered.

ω_B is the shift of the frequency of the scattered light from that of the incident light.

ω_L is the frequency of the incident light.

$\omega_s = \omega_B$ is the frequency of the scattering sound wave.

v is the velocity of sound in the medium.

c is the velocity of light in vacuo.

Section 2.2 (continued)

$\Delta\rho$	is a change of density in the medium.
t	is time.
Γ_B	is a constant characteristic of damping in the medium.
R	is a random fluctuation.
ω	is the frequency of a temporal Fourier component of R.
k	is the wave vector of a spatial Fourier component of R.
I	is the intensity at a particular frequency of the spontaneously scattered light.
$\Delta\omega$	is the difference in frequency between the incident and scattered light.

	In the denominators of the equations for depolarized scattering only.
I	Is the molecular moment of inertia.
k	is Boltzmann's constant.
T	is the temperature of the medium.
ξ	is the viscosity of the medium.
μ	is an elastic constant for the oscillation.

Γ_R	is the half width at half intensity of the frequency spread in Rayleigh line scattering.
k	is the wave vector of a thermal wave in the medium.
D	is the thermal diffusivity of the medium, $D = \frac{K}{\rho_o c_p}$,
K	is the thermal conductivity of the medium ,
ρ_o	is the density of the medium when undisturbed,
c_p	is the specific heat at constant pressure of the medium.
ω_{Ram}	is the frequency of a Raman transition .
Γ_{Ram}	is the half-width of a Raman line.

Section 2.3

P is the polarization of the medium.

E is the electric field in the medium.

χ is the linear polarizability of the medium.

$\chi_1, \chi_2, \chi_3 \ldots$ are non-linear polarizabilities of the medium.

$P_L(E)$ is the linear polarization of the medium.

$P_{NL}(E^2, E^3 \ldots)$ is the non-linear polarization of the medium.

A_1, A_2 are the amplitudes of the electric fields of two light waves travelling along the x axis. (The analysis is restricted to one dimension except in Section 2.5.)

k_1, k_2 are the wave vectors of these waves.

ω_1, ω_2 are the frequencies of these waves.

x is the distance along the direction of propagation of the waves.

t is time.

A_3, k_3, ω_3 are the amplitude, wave vector and frequency of a third wave along the x axis.

k_4, ω_4 are the wave vector and frequency of the light wave produced by the non-linear interaction.

i, j, k are integers each of which may take the value 1, 2 or 3.

Section 2.4

x, t, n, c are as defined for Sections 2.2 and 2.3.

$E_1, k_1, \omega_1, E_2, k_2, \omega_2$ are as defined for Section 2.3 except that the suffix 2 now refers to a backward going wave.

$\Delta\varepsilon$ is the change in dielectric constant of the medium.

$\Delta\varepsilon'$ is the amplitude of the part of the wave of dielectric constant on phase with the component of E^2 producing it.

$\Delta\varepsilon''$ is the amplitude of the part of the wave of dielectric constant out of phase with the component of E^2 producing it.

Section 2.4 (continued)

$\Delta\rho$ is the change in density of the medium.

ΔT is the change in temperature of the medium.

c_p, c_v are the specific heats of the medium at constant pressure and constant volume respectively.

v is the velocity of sound in the medium.

η is the viscosity of the medium.

ρ_o is its density.

β is its volume coefficient of thermal expansion.

γ is the electrostrictive constant

$$\left[\gamma = \rho_o \frac{\partial \varepsilon}{\partial \rho} = (n^2 - 1) \text{ or } = (n^2 - 1)\left(\frac{n^2 + 2}{3}\right) \text{ or } = (n^2 - 1)\left(\frac{3n^2}{2n^2 + 1}\right)\right\} \text{ according to the local field correction used}^{(241)}.\Bigg]$$

A is the amplitude of a component of E^2.

k is the wave vector of that component.

ω is the frequency of that component.

$\Delta\rho'$ is the amplitude of the part of the density change which is in phase with the component of E^2 producing it.

$\Delta\rho''$ is the amplitude of the part of the density change which is out of phase with the component of E^2 producing it.

$\Delta T'$ is the amplitude of the in phase part of the temperature wave

$\Delta T''$ is the amplitude of the out of phase part of the temperature wave.

Section 2.4 (continued)

$$m = \frac{\gamma}{8\pi v^2}$$

$$\Gamma = \frac{Kk^2}{\rho_o c_p}$$

$$\Omega_1 = vk$$

$$\Omega_2 = vk\sqrt{\frac{K}{c_p \eta}}$$

$$\Omega_3 = \frac{2nc\,\alpha v^2 \beta}{c_p \gamma}$$

$$\omega_B = kv$$

$$\Gamma_B = \frac{\eta k^2}{2\rho}$$

$$\Gamma_R = \frac{Kk^2}{\rho_o c_p}$$

Γ is a frequency characteristic of damping of the oscillations responsible for $\Delta\varepsilon$.

Ω is a frequency characteristic of the oscillations responsible for $\Delta\varepsilon$.

K' is that part of the Kerr coefficient due to the process responsible for the oscillation with frequency Ω .

In the Rayleigh Wing Scatterubf Formulae for Ω and Γ, I, k, t, ξ and μ are as defined for depolarized scattering in Section 2.2.

Section 2.5

The symbols in this section are those defined in Section 2.4 plus the following:

p is any integer.

θ_{max} is the angle between the probe and scattering beams when the scattering of the probe is a maximum.

λ_a, λ_r are the wavelengths of the probe and scattering beams respectively.

n_a, n_r are the refractive indices of the medium, when undisturbed, for light of wavelengths λ_a and λ_r respectively.

k_a, k_r are the magnitudes of the wave vectors of the probe and scattering beams respectively.

θ is the angle between the probe and scattering beams.

I_I is the intensity of the incident probe beam.

I_R is the intensity of the reflected probe beam.

Δn_a is the difference between the maximum and minimum refractive index for probe light.

$N = \frac{2\, n_r L}{\lambda_r}$ is the number of wavelengths of the refractive index modulation within the interaction regions.

$\delta = \frac{\Delta n_a}{2 n_a}$

$\delta\theta$ is the angle between the directions for which the reflectivity has half its maximum value.

CHAPTER IV

Section 4.3

n_i is the initial population inversion (before Q-switch operation).

n_f is the final population inversion (after Q-switch operation).

n_p is that population inversion which gives a loop gain of exactly unity for light in the cavity.

Population inversion is defined as $\frac{N_2 - N_1}{N_1 + N_2}$.

N_1 is the number of chromium ions in the ruby rod in the ground state.

N_2 is the number of chromium ions in the ruby rod in the excited state.

Section 4.4

I_2 is the light flux travelling away from the layer in a backward direction.

I_3 is the light flux travelling away from the layer in a forward direction.

I_1 is the light flux from the ruby rod incident on the first beam splitter.

t_1 is the transmission of a beam splitter.

t_2 is the transmission of a cell wall.

r is the reflectivity of the layer.

a is the absorptivity of the layer.

R_1 is the ratio of the signals from the beam splitters in front of and behind the cell for light travelling in a backward direction.

R_2 is the same ratio for light travelling in a forward direction.

R_{10}, R_{20} are the values of R_1, R_2 respectively when $r = a = 0$.

CHAPTER V

The symbols are as defined for Section 2.1.

CHAPTER VI

θ_{max} is the angle between the probe and scattering light which gives maximum scattering.

λ_{probe} is the wavelength of the probe light.

λ_{ruby} is the wavelength of the scattering (ruby laser) light.

n_{probe}, n_{ruby} are the refractive indices of the medium for the probe and ruby laser light respectively.

θ and φ are the angles defining the beam direction in the A.D.P. crystal as shown in Fig.6.1.

CHAPTER VIII

The symbols used are those defined for sections 2.4 and 2.5 and also:-

Section 8.1

$\Delta\theta$ is the divergence of the argon-laser beam.

$\mathcal{L}_a$ is the diameter of the argon laser beam.

$\mathcal{L}_r$ is the diameter of the ruby laser beam.

R is the overall reflectivity of the phase grating for the argon laser beam incident at the angle giving maximum reflectivity.

Section 8.6

Z is the distance of the interaction region from the back face of the cell.

Section 8.7

τ is the relaxation time of the thermal grating.

t' is any time less that t.

N is the number of intervals into which the time t is split.

δt is the duration of one such interval.

P_c is the photomultiplier signal calculated to occur in the absence of electronic distortion.

P_o is the photomultiplier signal actually observed.

τ_i is the instrumental relaxation time.

MAGNITUDES OF PARAMETERS (236)

CHAPTER VIII

Section 8.2

Properties of the light beams

$\mathcal{L}_r \sim$ ·5 cm

λ_r = 6943Å

$k_r = \frac{2\pi}{\lambda_r} = 9{\cdot}0 \times 10^4$ cm^{-1}

λ_a = 4880 Å

$\theta_{max} = \cos^{-1} \frac{\lambda_a}{\lambda_r} \cdot \frac{\lambda_r}{n_a} = 45.5^o$

$\delta\theta \sim$ 2 m.rad

$I_1 = 3I_2 = 20$ MW cm^{-2}

Properties of the medium

$n_r = n_a = 1{\cdot}33$

α = ·15 cm^{-1}

$\beta = 1{\cdot}19 \times 10^{-3}$ $^oK^{-1}$

$\gamma = (n_r^2 - 1)$ = ·77

$K = 2{\cdot}05 \times 10^4$ ergs.sec^{-1}cm^{-1} $^oK^{-1}$

Section 8.7

$kr = 9{\cdot}0 \times 10^4$ cm^{-1}

Solvent	ρ_o gm cm^{-3}	$c_p \times 10^{-7}$ erg gm^{-1} $^oK^{-1}$	$K \times 10^{-4}$ erg sec^{-1}cm^{-1} $^oK^{-1}$	n_r	τ nsec	
					theo-retical	experi-mental
Methanol	·794	2·52	2.05	1·33	17·0	16·5 ± 2
Water	·998	4·18	5·97	1·33	12·1	12 ± 2
Acetone	·791	2·19	1·60	1·35	17·9	17 ± 2

REFERENCES

(1) LORD STOKES. Phil. Trans., vol.142-II, p.463, (1852)
vol.143-III, p.385, (1853)

(2) LORD RAYLEIGH, Phil.Mag., vol.xli, pp.107,274,447, (1871)
vol.47, p.375, (1899)

(3) BRILLOUIN, L., Ann. Phys. (Paris), vol.77, p.88, (1922)

(4) DEBYE, P., Ann. der Physik, vol.XXXIX, p.789, (1912)

(5) GROSS, E., Nature, vol.126, pp.201,400,603, (1930)

(6) MANDELSHTAM, L. J. Russ. Soc. Phys. Chem, vol.58, p.381, (1926)

(7) LANDAU, L. and PLACZEK, G., Phys. Z. Sow., vol.5, p.172, (1934)

(8) LEONTOVICH, M. Z. Phys., vol.72, p.247, (1931)

(9) DEBYE, P. and SEARS, F., Proc. Nat. Acad. Sci., vol.18, p.409, (1932)

(10) RAMAN, C. and NATH, N., Proc. Ind. Acad. Sci., vol.2A, pp.406, 413, (1935) and vol.3A, pp.75,119,459, (1936)

(11) RAMAN, C., Ind. J. Phys., vol.2, p.387, (1928)

(12) RAMAN, C., and KRISHNAN, K., Ind. J. Phys., vol.2, p.398, (1928)

(13) RAMAN, C., and KRISHNAN, K., Phil. Mag., vol.5, p.498, (1928)

(14) KRISHNAN, K. and RAO, R., Ind. J. Phys., vol.4, p.39, (1929)

(15) RAO, R., Proc. Ind. Acad. Sci., vol.2, p.236, (1935) and
vol.3, p.607, (1936)

(16) GROSS, E. Compt. Rend. Acad. Bulgare, vol.28, p.786, (1940)

(17) PLACZEK, G., Marx Handbuch der Radiologie, vol.VI, p.206, (1934)

(18) KOHLRAUSCH, F., 'Der Smekal-Raman Effekt', (1938)

(19) BHAGAVANTAM, S., 'Scattering of Light and the Raman Effect', (1942)

(20) RAO, R., Proc. Ind. Acad. Sci., vol.A8, p.163, (1938)

(21) VENKATESWAREN, C., Proc. Ind. Acad. Sci., (1942)

(22) RANK, D., McCARTNEY, J. and SZASZ, G., J. Opt. Soc. Am., p.287, (1948)

(23) FRENKEL, J., 'Kinetic Theory of Liquids', (1946)

(24) MANDELSHTAM, L. and LEONTOVICH, M., Zh. Exp. Teor. Fiz., vol.7, p.438, (1937)

(25) LEONTOVICH, M. J. Phys., U.S.S.R., vol.4, p.499, (1941).

(26) FABELINSKII, I., and SHUSTIN, O. Dokl. Akad. Nauk. S.S.S.R. vol.92, p.285, (1953)

(27) MOLCHANOV, V., amd FABELINSKII, I., Dokl. Akad. Nauk, S.S.S.R. vol.105, p.248, (1955)

(28) PESIN, M. and FABELINSKII, I., Sov. Phys. Doklady, vol.3, p.974, (1958)

(29) PESIN, M., and FABELINSKII, I., Sov. Phys. Doklady, vol.4, p.1264, (1959) and vol.5, p.1294, (1960)

(30) FABELINSKII, I., Sov. Phys. Usp., vol.5, p.667, (1963)

(31) ISAKOVICH, M. and CHABAN, A. Sov. Phys. J.E.T.P., vol.23, p.893, (1966)

(32) GORDON, J., ZEIGER, H., and TOWNES, C. Phys, Rev., vol.95, p.282, (1954)

(33) MAIMAN, T., Nature, vol.187, p.493, (1960)

(34) HELLWARTH, R., 'Advances in Quantum Electronics' (ed. J. Singer), p.334, (1961)

(35) McCLUNG, F., and HELLWARTH, R., J. Appl. Phys., vol.33, p.838, (1962)

(36) JAVAN, A., BENNETT, W., and HERRIOTT, D., Phys. Rev. Lett., vol.6, p.106, (1961)

(37) KLEINMAN, D. and KISLIUK, P., Bell. Syst. Tech. J., vol.41, p.453, (1962)

(38) McCLUNG, F. and WEINER, D. I.E.E.E. J. of Q. E., vol.1, p.94, (1965)

(39) HERCHER, M., Appl. Phys. Lett., vol.7, p.39, (1965)

(40) MAGYAR, G., Rev. Sci. Inst., vol.38, p.517, (1967)

(41) SOROKIN, P., LUZZI, J., LANKARD, J. and PETTIT, G., I.B.M. J. Res. & Dev., vol.8, (1964)

(42) KAFALAS, P., MASTERS, J. and MURRAY, E., J. Appl. Phys., vol.35, p.2349, (1964)

(43) DiDOMENICO, M. J. Appl. Phys., vol.35, p.2870, (1964)

(44) HARGROVE, L., FORK, R. and POLLACK, M.; Appl. Phys. Lett., vol.5, p.4, (1964).

(45) MOCKER, H., and COLLINS, R., Appl. Phys. Letts., vol.7, p.270, (1965).

(46) DeMARIA, A., STETSER, D. and HEYNAU, H., Appl. Phys. Lett., vol.8, p.174, (1966)

(47) GIORDMAINE, J., SHAPIRO, S. and WECHT, K. Appl. Phys. Lett. vol.11, p.216, (1967)

(48) WEBER, H., Phys. Lett., vol.27A, p.321, (1968)

(49) SONCINI, G., and SVELTO, O. Appl. Phys. Lett., vol.11, p.261, (1967)

(50) CUBEDDU, R., POLLONI, R., SACCHI, C. and SVELTO, O., I.E.E.E. J. of Q.E., vol.5, p.470, (1969)

(51) ARAKELYAN, V., KARLOV, N., and PROLOROV, A., J.E.T.P. Lett., vol.10, p.178, (1969).

(52) ERNEST, J., MICHON, M., and DEBRIE, J., Phys. Lett., vol.22, p.147, (1966)

(53) VUYLSTEKE, A., J. Appl. Phys., vol.34, p.1615, (1963)

(54) PENNEY, A., and HEYNAU, H., Appl. Phys. Lett., vol.9, p.257, (1966)

(55) BRADLEY, D., NEW, G. and CAUGHEY, S., Phys. Lett., vol.30A, p.78, (1969)

(56) SOROKIN, P., LANKARD, A., HAMMOND, E. and MORUZZI, V., I.B.M. Journal, vol.11, p.130, (1967)

(57) FABELINSKII, I., 'Molecular Scattering of Light', (1965)

(58) SKINNER, J., and NILSEN, W., J. Opt. Soc. Am., vol.58, p.113, (1968)

(59) McCLUNG, F., and WEINER, D., J. Opt. Soc. Am., vol.54, p.641, (1964)

(60) DeMARTINI, F., and DUCUING, J., Phys. Rev. Lett, vol.17, p.117, (1966)

(61) FETTER, A., Phys. Rev., vol.139A, p.1616, (1965)

(62) LOUDON, R., Advan. Phys., vol.13, p.423, (1964)

(63) BENEDEK, G., LASTOVKA, J., FRITSCH, K., and GREYTAK, T., J. Opt. Soc. Am., vol.54, p.1284, (1964)

(64) CHIAO, R., and STOICHEFF, B., J. Opt. Soc. Am., vol.54, p.1286, (1964).

(65) RANK, D., KIESS, E., and FINK, U., J. Opt. Soc. Am., vol.56, p.163, (1966)

(66) SHAPIRO, S., McCLINTOCK, M., JENNINGS, D., and BARGER, R., I.E.E.E. J. of Q.E., vol.2, p.89, (1966)

(67) SHAPIRO, S., GAMMON, R., and CUMMINS, H., Appl. Phys. Lett., vol.9, p.157, (1966)

(68) BENEDEK, G., and GREYTAK, T., Proc. I.E.E.E., vol.53, p.1623, (1965)

(69) CUMMINS, H., and GAMMON, R., J. Chem. Phys., vol.44, p.2785, (1966)

(70) LANSHINA, L., SHOROSHEV, Y., and SHAKPARANOV, M., Sov. Phys. Doklady, vol.12, p.220. (1967).

(71) EASTMAN, D., WIGGINS, T., and RANK, D., Appl. Opt., vol.5, p.879, (1966)

(72) MASH, D., STARANOV, V., and FABELINSKII, I., Sov. Phys., J.E.T.P. vol.20, p.523, (1965).

(73) DURAND, G. and PINE, A., I.E.E.E. J. of Q.E., vol.4, p.523 (1968)

(74) FABELINSKII, I., and STARUNOV, V., Appl. Opt., vol.6, p.1793, (1967)

(75) GEORGE, T., SLAMA, L., YOKOYAMA, M. and GOLDSTEIN, L., Phys. Rev. Lett., vol.11, p.403, (1963)

(76) LEITE, R., MOORE, R., PORTO, S. and RIPPER, J., Phys. Rev. Lett., vol.14, p.7, (1965)

(77) CUMMINS, H. and GAMMON, R., Appl. Phys. Lett., vol.6, p.171, (1965)

(78) RANK, D., HOLLINGER, A., and EASTMAN, D, J. Opt. Soc. Am., vol.56, p.1057, (1966)

(79) THIBEAU, M., OKSENGORN, B., and VODAR, B., Compt. Rend., vol.265B, p.722, (1967)

(80) STARUNOV, V., Sov. Phys. Doklady, vol.8, p.1205, (1964)

(81) STARUNOV, V., Opt. and Spect., vol.18, p.165, (1963)

(82) ZAITSEV, G., Opt and Spect., vol.23, p.175, (1967)

(83) ZAITSEV, G., and STARANOV, V., J.E.T.P. Lett., vol.4, p.37, (1966)

(84) SHAPIRO, S., and BROIDA, H. Phys. Rev., vol.154, p.129, (1966)

(85) COOPER, V., MAY, A., HARA, E., and KNAAP, H., I.E.E.E. J. of Q.E., vol.4, p.720, (1968).

(86) STARUNOV, V., TIGANOV, E., and FABELINSKII, I. J.E.T.P. Lett. vol.5, p.260, (1967)

(87) STEGEMAN, G., and STOICHEFF, B. Phys. Rev. Lett., vol.21, p.202, (1968)

(88) FABELINSKII, I., SABIROV, L., and STARUNOV, V. Phys. Lett., vol.29A, p.414, (1969)

(89) CUMMINS, H., KNABLE, K. and YEH, Y., Phys. Rev. Lett., vol.12, p.150, (1964)

(90) GREYTAK, T., and BENEDEK, G., Phys. Rev. Lett., vol.17, p.179, (1966)

(91) LASTOVKA. J., and BENEDEK, G., Phys. Rev. Lett., vol.17, p.1039, (1966)

(92) FORD, N., and BENEDEK, G., Phys. Rev. Lett., vol.15, p.649, (1965)

(93) MOUNTAIN, R., Rev. Mod. Phys., vol.38, p.205, (1966)

(94) MOUNTAIN, R., J. Res. Nat. Bur. Sci., vol.78A, p.207, (1966)

(95) RYTOV, S. Sov. Phys. J.E.T.P., vol.27, p.147, (1967)

(96) O'CONNOR, L., and SCHLUPF, J., J. Chem. Phys., vol.47, p.31. (1967)

(97) GORNALL, W., STEGEMAN, G., STOICHEFF, B., STOLEN, R. and VOLTERRA, V. Phys. Rev. Lett., vol.17, p.297, (1966)

(98) GRIFFEN, A., Phys. Lett., vol.17A, p.208, (1965)

(99) ENNS, R., and HAERRING, R., Phys. Lett., vol.21A, p.534, (1966)

(100) FABELINSKII, I., Sov. Phys. Usp., vol.8, p.637, (1966)

(101) BUCKINGHAM, A., Trans. Farad. Soc., vol.53, p.884, (1957)

(102) KAISER, W. and GARRETT, C., Phys. Rev. Lett., vol.7, p.229, (1961)

(103) GIORDMAINE, J., and HOWE, J., Phys. Rev. Lett., vol.11, p.207, (1963)

(104) SPAETH, M. and SOOY, J. Chem. Phys., vol.48, p.2315, (1968)

(105) HERCHER, M., CHU, W. and STOCKMAN, D., I.E.E.E. J. of Q.E., vol.4, p.954, (1968)

(106) GIULIANO, C. and HESS, L., I.E.E.E. J. of Q.E., vol.3, p.358, (1967)

(107) MACK, M., Appl. Phys. Lett., vol.12, p.329, (1968)

(108) GIBBS, W., Appl. Phys. Lett., vol.11, p.113, (1967)

(109) FRANKEN, P., HILL, A., PETERS, C. and WEINREICH, G. Phys. Rev. Lett., vol.7, p.118, (1961)

(110) BLOEMBERGEN, N, 'Non-Linear Optics', (1965)

(111) TERHUNE, R., MAKER, P., and SAVAGE, C., Appl. Phys. Lett., vol.2, p.54, (1963)

(112) MAKER, P., TERHUME, R., NISENOFF, M. and SAVAGE, C., Phys. Rev. Lett., vol.8, p.21, (1962).

(113) WANG· C., and RACETTE, G., J. Appl. Phys., vol.36, p.3281, (1965)

(114) ADAMS, N. and SCHOEFER, P., Appl. Phys. Lett., vol.3, p.19, (1963).

(115) ECKARDT, R., and LEE, C., Appl. Phys. Lett., vol.15, p.425, (1969)

(116) BASS. B., FRANKEN, P., WARD, J. and WEINREICH, G., Phys. Rev. Lett., vol.9, p.446, (1962)

(117) NIEBUHR, K., Appl. Phys. Lett., vol.2, p.136, (1963)

(118) MANLEY, J., and ROWE, H., Proc. I.R.E., vol.44, p.904, (1956)

(119) PETERSON, G., and YARIV, A., Appl. Phys. Lett., vol.5, p.184, (1964)

(120) GIORDMAINE, J., and MILLER, R., Phys. Rev. Lett., vol.14, p.973, (1965)

(121) HARRIS, S., Proc. I.E.E.E., vol.57, p.2096, (1969)

(122) AKHMANOV, S., FADEEV, V., KHOKLOV, R., and CHUNAEV, O., J.E.T.P. Lett, vol.5, no.85, (1967)

(123) HARRIS, S., OSHMAN and BYER, R., Phys. Rev. Lett., vol.18, p.732, (1967)

(124) ARMSTRONG, J., BLOEMBERGEN, N., DUCUING, J., and PERSHAN, P. Phys. Rev., Phys. Rev., vol.127, p.1918, (1962)

(125) BLOEMBERGEN, N., and PERSHAN, P., Phys. Rev., vol.128, p.606, (1962)

(126) BLOEMBERGEN, N. and SHEN, Y, Phys. Rev., vol.133A, 37, (1964)

(127) GRIVET, P. and BLOEMBERGEN, N. 'Proceedings of the Third International Conference on Qauntum Electronics Conference'(1966)

(128) MILES, P. 'Proceedings of the International School of Physics 'Enrico Fermi', (1964)

(129) KELLEY, P., LAX, B., and TANNENWALD, P. 'Proceedings of the Physics of Quantum Electronics Conference', (1966)

(130) BONCH-BRUEVICH, A., and KHODOVOI, V., Sov. Phys., Usp., vol.8, p.1, (1965)

(131) MINCK, R., TERHUNE, R., and WANG, C., Appl. Opt., vol.5, p.1595, (1966)

(132) MAKER, P., and TERHUNE, R., Phys. Rev., vol.137A, p.801, (1965)

(133) ASKARYAN, G., Sov. Phys. J.E.T.P., vol.15, p.1088, (1962)

(134) HERCHER, M., J. Opt. Soc. Am., vol.54, p.563, (1964)

(135) PILIPETSKII, N. and RUSTAMOV, A., J.E.T.P. Lett., vol.2, p.55, (1965)

(136) CHIAO, R., GARMIRE, E. and TOWNES, C., Phys. Rev. Lett., vol.13, p.479, (1964)

(137) GARMIRE, E., CHIAO, R., and TOWNES, C., Phys. Rev. Lett., vol.16, p.347, (1966).

(138) SHEN, Y., YOUNG, M., and COHEN, M., Phys. Rev. Lett., vol.19, p.1171, (1967)

(139) SHEN, Y., and SHAHAM, Y., Phys. Rev., vol.163, p.224, (1967)

(140) CHIAO, R., JOHNSON, M., KRINSKY, S., SMITH, H., TOWNES, C., and GARMIRE, E., I.E.E.E. J. of Q.E., vol.2, p.467, (1966)

(141) AKHAMANOV, S., SUKHOROKOV, A. and KLOKHLOV, R., Sov. Phys. J.E.T.P., vol.23, p.1025, (1966).

(142) AKHMANOV, S., SUKHOROKOV, A. and KHOKHLOV, R., Sov. Phys. Usp., vol.10, p.609, (1968)

(143) BREWER, R., and LEE, C. Phys. Rev. Lett., vol.21, p.267, (1968).

(144) POLLONI, R., SACCHI, C., and SVELTO, O., Phys. Rev. Lett., vol.23, p.690, (1969)

(145) LEITE, R., MOORE, R, and WINNERY, J., Appl. Phys. Lett., vol.5, p.141, (1964)

(146) AKHMANOV, S., KRINDACH, D., SUKHORUKOV, A. and KHOKHLOV, R., J.E.T.P. Lett., vol.6, p.38, (1967)

(147) CARMAN, R., and KELLEY, P., Appl. Phys. Lett., vol.12, p.241, (1968)

(148) DABBY, F., and WHINNERY, J., Appl. Phys. Lett., vol.13, p.284, (1968)

(149) KAPLAN, A., J.E.T.P. Lett., vol.9, p.33, (1969)

(150) BRODIN, M. and KAMUZ, A., J.E.T.P. Lett, vol.9, p.351, (1969)

(151) GIRES, F. and MAYER, G., Compt. Rend., vol.258, p.2039, (1964)

(152) MAKER, P., TERHUNE, R., and SAVAGE, C., Phys. Rev. Lett., vol.12, p.507, (1964)

(153) PAILLETTE, M., Compt. Rend., vol.262B, p.264, (1966)

(154) LONGAKER, P., and LITVAK, M., J. Appl. Phys., vol.40, p.4033, (1969)

(155) WOODBURY, E., and NG, W., Proc. I.R.E., vol.50., p.2367, (1962)

(156) ECKHARDT, G., HELLWARTH, R., McCLUNG, F., SCHWARTZ, S., WEINER, D. and WOODBURY, E. Phys. Rev. Lett., vol.9, 455, (1962).

(157) HELLWARTH, R., Phys. Rev., vol.130, p.1850, (1963)

(158) WEINER, D., SCHWARTZ, S., and McCLUNG, F., J. Appl. Phys., vol.36, p.2395, (1965)

(159) SHIMIZU, T., and SHIMIZU, F. Japan J. Appl. Phys., vol.5, p.948, (1966)

(160) LOUDON, R., Proc. Phys. Soc., vol.A82, p.393, (1963)

(161) GROB, K., Z. fur Phys., vol.207, p.235, (1967)

(162) SHEN, Y., and BLOEMBERGEN, N., Phys. Rev., vol.137A, p.1787, (1965)

(163) SHEN, Y., Phys. Rev., vol.138A, p.1741, (1965)

(164) BLOEMBERGEN, N., Am. J. Phys., vol.35, p.989, (1967)

(165) JONES, W., and STOICHEFF, B., Phys. Rev. Lett., vol.13, p.657, (1964)

(166) MINCK,R., TERHUNE, R. and RADO, W., Appl. Phys. Lett., vol.3, p.181, (1963)

(167) SACCHI, C., TOWNES, C., and LIFSITZ, J., Phys. Rev., vol.174, p.439, (1968)

(168) DENARIEZ, M. and BRET, G., Phys. Rev., vol.171, p.161, (1968)

(169) BRET, G., and MAYER, G., Compt. Rend., vol.258, p.3265, (1964)

(170) CHIAO, R., TOWNES, C. and STOICHEFF, B., Phys. Rev. Lett., vol.12, p.592, (1964)

(171) GARMIRE, E. and TOWNES, C. Appl. Phys. Lett., vol.5, p.84, (1964).

(172) BREWER, R. and RIECKHOFF, K., Phys. Rev. Lett., vol.13, p.334, (1964)

(173) BREWER, R., Appl. Phys. Lett., vol.5, p.127, (1964)

(174) WIGGINS, T., WICK, R., RANK, D. and GUENTHER, A. Appl. Opt., vol.4, p.1203, (1965)

(175) GIULIANO, C., Appl. Phys. Lett., vol.7, p.279, (1965)

(176) MASH, D., MOROZOV, V., STARUNOV, V., TIGANOFF, E., and FABELINSKII, I., J.E.T.P. Lett., vol.2, p.157, (1965)

(177) KRIVOKHIZHD, S., MASH, D., MOROZOV, V., STARUNOV, V., and FABELINSKII, I., J.E.T.P. Lett., vol.3, p.245, (1966)

(178) BREWER, R. Phys. Rev., vol.140A, p.800, (1965)

(179) PINE, A., Phys. Rev., vol.149, p.113, (1966)

(180) YARIV, A. I.E.E.E. J. of Q.E., vol.1, p.28, (1965)

(181) KROLL, N., J. Appl. Phys., vol.36, p.34, (1965)

(182) TANG, C., J. Appl. Phys., vol.37, p.2945, (1966)

(183) GROB, K., Z. fur Phys., vol.201, p.59, (1967)

(184) MASH, D., MOROZOV, V., STARUNOV, V., and FABELINSKII, I., J.E.T.P. Lett., vol.2, p.25, (1965)

(185) CHO, C., FOLTZ, N., RANK, D. and WIGGINS, T., Phys. Rev. Lett., vol.18, p.107, (1967)

(186) FOLTZ, N., CHO, C., RANK, D., and WIGGINS, T. Phys. Rev., vol.165, p.396, (1968)

(187) ZAITSEV, G., KYSYLASOV, Y., STARUNOV, V., and FABELINSKII, I. J.E.T.P. Lett, vol.6, p.35, (1967)

(188) STARUNOV, V., Sov. Phys. Doklady, vol.13, p.217, (1968)

(189) HERMAN, R., Phys. Rev., vol.164, p.200, (1967)

(190) POHL, D., MAIER, M. and KAISER, W., Phys. Rev. Lett., vol.20, p.366, (1968)

(191) LANDAU, L., and LIFSHITZ, E., 'The Electrodynamics of Continuous Media', (1960)

(192) STARUNOV, V., Phys. Lett., vol.26A), p.428, (1968)

(193) ZIATSEV, G., KYZYLASOV, Y., STARUNOV, V. and FABELINSKII, I. J.E.T.P. Lett., vol.6, p.255, (1967)

(194) BESPALOV, V. and KUBAREV, A., J.E.T.P. Lett., vol.6, p.31, (1967)

(195) MASH, D., MOROZOV, V., STARUNOV, V., and FABELINSKII, I. Sov. Phys. J.E.T.P., vol.28, p.1085, (1969)

(196) HERMAN, R. and GRAY, M., Phys. Rev. Lett., vol.19, p.824, (1967)

(197) RANK, D., CHO, C., FOLTZ, N., and WIGGINS, T. Phys. Rev. Lett., vol.19, p.828, (1967)

(198) CHO, C., FOLTZ, N., RANK, D., and WIGGINS, T., Phys. Rev., vol.175, p.271, (1968)

(199) GIRES, F. Compt. Rend., vol.266B, p.596, (1968)

(200) WIGGINS, T., CHO, C., DIETZ, D. and FOLTZ, N., Phys. Rev. Lett., vol.20, p.831, (1968)

(201) ROTHER, W., POHL, D. and KAISER, W., Phys. Rev. Lett., vol.22, p.915, (1969)

(202) POHL, D., REINHOLD, I., and KAISER, W., Phys. Rev. Lett., vol.20, p.1141, (1968)

(203) SHAPIRO, S., GIORDMAINE, J. and WECHT, K., Phys. Rev. Lett., vol.19, p.1093, (1967)

(204) MACK, M., Phys. Rev. Lett., vol.22, p.13, (1969)

(205) POHL, D., Phys. Rev. Lett, vol.23, p.711, (1969)

(206) BLOEMBERGEN, M., and LALLEMAND, P., Phys. Rev. Lett., vol.16, p.81, (1966)

(207) WICK, R., RANK, D., and WIGGINS, T. Phys. Rev. Lett., vol.17, p.466, (1966)

(208) CARMAN, R., CHIAO, R., and KELLEY, P., Phys. Rev. Lett., vol.17, p.1281, (1966)

(209) KAVAGE, W., Appl. Phys. Lett., vol.11, p.303, (1967)

(210) ZAITSEV, G., KYZYLASOV, Y., STARUNOV, V., and FABELINSKII, I. J.E.T.P. Lett., vol.6, no.180, (1967)

(211) CHABAN, A., J. Opt. and Spect., vol.24, p.429, (1968)

(212) GIORDMAINE, J. and KAISER, W., Phys. Rev., vol.144, p676, (1966)

(213) BOERSCH, H. and EICHLER, H., Z. fur Ang. P., vol.22, p.378, (1967)

(214) WALDER, J., and TANG, C., Phys. Rev. Lett., vol.19, p.623, (1967)

(215) WINTERLING, G., and HEINIKE, W., Phys. Lett., vol,27A, p.329, (1968)

(216) GIORDMAINE, J., Sci. Am., vol.210, p.38, (1964)

(217) GIBSON, A. Sci. Prog., vol.56, p.479, (1968)

(218) FRANKEN, P., and WARD, J., Rev. Mod. Phys., vol.35, p.23, (1963)

(219) McLEAN, T., Lecture Series (unpublished)

(220) RYTOV, S., Sov. Phys., J.E.T.P., vol.6, pp.401,513, (1958)

(221) CHIAO, R., GARMIRE, E, and TOWNES, C., Ref., vol.128, p.326, (1964)

(222) CHIAO, R., Ph.D. Thesis, M.I.T., Cambridge, (1965)

(223) STARUNOV, V., Dissertation, Phys. Inst. Acad. Sci., Moscow, (1965)

(224) GIRES, F., I.E.E.E. J. of Q.E., vol.2, p.624, (1966)

(225) HUNT, F., American Institute of Physics Handbook, vols.3-25, (1957)

(226) CHESTER, M., Phys. Rev., vol.131, p.2013, (1963)

(227) DeMARIA, A., GLENN, W., BRIENZA, M., and MACK, M., Proc. I.E.E.E., vol.57, p.2, (1969)

(228) BJORKHOLM, and STOLEN, R., J. Appl. Phys., vol.39, p.4043, (1968)

(229) GIBSON, A., Brit. J. Appl. Phys., Series 2, vol.1, p.993, (1968)

(230) BATEMAN, D., R.A.E. Farnborough Tech. Report no.66349, (1966)

(231) GIULIANO, C., Appl. Phys. Lett., vol.5, p.137, (1964)

(232) LENGYEL, B. 'Introduction to Laser Physics', (1966

(233) GEUSIC, J., and SCOVIL, H., Bell. Syst. Tech. J., vol.41, p.1371, (1962)

(234) KATZENSTEIN, J., MAGYAR, G. and SELDEN, A. Opto. Electronics, vol.1 p.13, (1969)

(235) BARNES, P. and RIECKHOFF, K., Bull. Am. Phys. Soc., vol.11, p.898, (1967)

(236) SELDEN, A., Private Communication.

(237) SELDEN, A., Brit. J. Appl. Phys., vol.18, p.743, (1967)

(238) ARMSTRONG, J., J. Appl. Phys., vol.36, p.471, (1965)

(239) BOYD, G., ASHKIN, A., DIEDZIC, J., and KLEINMAN, D., Phys. Rev., vol.137A, p.1305, (1965).

(240) GIORDMAINE, J., Phys. Rev. Letts., vol.8, p.19, (1962).

(241) VUKS, M., Opt. and Spect., vol.25, p.479, (1968).

(242) LETOKHOV, V., and PAVLIK, B., Sov. Phys. Tech. Phys., vol.13, p.251, (1968)

(243) DITCHBURN, R., 'Light', 1952.

(244) QUATE, C., WILKINSON, C. and WINSLOW, D., Proc. I.E.E.E., vol.53, p.1604, (1965).

(245) LITTLE, V., KEY, P., & HARRISON, R., Nature, vol.216, p.257, (1967)

(246) HARRISON, R., KEY, P., LITTLE, V., MAGYAR, G. and KATZENSTEIN, J. Appl. Phys. Lett., vol.13, p.253, (1968)

(247) KEY, P., HARRISON, R., HEYWOOD, G., and LITTLE, V., J. Sci. Inst. vol.2, p.374, (1969).

(248) HARRISON, R., KEY, P., and LITTLE, V., Brit. J. Appl. Phys., vol.3, p.758, (1970).

(249) KEY, P., HARRISON, R., LITTLE, V., and KATZENSTIEN, J., I.E.E.E. J. of Q.E., (In print)

[References 245-249 are bound with this thesis]

ACKNOWLEDGEMENTS

I would like to acknowledge the advice and guidance of my supervisor Dr V.I. Little who conceived this project and obtained the considerable financial support and laboratory facilities necessary for its completion.

The project was financed principally by the Scientific Research Council and carried out in the Physics Department at Royal Holloway College. The work done would however have been much less satisfactory without the provision of an argon ion laser and laboratory facilities by U.K.A.E.A. Culham Laboratory. My thanks are due principally to Prof. S. Tolansky and Dr J. Katzenstein respectively for the provision of these facilities.

I would also like to acknowledge the help of many colleagues at Royal Holloway College and Culham Laboratory. In particular I must mention Mr R.G. Harrison, with whom I collaborated closely throughout this project, R. Asby, G. Magyar, G. Hayward, A. Selden and Miss M. Mendelssohn, though many others deserve my thanks.

My special thanks are also due to Mrs I. Godwin whose expertise is responsible for the attractive presentation of this thesis.

(*Reprinted from Nature, Vol.* 216, *No.* 5112, *pp.* 257–258, *October* 21, 1967)

Interaction of Self-trapped Light Beams

PRELIMINARY experiments have been carried out on the interaction of two self-trapped light beams in water. The 200 MW, 20 nsec output from a Q-switched ruby laser* was split by prisms and focused into a glass cell containing water to form two self-trapped beams (Fig. 1). Photographs were taken using the light scattered sideways from these beams.

Two types of scattering from self-trapped beams were observed; type A occurred when high purity water was used; type B was only produced in water which had been allowed to stand in an uncovered cell. When type A scattering was observed, the beams were characterized by fineness, short length, sharp cut-off and a tendency to scatter from a large number of discrete centres along the beam (Fig. 2). When type B scattering was observed, the beams were much longer than those associated with type A and the scattered light was much more diffuse, so that it was not always clear whether self-trapping had occurred (Fig. 3).

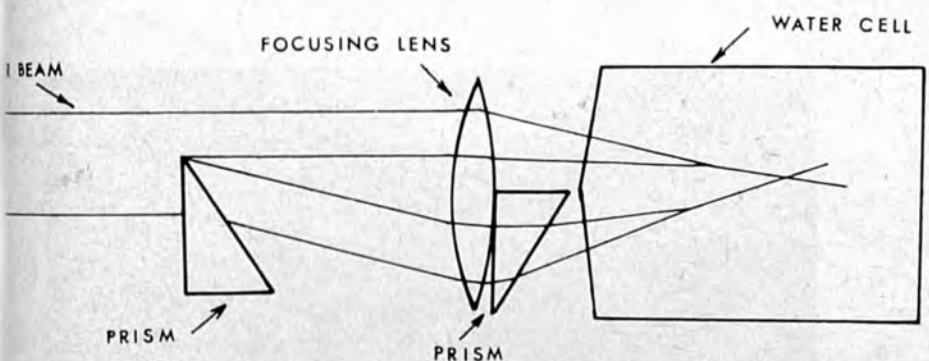

Fig. 1. Optical system used to produce two crossing self-trapped light beams.

* Ruby laser Bradley type *LH* 351, delivering 200 MW in 20 nsec distributed among a number of transverse modes (between 1 and 8). Beam divergence, 8 milliradians.

Fig. 2. Interaction of two crossing "type A" self-trapped beams. (×1.)

The apparatus used introduced distortion into the lower focused beam. The higher and lower edges of this beam were more intense than the centre, particularly the lower edge where self-trapping appeared to occur before the focal point was reached. Beyond the focal point two self-trapped beams were observed. The stronger beam travelled straight out from the end of the cone while the weaker appeared to be a continuation of the self-trapped lower edge of the cone. The weaker beam, after splitting from the stronger at the focus, bent and continued parallel with it.

Using the optical system shown in Fig. 1, the interaction of the two crossing light beams was observed. In the case of type A scattering, interaction was shown as an intense spot at the cross-over point (Fig. 2), but no significant effect on the beams could be observed because their scattering was not uniform. In the case of type B scattering, however, a considerable reduction in the intensity of the

Fig. 3. Interaction of two crossing "type B" self-trapped beams. (×1.)

upper beam was always observed (Fig. 3). It is possible that this upper beam was not self-trapped, in which case interaction was between a high intensity light beam and self-trapped light. A considerable amount of energy was lost by the upper beam. This could have been reflected into the liquid or back along the pipe by the reflexion coefficient of the cross-over point, or could have been converted into shock energy. Whatever the mechanism, it is notable that the loss occurred only from the upper beam.

V. I. Little
P. Y. Key
R. G. Harrison

Department of Physics,
Royal Holloway College,
University of London.

Received June 12, 1967.

Printed in Great Britain by Fisher, Knight & Co., Ltd., St. Albans.

Reprinted from

Volume 13, Number 8 APPLIED PHYSICS LETTERS 15 October 1968

BRAGG REFLECTION OF LASER LIGHT FROM A PHASE GRATING IN A Q-SWITCHING LIQUID

R. G. Harrison, P. Key, V. I. Little, and *G. Magyar*
Royal Holloway College, Englefield Green, Surrey, England

J. Katzenstein
U.K.A.E.A. Culham Laboratories, Abingdon, Berkshire, England
(Received 9 August 1968)

It is postulated that in a saturable dye absorber used for giant pulse laser switching a phase grating is formed. To prove this experimentally a frequency doubled part of the laser beam was reflected from this "Lippman plate" at the Bragg angle.

In the last few years many experimental and theoretical papers have been published on the phenomenon of laser Q-switching by saturable absorbers. Its principal features, like the relatively low power needed for saturation, mode-locking, etc., have been explained in terms of "spectral hole burning," i.e., the saturation of only a portion of the homogeneously broadened absorption line (see, e.g., Schwartz and Tan[1]). In this letter we propose an alternative explanation based upon the idea of a phase grating in the liquid, what we have called the Lippman plate mechanism[2] or what can also be described as spatial hole burning in the dye that forms the saturable absorber. Experimental evidence is cited to support this hypothesis: we report the first observation of Bragg reflected light from a phase grating created by the laser light in a Q-switching liquid.

The Lippman plate mechanism may be described as follows. The phenomenon of saturable absorption must be accompanied by an intensity-dependent variation of refractive index since these effects arise from the imaginary and real terms respectively of the nonlinear susceptibility.[3] If laser action commences in a single cavity mode, the resulting standing wave produces a periodic distribution of high and low electric fields, with a corresponding periodicity in the refractive index. The spatial period is half the wavelength of the mode. The situation can be described in the Mathieu–Hill equation:

$$\frac{d^2u}{dz^2} + \frac{\omega^2}{c^2}(n^2 - 2\delta n^2 \cos 2kz)u = 0 ,$$

where δn represents the intensity-dependent part of the refractive index and the cosine term stands for its spatial modulation. A medium with a periodically varying refractive index, a so-called Lippman plate, has a strong selective reflectivity for light of the same periodicity. Starting from the above equation, the reflectivity has been computed for various numbers of layers and depths of modulation.[4] It can be shown[5] that in a typical dye cell, for a few percent reflectivity the variation of refractive index required is $\delta n \sim 10^{-5}$. This value can be realized by the postulated nonlinear mechanism. Also, during the giant pulse there can be sufficient thermal energy deposited in the liquid to produce a similar variation of the refractive index.[5] The formation of such a Lippman plate effectively removes the absorption of the dye cell for those modes of the cavity whose periodicity closely matches that of the spatially varying refractive index. Thus, provided there is no mode-selective element present and the cell is sufficiently short in comparison with the total length of the resonator, this spatial hole burning facilitates mode-locking of the laser. The spatially selective bleaching also explains the relatively low power required for saturation.

The experimental arrangement is shown schematically in Fig. 1. The ruby laser was Q-switched using cryptocyanine in isopropyl alcohol. The Q-switch cell was in the shape of a regular hexagon having one inch square sides of Spectrosil-B glass, flat to $\lambda/10$. The fundamental light (typical power 30 MW) was frequency doubled with an efficiency of 3% in an ADP crystal, delayed around an adjustable optical path, and passed again through the cell at approximely 60° to the cavity radiation. The unique angle for Bragg reflection in this case is given by $2d \cos\theta = \lambda$, where $2d$ is the fundamental wavelength and λ is the second harmonic wavelength in the liquid. After adequate filtering of the red light, the transmitted and reflected frequency doubled beams were photographed using two cameras focused on infinity. The pulse shape and the spectral

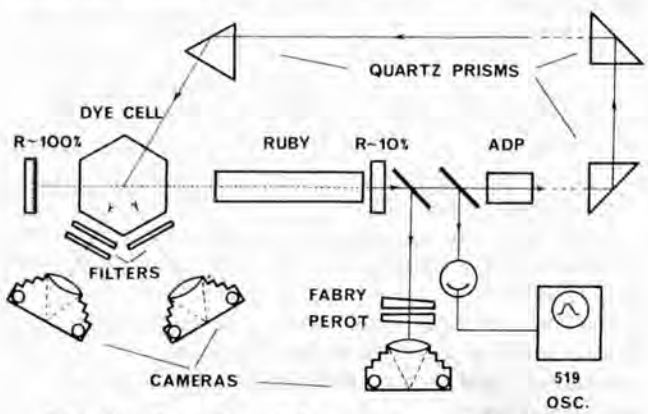

Fig. 1. Experimental arrangement for the observation of the Bragg-reflected second harmonic beam from the "Lippman plate" in a Q-switching dye.

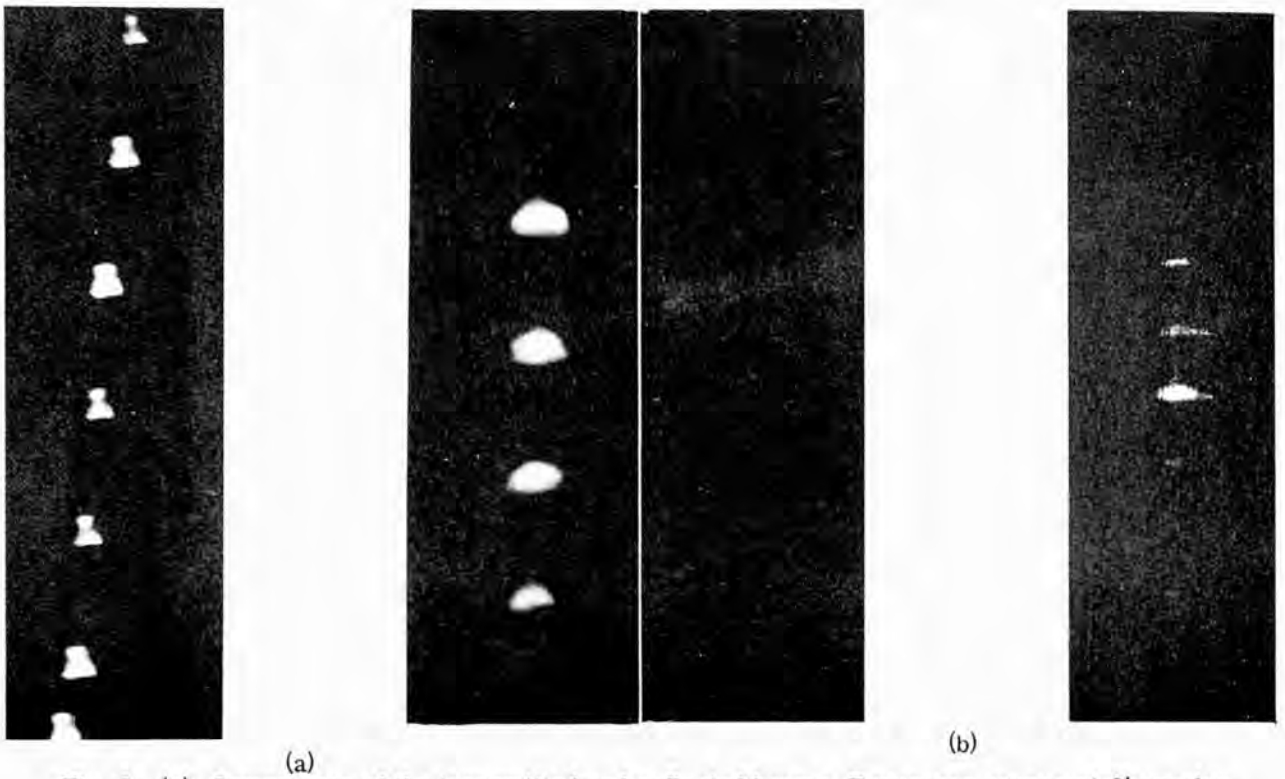

(a) (b)

Fig. 2. (a) Comparison of the transmitted and reflected beams. Exposures represent 6′ angular intervals. Transmitted beam is attenuated by ~ 200. Beam divergence: ~ 5 mrad. (b) Same with beam divergence reduced to ~ 2 mrad. Angular intervals of 2′.

composition were separately monitored.

Typical results are shown in Fig. 2. Figure 2(a) represents successive exposures of the transmitted and reflected beams taken at angular intervals of 6′, covering the angle for Bragg reflection. The transmitted light (left) is attenuated two-hundred-fold. The reflected light exhibits a critical dependence on angle of incidence, the intensity falling to half-value for a deviation of ±10′. Figure 2(a) corresponds to an incident beam divergence of 5 mrad, and about 1% of the beam is reflected. The amount of light reflected will be related to a number of factors, e.g., the amplitude of the induced periodic structure, filamentary processes, beam divergence, etc. Figure 2(b) shows the effect of restricting the incident beam by means of stops in the central portion to a divergence of 2 mrad. The exposures now represent increments of 2′ in the angle of incidence. 3% of the light is now reflected, and the intensity falls to half-value at ± 4′.

To eliminate the possibility that the phenomenon results from a spurious reflection, the ADP crystal was removed, and a photograph was taken under identical conditions but without the ultraviolet filter. The resulting plate showed a diffuse fogging due to scattered light, but no evidence of a well-defined reflected beam.

The effect of introducing delays of up to 30 nsec into the probing beam was also investigated. It was found that the relative intensity of the reflected light was not diminished, even for maximum delay (for which the overlap of the probing pulse and the fundamental pulse was less than 20%). The implication of this result was that the processes governing the decay of the ordered structure in the liquid were probably thermal. There was also an indication that the reflected intensity had a maximum for a delay time of 15 nsec. This could be explained by an integration of the thermal contribution to the amplitude of the structures in the liquid during the giant pulse.

Analysis of the spectral composition of the light showed that Bragg reflection took place for power levels well below the threshold for the stimulated Brillouin effect, as well as above it. We conclude from this that an ordered structure analogous to a Lippman plate was formed in the liquid in the Q-switching cell of the giant pulse laser.

This technique should prove valuable in the measurement of relaxation times and associated phenomena in liquids. Further experiments are in progress involving longer delay times and differing liquid temperatures. A further experiment is planned in which the dye cell will be probed continuously with a beam from a high power gas laser, the Bragg reflection being detected photoelectrically. Such an experiment would give more detailed information of the evolution of the processes taking place.

Three of us, Little, Harrison, and Key, wish to acknowledge the assistance of the Science Research Council in financing this experiment.

[1] S. E. Schwartz and T. Y. Tan, Appl. Phys. Letters 10, 4 (1967).
[2] G. Lippman, Compt. Rend. 112, 274 (1891).
[3] N. Bloembergen, Am. J. Phys. 35, 989 (1967).
[4] M. Iwata, R. Makabe, and S. Katsube, Japan. J. Appl. Phys., Suppl. 1, 4, 347 (1965).
[5] J. Katzenstein, G. Magyar, and A. C. Selden, Opt. Electron. (to be published).

Journal of Scientific Instruments (Journal of Physics E)
1969 Series 2 Volume 2

A high precision spectrometer table

P Key, G Hayward, R G Harrison and V I Little
Department of Physics, Royal Holloway College (University of London), Egham, Surrey
MS *received 3 January 1969*

Abstract In this note a novel form of spectrometer table is described. It has easily demountable arms and an incremental accuracy to 10^{-5} radian.

A versatile spectrometer table with removable arms has been designed by using kinematic principles. Such design allows various optical systems to be set up and positioned with considerable accuracy and with the minimum of effort. A table of this kind has been used successfully by the authors (Harrison *et al.* 1968) in an experiment in which laser light was Bragg-reflected from a laser-induced structure in a liquid.

The design is shown in figure 1. The movable arm has two ball bearings rigidly fixed to its underside. These rest in a

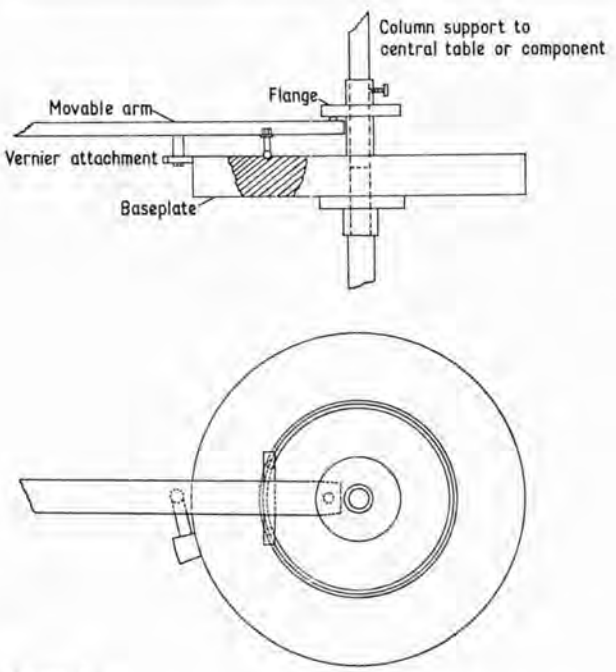

Figure 1

circular groove of V-shaped cross section, cut in the baseplate. A third ball bearing fixed to the upper face of the arm and positioned at its end makes contact with the underside of a flange machined parallel to the baseplate. Thus five points of contact are made between the arm and the fixed part of the instrument leaving one degree of freedom, i.e. rotation about a central axis. When the balls are correctly located, as shown in the diagram, the system is in neutral equilibrium provided the centre of mass of the arm lies outside the V-groove circle. A number of arms may be positioned simultaneously, and arms may easily be interchanged.

Angular displacements of an arm may be estimated with the help of a vernier scale attached to the arm and a circular scale engraved on the baseplate. A micrometer screw may be adapted to the system and used to achieve more precise adjustments.

The accuracy with which the groove and the flange have been machined sets an upper limit to the precision with which changes in the angular position of an arm may be made. For the system described, machining tolerances of the order 1 in 10^4 imply that a displacement of the order 10^{-1} radian will be subject to angular errors no greater than 10^{-5} radian, assuming of course that the machining errors are distributed and not localized over a narrow angular range.

References

Harrison R G Key P Y Little V I Magyar G and Katzenstein J 1968 *Appl. Phys. Lett.* **13** 253–5

Fluorescence due to excited state absorption in saturable absorbers

R. G. HARRISON, P. Y. KEY and V. I. LITTLE

Royal Holloway College, University of London

MS. received 5th November 1969, in revised form 26th January 1970

Abstract. Blue fluorescence has been observed from saturable absorbers excited by ruby laser light. The intensity dependence of this fluorescence showed that it was a result of excited-state absorption to the second singlet state. This intensity dependence also indicated the power density required to saturate the first excited singlet state for each dye. A similar fluorescence due to two photon absorption was observed in certain solvents.

1. Introduction

The use of an organic dye solution for the Q-switching of a laser depends on the intensity dependent reduction of the absorption coefficient of the dye at the laser frequency (Szabo and Stein 1965). In those dyes found suitable for Q-switching it is the transition from the ground state (0) to the first excited singlet state (1) which is responsible for this adsorption. The absorption coefficient is reduced when the laser intensity is such that the population of state (1) approaches that of state (0). There is, however, a residual absorption due to the transition from (1) to the second excited singlet state (2) (Guiliano and Hess 1967, Hercher *et al.* 1968). The subsequent spontaneous transition (2) to (0) results in the blue fluorescence (Gibbs 1967) studied in this experiment.

The equilibrium population of state (2) for the three-level system described, may be easily shown to follow the equation

$$N_2=I^2\sigma_1\sigma_2N\{I\sigma_2(3I\sigma_1+T_1^{-1}+T_{20}^{-1})+(2I\sigma_1+T_1^{-1})\,T_2^{-1}\}^{-1}$$

where σ_1, σ_2 are cross sections for transitions (0) $\rightarrow$(1) and (1) $\rightarrow$(2) respectively. T_1, T_2 are the total lifetimes of levels (1) and (2) respectively. T_{20} is the lifetime characterizing the transition (2) $\rightarrow$(0).

When I is very small

$$N_2=I^2\sigma_1\sigma_2T_1T_2N$$

thus the response is square law.

When I is very large

$$N_2=\tfrac{1}{3}N$$

and there are equal populations of the three states.

Now the lifetime of state (2) for the dyes used was about 10^{-13} s (Kasha 1950 and Gibbs 1967) whilst that of state (1) is greater than or approximately equal to 10^{-10} s (Gires 1966 and Selden 1967).

Also the low excited-state absorption of these dyes indicates $\sigma_2\ll\sigma_1$ (Gibbs 1967, Guiliano and Hess 1967). Thus the transition (0) $\rightarrow$(1) saturates at a very much lower power than (1) $\rightarrow$(2) and

$$N_2=I^2\sigma_1\sigma_2N(3I^2\sigma_1\sigma_2+2I\sigma_1T_2^{-1}+T_1^{-1}T_2^{-1})^{-1}.$$

Now for $I\sigma_2\ll T_2^{-1}$ i.e., for powers insufficient to saturate the transition (1) $\rightarrow$(2).

$$N_2=\frac{I^2\sigma_1\sigma_2N}{(2I\sigma_1+T_1^{-1})\,T_2^{-1}}.$$

Let $\sigma_1^{-1}T_1^{-1}=I_c$ then

$$N_2=\sigma_2 N T_2 I_c \frac{I^2/I_c^2}{1+2I/I_c}.$$

Since the number of fluorescent transitions $(2)\rightarrow(0)$ is proportional to N_2

$$\text{fluorescence}\propto\frac{I^2/I_c^2}{1+2I/I_c}.$$

2. Experimental details

A Q-switched ruby laser with an output of up to 200 MW and a pulse duration of about 15 nanoseconds was used to excite a dye solution. This solution was contained in a short cell which was misaligned with respect to the ruby beam. The light intensity incident on this cell was controlled by varying the concentration of a solution of copper sulphate placed in the path of the ruby laser light. This intensity was monitored using a calibrated beam splitter and photodiode connected to a Tektronix 454 oscilloscope. The blue fluorescence was detected by a Mullard 56 AVP photomultiplier connected to the same oscilloscope via a delay line. Scattered ruby laser light and red fluoresence was eliminated by use of Jena BG 18 green filters. Noise due to the flashlight from the ruby cavity was minimized by use of a Wratten 29 filter placed after the copper sulphate attenuator. Two-photon absorption (Garrett and Kaiser 1961, Bloembergen 1967) in this filter caused a small amount of blue fluorescence. This gave a negligible signal on the photomultiplier providing the distance of the dye cell from the filter was sufficiently long.

It was necessary to use dilute dye solutions contained in a narrow cell in order to minimize intensity variations due to absorption of the ruby beam. The thin misaligned cell also eliminated the possibility of stimulated non-linear effects (Bloembergen 1967, Minck *et al.* 1966).

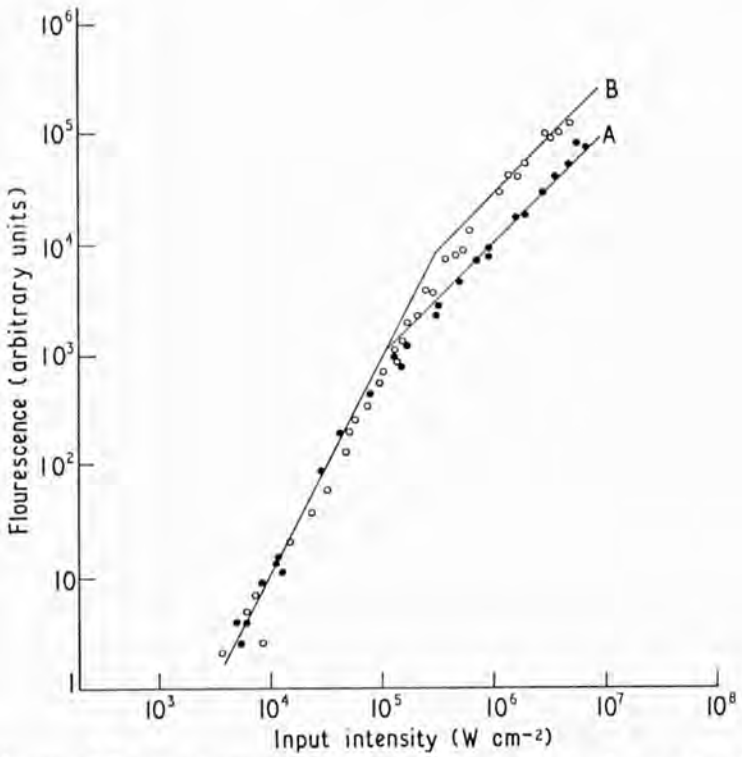

Figure 1. Dependence of fluorescence on input intensity. Curve A, CAP in chloronaphthalene; curve B, CAP in methanol. (In each figure I_c is the value of input intensity at the intersection of the theoretical lines representing fluorescence $\propto I^2$ and fluorescence $\propto I$.)

3. Results

The intensity of the blue fluorescence was measured as a function of the incident intensity, for the dyes chloroaluminiumphthalocyanine (CAP) (Gibbs 1967), cryptocyanine and vanadium–phthalocyanine (VnOPc).

Curves A and B of figure 1 show the dependence of fluorescence on incident intensity for solutions of CAP in chloronaphthalene and in methanol respectively.

At low inputs the fluorescence of both solutions follows the expected square law dependence on input intensity. With an increase of intensity this dependence changes and tends

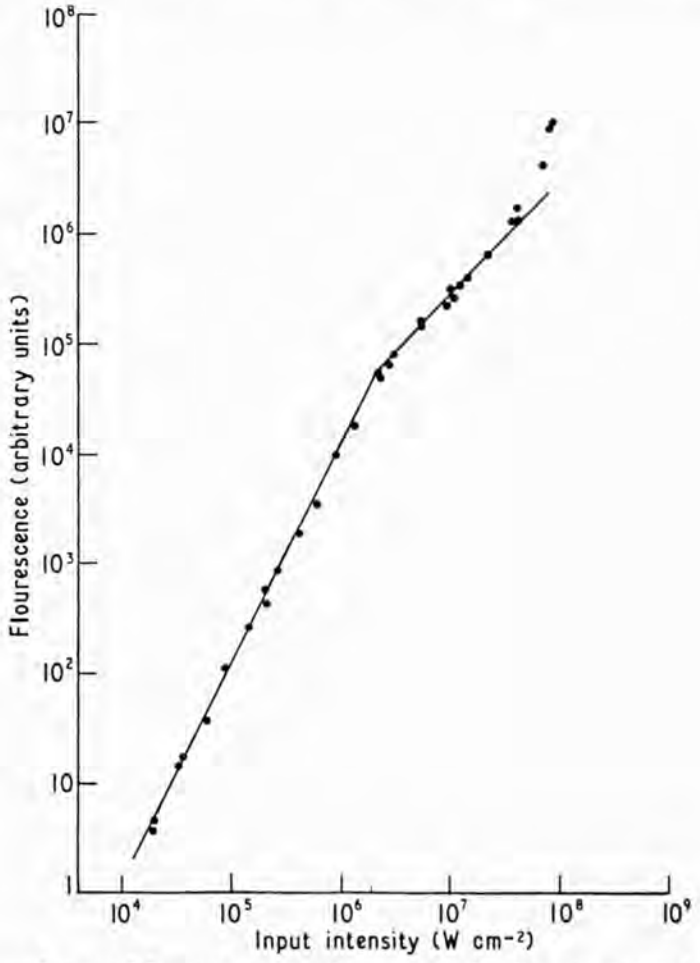

Figure 2. Dependence of fluorescence on input intensity for cryptocyanine in methanol.

towards a linear law as predicted by the theoretical law. (The non-linear breakdown of this law at still higher powers is attributed to chemical decomposition of the solution.) This corresponds to saturation of the first excited singlet state of the dye. The characteristic intensity I_c at which this occurs is about 10^5 W cm^{-2} in the case of the chloronaphthalene solution and about 3×10^5 W cm^{-2} for the methanol solution. The different powers I_c, for the two solutions are due to the different positions of the peaks of their absorption spectra. The peak of the spectrum of the solution in chloronaphthalene is much closer to the ruby wavelength (6943 Å) than that of the solution in methanol. Consequently the absorption cross section σ_1 is much greater and I_c much smaller in this case.

The dependence of fluorescence on input intensity for a solution of cryptocyanine in methanol (figure 2) has the same features as that for CAP in chloronaphthalene. However, although the absorption cross section for cryptocyanine in methanol ($\sigma_1=8{\cdot}1\times10^{-16}$ cm^2) is greater than that for CAP in chloronaphthalene ($\sigma_1=3\times10^{-16}$ cm^2) (Gires 1966, Selden 1967), I_c is greater for the cryptocyanine solution by over an order of magnitude

($I_c \sim 2{\cdot}5 \times 10^6$ W cm^{-2}). This is a result of the very much shorter lifetimes of the first excited state of cryptocyanine ($T_1 \sim 10^{-10}$ s). For CAP, $T_1 \sim 5 \times 10^{-9}$ s (Gires 1966, Selden 1967).

Thus theoretically

$$\frac{I_c(\text{cryptocyanine})}{I_c(\text{CAP})} \sim 25.$$

This is confirmed experimentally.

The dependence of fluorescence on input intensity for the VnOPc in nitrobenzene (figure 3) is similar to that of the other solutions. In this case saturation occurs at about $2{\cdot}5 \times 10^5$ W cm^{-2} as expected from the values $\sigma_1 = 4{\cdot}1 \times 10^{-16}$ cm^2 and $T_1 \sim 2 \times 10^{-9}$ s (Gires 1966). These values of I_c confirm the results obtained by other workers using transmission and single-photon fluorescence measurements (Armstrong 1965, Gires 1966 and Giuliano and Hess 1967).

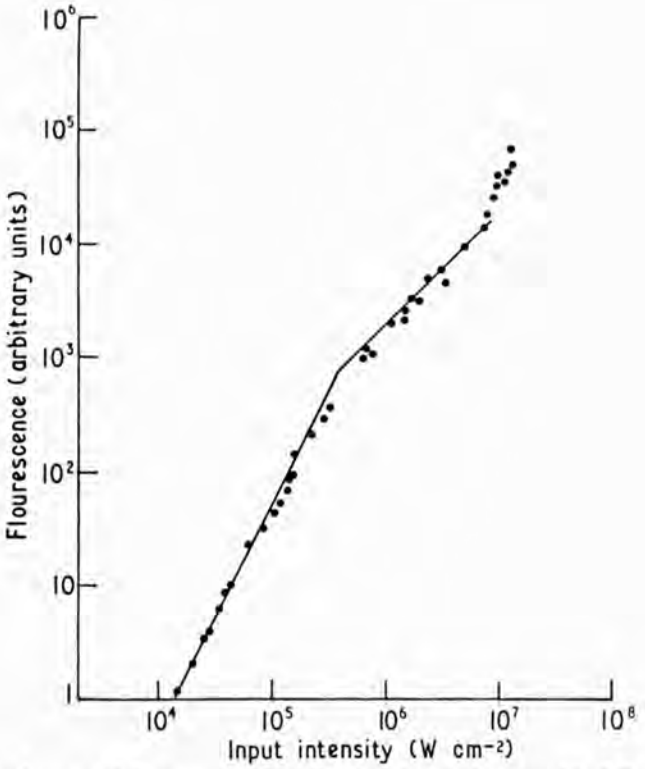

Figure 3. Dependence of fluorescence on input intensity for VnOPc in nitrobenzene.

The spectrum of the blue fluorescence was in all cases a fairly broad band (width about 800 Å). The peak of this emission was at about 4000 Å for CAP (Gibbs 1967) and at a somewhat longer wavelength about 4700 Å in the case of cryptocyanine. The true spectrum for VnOPc could not be determined because of absorption of wavelengths less than 4400 Å by the nitrobenzene solvent.

A small amount of blue fluorescence was observed from the solvents chloronaphthalene and nitrobenzene. This followed a square-law dependence on input power. These solvents have no absorption at the ruby frequency, but have a considerable absorption at twice this frequency. We therefore attribute this fluorescence to two-photon absorption (Giordmaine and Howe 1963). At very high intensities chemical breakdown of the solvents occurred. This was accompanied by a marked increase in fluorescence as seen on the graphs. A change in the fluorescence mechanism at these intensities was also suggested by the marked increase of the relaxation time of the fluorescence. This reached about 50 ns whereas at low intensities it was considerably shorter than the laser pulse duration ($\sim$15 ns).

CLM-P224

United Kingdom Atomic Energy Authority

RESEARCH GROUP

Preprint

BRAGG REFLECTION FROM A PHASE GRATING INDUCED BY NON-LINEAR OPTICAL EFFECTS IN LIQUIDS

P. Y. KEY
R. G. HARRISON
V. I. LITTLE
J. KATZENSTEIN

Culham Laboratory
Abingdon Berkshire

1969

CLM - P 224

BRAGG REFLECTION FROM A PHASE GRATING INDUCED BY NON-LINEAR OPTICAL EFFECTS IN LIQUIDS

by

P.Y. KEY*
R.G. HARRISON*
V.I. LITTLE*
J. KATZENSTEIN

(To be submitted for publication in IEEE Journal of Quantum Electronics)

ABSTRACT

Bragg reflection of light from a phase grating has been used as a technique for the investigation of non-linear optical phenomena. A continuous argon ion laser was used to probe the structure induced in a liquid by the non-linear interaction of a high intensity ruby laser beam with that liquid. This arrangement had the advantage of allowing direct space and time resolved measurements of the induced effects.

*Royal Holloway College (London University), Egham, Surrey, England.

U.K.A.E.A. Research Group,
Culham Laboratory,
Abingdon,
Berks.

October, 1969 (MEJ)

C O N T E N T S

1. INTRODUCTION

The strong electric field of the light output of a ruby laser affects the refractive index of a medium through which it passes in a number of ways. The most significant of these are:-

1. Electrostriction
2. Kerr effect
3. Thermal effects - in absorbing media.

When the light is reflected back along its own path, large oscillating fields exist at the antinodes of the resulting standing wave. As the above effects are dependent on the square of the field a spatially periodic variation of refractive index is set up proportional to the mean square of the local field (Fig.1). If the frequency of the back-reflected light is slightly shifted, the nodes and antinodes will propagate through the medium. The distortion associated with each of the above effects also has a characteristic velocity of propagation. (Electrostriction gives acoustic phonons - the Kerr effect gives optical phonons - the thermal fluctuations decay but do not propagate.) When the velocity of propagation of the nodes of the field matches that of the distortion of the medium, the effect on the medium has a resonant maximum. (It is this situation which, at sufficiently high laser powers, can give rise to the stimulated scattering associated with each of the interactions, i.e. electrostriction gives stimulated Brillouin scattering[1,2], the Kerr effect gives stimulated Rayleigh Wing[3,4] and stimulated Raman scattering[5], the thermal effect gives stimulated thermal Rayleigh scattering[6,7]). Thus by choosing the appropriate feedback frequency we can select the form of interaction we wish to investigate.

The refractive index variation set up in this way, by the ruby laser light, acts as a phase grating[8,9,10] upon a probing argon laser beam traversing the medium. Each layer of high and low index reflects a small portion of the incident argon light. When these portions add in phase, a maximum overall reflectivity is reached. The condition for this is the Bragg condition:

$$\theta_o = \cos^{-1} \frac{\lambda_a}{\lambda_r} \cdot \frac{n_r}{n_a} = 45{\cdot}5^o$$

where θ_o is the angle between the two beams, and suffices a and r refer to the argon and ruby wavelengths respectively. At this angle, providing the reflectivity is small

$$\text{reflectivity} = \left(\frac{\pi N \delta}{2\cos^2\theta} \right)^2 \qquad \text{(see Appendix)}$$

where N = number of modulations crossed

$\delta = \frac{\Delta n_a}{2n_{ao}}$

Δn_a = difference between maximum and minimum refractive index (for argon light) induced by the standing wave.

n_{ao} = refractive index of the undisturbed medium for argon light.

When $\Delta n \sim 2 \times 10^{-6}$ and length of interaction region $\sim$ 1 cm

reflectivity $\sim$ 1%.

The angular width at half reflectivity is

$$\frac{4 \times 1{\cdot}39}{\pi N \tan\theta_o} \qquad \text{(see Appendix)}$$

For 1 cm interaction length

angular width $\sim 5 \times 10^{-5}$ radians $\sim$ 10 seconds.

2. EXPERIMENTAL

Fig.2 shows the experimental arrangement. Single longitudinal mode output of the ruby laser was achieved by the use of two narrow dye cells for Q-switching and a resonant reflector as the output mirror. An aperture was used to cut down the divergence of the beam, and power densities of up to 100 MW/cm^2 were transmitted. The pulse duration was of the order of 15 nsec.

The argon laser gave 1 W output at 4880 Å with a beam divergence of 1 mrad. Accurate adjustment of the Bragg angle between the argon light and ruby induced structure was achieved by sensitive control of mirror M_1. A Fabry-Perot interferometer was used to check the single mode output of the ruby laser and to measure the frequency shift of the backward-going beam. These beams were distinguished by the use of the $\lambda/4$ plate and polaroid quadrant[7], as shown in the diagram. The reflected beam could either be shifted or unshifted in frequency. An unshifted frequency was obtained simply by the use of a mirror normal to the ruby beam. A shifted frequency was generated by stimulated back-scattering of light focussed into cell (2), as shown in the diagram. The frequency shift was determined by the liquid contained in cell (2).

An advantage of this set up was that the detectors D_1, D_2 measured the incident ruby beam in each direction while P and D_3 simultaneously measured the amplitude of the refractive index modulation in the cell and the amplification which it caused in the backward beam. This was achieved by the use of cable delay lines allowing simultaneous display of four pulses on a single trace of a Tectronix 454 oscilloscope.

The intensities of the beams were controlled (and feed-back into the laser minimised) by the use of $CuSO_4$ attenuators. The Bragg angle of $45{\cdot}5^{o}$ between the ruby and argon laser beams permits the very simple geometry of cell (1) and normal incidence of the argon beam as shown. Spatial resolution could be directly achieved by longitudinal movement of the cell along the ruby beam.

3. RESULTS

The experimental investigations were carried out mainly in absorbing media using unshifted frequency feedback. The thermal effect was therefore dominant.

(a) Angular Dependence

Using a solution of copper acetate in methanol with absorption coefficient $\alpha = 0{\cdot}15\ cm^{-1}$ the angle giving maximum Bragg reflection was measured to be $45{\cdot}5 \pm 0{\cdot}1^{o}$, and was equal to the theoretical value given by $\cos^{-1} \frac{\lambda_a}{\lambda_r} \cdot \frac{n_r}{n_a}$. While the angle could only be measured absolutely to $\pm 0{\cdot}1^{o}$, small incremental adjustments could be made much more accurately[11]. The angular width at half reflectivity was found to be ~ 5 minutes corresponding to the divergence of the argon laser beam.

(b) Magnitude of Reflectivity

The refractive index modulation due to thermal effects is given by[12]

$$\Delta n = \gamma \frac{P}{2\ell\chi(n_r k_r)^2} \left(\frac{\partial n}{\partial T} \right)$$

where γ is a numerical factor such that $0{\cdot}5 < \gamma < 1$ and P is the power per unit area absorbed in the medium of length ℓ and thermal conductivity χ.

Hence with the same solution as in (a), with an intensity of 23 MW/cm^2 and $\ell \sim 4$ cm

$$\Delta n \sim 4 \times 10^{-6}$$

Now reflectivity $= \left(\frac{\pi N \delta}{2 \cos^2 \theta} \right)^2 \sim 4\%$ for argon light incident at the Bragg angle. However, the theoretical angular width at half reflectivity of the Bragg is of the order of 10 seconds for a non-divergent beam (see Introduction), whereas the divergence of the argon laser beam was about 5'. Hence only about 3% of the argon beam was available for reflection, and thus resultant reflectivity ~ 0·1%. This estimate was experimentally confirmed.

(c) Dependence of Reflectivity on Ruby Laser Power

The change in refractive index at any point is proportional to the mean square of the local field. Let $\underline{E_1}$ and $\underline{E_2}$ be the electric vectors of the forward- and backward- going beams respectively.

Now

$$E_1 = A_1 \sin(kz-\omega t)$$

$$E_2 = A_2 \sin(-kz-\omega t).$$

The local field $E = E_1 + E_2$

$$= A_1 \sin(kz-\omega t) + A_2 \sin(-kz-\omega t)$$

$$\bar{E}^2 = \tfrac{1}{2}A_1^2 + \tfrac{1}{2}A_2^2 + \frac{A_1 A_2}{2} \cos 2kz$$

therefore the difference between maxima and minima of the mean square of the local field $= A_1 A_2$.

Hence the difference between the maxima and minima of the refractive index $\delta n \propto A_1 A_2$.

Now reflectivity of grating $\propto (\delta n)^2$ (see Introduction)

$\propto I_1 I_2$ where I_1, I_2 are the intensities of the forward- and backward- going beams respectively. Fig.3

shows the dependence of reflectivity of a solution of copper acetate in methanol ($\alpha = 0{\cdot}15\ cm^{-1}$) on I_1 when $I_2 = 0{\cdot}33\ I_1$. In this case reflectivity $\propto I_1^2$ as is confirmed by the graph. We ascribe the errors mainly to variation of the divergence of the ruby light due to lack of transverse mode control.

Fig.4 shows that the reflectivity is proportional to I_2 when I_1 is kept constant. These two results confirm the theoretical relationship.

Further power dependence investigations were made in the case of a saturable absorber (cryptocynanine in methanol). As was expected, the I_1^2 dependence breaks down at about 10 MW/cm^2 owing to the bleaching of the dye[13,14,15] (Fig.5).

(d) Dependence of Reflected Power on Incident Argon Laser Power

To ensure that the argon light was acting solely as a probe and not contributing significantly to the non-linear effects, the dependence of reflected power on the incident argon power was investigated. For solutions not absorbing at the argon wavelength, e.g. copper acetate in methanol, the expected linear dependence was observed (Fig.6). However, for solutions having even a slight absorption at the argon wavelength, e.g. nitrobenzene, thermal de-focusing[16] of the argon beam greatly reduced the Bragg reflection.

(e) Dependence of the Reflectivity on Concentration

The reflectivity of the grating was also investigated as a function of the absorption coefficient. As expected, different solutes in the same solvent gave equal reflectivities when the absorption coefficients of the solutions were equal.

The measurement of the reflection as a function of the absorption coefficient α was complicated by the fact that variation of α affects the values of E_1 and E_2. This can only be corrected for as long as the non-linear effect in the cell has a negligible effect on the ruby beam, a condition that requires a much shorter cell than that used in this experiment.

(f) Time Resolution

Each of the non-linear effects mentioned earlier has a characteristic relaxation time[17]. These have the following orders of magnitude:

Electrostriction - 10^{-9} to 10^{-10} sec

Kerr effect - 10^{-11} to 10^{-12} sec

Thermal effect - 10^{-7} to 10^{-8} sec.

The length of the ruby pulse (~ 15 nsec) and the resolution of the instruments (~ 7 nsec) only allowed investigation of the thermal relaxation.

Fig.7 shows the time profile of the ruby laser pulse and the resulting Bragg reflected pulse in the thermal and the electrostrictive cases. The relaxation time of the effect of electrostriction is very fast (compared with the pulse profile and instrument resolution). Hence the profile of this pulse provides a measure of the resolution of the instruments, (7 nsec). The relaxation time of a thermal grating is calculated from the bulk properties of the medium by the formula[7]

$$\tau = \frac{c\rho}{\chi(2k_r n_r)^2}$$

where c = specific heat at constant pressure and ρ = density. This gives a value of 16·5 nsec for methanol. The points marked on Fig.7

are the theoretical points given this relaxation time and the resolution time of the instruments. There is good agreement for this value of relaxation time and significant misfit if it is varied by more than 2 nsec.

Similar agreement was obtained in the case of a number of other liquids.

This technique can be used more generally for investigation of any non-linear optical effect dependent on E^2. In particular short pulses and better detector resolution will allow direct measurement of the lifetimes of the phonons generated by the stimulated Brillouin effect.

REFERENCES

1. R.Y. Chiao., C.G. Townes and B.P. Stoicheff, "Stimulated Brillouin scattering and coherent generation of intense hypersonic waves", Phys. Rev. Letters, vol.12, pp.592-595, May 1964.

2. K. Grob, "On the theory of stimulated Brillouin scattering in liquids", Z. Physk, vol.201, pp.59-68, April 1967.

3. D.I. Marsh, V.V. Morozov, V.S. Starinov and I.L. Fabelinskii, "Stimulated scattering of light of the Rayleigh Line Wing", JETP Letters, vol.2, pp.25-27, July 1965.

4. V.S. Starinov, "The theory of the stimulated Rayleigh Wing Scattering", Sov. Phys. Dokl., vol.13, pp.217-219, September 1968.

5. N. Bolembergen, "The stimulated Raman effect", Am. J. Phys, vol.35, pp.989-1023, November 1967.

6. R.M. Herman and M.A. Grey, "Theoretical predictions of the stimulated thermal Rayleigh scattering in liquids", Phys. Rev. Letters, vol.19, pp.824-828, October 1967.

7. D.H. Rank, C.W. Cho, N.D. Foltz and T.A. Wiggins "Stimulated thermal Rayleigh scattering", Phys. Rev. Letters, vol.19, pp.828-830, October 1967.

8. R.G. Harrison, P.Y. Key, V.I. Little, G. Magyer and J. Katzenstein, "Bragg reflection of laser light from a phase grating in a Q-switching liquid", Appl. Phys. Letters, vol.13, pp.253-255, October 15, 1968.

9. J. Walder and C.L. Tang, "Photoelastic amplification of light and generation of hypersound by the stimulated Brillouin process", Phys. Rev. Letters, vol.19, pp.623-626, Spetember 1967.

10. H. Boersch and H. Eichler, "Beugung an einen mit stehenden Lichtwellen gepumpten Rubin", Z. Angew. Phys. vol.22, pp.378-379, 1967.

11. P.Y. Key, R.G. Harrison, G. Hayward and V.I. Little, "A high precision spectrometer table", J. Sci. Instr., series 2, vol.2, pp.374-375, April 1969.

12. V.S. Letokhov and B.D. Pavlik "Theory of the resonant feedback laser", Sov. Phys. -Tech. Phys. vol.13, pp.251-259, August 1968.

13. F. Gires, "Experimental studies of saturable optical absorption", IEEE J. Quantum Electronics, vol.QE-2, pp.624-626, Spetember, 1966.

14. C.R. Guiliano and L.D. Hess, "Nonlinear absorption of light", IEEE J. Quantum Electronics, vol.QE-3, pp.358-367, August 1967.

15. R.G. Harrison, P.Y. Key and V.I. Little "Fluorescence due to excited state absorption in saturable absorbers", Brit. J. Appl. Phys., to be published.

16. S.A. Akhlmanov, D.P. Krindach, A.P. Sukhorukov and R.V. Khokhlov, "Nonlinear defocusing of laser beams", JETP Letters, vol.6, pp.38-42, July 1967.

17. M. Denariez and G. Bret, "Investigation of Rayleigh Wing and Brillouin stimulated scattering in liquids", Phys. Rev. vol.171, pp.160-171, July 1968.

APPENDIX

Let θ = angle of incidence at a refractive index boundary

θ' = angle of refraction at a refractive index boundary

A_i = amplitude of wave incident on boundary

δA_r = amplitude of wave reflected from boundary

δn = very small change of refractive index at boundary

then $$\frac{\delta A_r}{A_i} = \frac{-\sin(\theta-\theta')}{\sin(\theta+\theta')} \sim \frac{-\delta n}{2n_{ao}\cos^2\theta}$$ for parallel polarisation

$$\text{in limit } \underset{\delta n \to 0}{} \frac{1}{A_i} \cdot \frac{dA_r}{dn} = \frac{-1}{2n_{ao}\cos^2\theta}$$

Now let

n_{ao} = undisturbed refractive index for argon light

n_{ro} = undisturbed refractive index for ruby light

Δn_a = difference between max and min refractive index for argon light

λ_a = wavelength of argon light in vacuo

λ_r = wavelength of ruby light in vacuo

$$k_a = \frac{2\pi}{\lambda_a}$$

$$k_r = \frac{2\pi}{\lambda_r}$$

z = distance along ruby beam direction

then $$n_a = n_{ao} + \frac{\Delta n_a}{2} \sin 2k_r n_{ro} z$$

$$\frac{dn_a}{dz} = \frac{\Delta n_a}{2} \, 2k_r n_{ro} \cos(2k_r n_{ro} z)$$

$$\therefore \quad \frac{1}{A_i} \cdot \frac{dA_r}{dz} = \frac{-\Delta n_a \cdot k_r n_{ro} \cos(2k_r n_{ro} z)}{2n_{ao} \cdot \cos^2\theta} \cdot$$

Now light reflected from boundary at z has phase lag of $2n_{ao}k_a z\cos\theta$ at $z = 0$

$$\therefore \quad \frac{1}{A_i}\frac{dA_{ro}}{dz} = \frac{-\Delta n_a \cdot k_r n_{ro}}{2n_{ao}\cdot\cos^2\theta} \cdot \cos(2k_r n_{ro} z) \cdot \ell^{i2n_{ao}k_a z\cos\theta}$$

where A_{ro} is the amplitude at $z = 0$ of the wave reflected from a depth z of grating. Then total amplitude, A_R, of wave at $z = 0$ reflected from grating of depth L is given by

$$\frac{A_R}{A_I} = \int_0^L \frac{1}{A_i}\cdot\frac{A_{ro}}{dz}\cdot dz = \frac{-\Delta n_a k_r n_{ro}}{2\cos^2\theta\ n_{ao}}\int_0^L \cos(2k_r n_{ro} z)\ell^{i2n_{ao}k_a z\cos\theta}dz$$

assuming $A_i \sim \text{const} = A_r$ i.e. total reflectivity $\ll 1$ where L = total length of modulations probed.

Now let $\quad 2k_r n_{ro} = k$

$$2k_a n_{ao}\cos\theta = k'$$

$$\left(\frac{A_R}{A_I}\right) = \frac{-k\ \Delta n_a}{4\cos^2\theta n_{ao}}\int_0^L \cos kz\ \ell^{ik'z}dz$$

$$\left(\frac{A_R}{A_I}\right) = \frac{-k\Delta n_a}{8\cos^2\theta n_{ao}}\left[\frac{\sin(k'+k)L}{k'+k} + \frac{\sin(k'-k)L}{k'-k} + \right.$$

$$\left. + i\left[\frac{1-\cos(k'+k)L}{k'+k} + \frac{1-\cos(k'-k)L}{k'-k}\right]\right]$$

for $k' \sim k$ terms with $k'-k$ denominator $\gg$ terms with $k'+k$ denominator

$$\therefore \quad \left|\frac{A_R}{A_I}\right|^2 = \left(\frac{k\Delta_{na}}{8\cos^2\theta n_{ao}}\right)^2\left[\frac{\sin^2(k'-k)L+(1-\cos(k'-k)L)^2}{(k'-k)^2}\right]$$

$$= \left(\frac{k\ \Delta n_a\ L}{8\cos^2\theta n_{ao}}\right)^2\left[\frac{\sin\left(\frac{k'-k}{2}\right)L}{\left(\frac{k'-k}{2}\right)L}\right]^2$$

This has maximum when $k' = k$

i.e. when $\cos\theta = \frac{\lambda_a}{\lambda_r} \cdot \frac{n_{ro}}{n_{ao}}$

then $\frac{I_R}{I_I} = \left|\frac{A_R}{A_I}\right|^2 = \left(\frac{k \Delta n_a L}{8 \cos^2 \theta n_{ao}}\right)^2$

where I_R, I_I are the reflected and incident intensities

$$\boxed{\text{reflectivity} = \frac{I_R}{I_I} = \left(\frac{\pi N \delta}{2 \cos^2\theta}\right)^2}$$

where $N = \frac{2n_{ro}L}{\lambda r}$

$$\delta = \frac{\Delta n_a}{2n_{ao}}$$

At half reflectivity $\frac{\sin\left(\frac{k'-k}{2}\right) L}{\left(\frac{k'-k}{2}\right) L} = \frac{1}{\sqrt{2}}$

now $k'-k = 2k_a n_{ao} \cos\theta - 2k_r n_{ro}$

let $\theta = \theta_o + \delta\theta$ where $\theta_o = \cos^{-1} \frac{k_r n_{ro}}{k_a n_{ao}}$

$$k' - k = -\delta\theta \sqrt{k_a^2 n_{ao}^2 - k_r^2 n_{ro}^2}$$

$$\therefore \frac{\sin\left(\frac{\delta\theta}{2} \sqrt{k_a^2 n_{ao}^2 - k_r^2 n_{ro}^2} \cdot L\right)}{\frac{\delta\theta}{2} \sqrt{k_a^2 n_{ao}^2 - k_r^2 n_{ro}^2} \cdot L} = \frac{1}{\sqrt{2}}$$

$$\therefore \frac{\delta\theta}{2} \sqrt{k_a^2 n_{ao}^2 - k_r^2 n_{ro}^2} \cdot L = \pm 1{\cdot}39 \text{ radians}$$

$$\therefore \delta\theta = \pm \frac{2 \times 1{\cdot}39}{\pi N \sqrt{\left(\frac{k_a n_{ao}}{k_r n_{ro}}\right)^2 - 1}}$$

$$\therefore \boxed{\text{angular width at half reflectivity} = \frac{4 \times 1{\cdot}39}{\pi N \tan\theta_o}}$$

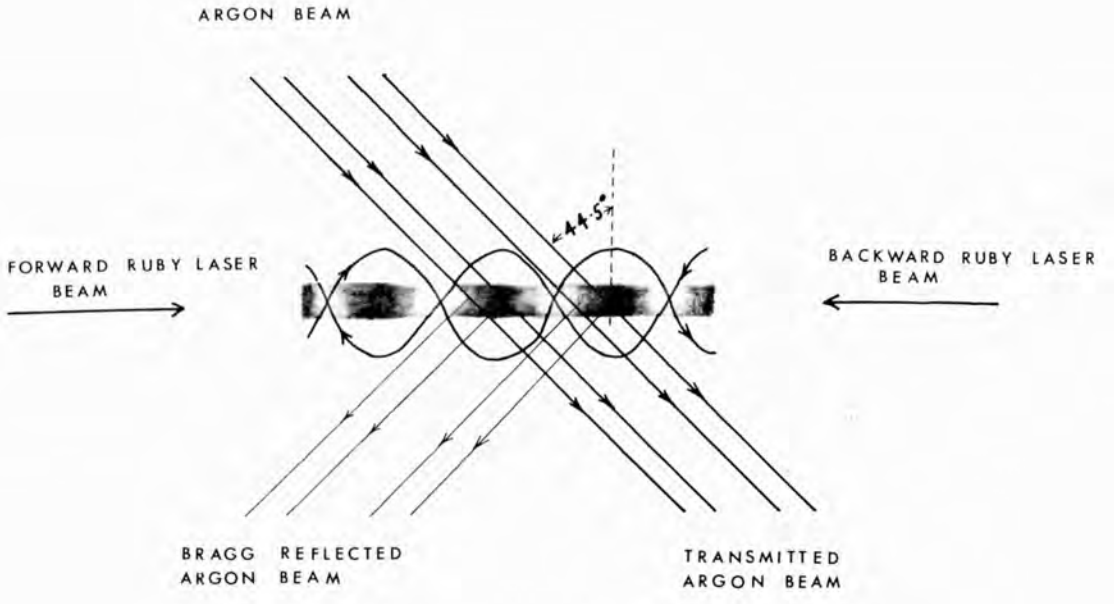

Fig.1 Illustrative diagram showing Bragg reflection of a continuous argon beam from a periodic structure induced in a liquid by the standing wave of a ruby laser beam.

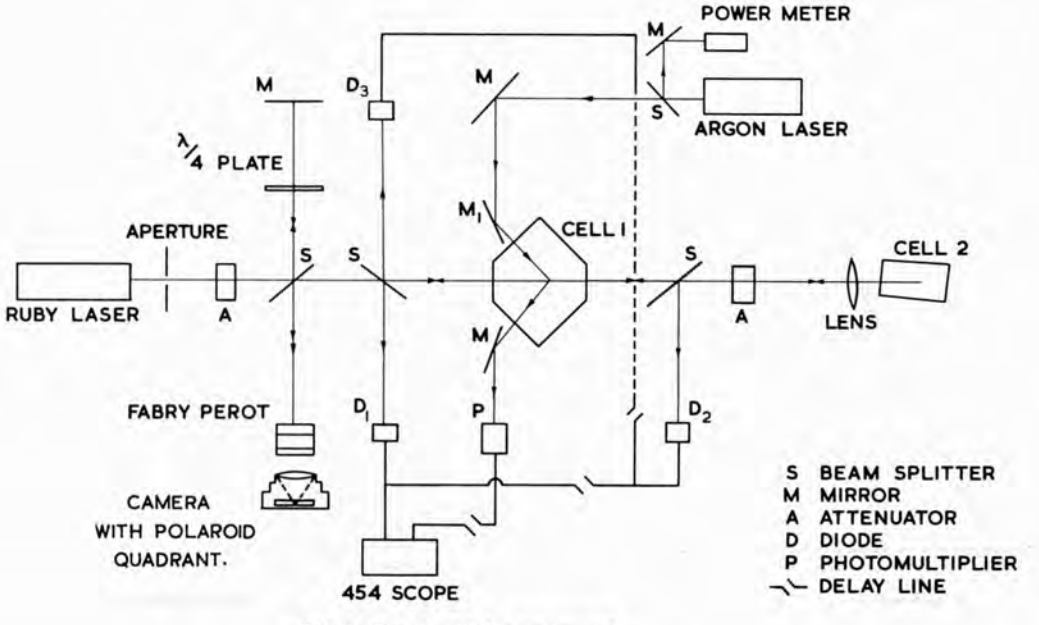

Fig.2 Experimental arrangement

CLM-P224

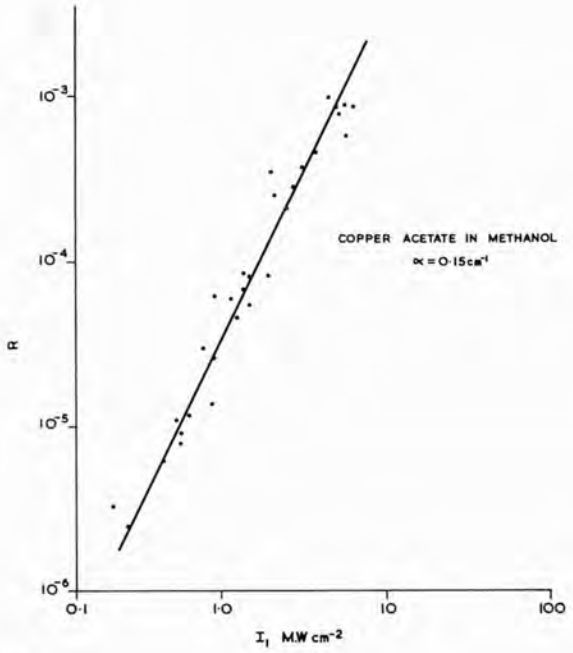

Fig.3
Reflectivity (R) of the phase grating as a function of the intensity (I_1) of the forward-going beam with $I_2 \propto I_1$. The line shows the theoretical square law.

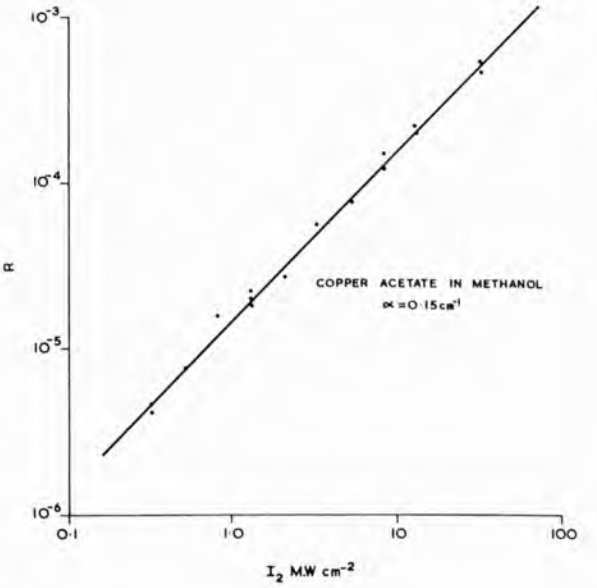

Fig.4
Reflectivity (R) of the phase grating as a function of the intensity (I_2) of the backward-going beam with I_1 constant at 71 MW cm^{-2}. The line shows the theoretical linear law.

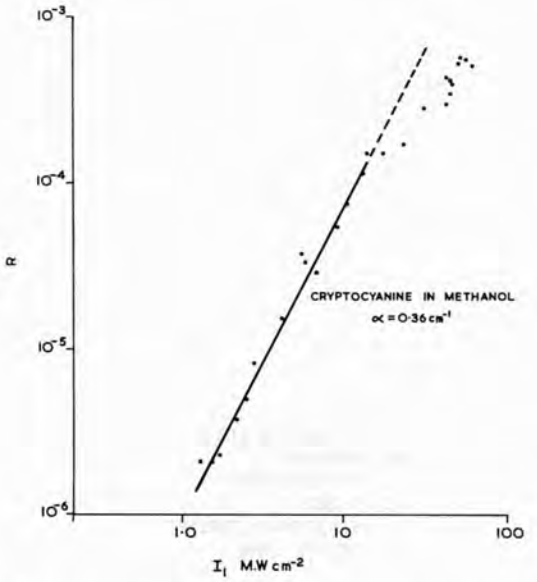

Fig.5
Reflectivity of phase grating as a function of I_1 for a saturable absorber.

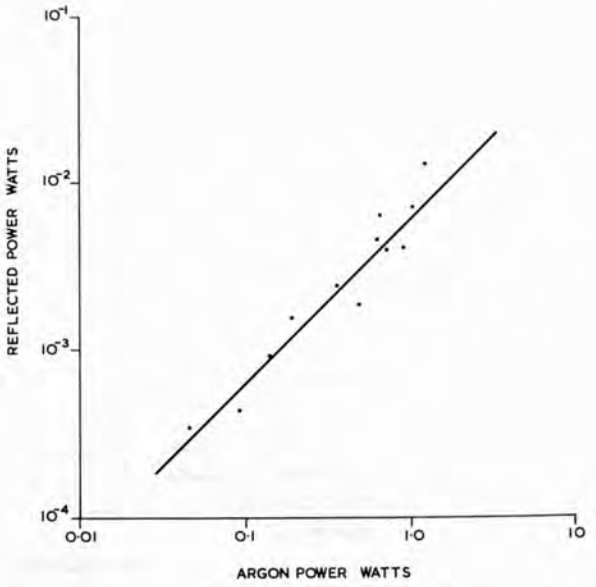

Fig.6
Reflected power as a function of incident argon laser power.

CLM-P224

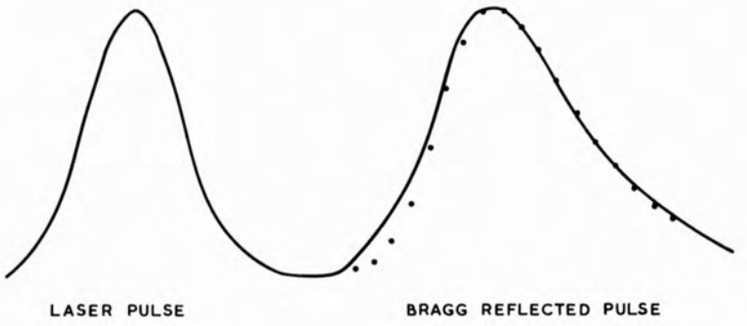

THERMAL

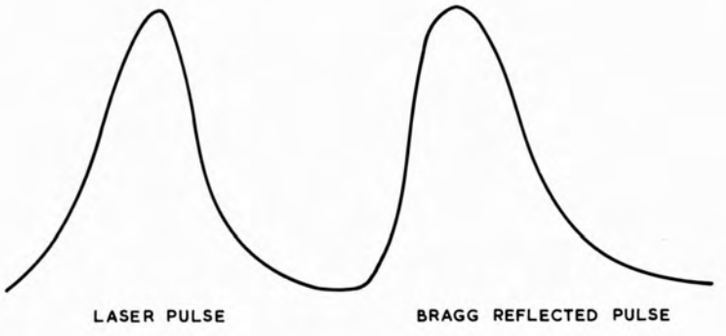

ELECTROSTRICTIVE

Fig.7 Time profile of the ruby laser pulse and the resulting Bragg reflected pulse in the thermal and electrostrictive cases. The points marked are those calculated given the theoretical relaxation time.

CLM-P224